1956 National Convention

IRE Convention Record

Part 7
Audio and Broadcasting

SESSIONS ON

Trends in TV Equipment
Audio Techniques
TV Transmitting Equipment and Techniques
High Quality Sound Reproduction
Color Television Tape Recording
Broadcast Transmission Systems—New Horizons

SPONSORED BY
IRE PROFESSIONAL GROUPS ON

Audio
Broadcast Transmission Systems

Presented at the IRE National Convention, New York, N. Y., March 19-22, 1956

The Institute of Radio Engineers

Additional Copies

Additional copies of 1956 Convention Record Parts may be purchased from The Institute of Radio Engineers, 1 East 79 Street, New York 21, N.Y., at the prices listed below.

PART	TITLE	Prices for Members (M) College and Pub. Libraries (L) Non-Members (NM)		
		M	L	NM
1	Telemetry, Antennas and Propagation Sessions: 5, 14, 22, 24, 28, 33, 38, 40	$3.00	$7.20	$9.00
2	Circuit Theory Sessions: 30, 41, 49	1.25	3.00	3.75
3	Electron Devices and Receivers Sessions: 16, 23, 29, 37 43, 50	2.50	6.00	7.50
4	Computers, Information Theory, Automatic Control Sessions: 7, 10, 32, 39, 42, 46, 53	3.50	8.40	10.50
5	Microwave and Instrumentation Sessions: 1, 26, 34, 47, 48, 54	2.75	6.60	8.25
6	Manufacturing Electronics Sessions: 6, 8, 17, 27, 35, 44, 45, 52	3.25	7.80	9.75
7	Audio and Broadcast Sessions: 12, 13, 20, 21, 25, 55	2.25	5.40	6.75
8	Aeronautical, Communication and Military Electronics Sessions: 3, 4, 11, 15, 19, 31, 36	2.75	6.60	8.25
9	Ultrasonics, Medical and Nuclear Electronics Sessions: 2, 9, 18, 51	1.50	3.60	4.50
	Complete Convention Record (All Nine Parts)	$22.75	$54.60	$68.25

Responsibility for the contents of papers published in the IRE Convention Record rests solely upon the authors, and not upon the IRE or its members.

IRE CONVENTION RECORD

1956 NATIONAL CONVENTION

PART 7 - AUDIO AND BROADCAST

TABLE OF CONTENTS

Session 25: Color Television Tape Recording
(Sponsored jointly by the Professional Groups on Audio and on Broadcast Transmission Systems)

Session 55: Broadcast Transmission Systems—New Horizons
(Sponsored by the Professional Group on Broadcast Transmission Systems)

HIGH STABILITY TELEVISION SYNCHRONIZATION GENERATOR

Francis T. Thompson

Westinghouse Research Laboratories
Pittsburgh 35, Pennsylvania

Abstract

A method for obtaining a new order of phase stability in frequency dividers is described. The output of a high frequency crystal oscillator is sampled in order to obtain an output corresponding to a half cycle of a high frequency reference. The application of this method to television results in accurately phased horizontal and vertical synchronization pulses. This method is particularly applicable to television systems which utilize dot interlace.

Problem

The function of a television synchronization generator is to provide timing pulses which assure that the picture information will be displayed in the correct location. The timing accuracy that is required depends upon the particular television system that is being used. The greater the number of picture subdivisions employed, the higher the required timing accuracy.

In conventional monochrome television, two timing signals are required: the horizontal synchronizing pulse which controls the starting of each line and the vertical synchronizing pulse which controls the starting of each field. The NTSC monochrome television standards specify that the time interval between the leading edges of successive horizontal pulses shall vary less than 0.5 percent of the average interval.[1] The tolerance of the vertical synchronization repetition frequency, nominally 60 cycles, is wide enough to allow the 60 cycle power frequency to be used as a reference for the system. In order to achieve good interlace it is desirable that the time between successive vertical pulses vary less than 10 microseconds or 0.06 percent of the average vertical interval which is 262.5 times the average horizontal interval. This relationship may be alternately expressed as a phase relationship between the vertical and horizontal synchronizing signals.

The introduction of the color subcarrier in compatible color television necessitated more accurate control of the timing signals. The frequency specification of the color subcarrier 3.579545Mc± 0.0003%, is necessary to assure proper operation of color reference oscillators in color receivers.[2] This frequency forms the reference for the timing pulses in compatible color, thereby precluding the possibility of synchronization with the 60 cycle power frequency. In order to obtain interlacing of luminance and chrominance information, the color subcarrier frequency was chosen to be an odd multiple of one-half the horizontal line frequency (455/2). This relationship reduces the degradation of the luminance signal caused by the chrominance signal because a 180 degree phase shift of the chrominance signal occurs between successive scans of identical areas. The cancellation of the dot pattern caused by the chrominance signal occurs at a 30 cycle rate if the phase relationship between the color subcarrier and the horizontal synchronizing pulse is accurately maintained. A phase shift of 0.8 degrees at 15734 cps in the horizontal synchronizing pulse during this 1/30 sec. will cause the dot pattern to be reinforced, rather than cancelled.

The requirement for proper phasing between the horizontal and vertical synchronizing pulse to achieve good vertical interlacing remains the same as in monochrome television.

Television systems which use a higher order of interlace to achieve high definition require an even greater timing accuracy. A high definition system which provides 1016 horizontal picture elements and 1050 vertical picture elements[3] samples the video presented on a single line during a single field into 254 dots. The other 762 dots are placed in between these 254 dots during subsequent fields. In order to achieve good interlace of these dots, it is desirable that the phase of the horizontal synchronizing pulse vary less than 0.12 degrees at 15.7 kc with respect to the phase of every 254th dot. This requires that the interval between horizontal pulses be maintained to within .02 microseconds. The timing of the vertical synchronizing pulse must be twice as accurate as in conventional television, since a vertical interlace ratio of four is used.

The synchronization generator, which is described in this paper, was developed in conjunction with the dot interlaced television system described above. The principles are applicable to synchronization generators in general.

Timing inaccuracies in a television system are caused by inaccuracies in the transmitter and the receiver. It is economically desirable to provide more accuracy in the transmitter so that most of the allowable tolerance may be

employed at the receiver.

Stability

The timing accuracy required in dot interlacing television systems dictates the use of a highly stable frequency reference. A temperature-controlled crystal oscillator provides a very satisfactory reference. It will be assumed in the discussion that follows that this reference frequency remains perfectly constant during the period of time required to complete an interlaced picture.

Stability of the timing signals produced by the synchronizing generator will be divided into the following two classes: frequency stability and phase stability. Although they are related by a time derivative, they will be defined for the purpose of this paper as follows:

Frequency Stability - The ability to maintain the period between consecutive timing pulses accurately enough so that the desired number of crystal oscillator reference pulses occurs during each of these periods.

Phase Stability - The ability to maintain the phase of the timing pulses with respect to the crystal oscillator reference pulses within the desired limits.

A loss of frequency stability results in counting down by the wrong number of pulses. This type of instability is associated with tearing or rolling of the picture. Frequency stability is necessary before phase stability can be considered. Phase instability is associated with pairing of interlaced lines or dots in the picture.

Present-day commercial synchronization generators provide excellent frequency stability. It is the purpose of this paper to investigate methods of improving the phase stability of existing synchronization generators.

Sinusoidal Divider Chain

The sinusoidal divider chain illustrated in Figure 1 divides from a crystal reference frequency f by integral factors n and m to a frequency f/mn. Let us assume that each dividing stage counts down by the proper integer and that the phase of the output of each stage is related to the input of that stage as follows:

Divider m input phase θ_m output phase $\theta_m \pm \phi_m$

Divider n input phase θ_n output phase $\theta_n \pm \phi_n$

Input and output phase angles of each stage are referred to the input frequency of that stage.

The $\pm \phi$ terms represent the limits of the phase jitter in each divider. The phase jitter in a cascaded divider of this type is cumulative. The phase jitter of the output of the divider chain referred to the input frequency f is $\phi_m + m \phi_n$.

It can be seen that small amounts of phase jitter in the low frequency divider, n, cause a large jitter of the output phase with respect to the phase measured at the reference frequency f.

Sinusoidal Divider Chain With Sampling

The sinusoidal divider chain illustrated in Figure 2 is identical with that of Figure 1. Equal amplitudes of the reference frequency f and the outputs of dividers m and n are added in a divider network. The addition of three sinusoids of frequencies f, f/4, and f/16 is illustrated in Figure 3. These three sinusoids add together periodically to produce a small peak which has a higher amplitude than the other peaks.[4] The repetition rate of this small peak corresponds to the repetition rate of the lowest frequency sinusoid. The phase of this peak is identical with one of the peaks of the reference sinusoid to a first approximation.

This peak may be selected by a clipper to obtain a synchronizing pulse at a frequency of f/mn cps. The phase jitter of this pulse is much lower than that of the f/mn cps sinusoid because of the sampling process of adding the various sinusoids and selecting the desired pulse.

Amount of Reduction of Phase Jitter

The sampled pulse does not remain exactly in phase with the reference sinusoid frequency f. Phase shifts in the various divider output sinusoids, which are added to the reference sinusoid, cause a slight shift in the location of the peak of the sampled output pulse. The amount of the shift of the sampled output pulse is equal to the sum of the shifts caused by each of the divider sinusoids.

The shift of the peak of the sampled pulse is plotted in Figure 4 as a function of the shift of a divider output sinusoid for several values of r, the ratio of the reference frequency to the divider output frequency. All angles are referred to the reference frequency f. It is assumed that the amplitude of the sinusoids f and f/r are equal and that their peaks are initially in phase.

It can be seen that the phase shift caused by the divider output decreases as the ratio r is increased. The importance of this fact can be understood by considering the previously described sinusoidal divider chain. The phase jitter of the lowest frequency output sinusoid with respect to the reference sinusoid is $\phi_m +$

$m\phi_n$. This jitter is large because it represents the cumulative jitter of both dividers. The ratio, r, of the reference frequency f to the frequency of the divider sinusoid f/mn is equal to mn. This large ratio results in a small jitter in the sampled output pulse even though the jitter of the f/mn sinusoid is large.

The phase shift of the leading edge of the sampled pulse has been found to be even smaller than the phase shift of the peak. This is to be expected because of the steep slope of the front edge of the sampled pulse.

Low Frequency Pulse Sampling

A highly stable pulse can be obtained from a pulse dividing chain by adding the outputs of the various divider stages and using them to sample the input pulse as illustrated in Figure 5. Astable multivibrator dividers were used in this particular chain, although the principle is applicable to bistable multivibrators and phantastron dividers. Figure 6 illustrates how the positive pulse duration of each divider was selected so as to select one of the p pulses that it divides by. The relative phase of these square pulses was chosen to insure that the output pulse is sampled by the flat portion of the square wave top. The peak square pulse allows one of the input pulses to pass through the gate insuring that the output is in phase with the input. Jitter in the firing time of the chain multivibrators has no effect on the phase of the output pulse as long as the counting ratio remains constant and the pulse is sampled by the flat portion of the square pulse peaks.

Experimental Equipment

High Frequency Divider

This divider was built as a part of a dot interlacing bandwidth reduction television system. Block and circuit diagrams are shown in Figures 7 and 8. Regenerative dividers were used in the sinusoidal dividing chain which divided from 2.47 Mc to 58.8 kc in steps of 6 and 7. Figure 9 is a photograph of the waveform obtained at the cathode of V10. The peak of this waveform causes pulses of cathode current to flow in V11. The outputs from the 14.7 kc and 7.35 kc multivibrators are added and applied to the suppressor of V11. Every eighth pulse of cathode current is drawn from the plate, while the other seven draw screen current. The narrow plate pulse, which has a 7350 cps rate, is amplified and inverted in V12 and applied to cathode follower V13. The 100 μμf condenser is rapidly charged by this pulse through the 1N48 diode. The condenser discharges exponentially through the 270 K resistor. This pulse widening circuit provides the output pulse shown in Figure 10.

Low Frequency Divider

This divider shown in Figure 11 divides from 14700 cps to 60 cps using multivibrator dividers. Block and circuit diagrams are shown in Figures 12 and 13. The synchronizing pulse to the first multivibrator is delayed by 14 microseconds to assure that a portion of the pulse triggering the multivibrator is not sampled by it. The phase relationships of synchronizing and sampling are illustrated in Figure 6. The sampling waveform which is applied to the suppressor of V12 is shown in Figure 14. The sampled output pulse is widened as explained previously.

Experimental Results

A simple experiment was performed to illustrate the improvement in phase stability obtained by sampling. The B^+ voltage of the low frequency divider was slowly varied from 200 to 300 volts. Time exposures of the 14.7 kc input pulse, Figures 15 and 16, were taken while this voltage was varied. In Figure 15, the time sweep was synchronized by the 60 cps sampled output pulse. In Figure 16, the time sweep was synchronized by a pulse obtained from the 60 cps multivibrator. The pulse from the 60 cps multivibrator represents the output of a conventional divider chain. The relative phase stability of the input and output pulses using sampling and conventional techniques is clearly illustrated.

Conclusion

The methods of sampling described in this paper provide a significant improvement in the phase stability of synchronization generators. These methods are applicable to most divider chains and should prove particularly valuable in color television. A color television synchronization generator which uses these sampling methods is being built in our laboratories.

References

1. National Television System Committee, Television Standards and Practice, p. 367, New York, McGraw Hill Book Company, First Edition, (1943.)

2. Fink, D. G., "NTSC Color Television Standards." Electronics, December 1953.

3. F. T. Thompson, P. M. G. Toulon, "A High Definition Monochrome Television System," 1955 IRE Convention Record, Part 7, PP. 153-164.

4. P. M. G. Toulon, U.S. Patent 2,565,102, August 1951.

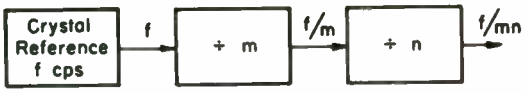

Fig. 1
Sinusoidal dividing chain

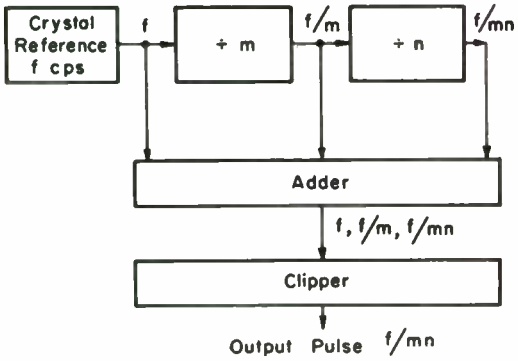

Fig. 2
Sinusoidal dividing chain with sampling

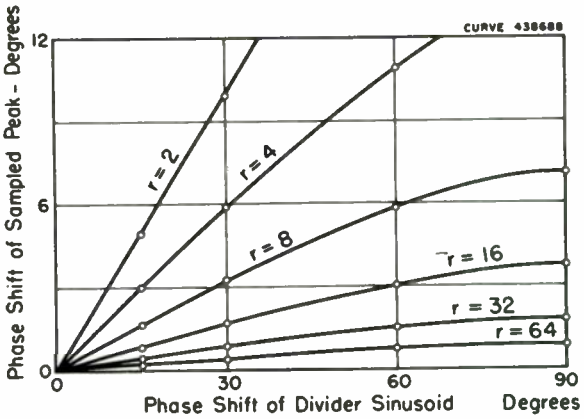

Fig. 4
Reduction of phase jitter

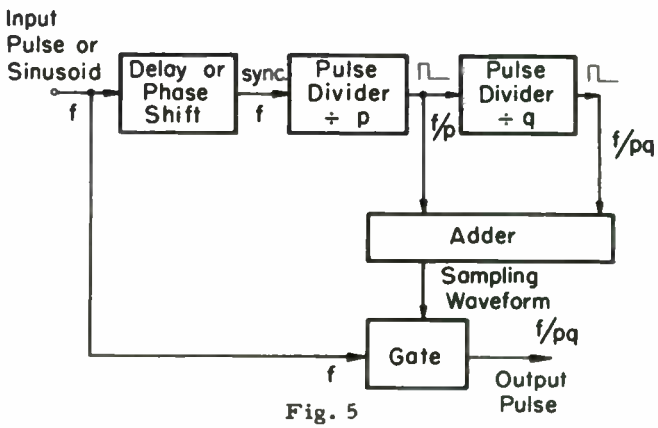

Fig. 5
Pulse dividing chain with sampling

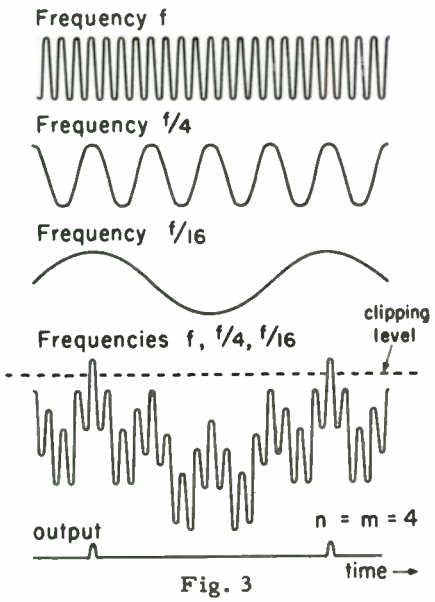

Fig. 3
Sampling dividing waveforms

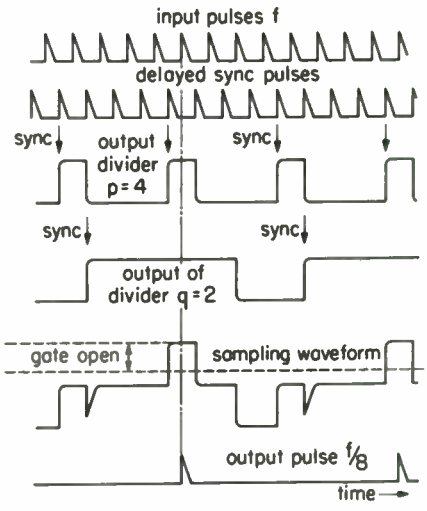

Fig. 6
Sampling dividing chain with pulse input

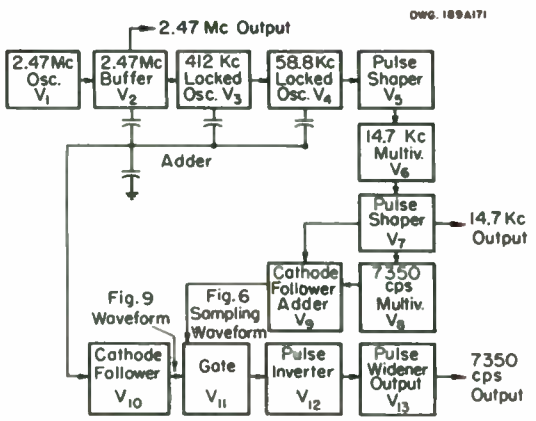

Fig. 7
High frequency divider

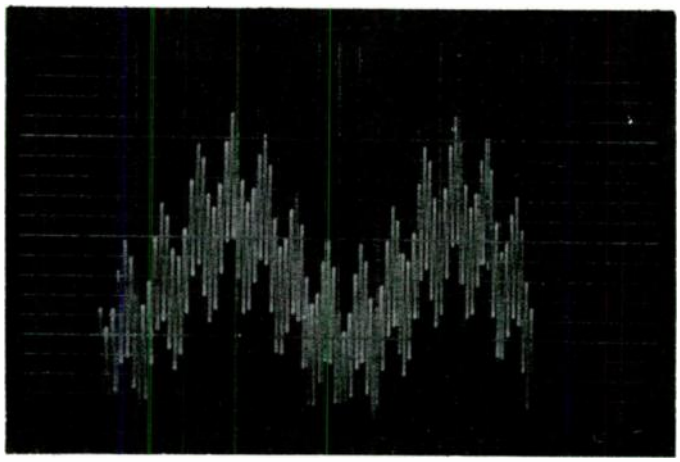

Fig. 9
Addition of sinusoids

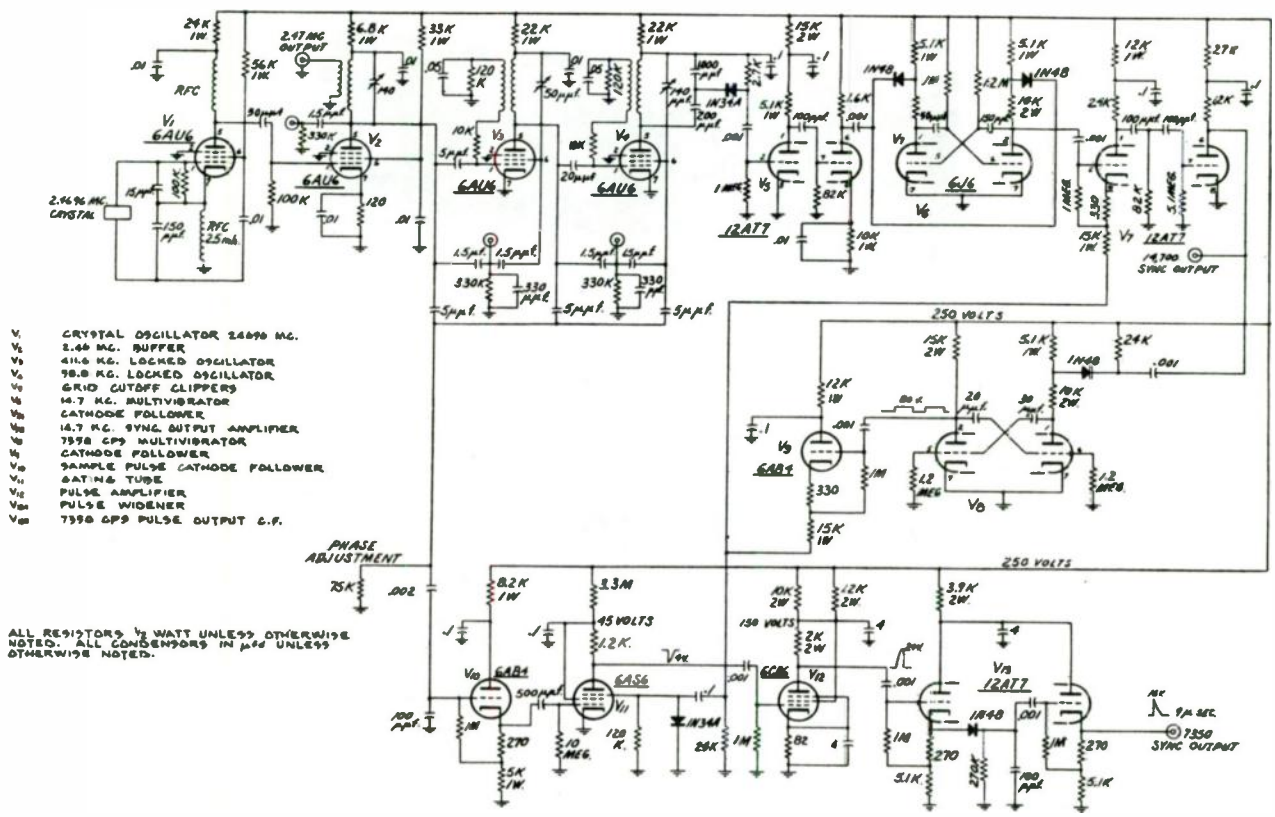

Fig. 8
High frequency divider

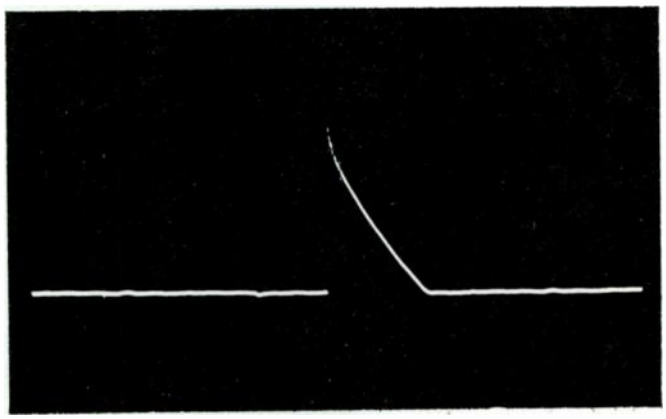

Fig. 10
7350 cycle sampled output

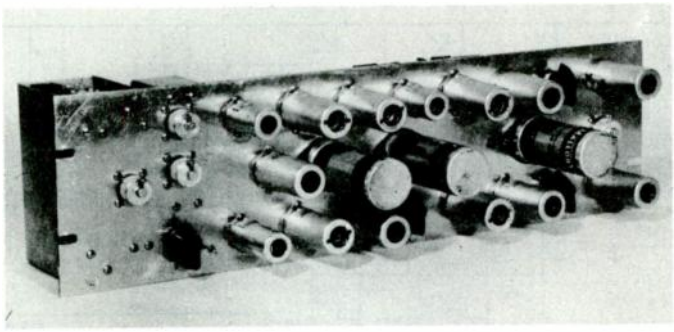

Fig. 11
Low frequency divider

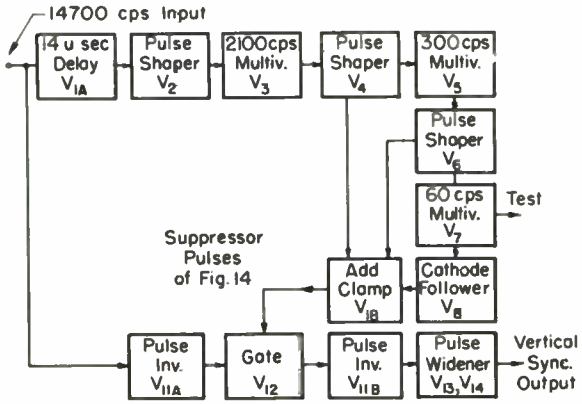

Fig. 12
Low frequency divider

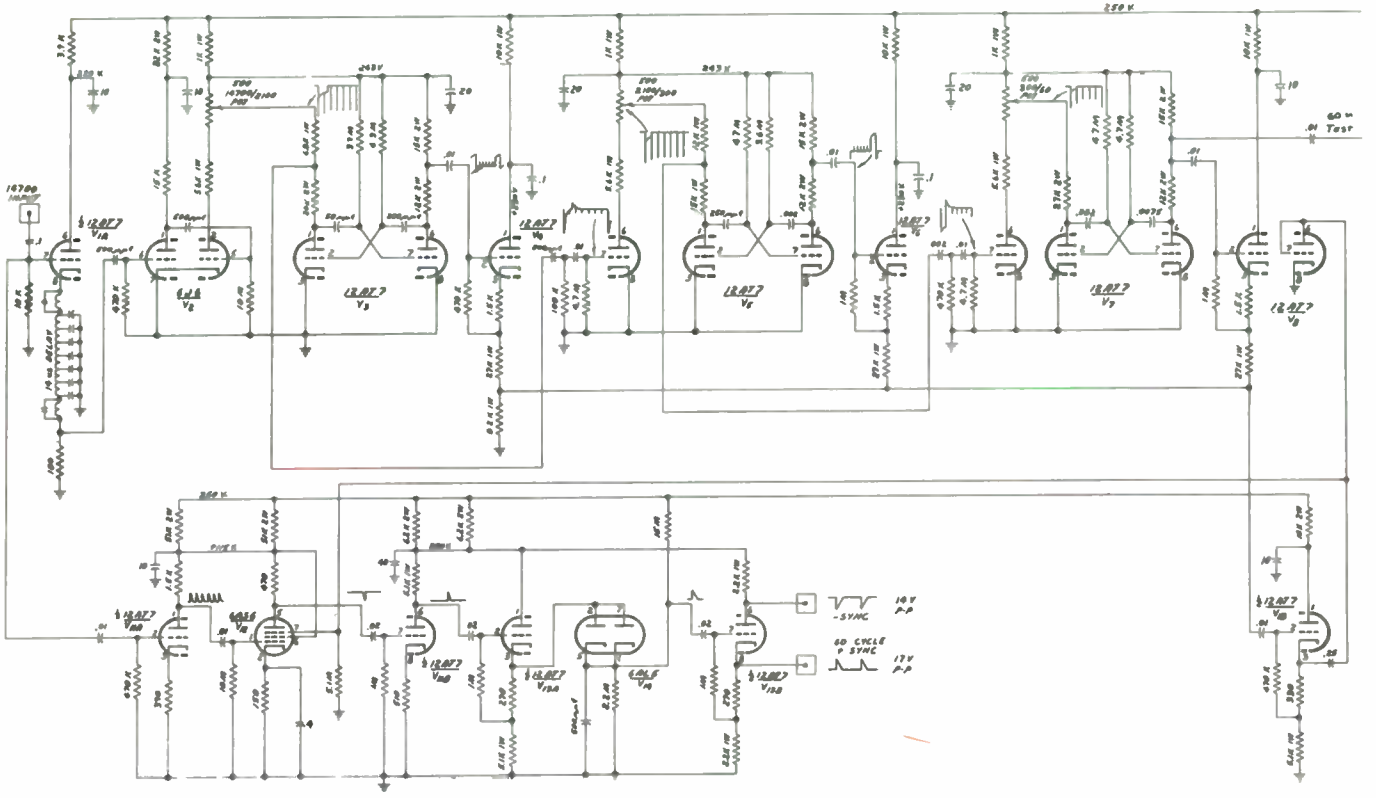

Fig. 13
Low frequency divider

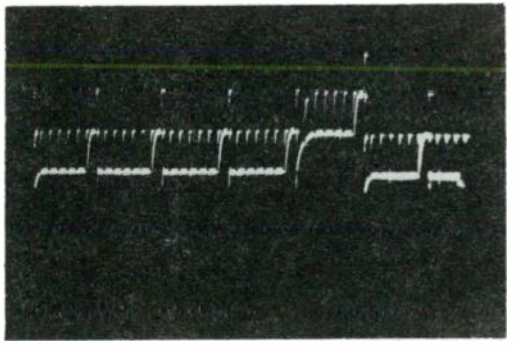

Fig. 14
Low frequency divider gating waveform

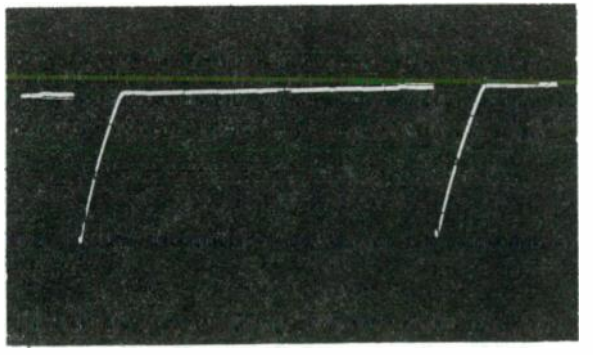

Fig. 15
Jitter between input and sampled output

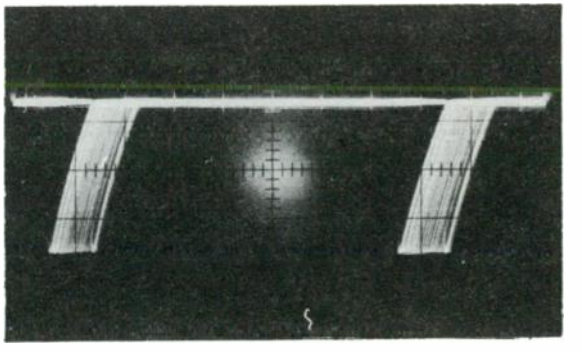

Fig. 16
Jitter between input and conventional output

PEDESTAL PROCESSING AMPLIFIER FOR TELEVISION

Ralph C Kennedy
National Broadcasting Company
New York, N.Y.

Summary

The Pedestal Processing Amplifier is intended to provide the essential signals for a color genlock system. Since a unique method of sync cancellation is used, it is felt that the term stabilizing amplifier, as commonly known for monochrome, should not be used to describe this equipment. Additionally, an improved sync separator is described which provides constant output sync amplitude for input signal level variations of ± 14 db.

Introduction

Television has presented many interesting challenges to the engineer. This is true not only in the area of transmission where many new problems have arisen but also in the areas of various special effects where continuing attempts have been made to try to accomplish the same results as the motion picture producer realizes on film.

With the advent of color television, a whole new transmission system has had to be designed. Manifestly the range of color special effects has been considerably greater than for monochrome and it has generally been more difficult to find satisfactory solutions.

Special Effects Require Genlock Operation

One of the procedures used in monochrome television to facilitate various special effects is to lock the sync generators together which provide the pulses for the various signals. This is known as genlocking and is used to create various video effects which require the simultaneous appearance on the screen of signals from two different locations. Such signals are used to produce split screen, video inset, lap dissolve and other types of effects. The introduction of commercials, which generally are on film and originate in the film studio, into the live program sequence originating in another location requires genlocking. In fact, without genlocking television would be at a very distinct disadvantage.

Stabilizing Amplifiers

Genlock operation has been successful due primarily to the availability of stabilizing amplifiers. These are capable of recovering the sync signal from the composite monochrome video signal and of clipping the sync signal from the incoming composite so as to reduce it to a simple video signal. The sync recovered from the signal has been used to lock the sync generators together while the video signal free of sync has permitted it to be introduced into the studio switching system in the same manner as a normal camera signal.

Such stabilizing amplifiers, however, are not usable on a color signal. The recovery of the sync signal permits the burst and chroma components, which extend below the blanking level, also to be present. Further, the clipping of sync from the signal to produce a simple video waveform simultaneously results in burst and many chroma components being clipped.

Two Line Genlock Operation

To circumvent the lack of a suitable stabilizing amplifier, color genlocking has heretofore been accomplished by using two wideband circuits. One has carried the sync and burst to lock the generators. The simple video signal free of sync to be introduced into the switching system has been carried on the other circuit. Clamper amplifiers in the Telco circuits, since they clamp on the tip of sync, have clamped on the blanking signal and operated satisfactorily. Further genlock operation has been attempted only on film camera signals. Pedestal has been easily controlled and no chroma components nor burst have been allowed to extend far enough below blanking to cause confusion in the clamper amplifiers.

However, when live pickups have been attempted the pedestal has not been so easily controllable and burst and chroma components have extended so far below the blanking level that the clampers have stopped functioning properly.

The Pedestal Processing Amplifier

This equipment has been designed and built with the main objectives being to recover the sync signal from an incoming composite video signal, either monochrome or color, and to produce a simple video signal as well. This eliminates the need for two circuits when genlocking and restores genlock operation to the same procedures as are used on monochrome

television. Needless to say, the saving in line costs is substantial.

The operation of the unit may be described briefly in the following manner. A composite monochrome or color signal is introduced at the input terminals where it branches in two paths. In one the sync is recovered. Further a circuit permits adjusting the location of the back edge of sync so as to produce sync having adjustable width. Clamp pulses are also developed from this sync.

The second path has an adjustable video delay line for delaying the composite video signal. This delayed signal is fed to a clamped adder tube which is also fed the sync signal. The sync is added in the same polarity as that in the composite video. Enough is added to cause the sync in the resultant output to extend well below the negative peaks of burst. The sync is clipped so as to produce a clean tip but it is not clipped enough to distort the burst. This signal is fed to another clamped adder tube which is likewise fed the sync signal. The polarity of the sync in the composite signal is opposite to that of the sync being added. This causes the sync in the output signal to be reduced to zero, i.e., blanking level by proper adjustment of the amount of the sync introduced.

The proper timing of the front edges of the sync in the composite signal and the added sync is realized by adjusting the video delay line. The timing of the back edges of the two syncs is adjusted with the pulse width control.

Three outputs are available from the unit. One is processed sync whose output remains constant for input level variations of ± 14 db from a standard one volt peak-to-peak signal. A second output is a composite signal having processed sync. The third output is a simple video signal having a processed pedestal.

The evolution of these three signals from the original composite signal may be understood by referring to Figure 1. The 417-A-1 is a high gain amplifier. It is coupled through an L-C circuit anti-resonant at a frequency 3.579 mc/s to the grid of 6BN6-2. The tuned circuit removes the chroma components and burst from the signal. About 10 volts of sync is present in the signal at the grid of 6BN6-2. This is sufficient to produce very positive gating action for input signal level variations of ± 14 db. This circuit is essentially the key to the success of the whole unit since variations in input are removed. As a result constant amplitude sync and clamp pulses are assured which eliminates many of the usual stabilizing amplifier problems.

The output of 6BN6-2 is amplified in 12AT7-3 and is again gated in 6BN6-4. The accelerator output of this tube is amplified in 5687-5 to produce a sync output of between 4 and 5 volts into 75 ohms.

The plate output of 6BN6-4 is fed to 12AU7-6. The first half has a number of open circuited delay lines of varying lengths in its plate circuit which is used to control the location of the back edge of sync. A base clipper is used to couple the pulse to the second half of 12AU7-6. A tip clipper couples the plate to 12AT7-7.

This tube acts as a cathode follower having one fixed output and two adjustable outputs. The two adjustable outputs are the sync addition and subtraction controls. Since processed sync is first introduced into the signal to drive the original impure sync below clipping level and thereby removing it, it is necessary to have the identical sync for cancellation. This is realized by feeding the syncs to the two adder tubes from the same source.

The fixed sync output from the cathode follower is amplified and differentiated in 12AX7-8 to form clamp pulses. The base is clipped and the pulse is coupled to 5687-9. This tube amplifies the pulse and splits its phase to drive the clamp tubes 6AL5-13 and 6AL5-17.

As mentioned earlier, the input signal to the unit split in two paths. The second is to a 12AU7-10. This tube is a cathode follower gain control which allows adjustment of the overall video gain of the unit.

The second tube in the video circuit is 417A-11 which has a 75 ohm adjustable delay line in its plate circuit. The delay of this line is 0.3 usec. The last 0.1 usec is tapped at each 0.01 usec. This line has response variations of about 5% at most to 5 mc/s.

The line output feeds 12AT7-12 which is a straight amplifier feeding clamped amplifier 6U8-14. The triode section of this tube is a sync amplifier which injects the sync on the cathode of the pentode section. The polarity of the sync adds to that of the composite signal in the adder tube. The 6U8-14 has a clipper 6AL5-15 in its plate to clip sync.

Precise clipping is realized by regulating both the screen and plate voltages of the pentode section of 6U8-14. The 6BQ7-19 acts as the regulator for these two voltages.

At the output of 6AL5-15 the signal is composite video having processed sync. The timing of the front edge of the inserted sync is made to coincide with that of the original

signal by adjustment of the delay line in the video path. The back edge of these same pulses coincides by adjusting the pulse width in the pulse path.

The signal out of 6AL5-15 divides into two paths. One is through 12AU7-16 which is a straight video amplifier into a 2:1 gain line amplifier. This signal is composite video with processed sync.

The second output is fed to the clamped grid of adder tube 12AU7-18. Processed sync is fed to the second grid of this tube. The inserted sync is out of phase with the composite signal sync so that, by adjusting the amplitude of the inserted sync, cancellation of sync results. The signal out of 12AU7-18 is a simple video signal including burst and chroma. This is fed through a second line amplifier having a gain of 2 to 1. This signal having a processed pedestal is now in condition to enter a conventional switching system.

Adjustment of the Apparatus

As previously mentioned, the primary purpose for the Pedestal Processing Amplifier is to provide a video signal from a composite color signal. This objective is kept in mind when adjusting the apparatus. The power requirement is 115 volts ac for heater power and 585 ma at +285 volts dc for plate and screen power.

The apparatus should have a few minutes to stabilize after applying power. Referring to Figure 1 it is seen that test point A may be used to monitor the input signal. This signal should be 1 volt peak-to-peak composite. A color bar signal appears at this point as shown in Figure 2.

Test point B shows the signal after amplification and chroma filtering. The trap circuit ordinarily requires no adjustment except during the initial installation. Figure 3 shows the signal when the trap is properly adjusted. If chroma is present, readjust the chroma trap condenser to eliminate the chroma.

Test point C shows in Figure 4 a correctly recovered sync signal at the single terminated sync output.

Test point D and Figure 5 shows the signal at the cathode follower video gain control output. This signal should be the same as that at test point A except at a lower level.

Test points E and F permit monitoring several adjustments. They allow the two pulse shaping clippers associated with 12AU7-6 to be properly adjusted and also they indicate the level of addition and cancellation syncs. The controls #6 and #7 should be rotated clockwise as should also the pulse width control. Control #1 should be adjusted so that the base of the pulse is just clipped clean as viewed at points E or F. Control #2 is adjusted so that the tip of the pulse is also clipped clean. When the clippers are properly adjusted the sync signal at points E or F appears as shown in Figure 6.

Test point G permits monitoring the clamp pulse and is shown in Figure 7. The clamp pulse should begin just after the back edge of sync and last throughout the duration of burst. The variable coupling condenser between the two halves of 12AX7-8 controls the location of the back edge of the clamp pulse.

At this point controls #6 and #7 should be returned to zero so that no signal is present at points E and F. Rotate controls #5, #8, and #9 clockwise to attain maximum output.

Controls #8 and #9 are intended to adjust the level of the composite and video signals into the two line amplifiers. The usual procedure is to set each for maximum output observing the level of the video at the input to each line amplifier. Next reduce the amplitude of whichever signal is greater so that the video level in each signal is the same. Now adjust control #5 for the desired output level from the line amplifiers.

By adhering to this procedure the level through the whole equipment is operated at the lowest value possible, thereby causing the differential phase distortion to be kept to a minimum.

Adjust control #3 so that the tip of sync is barely clipped as it appears at the test point of the input to the video signal line amplifier. Adjust control #6 so that sync is driven back up to the pedestal. Adjust the video delay line so as to minimize the transient at the previous location of the front edge of sync. Adjust the pulse width control to minimize the transient where the back edge of sync previously occurred. Further reduction of the magnitudes of the transients may be affected by adjusting control #7.

The realization of the optimum cancellation condition is more of an art than a science. Sequential adjustments of controls #3, #6, and #7 will produce a pedestal having less than ± 3.5% of peak transient ripple in the processed pedestal region. Figures 8 and 9 show the signal at the inputs to the two line amplifiers. It should be emphasized that no attempt is made to cause the composite output signal to have the correct sync to video ratio. Only the optimum video pedestal adjustment is important. The sync in the composite output is always great enough to extend beyond the blacker than black tips of burst so that it can be used wherever a

composite signal is acceptable. Control #4 is the clamp balance of the sync cancellation circuit. This should be set so that 12AU7-18 grid #7 is about -0.1 volts with respect to the chassis as ground.

Test Results

Three of these equipments have been built and used commercially. The first time this method of genlocking was attempted commercially was during the 1955 World's Series where in 6 days a total of 21 hours time genlocking was maintained. The "Great Waltz" and "Producer's Showcase" have also used this method of genlocking. In the latter case, Brooklyn was locked to Radio City, which in turn was locked to Burbank. Split screen and numerous fast switches between the East and West Coast were made with no loss of genlock.

Another test included genlocking a film studio whose output was a continuous loop of film leader which causes extreme signal variations. This signal was fed for half an hour with no interruptions in genlocking.

Performance Data

As has been mentioned earlier the dc power requirements are 285 volts at 585 ma. Additionally, the response is dependent upon the video delay line which has been covered previously. The differential gain is less than 2% while the differential phase is $\pm \frac{1}{4}°$.

Conclusion

The Pedestal Processing Amplifier is a device which makes color genlock operation a practical procedure. The unit may be used either on color or monochrome signals. With such a device it is now possible to begin work on a "fail safe" type of genlock system, having automatic relocking facilities upon restoration of the signal. Large yearly savings in line costs are possible since only one line is required instead of two. Further, coast to coast genlock heretofore was impossible, since there are only two color circuits. On the old two line system no spares were available.

APPENDIX

It is well to consider the transient conditions during the sync cancellation period. The situation may be better understood by referring to Figure A. The sync pulse is shown having two different rise times, τ_1 and τ_2. τ_1 is the rise time of the leading edge of sync and is shorter than τ_2. This is the sync in the incoming composite signal after it has been clipped to smooth the tip but prior to the insertion of the inphase processed sync. The values for τ_1 and τ_2 will vary depending upon the sync generator output, transmission path, etc; however, for an average $\tau_1 = 0.2$ usec and $\tau_2 = 0.3$ usec.

Figure B shows the inphase sync to be added to Figure A sync. The rise time is about 0.1 usec for both τ_3 and τ_4

The result of the inphase addition is shown in Figure C where the front edge has a rise time of 0.2236 usec while that of the back edge is 0.3162 usec.

In Figure D is shown the result when sync cancellation occurs. Theoretically the condition of minimum ripple occurs when two pulses having identical rise times are added exactly 180° out of phase. Since the recovery of sync without changing the pulse rise times and width is next to impossible it then becomes a matter of compromise. Further, alteration of the pulse is minimized by making the rise time of the recovered sync as short as possible. However, here again a practical limit on circuit complexity dictates something of the order of 0.1 usec.

Finally, since we know that the minimum amount of overshoot and optimum phase linearity occurs for a transition approaching a unit doublet response, the video delay line is adjusted to realize that objective where the leading edge of sync occured. The pulse width control is adjusted to try to improve matters in the region of the back edge of sync.

The resultant signal after it has passed through switching and has had new sync added, has resulted in a signal having no observable ripple on the edges of sync. This fact serves to justify the rather loose approach used to solve the transient problem.

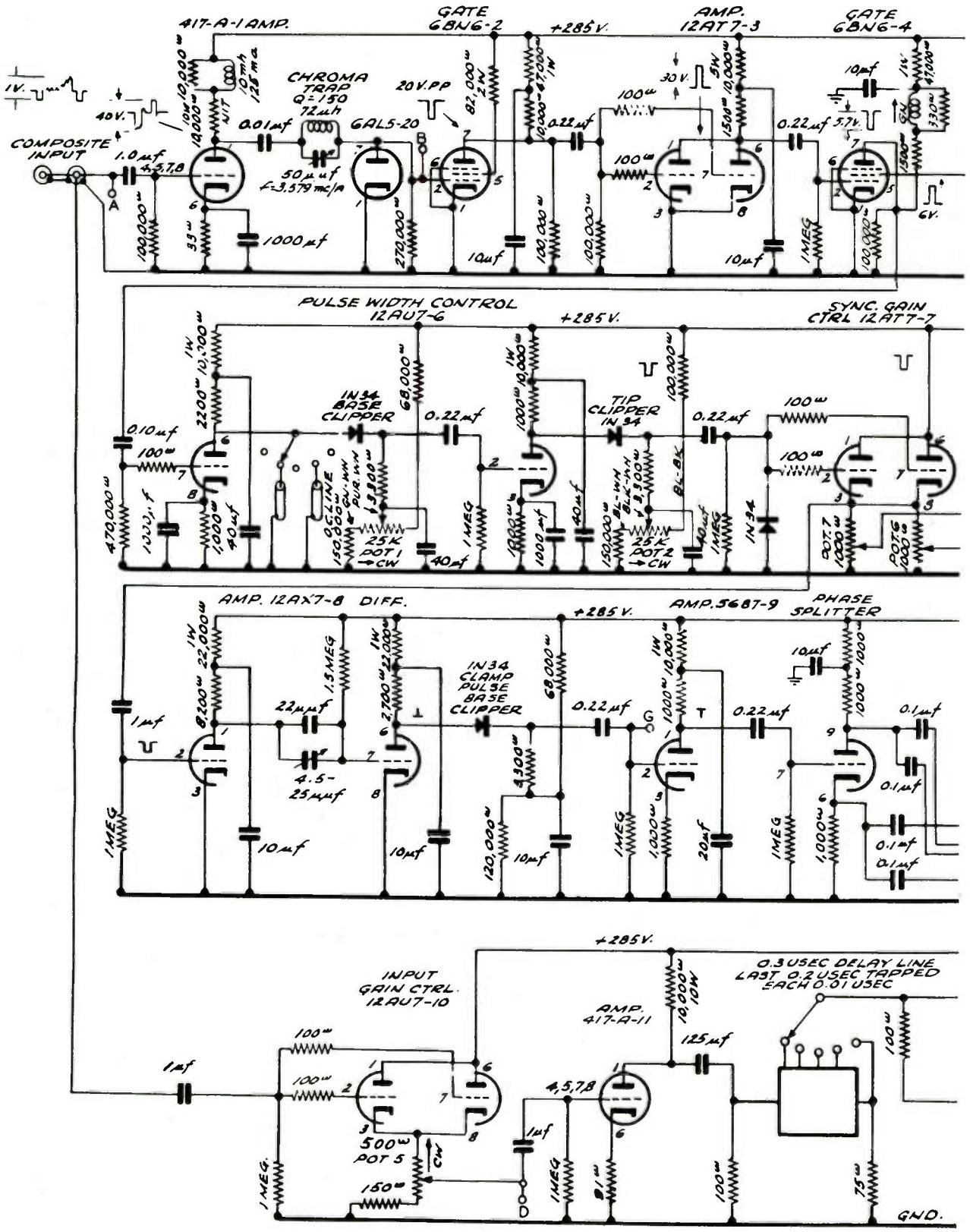

Fig. 1a
Circuit diagram of pedestal processing amplifier

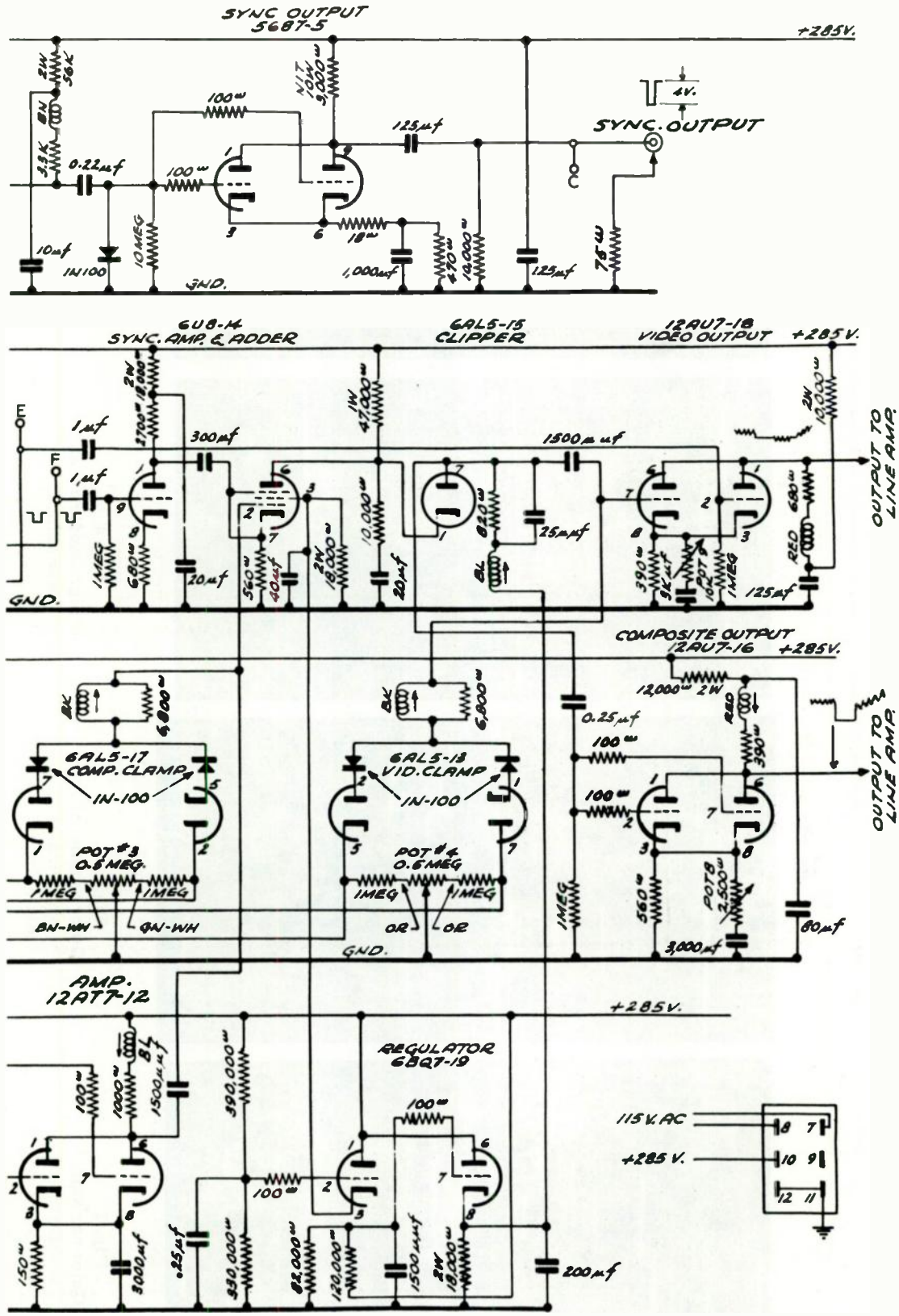

Fig. 1b
Circuit diagram of pedestal processing amplifier

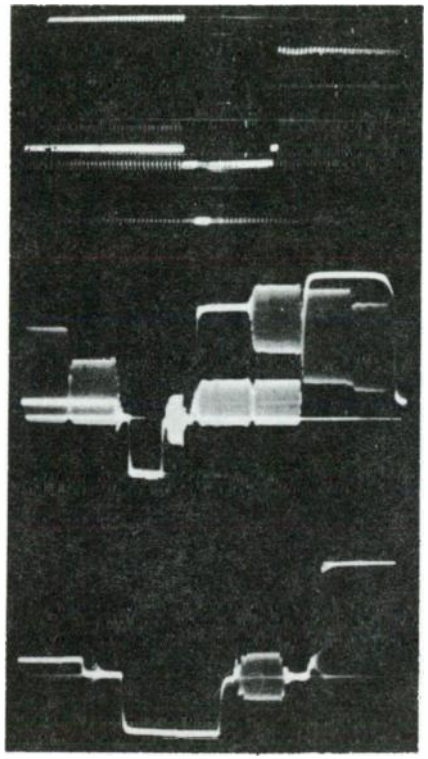

Fig. 2
Color bar signal
waveforms at
test point A

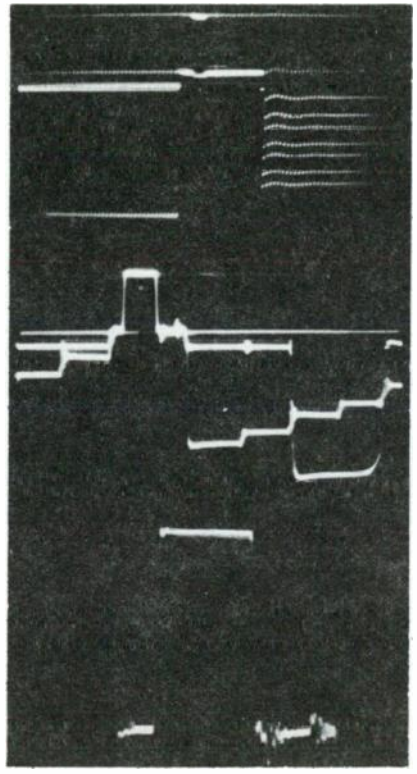

Fig. 3
Color bar signal
waveforms at
test point B

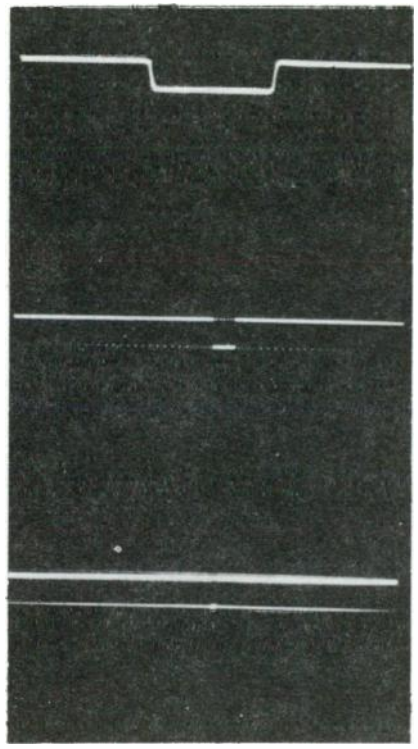

Fig. 4
Sync waveforms at
test point C

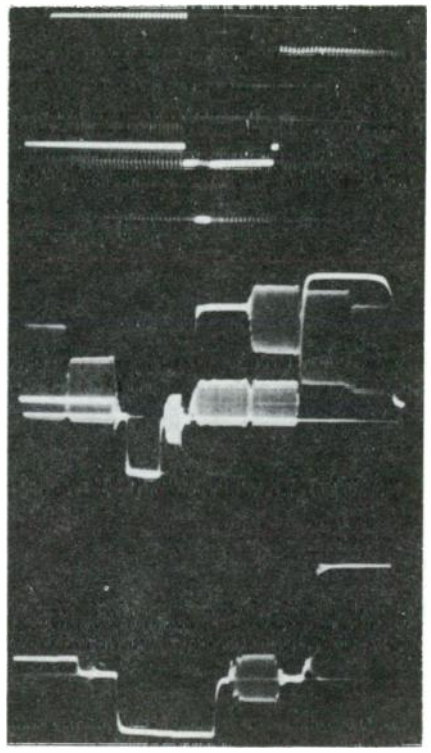

Fig. 5
Color bar signal
waveforms at
test point D

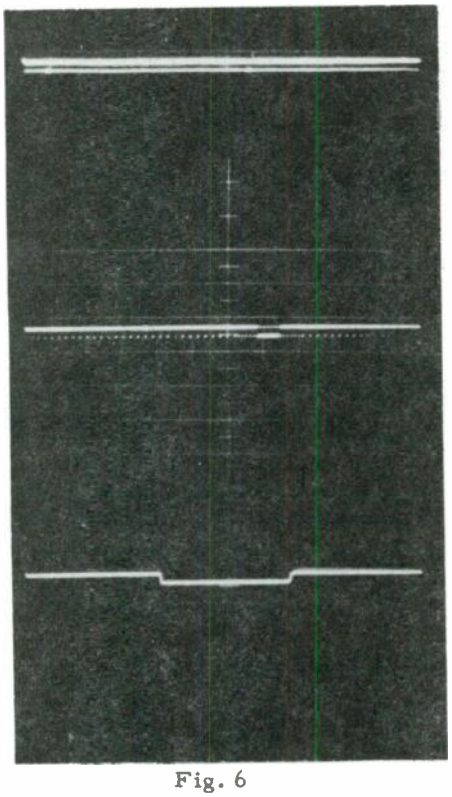

Fig. 6
Sync waveforms at test points E or F

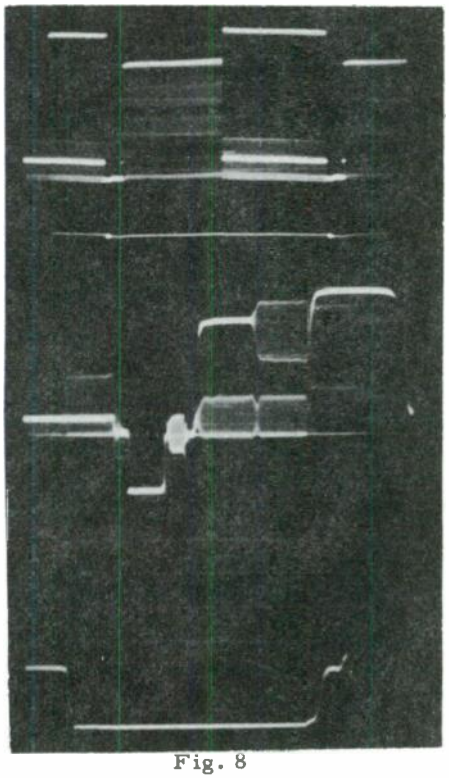

Fig. 8
Color bar signal waveforms of composite output signal

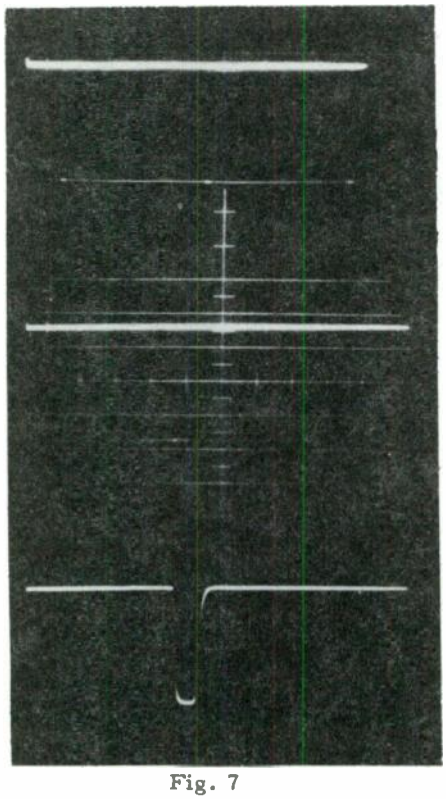

Fig. 7
Clamp pulse waveforms at test point G

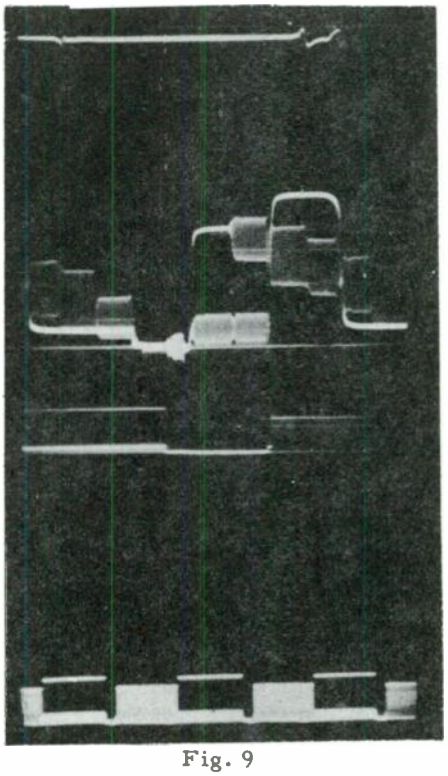

Fig. 9
Color bar signal waveforms of video output signal

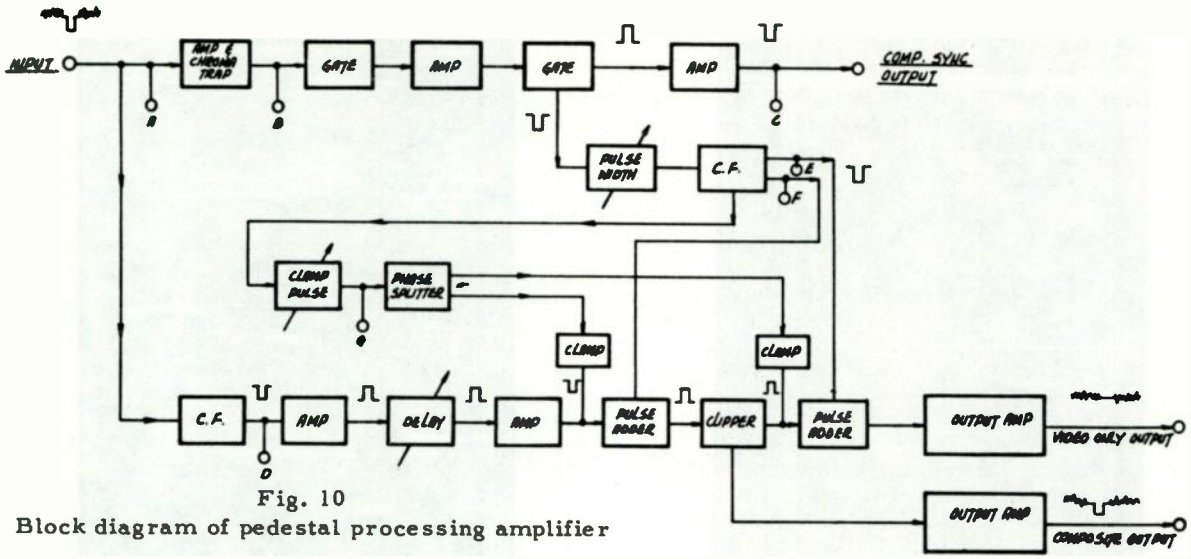

Fig. 10
Block diagram of pedestal processing amplifier

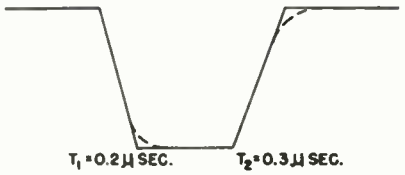

FIG. A

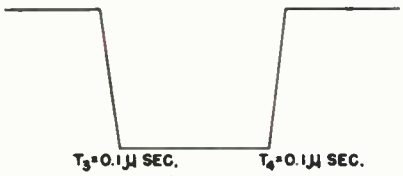

FIG. B

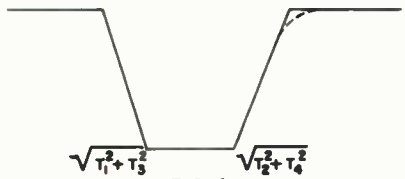

FIG. C

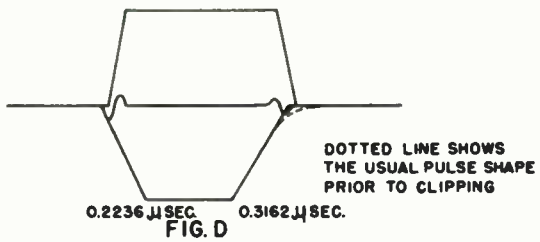

FIG. D

Fig. 11
Sync waveforms described in the appendix

A NEW ELECTRONIC MASKER FOR COLOR TELEVISION

Jesse H. Haines
Allen B. Du Mont Laboratories, Inc.
Circuit Research Laboratories
Passaic, New Jersey

Summary

A new color masker is described having improved performance, operational convenience, and efficiency. The color-difference mask signal is formed by a specially designed video mixing transformer, thus permitting major circuit simplification and greatly improved neutral balance stability. Use of the narrow-band mask principle substantially reduces luminance noise crosstalk into the encoded chroma signal. The philosophy of masking controls is discussed. Trilinear colorimetric plots illustrate the color shifts produced by incremental changes in the masking controls of various proposals.

Introduction

Early in 1954, electronic color masking was just emerging from the laboratory into practical broadcasting use. The first pioneering papers on the subject, from Burr of Hazeltine, and Brewer, Ladd, and Pinney of Kodak, had just appeared in the literature.[1,2]

Two years ago at this convention, we presented a paper concerning the use of electronic masking in color broadcasting.[3] Mentioned in the paper was a masker we had developed and which soon went into production under the name of the Du Mont Electronic Masker, Type 9005B. This is pictured in Figure 1.

Since the introduction of the 9005B masker, our efforts have been directed at developing an improved masker. In general, the aim was to achieve major circuit simplifications, improved reliability and stability, and certain performance improvements. One specific improvement was to incorporate narrow-band masking, which was first proposed in the previous paper. Another aim was to investigate the proper function of the various masking controls to be made available to the operator.

At last year's IRE Convention, Brewer, Ladd, and Pinney presented the paper[4], "Proposed Controls for Electronic Masking in Color Television." These proposed controls were fundamentally different from the controls used by Burr and also used in our masker. A masker employing these different controls was subsequently built and tested.

This paper is thus divided into two major parts. First, the results of the new masker circuit development are described. Secondly, a detailed comparison is made of the various control philosophies leading to the final choice.

Before proceeding, however, it may be in order to give a very brief definition of color masking. A mask operates on a color picture to change the relative luminance and saturation of some colors, or to shift the hue of some colors. This is often necessary, when televising color film, to compensate for improper taking emulsion sensitivities and improper dyes having overlapping and unwanted absorptions. The table below points out the more familiar shortcomings of a typical color film.[5]

Original	Reproduction
Gray scale	Higher contrast
All colors	Desaturated
Red	Only slightly desaturated
Green	Much darker, hue shifted slightly toward blue
Blue	Darker, hue shifted slightly toward green
Yellow	Hue shifted toward red
Magenta	Greatly desaturated, hue shifted toward red
Cyan	Much darker

Depending on the exact color process involved, certain variations in the above table will occur. Indeed, colorimetric differences between reversal and negative-positive processes, such as Anscochrome and Eastmancolor. occur specifically because it is feasible photographically to incorporate color masking in the negative-positive processes, but not in the reversal processes. Nevertheless, with all

color films, due chiefly to the dye deficiencies, it is characteristic that luminance and saturation of all saturated primaries are reduced. There are also minor shifts in the hue of some colors.

It should also be clearly understood that the statements above apply strictly to the objectively measured aspects of color film reproduction. On the other hand, it is not at all uncommon for the photographer to purposely predistort the colors and luminances in the original scene so as to produce the desired result on the film. In such a case, it is quite possible that no masking would be required. Thus, in the final analysis, the specific masking selected is a subjective matter and hence the importance of the proper controls becomes obvious.

As now used in color TV, maskers perform a linear transformation on R, G, B input voltages prior to encoding to produce the corrected R', G', B' outputs. In a mathematical sense, a color masker is simply a linear 3 x 3 matrix, represented by the equation:

$$R' = a_{11}R + a_{12}G + a_{13}B$$

$$G' = a_{21}R + a_{22}G + a_{23}B$$

$$B' = a_{31}R + a_{32}G + a_{33}B$$

However, practical broadcast operational techniques dictate that control of the coefficients be suitably linked together, rather than having a gain control for each of the nine coefficients. The first and most important operational requirement is that an input neutral scale of equal R, G, B signals remain perfectly neutral in the output. This is satisfied when the sum of the coefficients in each equation always equal unity. This condition reduces the number of independent variables from nine to six, as seen below.

$$R' = (1-a_{12}-a_{13})R + a_{12}G + a_{13}B$$

$$G' = a_{21}R + (1-a_{21}-a_{23})G + a_{23}B$$

$$B' = a_{31}R + a_{32}G + (1-a_{32}-a_{33})B$$

Because of the necessity for increased saturation, it is also characteristic of color TV maskers that all of the off-diagonal coefficients are negative. Typical coefficients found in mask equations are shown below.

$$R' \quad 1.10R - .05G - .05B$$

$$G' \quad -.30R + 1.60G - .30B$$

$$B' \quad -.20R - .20G + 1.40B$$

Note that the off-diagonal terms are small and negative while the diagonal terms are large and positive. With no masking, the off-diagonal terms would be zero, the diagonal terms unity. In the example shown, the Green channel could thus be said to have a .6 mask amplitude.

Basic Circuit Design

Figure 2 shows the block diagram of the Mask Amplitude-Mask Makeup control scheme used in the 9005B masker. As can be seen, the Mask Makeup selects the amount of the off-diagonal terms relative to each other. The Neutral Balance adjustment insures that when the input is neutral, complete signal cancellation occurs so that no mask signal is produced. The Mask Amplitude determines the total amount of masking. With these two operating controls in each channel, any desired mask equation can be produced. Thus two controls in each channel, six in all, provide complete control of the six independent coefficients in the masking equation.

In translating the block diagram above into actual circuitry, the adding and subtracting circuits cause the most difficulty. The problem is completely analogous to that found in many other kinds of color TV broadcast equipment. That is, there should be no color-difference output for equal R, G, B inputs.

In the very simplified single-channel schematic of the 9005B masker, Figure 3, it is apparent that three tube sections are required to form the mask. One tube simply inverts the signal polarity and the other two, with plates tied together, add the negative and positive signals to form the mask. This color-difference signal, which may be either positive or negative depending on picture content, is then added to the direct signal in the plates of the output tubes. Obviously, if the gain of any one tube drifts in the mask mixer, an unwanted color-difference signal will appear on white. Actually, the above circuit is not at all unstable. Nevertheless, tubes inevitably age and this drift must be checked occasionally. Fortunately, this is quickly and easily done. But it is much better to eliminate the probelm completely.

As also seen in Figure 3, the approach taken with the new masker to eliminate the Neutral Balance drift problem was to employ completely passive circuit elements to form the mask signal. This was accomplished by employing a specially designed video mixing transformer. As before, the resistive signal addition of the Mask Makeup selects the ratio of subtracting coefficients, although the signals are still actually positive at this point. By feeding voltages of the same polarity at either end of the center-tapped transformer primary, a difference signal is automatically formed, without the need for an inverter stage. Thus, the color-difference mask signal is produced with passive circuitry and the tube drift problem is completely avoided. The Neutral Balance control is set once and locked at time of manufacture of the unit. Over a test period of several months, no readjustment of the prototype unit was necessary, indicating that the resistances in the divider did not change. A possible disadvantage of the transformer type of mixing circuit is that to avoid crosstalk, resistive isolation must be provided, thus giving a certain loss in gain. In the circuit above, there was no problem in restoring the gain.

The specially designed video transformer is toroidal wound on an extremely high permeability core of Arnold Supermalloy. Fortunately, experience with a wide variety of pictures has shown that the mask signal contains no significant low-frequency components, the black level base line being absent, and thus a primary inductance of several henrys, giving a few percent tilt at 1000 cycles, is quite adequate. Due to the stray capacity and leakage inductance of the transformer, the high-frequency response falls off at about 2 mc and this, in combination with the peaking in the next stage, provides the desired low-pass response for the mask channel. The frequency response specifications of the narrow-band mask are $\pm \frac{1}{2}$ db to 1 mc, less than 3 db down at 1.3 mc, and greater than 20 db down at 3.6 mc. Rise time is .3 μs with less than 2% overshoot. Because of the delay caused by the narrow-band mask, a .25 μs delay line is employed in the direct channel.

The narrow-band mask is used to insure that the masking process does not add noise to the luminance signal which would be demodulated into the chroma channel of the receiver. It is inherent with masking that any noise existing in the input signals is increased. This is because even though the mask signal is cancelled out on a gray scale, the added noise coming from the cancelling signals will remain. If this noise occurs near 3.6 mc, it will be demodulated at the receivers to low frequencies and will form coarse bluish noise, since the B-Y gain is the highest. By rejecting the mask signal above 3 mc, where it is not needed anyway, this added noise is eliminated.

The direct and mask channel are added in the plates of two pentodes and a high-efficiency double-cathode follower provides the output. By incorporating video mixing transformers, not only does the new C masker exhibit improved performance over the B masker, but 6 less tubes are employed. Although not shown in the schematic, the C unit has dual output stages, compared to the single outputs of the B masker. While the new unit provides twice the number of outputs, it draws only one-half the power and occupies only one-half the space. Quite obviously in this particular application, the use of video transformers permits an impressive improvement in the overall circuit design. It is to be hoped that a fresh evaluation of this long-neglected circuit component for video design will be made by other workers in this field. There appear to be many possible applications for the impedance matching and mixing properties of video transformers.

In passing, the basic circuit required by the Hue Shift, discussed later, is considerably more complex than the Mask Makeup control since it involves cross linkages between all three channels. Fortunately, by using video mixing transformers, no tubes were required and such a circuit was rather easily constructed. Without the transformers, perhaps 12 tube sections would have been required. Actually, it was substituted directly into the C masker, the chief cost being 3 more transformers, 3 dual pots and a few resistors.

Manual Controls

In actual TV operation over the past few years, good results have been obtained with the Mask Amplitude-Mask Makeup controls provided in the 9005B masker. However, before completing the 9005C design, it was decided to conduct a rigorous investigation of the philosophy of manual controls for maskers, particularly in reference to the proposals for Saturation-Hue Shift controls.

In evaluating the various control schemes, two considerations were uppermost:

1. The masker control knobs should directly correct for the known deficiencies of color film reproduction.

2. The masker control knobs should be related as directly as possible to resultant visual effects.

The investigation of masker control philosophy was divided into two parts. First, a theoretical analysis, involving colorimetric calculations, was made up of the various candidates for masker controls. Secondly, on the basis of the theoretical analysis, two different maskers were built and tested, incorporating the most promising control schemes. Side-by-side operational comparisons were made with a wide variety of color slides over a complete color TV system. For the theoretical analysis, a number of relatively desaturated colors were selected for masking. Then, an arbitrary mask equation was applied. From this reference point, differential changes were made with the four proposed controls. In the calculations, a square-law reproducer was assumed. White luminance, which does not change with masking, was set at 100, the luminance of other colors was specified relative to white.

The unmasked starting colors, and the changes when the reference mask is applied, are shown in Figure 4. Although the CIE plot is perhaps more familiar, a simple trilinear plot eliminates considerable computational labor and will be used in all subsequent plots. Figure 5 shows exactly the same data on a trilinear plot.

Since the colors to be masked were chosen quite arbitrarily, the computing time was further reduced by choosing the rather regular set of starting voltages shown, actually desaturated color bars. The reference mask was likewise chosen for the same reasons of symmetry.

With the reference mask initially set, differential changes were then made in the mask equations by turning the various knobs that are candidates for the attention of the operator. Following the terminology of the previous proposals, the following controls were considered: Mask Amplitude, Mask Makeup, Hue Shift, and Saturation. In all cases, the coefficient differentials are of the same size.

Figures 6, 7, 8 show the changes produced by each of the four proposals by the knobs labelled, respectively, Red, Green and Blue.

The changes produced in the Green controls will be considered in detail. The actual equation coefficient changes for the Green controls are summarized below.

Green Control Knob Changes

Mask Amplitude	$-\Delta a_{21}$ and Δa_{23}	are equal
Saturation	$-\Delta a_{12}$ and Δa_{32}	are equal
Mask Makeup	$-\Delta a_{21}$ and Δa_{23}	are equal and opposite
Hue Shift	$-\Delta a_{12}$ and Δa_{32}	are equal and opposite

The really basic differences between the Mask Amplitude and the Mask Makeup controls on the one hand, and the Hue Shift and Saturation controls on the other, are very simple. In the Mask Amplitude and Mask Makeup, the changes affect only the one channel labelled by the knob, but with the Hue Shift and Saturation, the other two channels are the ones affected. Thus, in the former cases, only the Green signal is affected. In the latter cases, the Red and Blue signals are affected, but not the Green.

Referring to Figure 7, the Green Mask Amplitude control is considered first. Increased masking, indicated by the solid arrows, is applied. Note here the increase in Green saturation, but especially the major increase in Green luminance due to the increase in the Green signal. Yellow and Cyan, the other colors containing considerable Green, have a smaller increase in the green signal, thus give a smaller hue shift towards Green. The other colors show practically no change because of the very small changes in luminance. In simple terms, it suffices to say that increasing the Green Mask Amplitude will increase Green color differences.

The Green Saturation control is next considered. The amount of saturation increase is slightly more than with the Mask Amplitude. However, the luminance remains relatively constant, in fact, decreases slightly. Magenta saturation is not affected. The other colors apparently suffer small changes.

The Green Mask Makeup control is seen next. Interestingly enough, Green Mask Makeup has no effect on colors lying along the Green-Magenta axis. In general, hues are shifted but in small, nearly equal amounts in all the colors except Green and Magenta.

Next is seen the Green Hue Shift control. Here, as desired, the hue shift rotates the Green-Magenta axis. The off-axis colors are affected very little. It is immediately obvious that considerably more shift is given to Magenta than to Green. Virtually no changes occur in Yellow and Cyan, but luminance changes occur in Red and Blue. As proposed, the Hue Shift appears theoretically to perform its purpose.

As described previously, the next step in evaluation was to compare the operation of masking units incorporating different control philosophies. At this point, it was decided to limit the possible control schemes to only two. Further consideration of the "Saturation" control was discontinued. The reasons for eliminating the Saturation control from consideration is simply that in all color films, the nature of the dyes are such that a decrease in saturation of either Red, Green or Blue is always accompanied by a decrease in luminance relative to white. It should be kept in mind that the dye errors are substantially greater than errors contributed by the color reproduction capabilities of the TV system. Thus, it is most logical to provide a single control in each channel which simultaneously increases both saturation and luminance. Hence, the Mask Amplitude control is to be clearly preferred over the Saturation control. The remaining question is thus whether the remaining controls should be Hue Shift or Mask Makeup.

A new masker was then built of the "Mask Amplitude-Hue Shift" variety and compared critically with the "Mask Amplitude-Mask Makeup."

The evaluation of the two control schemes employed 2" x 2" slides displayed on high-quality color monitors and receivers. The signal originated from a flying-spot scanner and obeyed a half-power transfer characteristic. Twenty slides were utilized, 5 original Kodachromes, 5 Kodachrome duplicates selected from the old NTSC set, 5 Eastmancolor and 5 Anscochrome from the new SMPTE set.

Before comparing the maskers, a determination was made of the required Mask Amplitude settings. In evaluating the results obtained, the amount of gamma correction employed is important. The half-power gamma correction used corrected only for the TV system but not for the high gamma reproduction of the color film. If additional gamma correction had been used, even more mask amplitude would have been required. For this test, Hue Shift and Mask Makeup were put in the center of the range and thus both maskers yielded exactly the same equations initially.

Although the amount of masking varied somewhat, depending on the type of color film, several observations stood out clearly.

First - all slides required considerable Green Mask Amplitude. Amounts ranged from .5 to 1.0.

Second - all slides required very little Red Mask Amplitude. A figure of .1 gave good results with all slides.

Third - all slides gave acceptable pictures, improved by masking, in regard to hue.

Fourth - all slides gave excellent hue reproduction with the Hue Shift or Mask Makeup in the normal position in the middle of the range.

It thus became apparent that the need for a Hue Shift control was not urgent compared to the need for the Mask Amplitude control. The Mask Amplitude controls alone were extremely effective and positive in action. In looking at the pictures, "Brilliance" suggested itself as a more descriptive name for the Mask Amplitude control.

Actually, even without changing Hue Shift or Mask Makeup, one specific hue shift did occur due to the fact that the Mask Amplitudes were not equal. Since the Green mask amplitude was always considerably greater than the Red, a very definite shift toward Green occurred in Yellows. However, this appeared to compensate very well for the opposite hue shift deficiency found in all color films. Figure 9 shows the color changes caused by the typical mask equation, previously given, which gave good results in the preceding tests.

The Hue Shift control was next tested. To simulate the calculations, desaturated color bars were used. As predicted by the trilinear plots, the complementary color shifts were quite marked. However, with relatively saturated primaries, no hue shift was visually detectable, although the proper shift voltages were seen on the waveform monitors. This result was apparently caused by the display devices having greater than a square-law transfer characteristic. Unfortunately, a very serious defect of the Hue Shift control was noted in that the luminance changes of color colors off the hue shift axis were visually quite annoying. Apparently, the luminance changes were greater than predicted by the calculations.

On the slide material, the same conclusions were reached. Since saturations were somewhat less, hue shift in primary colors was seen. It was most apparent in Reds, considerably less in Blues and practically indistinguishable in Greens. In all slides, the unwanted luminance changes in other colors were noted. Another annoying feature was that with the Red and Blue Hue Shift knobs at certain ends of their range, it was impossible to obtain Green mask amplitude. This could happen with other combinations, for example, but not simultaneously. In general, however, out-of-channel Hue Shift settings determine the amount of Mask Amplitude obtainable. In short, the operation of the Hue Shift controls left a great deal to be desired.

Attention next turned to the Mask Makeup control. Here the pictorial changes were actually more predictable than with the Hue Shift. Furthermore, the bad side effects were not present. As compared to the Hue Shift control, no matter where the Mask Makeup is set, full Mask Amplitude is always obtainable.

Changes in Mask Makeup in any channel will shift the hue in saturated colors containing that primary color. Thus, the Green Mask Makeup will effect the hue of saturated Yellows and Cyans, although only saturated Yellows will actually be found in nature. While theoretically the Red Makeup will also affect the hue of saturated Yellows, it will have little effect because of the normally low mask amplitude of Red. Magentas, found much less frequently in nature, will have their hues affected chiefly by the Blue rather than Red Mask Makeup. Thus, as a practical matter, Green Mask Makeup will control Yellow hue and Blue Mask Makeup will control Magenta hue.

Before making a final evaluation of the two proposed control schemes, it is in order to take a quick look at some of the other problems confronting the color film video operator. Aside from other auxiliary controls required in certain types of television reproducing equipment afflicted with spurious shading signals, the operator will have up to eight video controls. These might be master gain and black level control plus individual R, G, B gain and black level controls. Very often, it is possible to preset the R, G, B black levels and operate satisfactorily with only the master black level control. However, it is still true that the video modulation in most color films varies enough so that the operator is often quite busy adjusting the master gain control so as to maintain a reasonably constant level of modulation at the TV transmitter. He probably will also be adjusting individual R, G or B gain controls in order to compensate for shifts in white balance in the film. These variations are not only quite frequent in the film but they become much more bothersome in the home than in the theatre because of the closer tolerances, both electrical and visual, under which the system operates. It should be clearly understood that the above adjustments must be proper at all times for the mask to be most effective. The masker controls simply cannot be used to correct for errors in the gain and black levels of the R, G, B channels.

It is clear then why there is a certain resistance to using any masking at all, purely from the standpoint of video operator fatigue. Certainly we wish to keep the mask controls as simple as possible, preferably using 3, not 6. Fortunately, Mask Amplitude meets these requirements admirably for two reasons. First, it directly compensates for the chief colorimetric failing in the film - simultaneous loss of saturation and luminance of saturated colors, relative to neutrals. Secondly, the results produced are straightforward - an increase in any Mask Amplitude knob will always increase the brilliance of that color.

Experience has shown that the need for the shifting of hues is relatively unimportant. Neither Hue Shift nor Mask Makeup need be an operational control. On the basis of simplicity, Mask Makeup is favored. Thus, the new 9005C masker employs Mask Amplitude-Mask Makeup controls.

References

1. W. L. Brewer, J. H. Ladd, J. E. Pinney, "Brightness Modification Proposals for Televising Color Film", PROC IRE, Vol. 42, PP 174-191, January, 1954.

2. R. P. Burr, "The Use of Electronic Masking in Color Television," PROC IRE, Vol. 42, PP 192-200, January, 1954.

3. J. H. Haines, "Color Characteristics of a Television Film Scanner," IRE 1954 National Convention Record, Part 7, Broadcasting and Telecasting, PP 100-104, 1954.

4. W. L. Brewer, J. H. Ladd, J. E. Pinney, "Proposed Controls for Electronic Masking in Color Television," IRE 1955 National Convention Record, Part 7, Transmitters, Receivers, and Audio, PP 63-68, 1955.

5. R. M. Evans, W. T. Hanson, W. L. Brewer, "Principles of Color Photography," John Wiley and Sons, Inc., New York, 1953.

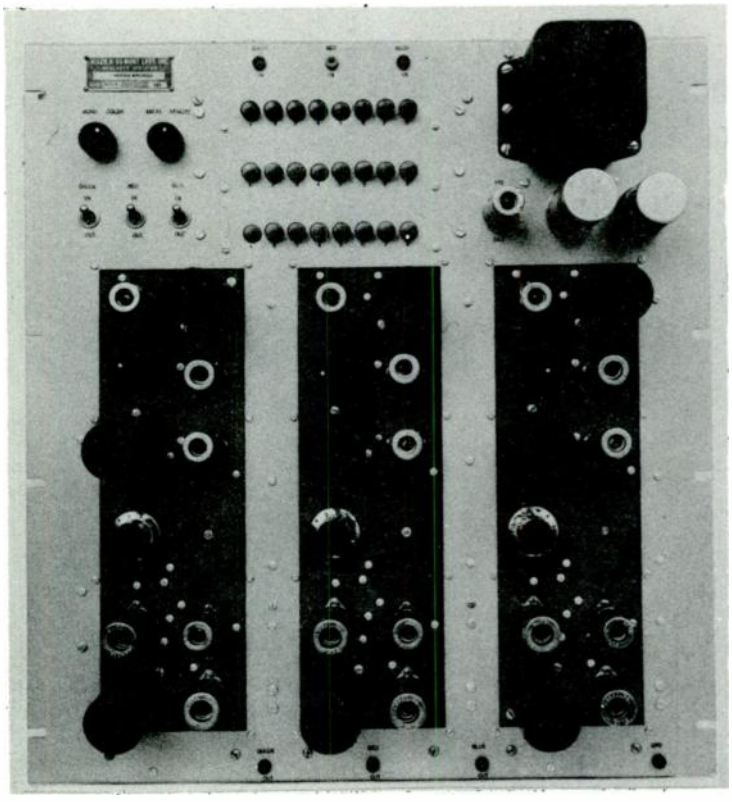

Fig. 1
Type 9005B electronic color masker

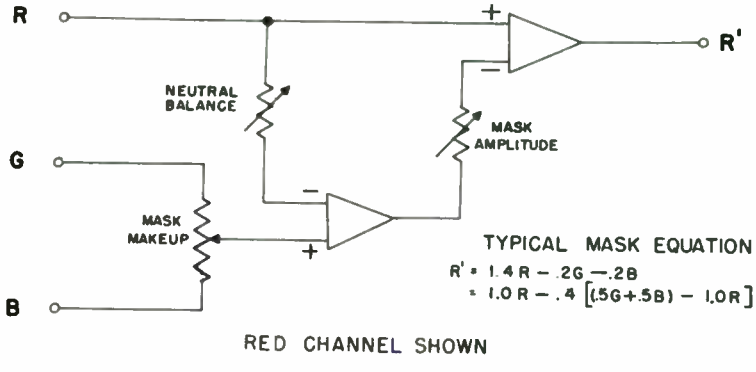

Fig. 2
Mask amplitude-mask makeup block diagram

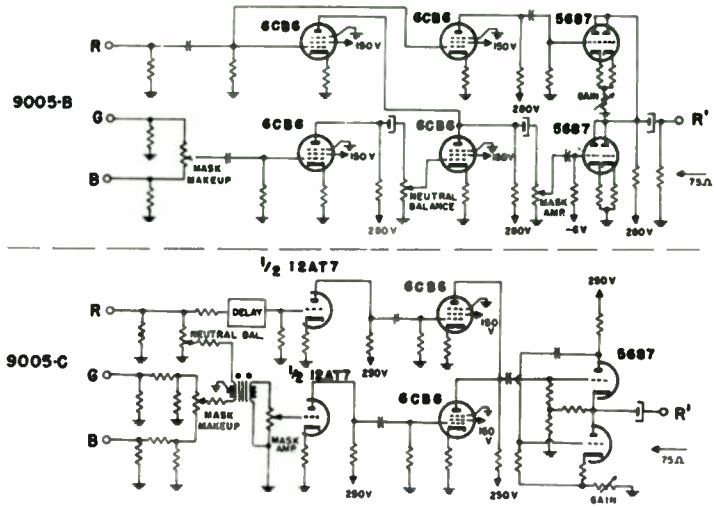

Fig. 3
Simplified schematics, 9005B and 9005C maskers (red channel)

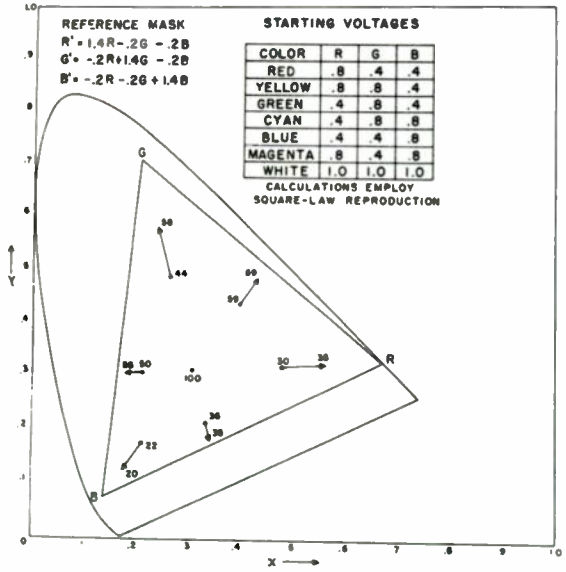

Fig. 4
Starting colors and reference mask (CIE diagram)

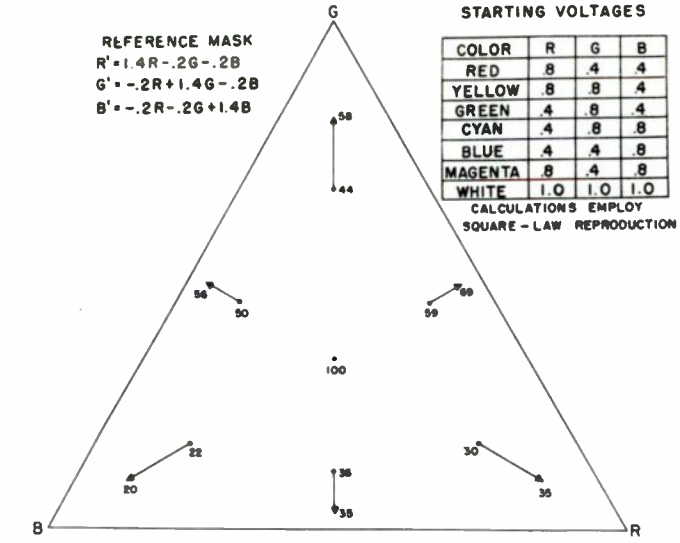

Fig. 5
Starting colors and reference mask (trilinear plot)

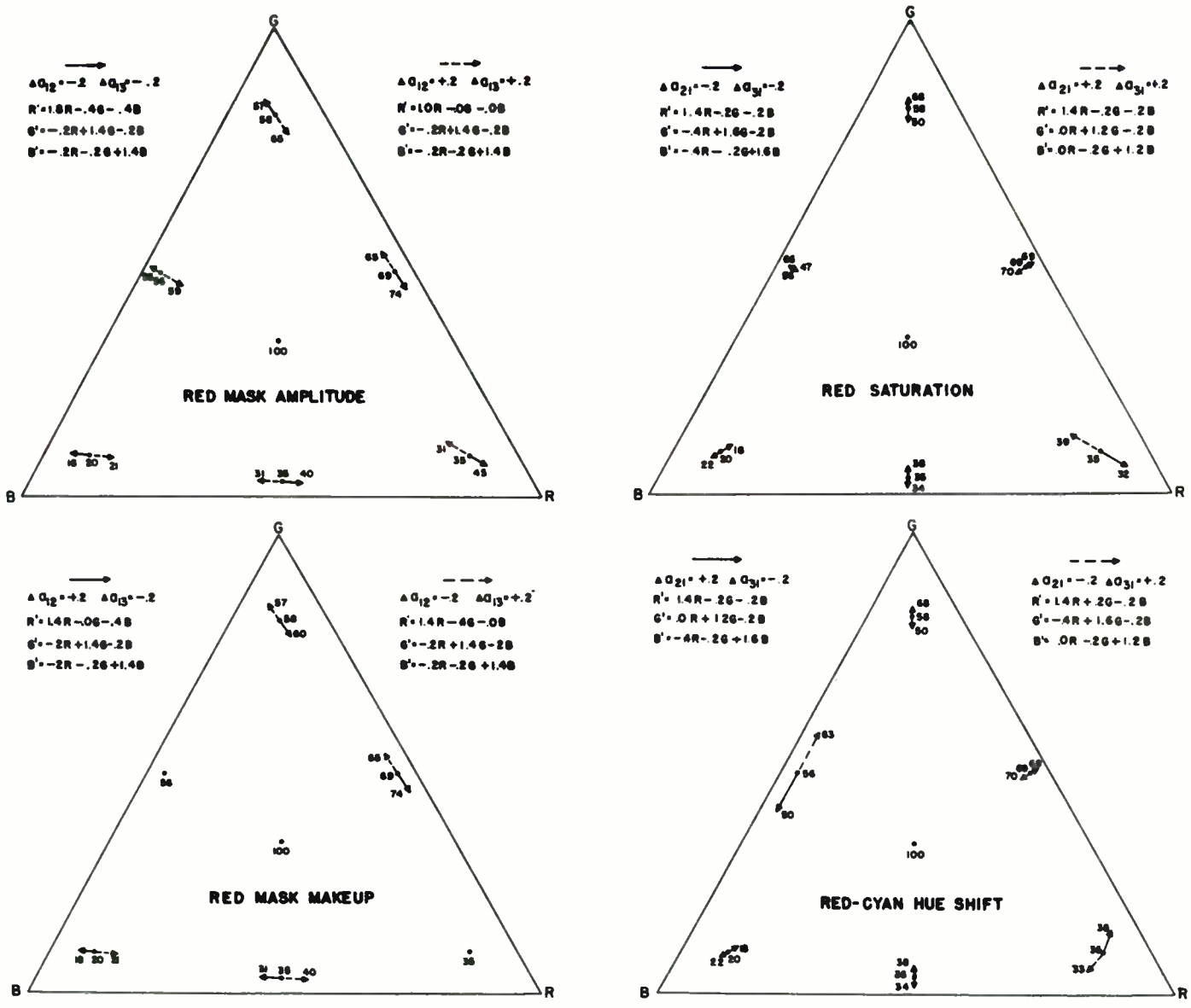

Fig. 6
Red knob control differential changes

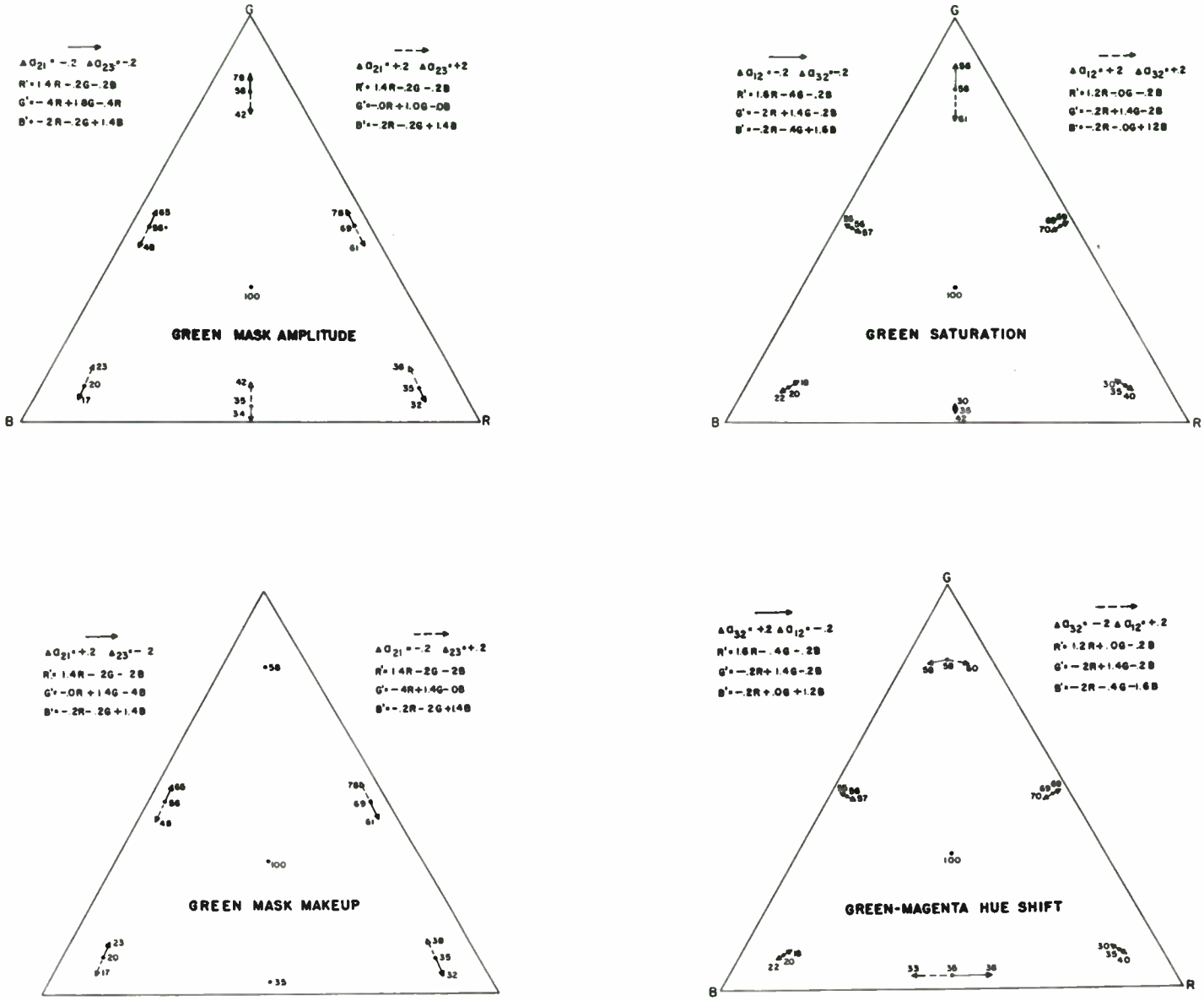

Fig. 7
Green knob control differential changes

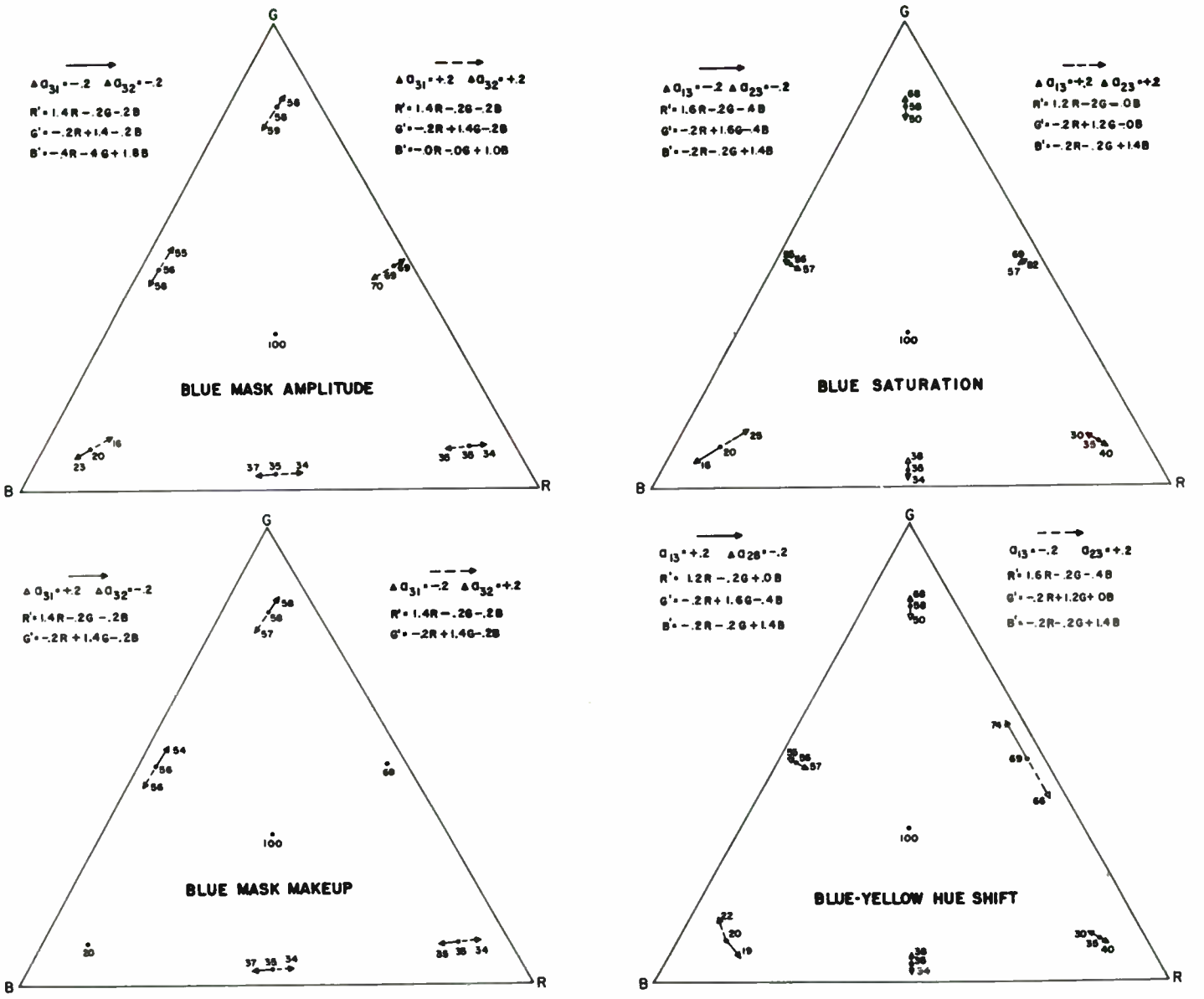

Fig. 8
Blue knob control differential changes

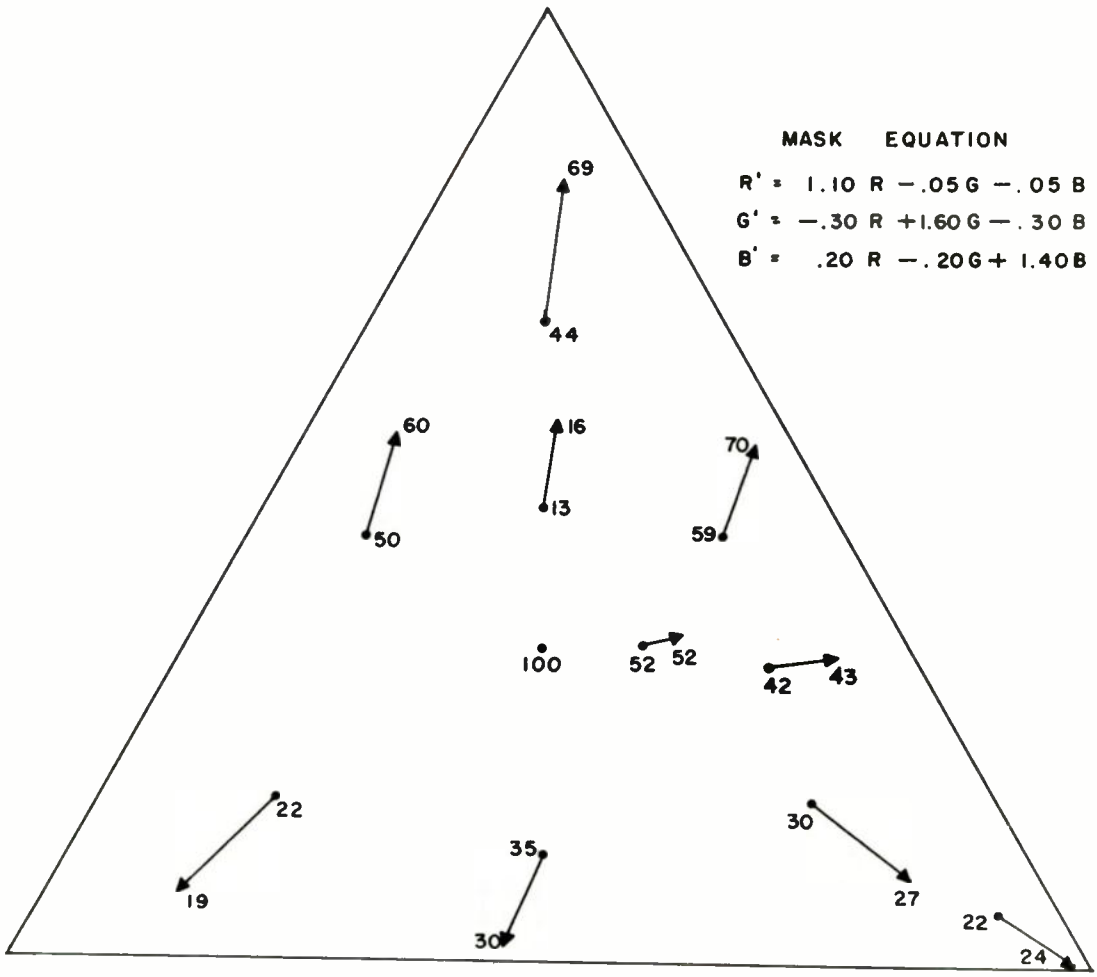

Fig. 9
Color changes with typical mask

REWORKING THE NETWORK OR REMOTE VIDEO SIGNAL

Ray R. Embree
Engineering Department, KING-TV
320 Aurora Avenue, Seattle, Washington

Summary

The network or remote picture signal can be improved locally to a varying extent, depending on the nature of its discrepancies. These improvements will be in the regions of synchronization and gamma. The defective signal is also shown to further deteriorate in passing through amplifiers employing keyed clamps. Pictures included show clearly the results for some deficiencies. Reasons for the inadequacy of presently available gear are discussed. The methods of circumventing many of the overlooked problems are incorporated in the circuitry and external hookup of the sync generator locking device called "Betterlok." This device, that will work under more adverse video signal conditions, is fully described.

The Problem of Airing a Defective Video Signal

Various attempts have been made to improve the video signal at points too far along the path of transmission to permit corrections of the original fault. It would be preferable to correct the trouble at the point of origin, but since this so often is not known, it is expedient to do what can be done locally.

Attempts to locate the origin of such troubles are not only time consuming, but often futile. In the interim, one is faced with having to broadcast the signal the best way one can. While it is impossible to restore lost resolution, or to entirely remove noise or snow from the picture, it is possible to restore good synchronizing information and to improve gamma on many signals. The most difficult problem with which we must deal in broadcasting a defective video signal is one on which the sync is erratic, or far enough removed from standards in one or more respects that the keyed clamps (driven) fail to function properly. Such a signal will often show up better if displayed on a picture monitor before going through a stabilizing amplifier.

The above observation led the author to develop a circuit called "Betterlok." The explanation of the necessity to design a new piece of gear and the method of its incorporation with associated equipment will be attempted in the following paragraphs.

The main variances from the standards that we encounter and correct by the use of the described circuits are listed below:

1. Insufficient back porch width
2. Too narrow sync pulse width (horizontal)
3. Extreme tilt of porches
4. Too narrow equalizing pulse width on one or both fields
5. Video spikes in the sync pulse region
6. Erratic replacement of some of the first in the group of leading equalizing pulses with the equivalent of vertical block pulses
7. Amplitude offset in front and back porches

Obviously, if a stabilizing amplifier, due to its poor clamping action, renders a less presentable picture than a plain video amplifier, the signal should not be run through it unless it is absolutely necessary. However, in some cases it will be necessary, or highly desirable, to have separate control of video and sync which a stabilizing amplifier provides. In cases where a separate amplitude linearity corrective amplifier is used in a compatible color system keyed clamps are also employed. Here too poor clamping action leads to the desire to get around this piece of gear as well. The one unit which usually employs keyed clamps and around which the video signal may not be shunted is the video modulator. Without going further, even the least experienced can see the desirability of having good sync on the video signal. A snowy or low resolution picture can be broadcast, but a picture that is streaking, tearing, jumping and rolling might better remain unaired.

If the defective sync could be replaced with clean, locally generated sync before having to pass through any amplifiers having keyed clamps, the signal could then pass through all normal channels in good order. Of course, in order to replace the defective sync with good sync, it is necessary to lock a local sync generator to the remote signal.

Why Available Equipment Has Fallen Short

Sync generator locking devices comercially available require that standard, reasonably clean sync, stripped from the network or remote

composite video, be fed to them. The usual method is to obtain this network sync from a stabilizing amplifier that employs keyed clamps. This number one step in locking a local sync generator to the network signal has already run into a snag if the network signal will not properly operate the keyed clamps in the stabilizing amplifier performing the stripping action.

Therefore, stripped sync is not obtained from a stabilizing amplifier to feed the "Betterlok." No criticism is intended to the engineers or manufacturers who recommend such hook-ups. They expected a normal signal from the network (or remote), and desired only to allow the local studio to treat the network signal as a local picture signal. Provided with such a normal signal this hook-up permitted superimposition and cross fades, etc., with other studio originated signals, with certain limitations. We are primarily concerned with reworking the network signal so that it will make a better picture.

The manner in which the aforementioned signal discrepancies cause further picture degradation in passing through amplifiers employing keyed clamp circuits must be explained on an individual fault basis. In the case where the back porch is too short in duration, the back porch clamping pulse that is applied to the clamping diodes occurs on or later than the trailing edge of blanking. When this happens, the clamping action is erratic, and changes as the picture content changes. This shows up as streaking, tearing, or black bars at various points along the raster, and changing in character as the picture content changes. Too narrow horizontal sync pulses can cause trouble in various manners, depending on the extent of its narrowness and the exact type of keyed clamp being used. An extreme case of sync narrowness will develop insufficient amplitude and jagged shapes in the clamp keying pulses. If peak of sync clamping is used, and the clamp keying pulse is formed from the leading edge of sync, the clamping pulse may occur wholly or partly on the trailing edge of sync. Anytime a clamp keying pulse is applied during an interval of fast signal voltage change, such as on the edge of a pulse or a video voltage excursion, erratic clamping takes place. The clamping action is intended to, among other things, remove low frequency discrepancies from the video signal. High frequency discrepancies are not only not removed, but if their amplitude is very high and they occur during the clamping pulse, the signal is imparied by passing through the clamping amplifier.

The first attempts at adding on locally generated sync to the stripped network signal were done with commercially available sync generator locking devices. The problem already described plus others were evident. The other most disconcerting problem was the loss of vertical in phase condition at random times. Then, too, was the time involved in regaining the vertical in phase condition each time it was lost. The reason the vertical in phase condition was so often lost is quite easily shown to be due to random long period noise bursts on the network signal. These noise bursts would get through the integrator in the locking device, and thus to the sync generator counters.

Betterlok Circuitry and Features

Reference to the block diagram and schematic should be made as often as necessary to aid in understanding the following explanations.

The network (or remote) video signal is looped by the video input, and thence to the GE TV16B stabilizing amplifier. The interstage coupling between V1 and V3 has a fast time constant with a section of V2-a 6AL5 diode connected as d. c. restorer to remove any hum or low frequency discrepancies at the grid of the sync separator V3. An a. f. c. voltage for the sync generator master oscillator is developed by the bridge circuit of V6 by comparing the output of the horizontal blocking oscillator synchronized by the network signal to a pulse developed at V8 locked to the local sync generator horizontal drive. To control the GE PG2 sync generator, a positive voltage is applied in series with this bridge. The stripped network and local vertical sync are treated almost identically to develop 30 V positive pulses representing the trailing edges of the last vertical block pulse at V10B and V20A. The trailing edge of vertical sync was chosen to avoid the aforementioned occasional problem with leading group of equalizing pulses changing erratically to vertical block pulses.

In order to speed up the vertical lock-in time, the pulse width of the vertical phase correction pulse fed to the sync generator is increased to a maximum value of about 6000 microseconds. This is accomplished by phanastron pulse generators for the network and local vertical sync separately. The phanastrons put out a pulse for each trigger pulse they receive from their respective vertical sync sources. The duration of a phanastron pulse is linear with the controlling d. c. voltage. Since this controlling voltage is common to both network and local phanastrons, their pulse durations have a fixed relation one to another. A vertical lock-in time of about one-quarter second is easily obtained from a maximum out-of-phase condition. This figure is about one eighth of the time necessary for other locking devices, and is

barely discernible to the average eye. The squared-up phanastron pulses are oppositely polarized in the mixer V28. When the local sync generator is in vertical phase with the network, no correction pulse is present at V27 output. Since the positive vertical phase correction pulse is coincident with, and resting in the notch of the wider and higher amplitude negative notch pulse, no pulse at all gets by the dual clippers of 1N48's and V27. When the above condition exists, the input to the vertical error output V26B is automatically disconnected by the open relay contacts of K2. If a vertical phase error does exist or occurs for any reason, it is basic that it will persist until K2 relay contacts close and pass the correction pulse to the local sync generator. On this premise the "door knocking" circuit of V17B, V29 and K2 was incorporated. This repetitious error pulse being rectified by V17B biases V29 and gains entrance to the sync generator. In a matter of a few correction pulses, the vertical in-phase condition will again exist, and K2 disconnects. This "door knocking" action to gain connection to the sync generator prevents long duration noise or other extraneous pulses from disrupting the vertical in-phase condition once gained.

An automatic drop-back for the local sync generator to power line control of the master oscillator and vertical phasing is provided by V24, V15B, V30, K1 and K4. This gives a positive control of the local sync generator at all times, and automatically provides for normal studio operation, even though the network signal drops out. The GE TV16B stabilizing amplifier was chosen to operate with this unit because it permitted, without modification, the passage of a composite video signal, or the addition of local sync and blanking within the one unit by merely operating the existing relay. This realy is automatically controlled by the network signal if switch S4 is in the automatic position.

Remote control is also provided for operational adjustments to the "Betterlok." These include a switch for selecting either local power-line or automatic network (or remote) control of the local sync generator.

Should the circuit be duplicated, there is the matter of reversal of the action of GE TV16B relay. This was done to make this unit interchangeable in this respect with RCA TA5C and D, that were being used elsewhere in the station. The addition of local blanking besides sync in the GE TV16B provides a means of regaining lost setup, as well as straightening out a signal with porches at different amplitude levels. Grass or noise at black level will also be removed completely by the addition of blanking and properly setting the black clip-balance control. (Note that in a locked condition, local sync is used to key the clamps in the stabilizing amplifier!)

Hook-Up Requirements

Power

1. 115V a.c., 60 cycles -- 2 amps.
2. 300V d.c., regulated -- 325 mils.

Signal Inputs

1. Network or remote composite video -- 1.4V, P.P. sync negative
2. Local horizontal drive - Negative 3.5V P.P.
3. Local R.T.M.A. sync -- Negative 3.5V P.P.
4. D.C. locking voltage from the local sync generator power line lock discriminator.

Signal Outputs

1. AFC voltage for sync generator master oscillator external control.
2. Vertical phase correction pulses.

Remote Control and Connections

1. Switch permits the selection of local 60 cycle power line, or automatic locking of sync generator master oscillator to network signal.
2. Horizontal fine phase control.
3. Black clip balance control.
4. Connection from stabilizing amplifier relay to "Betterlok" relay, to provide automatic operation of stabilizing amplifier relay.

Initial Adjustments

1. Connect all voltages, signal inputs and outputs in accordance with the diagrams and tabulated information.

2. Set R2 in mid range.

3. Set S4 to "local 60 cycles."

4. Remove V1 and V5.

5. Adjust R4 to operate the horizontal blocking oscillator at its highest frequency as viewed at J2.

6. Set S1 to $\pm$ 0 Ref.

7. Connect a zero center V.T.V.M. from J4 to chassis, using a 3 volt scale. The Voltohmist is very satisfactory.

8. Adjust R5 to obtain zero reading on the V. T. V. M. This balances the bridge of V6.

9. (If a positive reference voltage is required, carry out this step, if not, pass on to #10.) Set S1 to Pos. Ref. Adjust R7 to obtain the required positive reference for the sync generator, as indicated by a V. T. V. M. at J5 to chassis.

10. Replace V1 and V5 and set S4 to "auto lock."

11. Adjust R11 to a point slightly beyond the complete removal of all video from the sync as viewed with a scope at J1. R3 is then adjusted to clean up the sync peaks.

12. Lock the blocking oscillator of V4B to the remote sync by adjusting R4. This may be done by feeding a signal from J2 to the positive external sync input on an oscilloscope, while displaying a few horizontal pulses of the network stripped sync from J1. R4 is adjusted to the center of its locking range which causes the scope pattern to remain stationery. A double check is to be made on the setting of R4 by resetting the scope to positive internal sync, but not changing the sweep timing. Then display the pulse at J2. The time interval or spacing between pulses should be the same as that between horizontal sync pulse in the initial adjustment.

13. The master oscillator in the sync generator should be locked now to the network signal. This may be checked by viewing the mixture of the network and local sync at J3. The signal at J3 will be much distorted, but all components should be locked together.

14. Remove V18 and observe the signal at J7 with the oscilloscope set to view vertical information. Adjust R8 to a point where the observed negative pulse is reduced to a minimum. Replace V18.

15. With the scope still set to display vertical information, observe the pulses at J6. If the positive lower amplitude pulse is not resting in the notch of the wider negative pulse, R9 should be adjusted slowly to increase the width of the negative notch pulse until the positive pulse comes to rest in negative notch pulse. When this condition exists the local sync generator is in vertical phase with the network signal. If it is desired to view the vertical correction pulse at J8, it will be necessary to disconnect the vertical output cable and interrupt the network signal.

16. Now the horizontal phase may need some fine adjustment. This may best be done at the remote control, which for convenience, is located close to the network stabilizing amplifier remote controls. Therefore, switch S4 is set to remote position and the remote control switch to auto-lock position. Adjust the horizontal phase control to line up the leading edges of local blanking with that of the network signal.

17. Adjust the stabilizing amplifier remote black clip for desired setup. The remote black-clip balance should then be adjusted to give the best black level appearance when the remote switch is in the "local 60 cycle" position. The one meg. black-clip balance control is paralleled with the regular remote black clip control.

18. If the blanking is too short or long in duration, correction may be made at the sync generator to match the network signal.

19. Switching the remote control to "local 60 cycle" position will allow composite operation of the network stabilizing amplifier and "power line" control of the local sync generator. This enables the operator to see just how much improvement is being made in the signal by this reworking and permits an easy method of getting in and out of locked operation.

Using the Unit in Normal Station Operation

It is the primary function of this locking device to permit the reworking of a defective video signal. However, it will permit cross fades and superimposition of network, or remote, and any locally originated picture signal, except from film or video tape. The latter two video sources may also be included, providing the film driving motors are powered by an A. C. that is locked to the remotely controlled sync generator and pulsed light is used with film. It is understood that the vidicon is not subject to this exclusion when used in a film chain, as it has a very long image retentivity.

There is an advantage in being able to devote one staibilizing amplifier and one sync generator to normally operate with the "Betterlok." The advantages are that the operation of the unit can be checked at any time without any regard to interference with locally scanned film, etc. Then, too, maintenance and adjustments may be made to any of the units just before airing the reworked signal. After any pre-adjustments have been made, the sync generator changeover switch may be operated, placing the network controlled sync generator in general studio use, if such a hook-up is desirable. The operator must keep in mind the above mentioned limitations in connection with film chains. In case it is impossible to

devote a separate sync generator to this use, it is possible to switch the remote control of the "Betterlok" to auto lock coincidentally with airing the network or remote. The lock-in time is so fast that the layman will not notice it, but it will be necessary to have the equipment previously adjusted. Usually the equipment will stay in adjustment over long periods of time, so that only minor adjustments need be made, and very successful operation with one sync generator may be had most of the time.

Since we have been primarily concerned with reworking the network signal, the equipment is located at our studios. This permits us to rework the signal immediately upon receiving it, and then sending it through all normal channels of switching and control. Others might find this piece of gear valuable at a transmitter site to rework all signals that are to be transmitted.

Any station that receives a video signal over which it does not have full control as to its perfection, will undoubtedly find at times a very good use for this type of reworking equipment. A system that will provide a solid lock of studio sync generator to a remote is also a very useful adjunct to a television station's programming facilities.

Credit must go to the station's management whose policies allow such developments, and to our Director of Engineering, James L. Middlebrooks, and to our Chief Engineer, Robert A. Ferguson. Also we recognize the aid of many others of the KING-TV engineering staff, especially Lee Mudgett, Mique Talcott and Kenneth Hermanson.

Credit must also go to the Edison Technical School in Seattle and particularly to Nick Foster, head of the Radio and Television Department, and to Mardo De Jaen.

Tabulation of Pictures & Diagrams

Defective Signals to be Reworked - Figures No.

1. Signal with 60 cycle hum and spiking (horizontal display)
2. Signal with 60 cycle hum (vertical display)
3. Signal with too short a back porch.

Poor Clamping - Figures No.

4. Output of stabilizing amplifier with signal of Figure No. 3 at input. (C.R.O. vertical display)
5. Picture monitor displaying the signal of Figure No. 4 showing resultant tearing and pulling.

Sync Separation Capabilities - Figure No.

6. Vertical sync at J1 of the schematic with the signal of Figure No. 1 at the input.

Reworked Video Signal - Figure No.

7. Horizontal display

Better-lok Front View - Figure No.

8.

Diagrams - Figures No.

9. Better-lok hookup for video signal reworking.
10. Block diagram of Better-lok.
11. Schematic diagram of Better-lok.

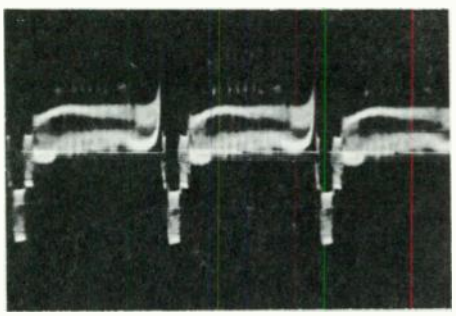

Fig. 1
Signal with 60 cy. hum and spiking
(horizontal display)

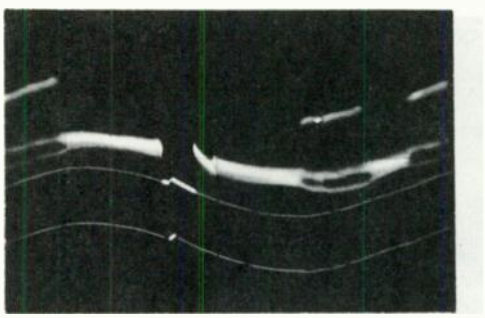

Fig. 2
Signal with 60 cy. hum
(vertical display)

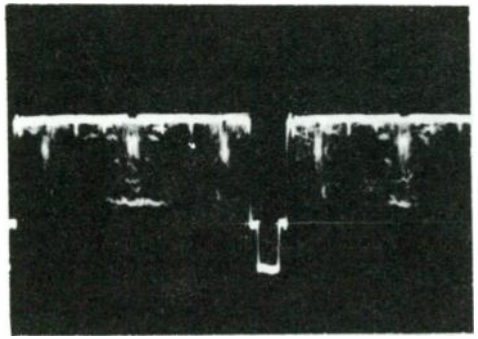

Fig. 3
Signal with too short a back porch

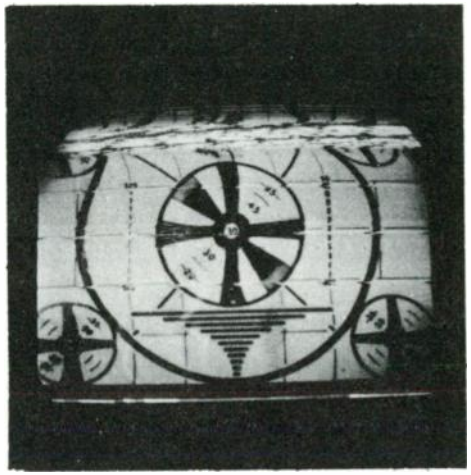

Fig. 5
Picture monitor displaying the signal of Figure 4 showing resultant tearing and pulling.

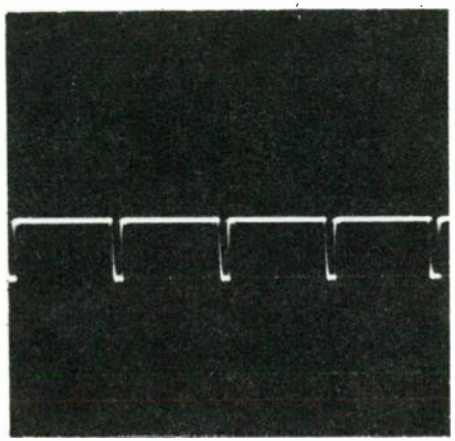

Fig. 7
Horizontal display

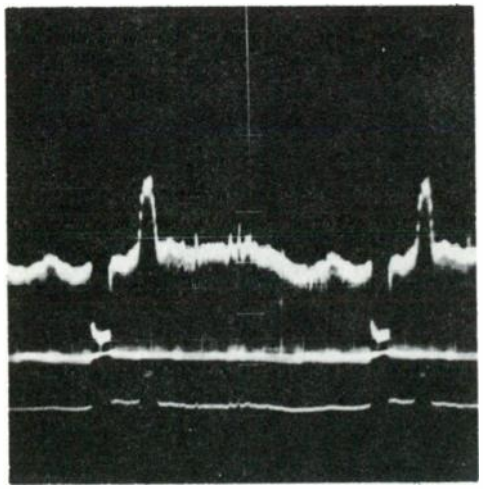

Fig. 4
Output of stabilizing amplifier with signal of Figure 3 at input (C. R. O. vertical display).

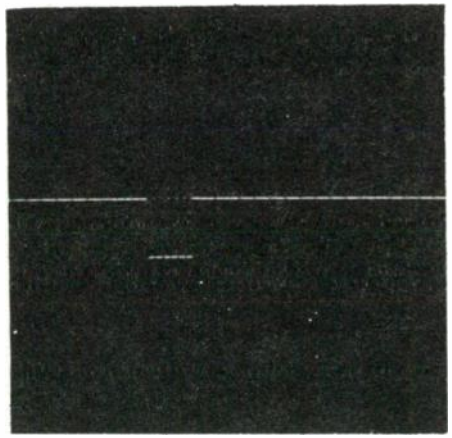

Fig. 6
Vertical sync at J1 of the schematic with the signal of Figure 1 at the input.

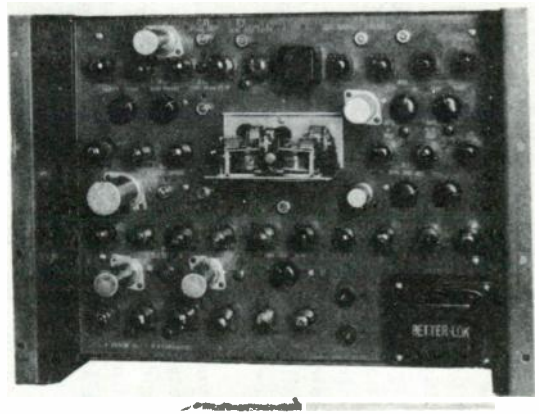

Fig. 8
Betterlok front view

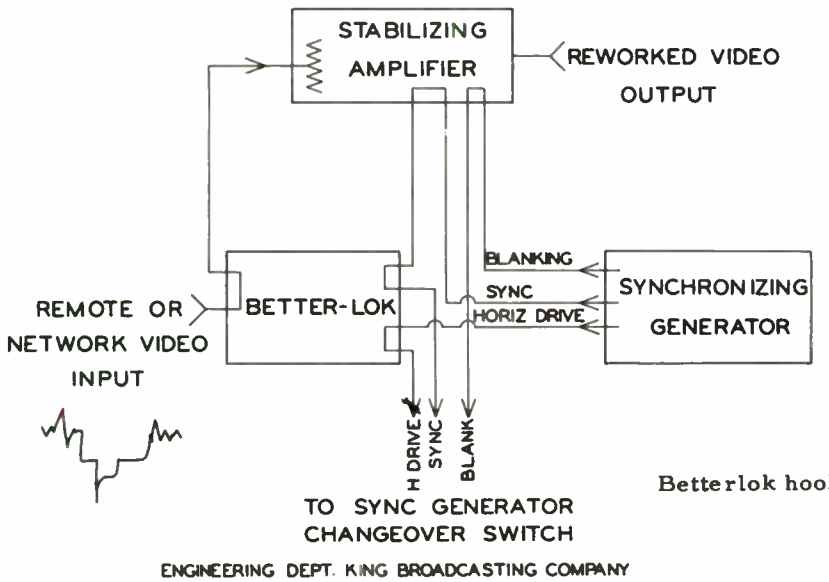

Fig. 9
Betterlok hookup for video signal reworking.

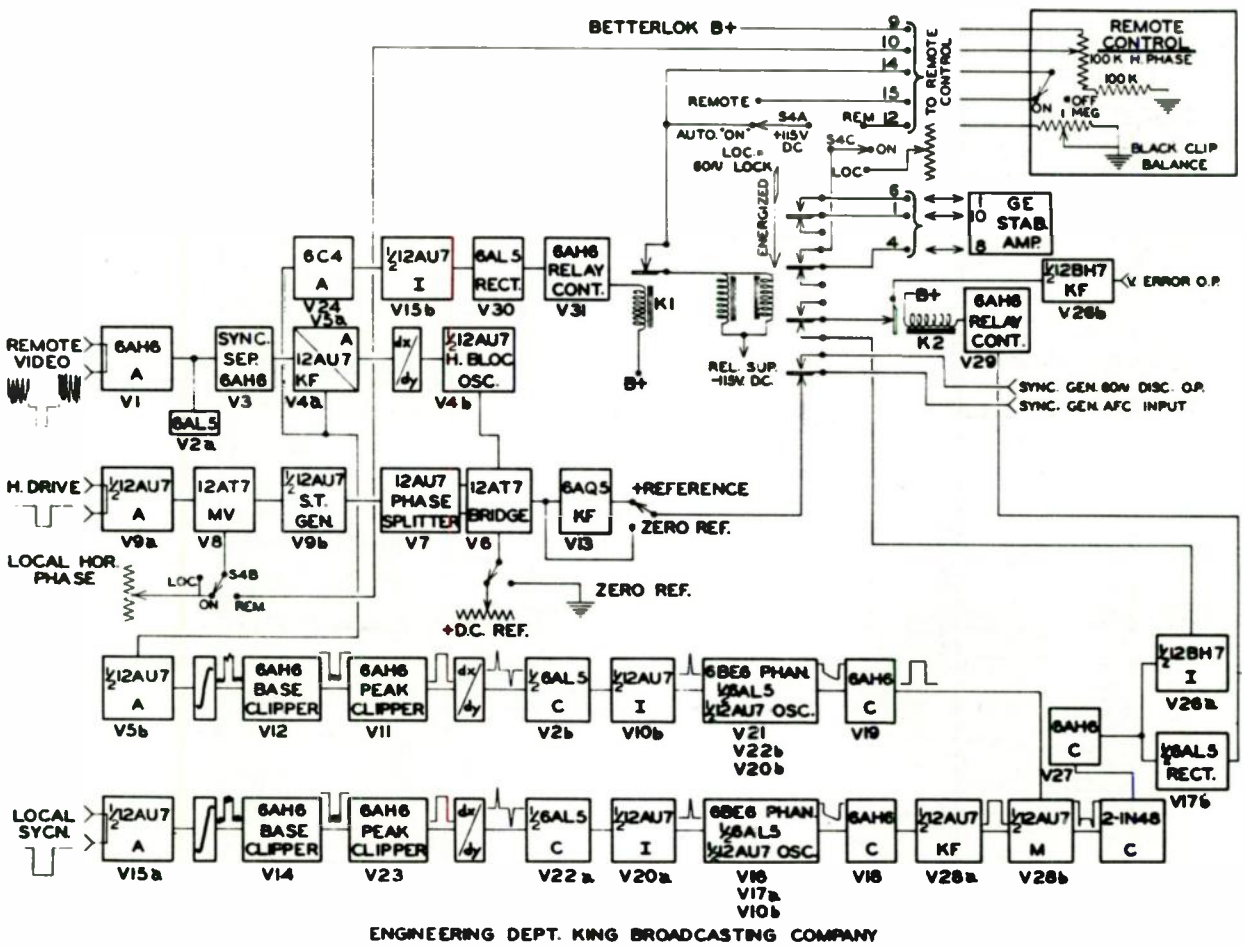

Fig. 10
Block diagram of Betterlok.

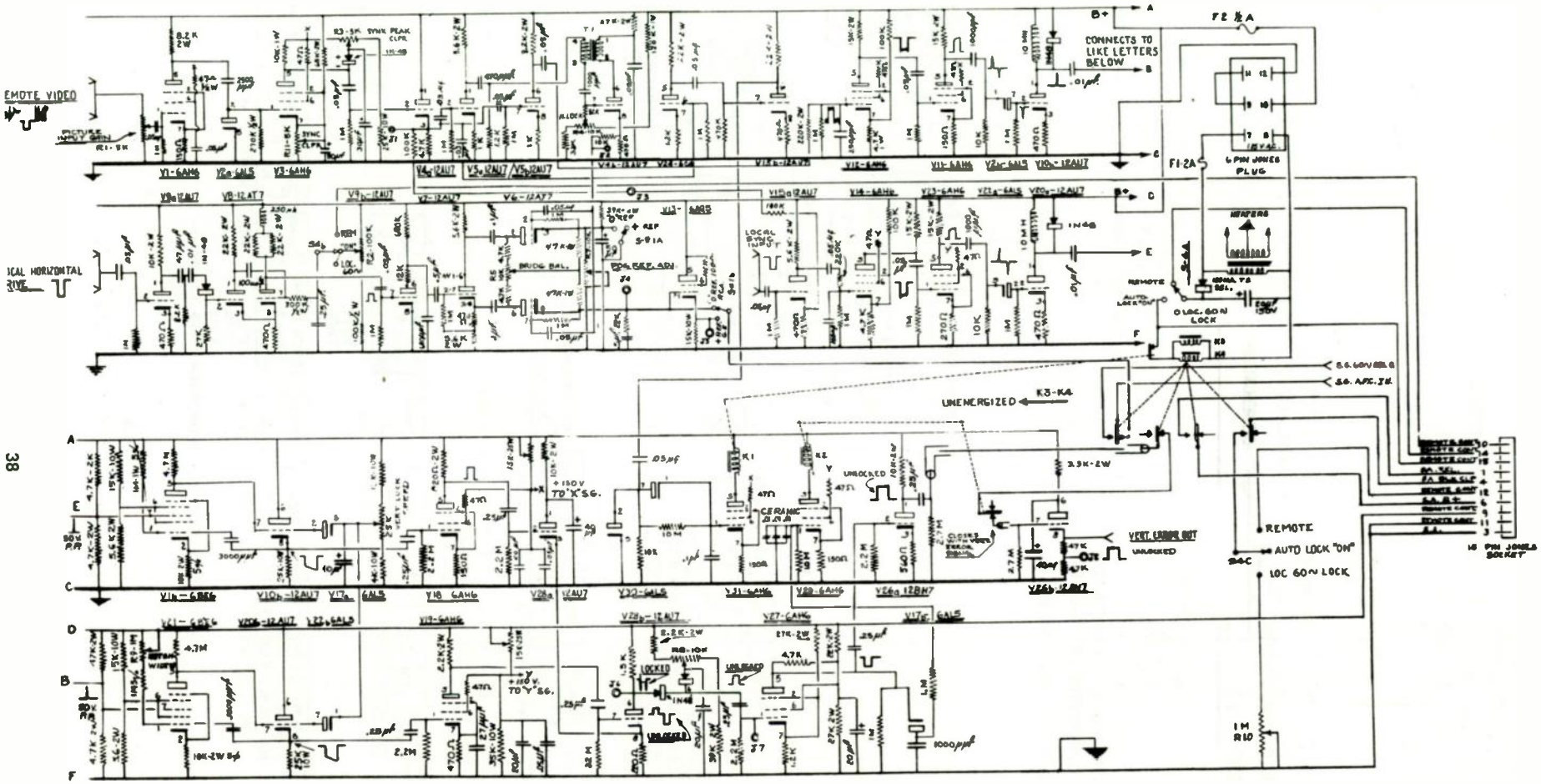

Fig. 11
Schematic diagram of Betterlok.

A 3-VIDICON COLOR TELEVISION CAMERA FOR LIVE PICKUP

Lannes E. Anderson
Studio Systems Supervisor
Broadcast Studio Engineering
Radio Corporation of America
Camden, New Jersey

In the development and production of color television cameras, RCA has followed a schedule which was dictated by the needs of the industry and the availability of suitable pickup tubes. Thus, the first color camera produced was the 3-image orthicon live pickup camera which was introduced commercially early in 1954. A subsequent version was introduced later having many improvements, both in the camera itself and in the associated control equipment.

At the same time, an intensive development and design program was undertaken looking toward the production of a color film camera, as it was expected that color films would play as important a part in color programming as in monochrome. This program resulted in a product similar in principle to the studio camera but employing vidicon pickup tubes. Although considerably less sensitive than the image orthicon, the vidicon tube is more satisfactory in several respects for film reproduction because, under conditions of high illumination, it can achieve better signal-to-noise ratio and can be made to provide excellent gray-scale reproduction. Its storage characteristics are well suited to such an application. Since standard television film projectors provide adequate light, the limited sensitivity of the vidicon is not a handicap.

Shortly thereafter it became apparent that the requirements imposed by certain application of live pickup color cameras could be better met by a camera employing vidicon tubes than by one employing image othicons. A vidicon camera is smaller, lighter, and somewhat more inexpensive to manufacture and operate. On the other hand, the lower sensitivity leads to a requirement of a much higher level of scene illumination for satisfactory performance. The vidicon camera is useful, therefore, where sufficient light is or could be made available and where considerations of size, weight, and operating cost are of special importance. To meet this need, RCA engineers have designed a 3-vidicon color camera for live pickup which will be described in this paper. A camera of this type has been used in a number of closed circuit demonstrations of medical television and has been field tested by the National Broadcasting Company. Production units, including many additional features and refinements, are scheduled for delivery shortly with the first ones allocated for installation at the Walter Reed Army Medical Center in Washington, D. C.

Many applications where the 3-vidicon live camera will be useful will be determined by its sensitivity. Electrically, the vidicon tube may be considered to be a generator having high internal impedance which, for a fixed set of electrical operating conditions, emits a signal current approximately proportional to the 0.65 power of the illumination of the photocathode. By increasing the d-c signal electrode voltage, this signal current can be made to increase very rapidly without increasing the illumination. Thus the sensitivity of the tube is a function of the signal electrode voltage. As the sensitivity is increased by raising the signal electrode voltage, however, the amount of time required to scan "off" the picture information is increased. This time lag may result in a smear behind moving objects. The adjusted sensitivity of the tube, therefore, is determined by the amount of lag which can be tolerated for a given application.

The voltage gain which may be employed in the video amplifier following the vidicon is limited by the permissible signal-to-noise ratio. Although the signal from the vidicon is virtually noise free and a very low-noise preamplifier is used, there is a practical limit to useful amplifier gain imposed by noise generated in the first stage.

The overall sensitivity of the camera is determined, therefore, (1) by the permissible lag which places a lower limit on the photocathode illumination and (2) by the permissible signal-to-noise ratio which limits the useful gain of the video amplifier. In the 3-vidicon color film camera it is possible to illuminate the photocathode intensely with the consequence that the camera signal has no noticeable lag and an excellent signal-to-noise ratio. With the 3-vidicon live camera, there will be certain practical operating limits with the available light; this will necessitate a mode of operation which involves a moderate compromise in lag and signal-to-noise ratio. The performance of the three color cameras with respect to sensitivity is summarized in Table I.

It is of interest to compare the light requirements of this new camera with light levels existing under other conditions. These are summarized in Table II.

TABLE I

COLOR CAMERA PERFORMANCE CHARACTERISTICS

Camera	Typical Scene Illumination	Photocathode Highlight Illumination (Nominal)	Remarks on Performance
3-Vidicon film camera	15,000 foot candles (f:1.5 lens system)	100 foot candles	No lag; excellent signal-to-noise ratio; free of "halos."
3-Vidicon live pickup camera	1200 - 1400 foot candles (f:2.1 lens systems)*	3 - 6 foot candles	Some lag on moving objects; good signal-to-noise ratio; free of "halos."
3-Image orthicon live pickup camera	250 foot candles (f:5.6 lens system)*		Negligible lag; good signal-to-noise ratio; image orthicon subject to "halos" and other edge effects under certain conditions

*Vidicon camera with f:2.1 lens system has depth of focus approximately equivalent to image orthicon camera operated at f:5.6

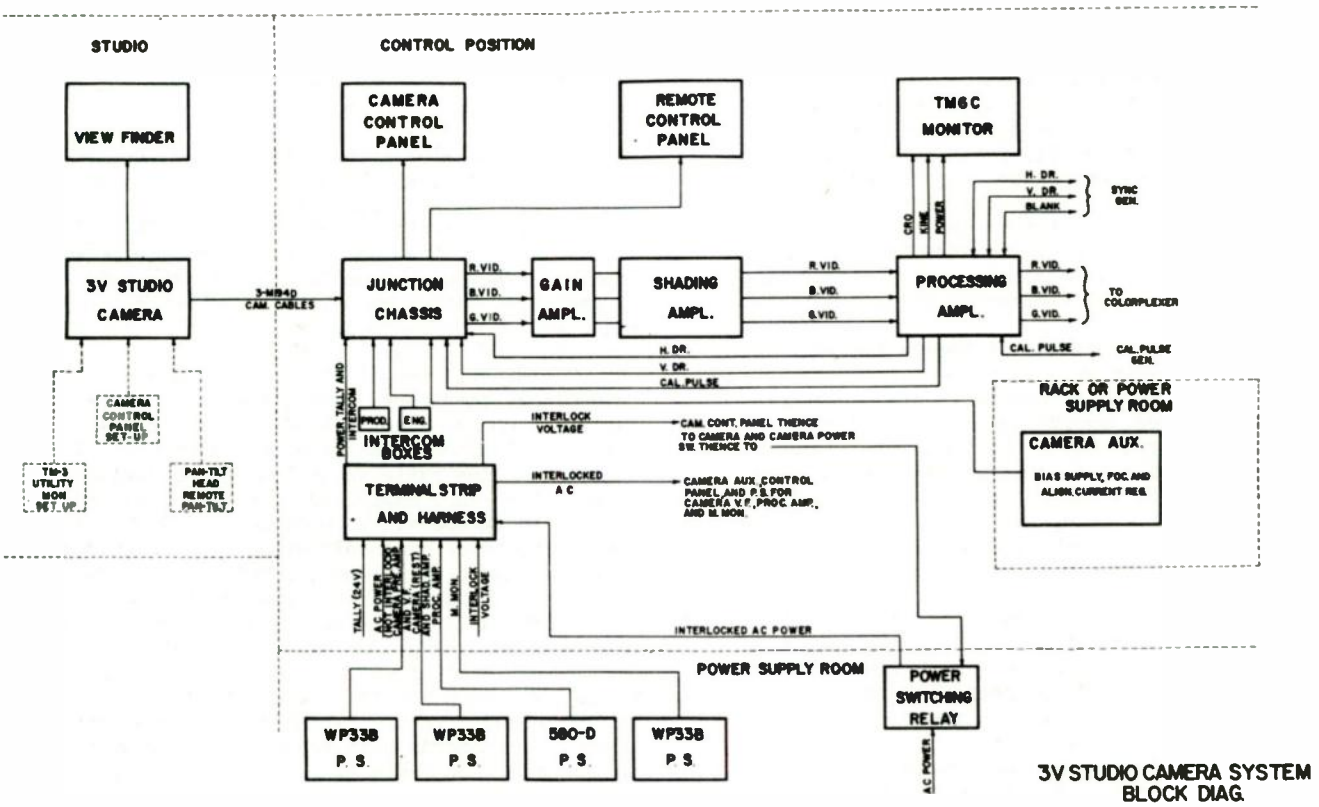

Fig. 1
Block diagram of 3-V studio camera chain

TABLE II

TYPICAL ILLUMINATION LEVELS

Direct sunlight	7500 - 10,000 ft. candles
Cloudy day	300 - 3000 ft. candles
Surgical operations	1500 - 3000 ft. candles
Department store show windows	1000 ft. candles
Indoor color photography	500 - 1000 ft. candles
Indoor monochrome photography	100 - 500 ft. candles
Monochrome television Studio	50 - 100 ft. candles

A desirable objective in the design of all electronic equipment and a primary objective in this camera design is to make it as small and light in weight as possible, consistent with good performance, reliability, and ease of maintenance. This objective has been achieved in this new camera. Its approximate dimensions, not including the viewfinder, are 26 inches long (less the lenses), 14 inches high, and 15 inches wide; the weight is about 100 pounds. Thus the camera is only slightly longer and heavier than the present RCA monochrome image orthicon camera. The standards of quality established in the image orthicon color camera have been maintained, and the signal processing and control equipment are identical. Because of the low cost and long life of the vidicon tubes, the operating cost will be low. On the basis of present field experience it is estimated that pickup tube replacement costs will be only about 60¢ per hour.

Although the lighting requirements of this camera are high, there are numerous applications in closed circuit and broadcast television where adequate illumination is available for satisfactory operation. It should be particularly useful where the subject matter consists primarily of inanimate objects. A representative, although by no means complete list of applications, is given in Table III.

TABLE III

TYPICAL APPLICATIONS
OF 3-VIDICON LIVE PICKUP CAMERAS

Broadcast commercials involving product displays or opaques.

Outdoor pickups on spring, summer, and bright fall days.

Medical and surgical instruction

- Operations
- Autopsies
- Microscopy

Military instruction

- Weapon operation and maintenance
- Aircraft operation and maintenance
- Electronic equipment operation and maintenance
- Target discrimination
- Camouflage detection

Industrial instruction

- Manufacturing proceses
- Mechanic training

Industrial and military remote monitoring

- Hazardous operations
- Remote operations
- Furnace observation
- Jet engine observation

A block diagram of a complete camera chain is shown in Fig. 1. As stated previously, the control and signal processing equipment is essentially identical to that used in the image orthicon color camera. The major elements are: the processing amplifier which amplifies, inserts pedestal and gamma correction, generates shading signals, and provides electronic switching facilities for monitoring signals; the modulation shading amplifier, the gain of which is varied in accordance with shading signals to compensate for residual variations in sensitivity in different areas of the photocathode in the vidicon tubes; the colorplexer which converts the simultaneous red, blue, and green signal into the standard color signal as specified in FCC Rules; a master monitor and a color monitor.

The camera head is shown in Fig. 2. An optional electronic view finder is available which can be used or removed depending on the application. In effect, the camera case contains three individual monochrome vidicon cameras, all identical and therefore, interchangeable. Each

receives a spectrally separated optical image, which is converted into a television signal and amplified to approximately 0.3 volts before leaving the camera. The three vidicon tubes are mounted in a vertical line on the left side of the camera with the taking lens directly in front of the center or red tube. Ease of servicing, plus better ventilation result from this arrangement, with more efficient use of the space for the lenses, mirrors, preamplifiers, deflection circuits, and wiring.

The unit has been provided with a knob and crank located at the lower right side rear of the camera for optical focusing control. A link drive to a shaft extending through the center of the camera moves the lens turret forward and backward in the focusing operation. This is similar to the focusing operation in the monochrome image orthicon camera which has proven to be very popular. When used in applications where the camera must be controlled remotely, optical focusing is controlled by a knob at the control console which in turn operates a driving motor that is attached to the camera.

A four lens turret similar to that used on image orthicon cameras is provided. This may be operated either remotely or by means of a handle at the back of the camera.

The same lenses may be used as are provided for the monochrome image orthicon cameras, thus allowing a wide variety of field sizes; for example,

Focal Length	Field Dimensions at Approx. 8 ft.
135 mm or 5½ inches	15 x 20 inches
8½ inches	9 x 12 inches
15 inches	4 x 5 inches
18 inches	2½ x 3 inches

For larger field coverage, wider angle lenses of 50 and 90 mm focal length are available. These permit coverage of any reasonable field size.

In addition to the camera units and optical system, the camera case contains the necessary deflection circuitry. It has been possible to make a significant reduction in the size of the deflecting yoke and focus assemblies by employing a new vidicon in which the side tip is eliminated. This makes it possible to fit the coil assembly snugly around the tube.

A unique feature of this camera is a plug-in control panel which may be used at the camera position for setup purposes and then transferred to a remote control location. An interlock relay for controlling power to the camera chain will remove dangerous voltages when the camera control panel is removed from any of its control points. This will protect personnel as well as the equipment.

A drawing of the camera fitted with a viewfinder and mounted on a standard tilt head is shown in Fig. 3.

Since the use of this camera for surgical instruction will be one of the most important, it is of interest to describe the mounting equipment designed for this application. This equipment with the camera mounted in place is shown in Fig. 4.

The light from the scene on the operating table passes through a ten inch circular opening in the center of a special surgical lamp and strikes the mirror which reflects the light into the horizontally mounted camera. The lamp may be tilted freely in any direction by the surgeon within wide angular limits. A gear reduction system automatically moves the mirror through one-half of the angular movement of the lamp when the lamp position is changed manually, thus maintaining the camera optical path in line with the light path. In addition, a clutch device allows the remote control operator to over-ride the local mechanical light adjustment. A joystick control can be provided in the camera control console for controlling the mirror angle.

The remote control features described above permit all necessary optical, mechanical and electrical adjustments to be made from a single control position. A locking device is available to permit the easy removal of the camera from the operating lamp. Access to the camera for servicing, while in its operating position, is possible because the locking device is located at a point that allows the side doors to be opened. Due care has been exercised in the design of the camera mount to prevent the camera from falling out of its cradle even though the locking device has not been properly secured.

The control position for the camera chain is shown in Fig. 5. All control and processing equipment is located here with the exception of the colorplexer and power supplies. These are normally mounted in a rack at another location. An alternative arrangement is shown in Fig. 6 in which all equipment is rack mounted. This system is particularly useful when space is at a premium since considerably less floor space is required.

In summary, it can be said that this camera, because of its small size and low operating cost, will extend the uses of color television to a large number of new applications in education, industry, and broadcasting. Under conditions of adequate light it will produce a compatible color signal of broadcast quality.

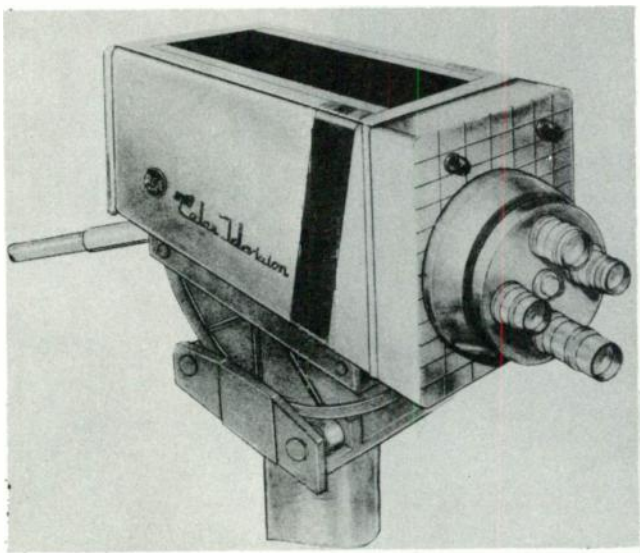

Fig. 2
Color camera on cradle mounting

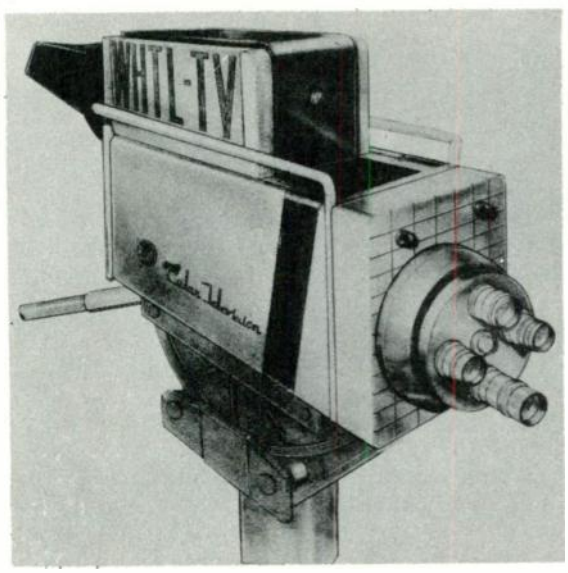

Fig. 3
Color camera with viewfinder on cradle mounting

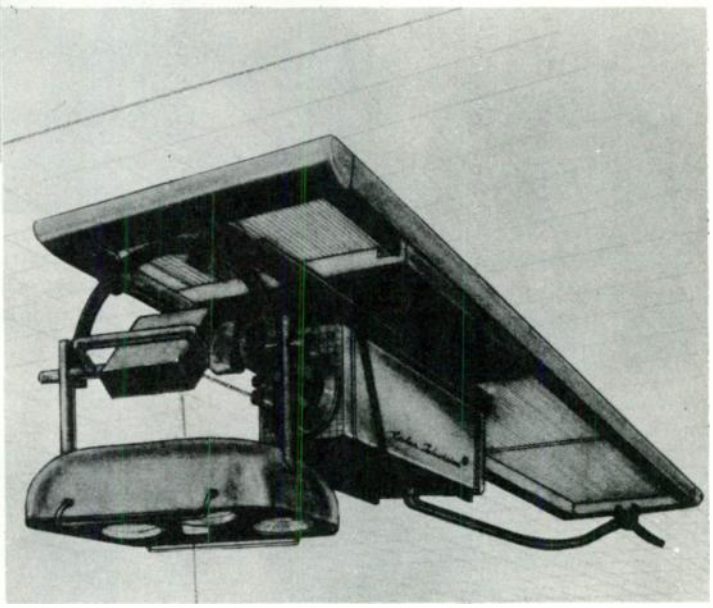

Fig. 4
Color camera without viewfinder mounted with hospital operating lamp

Fig. 5
Color camera control console and color monitor

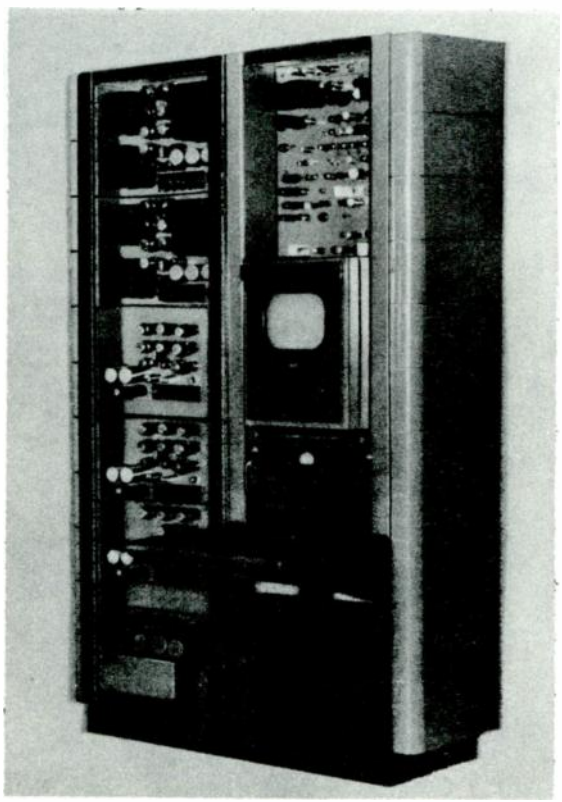

Fig. 6
Color camera control mounted in cabinet racks.

A SIMPLIFIED PROCEDURE FOR THE DESIGN OF TRANSISTOR AUDIO AMPLIFIERS

Albert E. Hayes, Jr., and William W. Wells
AUTONETICS
A Division of North American Aviation, Inc.,
Downey, California

Summary

A simplified procedure for the design of transistor audio-frequency amplifiers has been developed. This procedure involves the use of a set of approximate formulas which have been derived from the classical matrix form, in conjunction with special characteristic curves setting forth the variation of transistor parameters over a wide range of operating currents. The formulas used have been derived for practical circuits which incorporate external resistances in the emitter, base, and collector leads of the transistor. The effect of changes in circuit constants can be visualized directly from the formulas and characteristic curves, without the necessity of resorting to extensive computation, as has been the case heretofore.

This paper is divided into two portions. The first part is concerned with the derivation of the exact formulas of transistor circuits, incorporating the h-matrix parameters, while the second part presents approximate forms of these formulas which are shown to be of adequate accuracy for general use. A method of plotting transistor characteristic curves in a form particularly suitable for the requirements of the circuit designer, and particularly compatable with the simplified formulas, is described. Some examples of actual circuit designs in accordance with this paper are presented to show the generality of the method.

Characterizing The Transistor

A brief review of the origin of the so-called "h parameters" will be in order for those who may not be familiar with four-pole network theory. It is recommended that the reader who wishes to attain proficiency in matrix circuit methods study the references in the order set forth.

It must be pointed out, however, that matrix algebra, as such, is not used in the circuit design method set forth in this paper. The only mathematical operations required are those of simple arithmetic, applied to a set of symbols which have their origin in matrix circuit theory. As a matter of fact, the symbols used in the appended tables have been set forth in a form which eliminates even the appearance of matrix notation.

The General Network

Figure 1 illustrates a "black box" with a pair of terminals at each side. Those on the left side are numbered 1,1 and those on the right side are numbered 2,2. A voltage across the 1,1 terminals is designated v_1, and a similar voltage across the 2,2 terminals is designated v_2. A current flowing into the box through the upper 1 lead is designated i_1, and a current flowing into the box through the upper 2 is designated i_2. Polarities are standardized by convention in such a manner that currents flowing in the directions indicated by the arrows are positive, and voltages are positive when the upper terminal of a pair is at a higher potential than the lower terminal.

It is obvious that, no matter what is in the box, its performance can be described precisely if the interrelations among the two currents and two voltages are stated. Any two of these variables may be selected as the independent variables, with the remaining two selected as the dependent variables. Assuming that the circuit within the box is linear over the range of interest, the various combinations will lead to the six equations set forth below (equations (1) through (6)). It is to be noted at this point that the subscript 11 designates a coefficient associated with the 1,1 terminal pair, 22 designates a coefficient associated with the 2,2 pair, 12 denotes a coefficient associated with an effect at the 1,1 terminals produced by a cause at the 2,2 terminals, while the subscript 21 denotes a coefficient associated with an effect at the 2,2 terminals produced by a cause at the 1,1 terminals. In general, the letter designations used are arbitrarily selected, the exceptions being that the z terms are impedances, and the y terms are admittances. The dimensions of the other coefficients are readily apparent from a consideration of the voltage and current relationships, that is, they must be either impedance, admittance, voltage ratio, or current ratio.

$$v_1 = z_{11}i_1 + z_{12}i_2$$
$$v_2 = z_{21}i_1 + z_{22}i_2 \qquad (1)$$

$$i_1 = y_{11}v_1 + y_{12}v_2$$
$$i_2 = y_{21}v_1 + y_{22}v_2 \qquad (2)$$

$$v_1 = h_{11}i_1 + h_{12}v_2$$
$$i_2 = h_{21}i_1 + h_{22}v_2 \qquad (3)$$

$$i_1 = g_{11}v_1 + g_{12}i_2$$
$$v_2 = g_{21}v_1 + g_{22}i_2 \qquad (4)$$

$$v_1 = a_{11}v_2 - a_{12}i_2$$
$$i_1 = a_{21}v_2 - a_{22}i_2 \qquad (5)$$

$$v_2 = b_{11}v_1 - b_{12}i_1$$
$$i_2 = b_{21}v_1 - b_{22}i_1 \qquad (6)$$

Each of these six sets of equations is a complete characterization of the performance of the black box, and no decision can be made as to which is the most suitable set without knowing some of the limitations of the content of the box. If, for example, the box contained a grounded-cathode vacuum tube, the y set would have the following coefficients when translated into the familiar vacuum tube terminology:

$$y_{11} = 0,\ y_{12} = 0,\ y_{21} = G_m,\ y_{22} = 1/R_p$$

(As a comment on the universality of this system, note that $\mu = g_{21}$.)

Transistor Applications

In a transistor, if we wish to assume that to be the content of the box, we will generally have a low input impedance (perhaps across the 1,1 terminals) and a high output impedance. It develops that the h-set lends itself most readily to practical circuit measurements with such terminal conditions. The practical definition of the four h-parameters is, then:

h_{11} = Input impedance with the output terminals shorted.

h_{12} = Reverse-transfer (feedback) voltage ratio, with the input terminals open.

h_{21} = Forward-transfer current ratio, with the output terminals shorted.

h_{22} = Output admittance with the input terminals open.

In each case it will be seen that an open circuit is called for across a low-impedance circuit, and a short circuit is called for across a high-impedance circuit. The fact that a "short" can never be a true zero-resistance connection, and an "open" can never be a true zero-admittance connection, in practical test circuit arrangements, does not invalidate the terminal conditions of the h-parameter set of equations as applied to practical transistors. Each of the other sets contains at least one terminating condition which is difficult to approach with transistors.

In the preceding discussion it has been assumed that the 1,1 terminals comprise the "input" terminals, while 2,2 comprise the "output" terminals. Since transistors are used in common-emitter, common-base, and common-collector configurations, and since the several h-parameters differ with differing configurations, a convention must be established to enable transistors to be comparable regardless of their end use. In vacuum tubes, for example, the characteristic G_m has an ancillary connotation "in a grounded-cathode configuration." The characteristics of a tube could be set forth just as accurately in the cathode-follower or grounded-grid configurations, but the convention has become well established.

It can be demonstrated, and it will become apparent after reference to the formulas which are presented later, that closer control of the circuit characteristics of a transistor, in all configurations, will be attained if measurements are performed in the common-base configuration, rather than in either of the other possible configurations. The convention has therefore been adopted that all h-parameters are measured in the common-base configuration.

Notation

As has been pointed out earlier, the several h-parameters specify the performance of a generalized circuit, rather than the performance of a specific item, in this case a transistor. Further, transistors frequently appear as a portion of a circuit the h-parameters of which are desired. If, for example, a common-emitter transistor circuit is the subject of circuit analysis, two values of h_{11} must appear in the computation. One of these is the common-base h_{11} of the transistor itself, and the other is the h_{11} of the entire circuit incorporating the transistor. This can become confusing, and we have in the following pages incorporated the recommended notation of the joint IRE/AIEE Task Force 7.7.2 on semiconductor symbols, wherein the circuit equation becomes:

$$\left.\begin{aligned} v_1 &= h_i i_1 + h_r v_2 \\ i_2 &= h_f i_1 + h_o v_2 \end{aligned}\right| \text{ common base} \qquad (7)$$

from which it can be seen that:

h_i = Transistor input impedance with the output terminals shorted, in the common-base configuration.

h_r = Transistor reverse transfer voltage ratio, input terminals open, in the common-base configuration.

h_f = Transistor forward-transfer current ratio, output terminals shorted, in the common-base configuration.

h_o = Transistor output admittance, with the input terminals open, in common-base configuration.

These are the symbols which are used throughout the remainder of this paper.

Circuit Design Formulas

Figures 2, 3, and 4 are the exact formulas for the performance of transistors connected in the three possible circuit configurations. The h-parameters used are, as stated previously, those measured in the common-base configuration. It is believed that these figures constitute the first publication of exact circuit formulas including resistors external to the transistor, in each of the three legs of the circuit. No approximations have been used in the derivation of these formulas, since it is our belief that each user must tailor the degree of approximation in accordance with the limitations of the problem at hand.

The formulas are intended for use in the low-frequency region where the parameters are substantially independent of frequency. With most conventional transistors this range extends from DC up to one percent or more of the alpha-cutoff frequency. These formulas may be used at any frequency provided that (1) the parameters are measured at the frequency of operation, (2) the complex value of each parameter is measured, and (3) impedances and admittances are used in place of resistances and conductances.

The set of formulas in the bottom rows of Figures 2, 3, and 4 comprise expressions for the h-matrix parameters of the entire circuit including the transistor in the configuration shown, together with the associated resistances in the external leads. These formulas are presented for those accustomed to the use of matrix methods in computation.

A table of approximate formulas, useful under most circumstances, appears as Figure 5. These approximations are based on the assumption that R_L is much less than $1/h_o$, that R_g is larger than h_i, that h_r is of the same order of magnitude as $h_i h_o$, and the h_r is at least three orders of magnitude below unity.

Design Curves

It is a rare coincidence when a circuit uses a transistor at the particular values of bias set forth by the manufacturer as "standard test conditions." Taking the case of the USAF 2N43A, for example, the test conditions under which the common-base h-parameters are measured are V_c = -5 v., and I_e = 1 ma. The USAF 2N43A finds wide usage at collector voltages from 1.5 to 30 v., and at emitter currents from 50 uA to more than 10 mA. It is well known that all four h-parameters vary greatly with emitter current, and many manufacturers supply graphs showing the variation of each parameter, on a relative basis, with variation of emitter current. These graphs are not completely satisfactory, since it is necessary to enter the plot with the "standard test conditions" value, and perform an indicated multiplication or division in order to arrive at the correct value at the particular level of current at which it is desired to operate. Such a normalized plot, which expresses variations on a relative basis, suffers from the disadvantage that the variations in magnitude of the several parameters are not presented in a manner which enables the engineer to select optimum conditions directly from the plot.

In the reverse case, for example, when the engineer requires that a transistor have a value of h_i equal to 250 ohms, where the 1-ma I_e value of h_i is 30 ohms, it requires computation to determine that a current of 0.1 ma would provide the 250-ohm value. At the same time the problem of determining the magnitude of h_o at this latter value of bias current presents the requirement of another computation.

Practical Curve Presentation

A more convenient plot, more applicable to the day-to-day requirements of the design engineer, is introduced in Figure 6, which is a graph of the several h-parameters of the 2N43A transistor, plotted against collector current as the independent variable. In making use of this presentation it is necessary only to select the desired value of operating collector current, and then to read the value of the several h-parameters directly from the curve. Conversely, it is a simple task to select a point on one of the curves at which a desired value of an h-parameter appears, and then to read directly the value of collector current which would cause this value of the h-parameter to be presented to the circuit.

It was the single aim, in the preparation of this format, to enable the design engineer to obtain pertinent information as directly as possible, with the greatest practical accuracy, and with the minimum possibility of misinterpretation.

The collector current was selected as the independent variable since it is generally of more direct interest to the design engineer than is the emitter current. Collector current is plotted on a four-cycle logarithmic scale in order to maintain

the same accuracy throughout the useful operating range of the transistor.

Since the variation of parameters with collector voltage is generally less significant than with variation of current, plots are presented at a limited number of voltages, and those only when the value of the parameter is significantly affected. The values of the parameters at other voltages will be obtained with sufficient accuracy by interpolation or extrapolation of the plotted values.

Figures 7 through 10 are similar plots of the characteristics of several of the more popular transistors.

The parameters h_i, h_o, and h_r are plotted on the four-cycle ordinate scale in the obvious manner. Decade multiplying factors are indicated, as applicable, to normalize the values of the parameters to a common scale. On Figure 7, for example, the multiplier for the h_o curve is 10^8. This indicates that the value of the parameter is 10^{-8} times the plotted value. Since a logarithmic scale is used the percentage error is constant over the entire range of plotted values.

The forward-transfer current ratio (h_f), or "alpha" as it has been called, presented an interesting problem, since the value of h_f, by itself rarely appears in circuit computations. In fact, where h_f does appear alone the value, whether it be -.991 or -.992, has only an insignificant effect on the result.

The value of h_f is important, however, in the two forms in which it generally appears in transistor circuit computations: $1 + h_f$, and $\frac{h_f}{1 + h_f}$. It becomes apparent from a consideration of the foregoing expressions that a small change of h_f will produce a large change in the value of the functions, particularly for values of h_f approaching unity. Both of those functions are tabulated, together with the tabulation of h_f itself, on separate ordinate scales which cooperate with the curve labeled h_f. The quantity $\frac{h_f}{1 + h_f}$ is approximately the common-emitter short-circuit current gain, and is labeled h_{fe}. It is also known as "beta" in some circles.

The plot is laid in such a manner that the value of h_{fe} can be read to an accuracy of 10%, while the other parameters may be read to 20%.

Examples

Several examples will now be presented to demonstrate how the formulas and curves may be used to design audio amplifiers.

A One-Stage Amplifier

A very simple common-emitter single-stage amplifier is illustrated in Figure 11. The voltage gain of this amplifier may be computed by using the exact and approximate design formulas set forth on Figures 2 and 5, repectively. The numerical values of the h parameters used are those taken from the 2N43A curve family of Figure 6, for a collector supply of 3 ma and 5 v.

The values of the h parameter are:

$h_i = 12$

$h_r = 4.8 \times 10^{-4}$

$h_f = -.980$

$h_o = 1.4 \times 10^{-6}$

and $D = h_i h_o - h_r h_f = 4.9 \times 10^{-4}$

If the load resistor R_L is selected to be 1,000 ohms, the values of voltage gain computed from the exact and approximate formulas are:

$$D = h_i h_o - h_r h_f$$
$$= (12)(140)(10)^{-8} + (.98)(4.8)(10)^{-4}$$
$$= .168 \times 10^{-4} + 4.7 \times 10^{-4}$$
$$= 4.9 \times 10^{-4}$$

$$M = D - h_r + 1 + h_f$$
$$= 4.9 \times 10^{-4} - 4.8 \times 10^{-4} + .02$$
$$= .1 \times 10^{-4} + .02 = .0201$$

$$A_v = \frac{(4.9 \times 10^{-4} - .98)(10)^3}{12 + 4.9 \times 10^{-4} \times 10^3}$$
$$= \frac{979.5}{12.49} = 78.5 \qquad (8)$$

$$A_v \cong \frac{.98 \times 10^3}{12} = 81.6 \qquad (9)$$

Thus it can be seen that the approximate formula is less than 4% in error. This error will increase with higher values of R_L. Table I is the result of computations with both the exact and approximate formulas, together with the actual measurements made on the amplifier under consideration.

TABLE I

R_L ohms	Calculated Voltage Gain		Measured Voltage Gain - 5 Samples
	Approximate Formula	Exact Formula	
100	8.16	8.12	7.9
1K	81.6	78.5	81.0
10K	816.0	580.0	524.0
100K	8160.0	1600.0	1560.0

The Un-Bypassed Emitter Resistor

An unbypassed or partially bypassed emitter resistor is frequently added to a common-emitter amplifier to provide degeneration. This degeneration produces almost the same results we are accustomed to in vacuum tube circuits when the cathode resistor is left unbypassed -- the input impedance is increased, and the voltage gain is to a lesser extent a function of circuit variables. The circuit illustrated in Figure 12 is typical of this type of amplifier, and will be considered next.

The value of load resistor, 1K, selected for this example, is chosen to simulate to some extent the impedance the circuit would be working into if it were driving another common-emitter stage. The values of the h-parameters selected for this design are: (These values for 1 ma and 5 volts are slightly different from the published values because of the small sample used when plotting the curve.)

$$h_i = 28$$

$$h_r = 3.7 \times 10^{-4}$$

$$h_f = -.98$$

$$h_o = .55 \times 10^{-6}$$

$$\text{then } D = 3.8 \times 10^{-4}$$

$$\text{and } M = .02$$

It will be observed that in almost every computation encountered in small-signal design the assumption that $M = 1 + h_f$ will not materially diminish the accuracy of the result.

The load resistance into which the transistor is working is the parallel combination of R_L, (1,000 ohms) and the 5K collector supply resistor. The parallel combination comes to 832 ohms.

The series combination of all impedances between the emitter and ground yields the value of R_E to be used in the formulas. If the reactance of C is much smaller than 100 ohms it may be ignored and we can consider R_E to be equal to 100 ohms. In the event that the reactance of C is appreciable with respect to 100 ohms, the parallel combination of 1900 + jXc would be noted as R_E. In this case we will assume that the 1900-ohm resistor is adequately bypassed, and thus R_E = 100 ohms.

The formula for voltage gain, from Figure 3, is:

$$A_v = \frac{(D + h_f + h_o R_E)R_L}{h_i + DR_L + R_E[1 + h_o(R_B + R_L)] + R_B(M + h_o R_L)}$$

and thus the computed exact voltage gain is

$$D = h_i h_o - h_f h_r$$

$$= 2.8 \times .55 \times 10^{-6} + .98 \times 3.7 \times 10^{-4}$$

$$= 3.8 \times 10^{-4}$$

$$A_v = \frac{(3.8 \times 10^{-4} - .98 + 0.55 \times 10^{-6} \times 10^2)832}{28 + 3.8 \times 15^4 \times 832 + 10^2(1 + .55 \times 10^{-6} \times 832)}$$

$$= \frac{832 \times .98}{128.32} = 6.35 \qquad (11)$$

Using the approximate formula of Figure 5, the computed voltage gain is:

$$A_v \cong \frac{.98 \times 832}{28 + 100} = 6.36 \qquad (12)$$

where the two results are close to identical. If the emitter degeneration were removed, as would be the case if the emitter were effectively bypassed, the gain would be:

$$A_v \cong \frac{.98 \times 832}{28} = 29.1 \qquad (13)$$

The input impedance is, by the exact formula:

$$Z_i = \frac{(3.8 \times 10^{-4})832 + 28 + 100(14.55 \times 10^{-6} \times 832)}{.55 \times 10^{-6} \times 10^2 + 02}$$

$$= \frac{128.32}{.02} = 6430\,\Omega \qquad (14)$$

while, the approximate formula:

$$Z_i \cong \frac{28 + 100}{.02} = 6400\,\Omega \qquad (15)$$

Once again the error is of the order of 2%.

If the emitter were effectively bypassed to ground the input resistance would be.

$$Z_i = \frac{h_i}{1 + h_f} = \frac{28}{.02} = 1400\,\Omega$$

It is interesting to note that the gain and the input impedance are both changed by 4.58 times when the emitter impedance is varied between zero and 100 ohms.

APPENDIX

The transistor may be regarded, most generally, as a six-terminal network, of the form indicated in Figure 13.

This may at first appear surprising, since the transistor as we know it today has but three leads. However, let us assume that the primed leads are the emitter, base, and collector leads of the transistor, and that the unprimed leads are a y-connected common lead, with no connection whatever to the transistor itself. Figure 14 illustrates one such possible arrangement of the transistor.

For the sake of generality, however, we will not assume that the primed terminals are necessarily connected to the transistor elements in any particular order at this time.

We can define currents and voltages according to the following conventions: Currents are positive when a primed lead is at a higher potential than its unprimed associate. In the illustration of Figure 15 all currents and voltages indicated are positive.

It can be shown, by the method of Knight et al.,[1] that the interrelationship among these six voltages and currents may be expressed in the following form:

$$i_1 = y_{11}v_1 + y_{12}v_2 + y_{13}v_3 \qquad (17a)$$

$$i_2 = y_{21}v_1 + y_{22}v_2 + y_{23}v_3 \qquad (17b)$$

$$i_3 = y_{31}v_1 + y_{32}v_2 + y_{33}v_3 \qquad (17c)$$

The preceding equation family may be expressed in matrix notation as:

$$\begin{bmatrix} i_1 \\ i_2 \\ i_3 \end{bmatrix} = \begin{bmatrix} y_{11}y_{12}y_{13} \\ y_{21}y_{22}y_{23} \\ y_{31}y_{32}y_{33} \end{bmatrix} \begin{bmatrix} v_1 \\ v_2 \\ v_3 \end{bmatrix} \qquad (18)$$

If the unprimed terminals are assumed to be a common ground-lead, and if we choose to 'ground' one of the transistor elements to that lead, the following sets of equations will result from those connections.

Shorted Pair	Circuit Equations	
1', 1	$i_2 = y_{22}v_2 + y_{23}v_3$ $i_3 = y_{23}v_2 + y_{33}v_3$	(19)
2', 2	$i_1 = y_{11}v_1 + y_{13}v_3$ $i_3 = y_{31}v_1 + y_{33}v_3$	(20)
3', 3	$i_1 = y_{11}v_1 + y_{12}v_2$ $i_2 = y_{21}v_1 + y_{22}v_2$	(21)

If we assume that the pair 3', 3 represents the base terminal of the transistor and the common lead, the last of the preceding three equations is the complete circuit equation of the common-base transistor circuit, expressed in the terms of admittances. The general 'black box' equivalent of this type of equation is a two-terminal pair (or four-terminal network) as illustrated in Figure 16. The polarity conventions for voltage and currents are as set forth for the six-terminal network of Figure 15.

It will be noted that equation (21) expresses the operation of the two-terminal pair in terms of the independent variables v_1 and v_2. It will be obvious that five other sets of equations are possible, selecting other currents and voltages as the independent variables. The complete set, together with their matrix-notation equivalents, are set forth below. The notation is that of Shea.[2]

$$\begin{aligned} v_1 &= z_{11}i_1 + z_{12}i_2 \\ v_2 &+ z_{21}i_1 + z_{22}i_2 \end{aligned} \qquad \begin{bmatrix} v_1 \\ v_2 \end{bmatrix} = \begin{bmatrix} z_{11}z_{12} \\ z_{21}z_{22} \end{bmatrix} \begin{bmatrix} i_1 \\ i_2 \end{bmatrix} \qquad (22)$$

$$\begin{aligned} i_1 &= y_{11}v_1 + y_{12}v_2 \\ i_2 &= y_{21}v_1 + y_{22}v_2 \end{aligned} \qquad \begin{bmatrix} i_1 \\ i_2 \end{bmatrix} = \begin{bmatrix} y_{11}y_{12} \\ y_{21}y_{22} \end{bmatrix} \begin{bmatrix} v_1 \\ v_2 \end{bmatrix} \qquad (23)$$

$$\begin{aligned} v_1 &= h_{11}i_1 + h_{12}v_2 \\ i_2 &= h_{21}i_1 + h_{22}v_2 \end{aligned} \qquad \begin{bmatrix} v_1 \\ i_2 \end{bmatrix} = \begin{bmatrix} h_{11}h_{12} \\ h_{21}h_{22} \end{bmatrix} \begin{bmatrix} i_1 \\ v_2 \end{bmatrix} \qquad (24)$$

$$\begin{aligned} i_1 &= g_{11}v_1 + g_{12}i_2 \\ v_2 &= g_{21}v_1 + g_{22}i_2 \end{aligned} \qquad \begin{bmatrix} i_1 \\ v_2 \end{bmatrix} = \begin{bmatrix} g_{11}g_{12} \\ g_{21}g_{22} \end{bmatrix} \begin{bmatrix} v_1 \\ i_2 \end{bmatrix} \qquad (25)$$

$$\begin{aligned} v_1 &= a_{11}v_2 - a_{12}i_2 \\ i_1 &= a_{21}v_2 - a_{22}i_2 \end{aligned} \qquad \begin{bmatrix} v_1 \\ i_1 \end{bmatrix} = \begin{bmatrix} a_{11}a_{12} \\ a_{21}a_{22} \end{bmatrix} \begin{bmatrix} v_2 \\ -i_2 \end{bmatrix} \qquad (26)$$

$$\begin{aligned} v_2 &= b_{11}v_1 - b_{12}i_1 \\ i_2 &= b_{21}v_1 - b_{22}i_1 \end{aligned} \qquad \begin{bmatrix} v_2 \\ i_2 \end{bmatrix} = \begin{bmatrix} b_{11}b_{12} \\ b_{21}b_{22} \end{bmatrix} \begin{bmatrix} v_1 \\ -i_1 \end{bmatrix} \qquad (27)$$

A fine table setting forth the interrelations among the several sets of matrix parameters has been published.[2] By the use of such a table any of the coefficients may be expressed in terms of the coefficients may be expressed in terms of the coefficients of any of the other matrices.

It will be recalled at this point that the assumption has been made that the 3', 3 pair of the six-terminal network represented the base-common pair, and that the resultant four-terminal network comprosed a common-base configuration. In view of this, the convention has been adopted that the coefficient associated with a particular common-element configuration will have a third subscript indicating the common element. Thus the coefficients set forth in the preceding set of equations should, strictly speaking, be written as follows: z_{11b}, g_{12b}, etc. During the remainder of this discussion the common-base subscript will be assumed, and the complete forms will be reserved for the common-emitter and common-collector coefficients.

The Indefinite Y-Matrix

At this point a singular property of the y-matrix (equation 18) should be pointed out: The sum of the coefficients in each row is zero, and the sum of the coefficients in each column is zero. Thus, the entire 3 x 3 y-matrix, called the Indefinite Y-Matrix[3] can be written by inspection from the common-base y-matrix set forth above (23) as follows: (Equation 28)

$$\begin{bmatrix} i_1 \\ i_2 \\ i_3 \end{bmatrix} = \begin{bmatrix} y_{11} & y_{12} & -(y_{11}+y_{12}) \\ y_{21} & y_{22} & -(y_{21}+y_{22}) \\ -(y_{11}+y_{21}) & -(y_{12}+y_{22}) & y_{11}+y_{22}+y_{21}+y_{12} \end{bmatrix} \begin{bmatrix} v_1 \\ v_2 \\ v_3 \end{bmatrix}$$

Since the 3', 3 pair has been defined as representing the base-common pair of the six terminal network described above, and if we assume the 1', 1 pair to represent the emitter-common pair, and the 2', 2 pair to represent the collector-common pair, the common-emitter y-matrix may be expressed in terms of the common-base y-matrix by cancelling the 1 row and 1 column of the above matrix, and rearranging the terms in accordance with the customary input/output relationships where 1', 1 represents the input pair, and the 2', 2 represents the output pair. The result, the common-emitter y-matrix, in terms of the common-base y-matrix parameters becomes:

$$\begin{bmatrix} y_{11b} + y_{22b} + y_{21b} + y_{12b} & -(y_{12b} + y_{22b}) \\ -(y_{21b} + y_{22b}) & (y_{22b}) \end{bmatrix} \quad (29)$$

yielding the conversion table:

$$y_{11e} = y_{11b} + y_{22b} + y_{21b} + y_{12b}$$

$$y_{12e} = (y_{12b} + y_{22b})$$

$$y_{21e} = (y_{21b} + y_{22b})$$

$$y_{22e} = y_{22b}$$

Thus the indefinite y-matrix provides an avenue of translation between one circuit configuration and another. This was the method used in the derivation of the exact circuit formulas presented as Figures 2, 3, and 4.

By converting the h-parameters to their y-matrix equivalents, entering the result in the indefinite y-matrix, cancelling the appropriate row and column, and translating the resultant 2 x 2 y-matrix parameters back to h-matrix parameters, the following table of equivalents among the several sets of h-parameters is obtained:

TABLE (II)

Tabulation of the h-matrix parameters of the transistor connected in the three possible configurations expressed in terms of the common-base matrix parameters.

Configuration	Symbol	Equivalent
Common Emitter	h_{11e}	$\frac{h_{11b}}{M}$
	h_{12e}	$\frac{D - h_{12b}}{M}$
	h_{21e}	$\frac{-(h_{21b} + D)}{M}$
	h_{22e}	$\frac{h_{22b}}{M}$
	D_e	$\frac{D}{M}$
Common Collector	h_{11c}	$\frac{h_{11b}}{M}$
	h_{12c}	$\frac{1 + h_{21b}}{M}$
	h_{21c}	$\frac{h_{12b}^{-1}}{M}$
	h_{22c}	$\frac{h_{22b}}{M}$
	D_c	$\frac{1}{M}$

Where $D = h_{ib}h_{ob} - h_{fb}h_{rb}$

$$D_e = h_{ie}h_{oe} - h_{fe}h_{re} \text{ (etc)}$$

and $M = D - h_{rb} + h_{fb} + 1$

In this table the symbol D represents the value of the matrix, evaluated as a determinant, as follows: $D = h_{11}h_{22} - h_{12}h_{21}$. The symbol M represents: $D + h_f - h_r + 1$

Transistor Notation

While the preceding table of h-parameters represents a consistent set of parameters, the necessity to select one of these sets as the appropriate one to characterize a transistor, leads to a confusing situation when a configuration other than the "standard" is used in a circuit. The following example serves to illustrate this point:

Let us assume, as is the case, that the common-base set of h-parameters is defined as the set whereby the performance of a transistor is to be characterized. Let us assume further that the transistor in question is to be operated in a common-emitter circuit.

The following conditions will then prevail:

Input impedance of the transistor, with its output terminals shorted (measured in the common base connection) = h_{11b}.

Input impedance of the transistor circuit, with the output terminals shorted = h_{11e}.

Since, as is shown in Table (II), $h_{11b} \neq h_{11e}$ the subject of notation begins to become cloudy. For this reason, the following notation has been recommended by the Joint AIEE/IRE Task Force on Semiconductor Notations:

h_{ib} = Transistor small-signal, short-circuit, input resistance, measured in the common-base configuration.

h_{rb} = Transistor small-signal, open-circuit, reverse-transfer voltage ratio, measured in the common-base configuration.

h_{fb} = Transistor small-signal, short-circuit, forward-transfer, current ratio, measured in the common-base configuration.

h_{ob} = Transistor small-signal, open-circuit, output conductance, measured in the common-base configuration.

These symbols have been reduced to the practical symbols shown in Table III by invoking the rule that all transistor h-parameters are measured in the common-base configuration, regardless of the end use of the transistor.

TABLE III

OLD SYMBOL		NEW SYMBOL	
EXACT	PRACTICAL	EXACT	PRACTICAL
h_{11b}	h_{11}	h_{ib}	h_i
h_{12b}	h_{12}	h_{rb}	h_r
h_{21b}	h_{21}	h_{fb}	h_f
h_{22b}	h_{22}	h_{ob}	h_o

An Example

As an example of the use of matrix methods in the handling of complex transistor circuitry, the derivation of the formula for the voltage gain of a common-emitter transistor amplifier containing an external emitter resistor, as illustrated in Figure 17, will be carried through from the original common-base h-parameters.

This circuit may be redrawn, for the sake of analysis, as shown in Figure 18. This latter arrangement is seen to comprise two individual "black boxes" with their input terminals in series relationship, and with their output terminals similarly connected. According to Guilleman,[4] the z matrix of such a combination is equal to the sum of the z matrices of the individual boxes.

The h-matrix of the upper box containing the common-emitter-connected transistor is, from Figure 2.

$$\begin{bmatrix} \frac{h_i}{M} & , & \frac{D - h_r}{M} \\ \frac{-(h_f + D)}{M} & , & \frac{h_o}{M} \end{bmatrix} \qquad (30)$$

By using a table of matrix interrelations, the z matrix of the transistor "box" is found to be:

$$\begin{bmatrix} \frac{D}{h_o} & , & \frac{D - h_r}{h_o} \\ \frac{h_f + D}{h_o} & , & \frac{M}{h_o} \end{bmatrix} \qquad (31)$$

The z matrix of the lower "box", containing the resistor is, by inspection:

$$\begin{bmatrix} R_E & R_E \\ R_E & R_E \end{bmatrix} \qquad (32)$$

The z matrix of the combined circuit is the sum of these two matrices:

$$\begin{bmatrix} \frac{D}{h_o} + R_E , & \frac{D - h_r}{h_o} + R_E \\ \frac{h_f + D}{h_o} + R_E , & \frac{M}{h_o} + R_E \end{bmatrix} \qquad (33)$$

The voltage gain of a circuit, expressed in terms of the z matrix is[5]

$$A_v = \frac{Z_{21} R_L}{D_z + Z_{11} R_L} \qquad (34)$$

Substituting, from equation (33),

$$A_v = \frac{(\frac{h_f + D}{h_o} + R_E) R_L}{\frac{h_i + R_E}{h_o} + (\frac{D}{h_o} + R_E) R_L} \qquad (35)$$

$$= \frac{\frac{R_L(D + h_f)}{h_o} + R_E R_L}{\frac{h_i + R_E}{h_o} + \frac{D_{RL}}{h_o} + R_E R_L}$$

$$= \frac{R_L(D + h_f) + h_o R_E R_L}{h_i + R_E + D_{RL} + h_o R_E R_L}$$

$$A_v = \frac{(D + h_f + h_o R_E) R_L}{h_i + D_{RL} + R_E(1 + h_o R_L)} \qquad (36)$$

Which is the desired formula

REFERENCES

1. Measurement of the Small Signal Parameters of Transistors, G. Knight, et al., Proc. IRE, August 1953, p 983 ff.

2. Principles of Transistor Circuits, R. F. Shea, John Wiley and Sons, New York, 1953.

3. Matrix Representation of Transistor Circuits, J. Shekel, Proc. IRE, Nov. 1952, p 1493 ff.

4. Guillemin, E. A., Communications Networks, Vol. II, John Wiley and Sons, N.Y. 1935, P 146.

5. Shea, loc. cit., p 336.

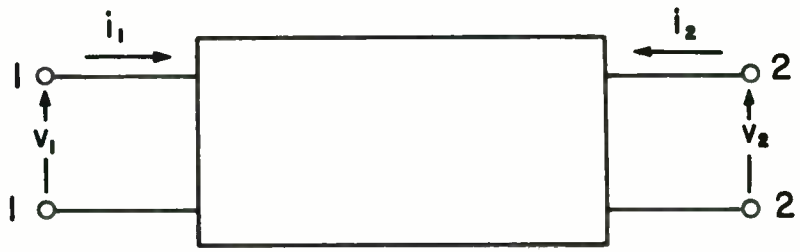

Fig. 1
The "classical" two-terminal pair, or four-terminal network, indicating the numerical designation of the terminals.

TRANSISTOR DESIGN FORMULAS IN THE SEVERAL COMMON-EMITTER ARRANGEMENTS

NOTE: THE h-PARAMETERS ARE MEASURED IN THE COMMON-BASE CONFIGURATION	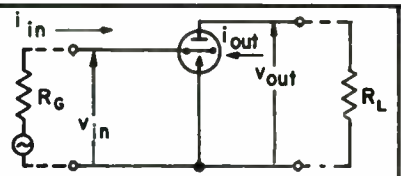	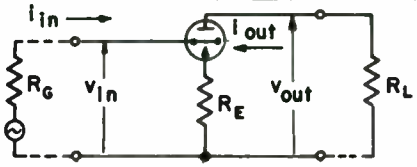	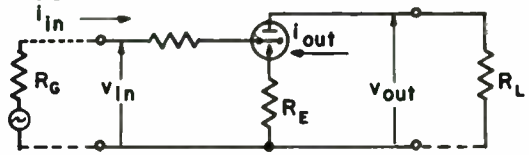
VOLTAGE GAIN $\left(\frac{v_{out}}{v_{in}}\right)$	$\frac{(D+h_f)R_L}{h_i+DR_L}$	$\frac{(D+h_f+h_oR_E)R_L}{h_i+DR_L+R_E(1+h_oR_L)}$	$\frac{(D+h_f+h_oR_E)R_L}{h_i+DR_L+R_E[1+h_o(R_B+R_L)]+R_B(M+h_oR_L)}$
CURRENT GAIN $\left(\frac{i_{out}}{i_{in}}\right)$	$\frac{D+h_f}{h_oR_L+M}$	$\frac{D+h_f+h_oR_E}{h_o(R_E+R_L)+M}$	$\frac{D+h_f+h_oR_E}{h_o(R_E+R_L)+M}$
INPUT RESISTANCE $\left(R_{in}\right)$	$\frac{DR_L+h_i}{h_oR_L+M}$	$\frac{DR_L+h_i+R_E(1+h_oR_L)}{h_o(R_E+R_L)+M}$	$R_B+\frac{DR_L+h_i+R_E(1+h_oR_L)}{h_o(R_E+R_L)+M}$
OUTPUT RESISTANCE $\left(R_{out}\right)$	$\frac{h_i+MR_G}{D+h_oR_G}$	$\frac{h_i+MR_G+R_E(1+h_oR_G)}{D+h_o(R_E+R_G)}$	$\frac{h_i+M(R_B+R_G)+R_E[1+h_o(R_B+R_G)]}{D+h_o(R_B+R_E+R_G)}$
EQUIVALENT h-MATRIX	$h_{11}=\frac{h_i}{M}$ $h_{12}=\frac{D-h_r}{M}$ $h_{21}=\frac{-(D+h_f)}{M}$ $h_{22}=\frac{h_o}{M}$	$h_{11}=\frac{h_i+R_E}{M+h_oR_E}$ $h_{12}=\frac{D-h_r+h_oR_E}{M+h_oR_E}$ $h_{21}=\frac{-(D+h_f+h_oR_E)}{M+h_oR_E}$ $h_{22}=\frac{h_o}{M+h_oR_E}$	$h_{11}=R_B+\frac{h_i+R_E}{M+h_oR_E}$ $h_{12}=\frac{D-h_r+h_oR_E}{M+h_oR_E}$ $h_{21}=\frac{-(D+h_f+h_oR_E)}{M+h_oR_E}$ $h_{22}=\frac{h_o}{M+h_oR_E}$
$D=h_ih_o-h_fh_r$			$M=D-h_r+1+h_f$

Fig. 2

The exact formulas for some of the properties of the common-emitter transistor amplifier, expressed in terms of the common-base h-matrix parameters. The resistors shown are all external to the transistor.

TRANSISTOR DESIGN FORMULAS IN THE SEVERAL COMMON-COLLECTOR ARRANGEMENTS

NOTE: THE h-PARAMETERS ARE MEASURED IN THE COMMON-BASE CONFIGURATION	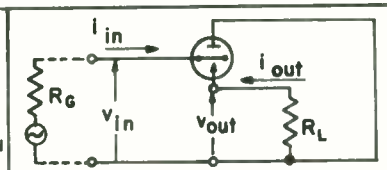	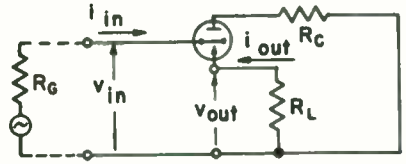	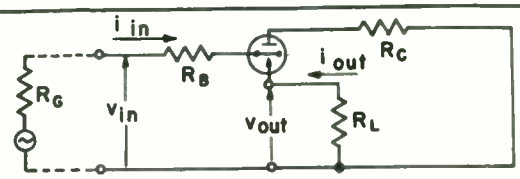
VOLTAGE GAIN $\left(\frac{v_{out}}{v_{in}}\right)$	$\frac{(1-h_r)R_L}{h_i+R_L}$	$\frac{(1-h_r+h_oR_C)R_L}{h_i+R_L(1+h_oR_C)+DR_C}$	$\frac{(1-h_r+h_oR_C)R_L}{h_i+DR_C+R_L\left[1+h_o(R_B+R_C)\right]+R_B(M+h_oR_C)}$
CURRENT GAIN $\left(\frac{i_{out}}{i_{in}}\right)$	$\frac{1-h_r}{h_oR_L+M}$	$\frac{1-h_r+h_oR_C}{h_o(R_C+R_L)+M}$	$\frac{1-h_r+h_oR_C}{h_o(R_C+R_L)+M}$
INPUT RESISTANCE $\left(R_{in}\right)$	$\frac{h_i+R_L}{h_oR_L+M}$	$\frac{h_i+R_L+R_C(D+h_oR_L)}{h_o(R_C+R_L)+M}$	$R_B+\frac{h_i+R_L+R_C(D+h_oR_L)}{h_o(R_C+R_L)+M}$
OUTPUT RESISTANCE $\left(R_{out}\right)$	$\frac{h_i+MR_G}{1+h_oR_G}$	$\frac{h_i+MR_G+R_C(D+h_oR_G)}{1+h_o(R_C+R_G)}$	$\frac{h_i+(M+h_oR_C)(R_B+R_G)+DR_C}{1+h_o(R_B+R_C+R_G)}$
EQUIVALENT h-MATRIX	$h_{11}=\frac{h_i}{M}$ $h_{12}=\frac{1+h_f}{M}$ $h_{21}=\frac{h_r-1}{M}$ $h_{22}=\frac{h_o}{M}$	$h_{11}=\frac{h_i+DR_C}{M+h_oR_C}$ $h_{12}=\frac{1+h_f+h_oR_C}{M+h_oR_C}$ $h_{21}=\frac{h_r-1-h_oR_C}{M+h_oR_C}$ $h_{22}=\frac{h_o}{M+h_oR_C}$	$h_{11}=R_B+\frac{h_i+DR_C}{M+h_oR_C}$ $h_{12}=\frac{1+h_f+h_oR_C}{M+h_oR_C}$ $h_{21}=\frac{h_r-1-h_oR_C}{M+h_oR_C}$ $h_{22}=\frac{h_o}{M+h_oR_C}$
$D=h_ih_o-h_fh_r$			$M=D-h_r+1+h_f$

Fig. 3

The exact formulas for some of the properties of the common-collector transistor amplifier, expressed in terms of the common-base h-matrix parameters.

TRANSISTOR DESIGN FORMULAS IN THE SEVERAL COMMON-BASE ARRANGEMENTS

NOTE: THE h-PARAMETERS ARE MEASURED IN THE COMMON-BASE CONFIGURATION	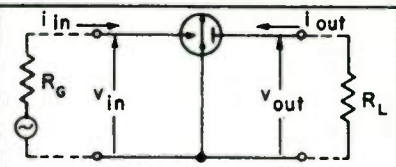	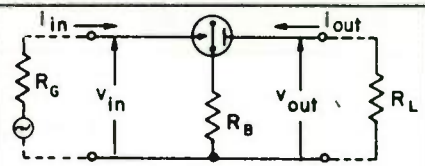	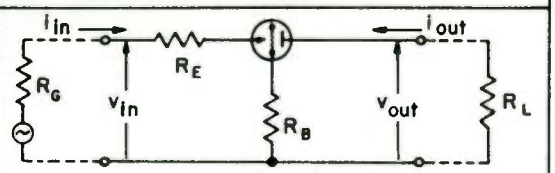
VOLTAGE GAIN $\left(\frac{v_{out}}{v_{in}}\right)$	$\frac{-h_f R_L}{h_i + D R_L}$	$\frac{R_L(h_o R_B - h_f)}{h_i + DR_L + R_B(M + h_o R_L)}$	$\frac{R_L(h_o R_B - h_f)}{h_i + DR_L + R_B(M + h_o R_L + h_o R_E) + R_E(1 + h_o R_L)}$
CURRENT GAIN $\left(\frac{i_{out}}{i_{in}}\right)$	$\frac{-h_f}{h_o R_L + 1}$	$\frac{h_o R_B - h_f}{1 + h_o(R_B + R_L)}$	$\frac{h_o R_B - h_f}{1 + h_o(R_B + R_L)}$
INPUT RESISTANCE $\left(R_{in}\right)$	$\frac{h_i + DR_L}{1 + h_o R_L}$	$\frac{h_i + DR_L + R_B(M + h_o R_L)}{1 + h_o(R_B + R_L)}$	$R_E + \frac{h_i + DR_L + R_B(M + h_o R_L)}{1 + h_o(R_B + R_L)}$
OUTPUT RESISTANCE $\left(R_{out}\right)$	$\frac{h_i + R_G}{D + h_o R_G}$	$\frac{h_i + R_G + R_B(M + h_o R_G)}{D + h_o(R_B + R_G)}$	$\frac{h_i + R_G + R_E + R_B[M + h_o(R_G + R_E)]}{D + h_o(R_B + R_E + R_G)}$
EQUIVALENT h - MATRIX	$h_{11} = h_i$ $\quad h_{12} = h_r$ $h_{21} = h_f$ $\quad h_{22} = h_o$	$h_{11} = \frac{h_i + MR_B}{1 + h_o R_B}$ $\quad h_{12} = \frac{h_r + MR_B}{1 + h_o R_B}$ $h_{21} = \frac{h_f - h_o R_B}{1 + h_o R_B}$ $\quad h_{22} = \frac{h_o}{1 + h_o R_B}$	$h_{11} = R_E + \frac{h_i + MR_B}{1 + h_o R_B}$ $\quad h_{12} = \frac{h_r + h_o R_B}{1 + h_o R_B}$ $h_{21} = \frac{h_f - h_o R_B}{1 + h_o R_B}$ $\quad h_{22} = \frac{h_o}{1 + h_o R_B}$
$D = h_i h_o - h_f h_r$		$M = D - h_r + 1 + h_f$	

Fig. 4

The exact formulas for some of the properties of the common-base transistor amplifier, expressed in terms of the common-base h-parameters. The resistors shown are all external to the transistor.

APPROXIMATE TRANSISTOR DESIGN FORMULAS

NOTE: THE h-PARAMETERS ARE MEASURED IN THE COMMON-BASE CONFIGURATION	COMMON EMITTER	COMMON COLLECTOR	COMMON BASE
	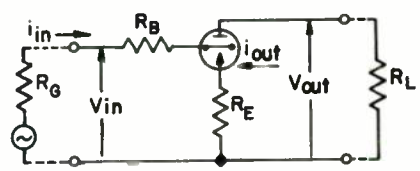	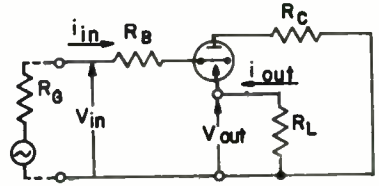	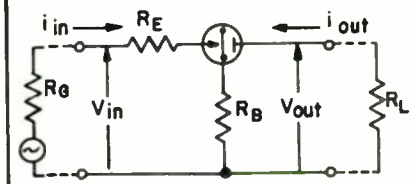
VOLTAGE GAIN $\left(\frac{V_{out}}{V_{in}}\right)$	$\frac{h_f R_L}{h_i + R_E + R_B(1+h_f)}$	$\frac{R_L}{h_i + R_L + R_B(1+h_f)}$	$\frac{-h_f R_L}{h_i + R_E + R_B(1+h_f)}$
CURRENT GAIN $\left(\frac{i_{out}}{i_{in}}\right)$	$\frac{h_f}{1+h_f}$	$\frac{1}{1+h_f}$	$-h_f$
INPUT RESISTANCE (R_{in})	$R_B + \frac{h_i + R_E}{1+h_f}$	$R_B + \frac{h_i + R_L}{1+h_f}$	$R_E + h_i + R_B(1+h_f)$
OUTPUT RESISTANCE (R_{out})	$\frac{h_i + R_E + (R_B + R_G)(1+h_f)}{h_O(R_E + R_B + R_G)}$	$\frac{h_i + (R_B + R_G)(1+h_f)}{1 + h_O(R_B + R_G + R_C)}$	$\frac{h_i + R_E + R_G + R_B(1+h_f)}{h_O(R_E + R_B + R_G) + D}$ $D = h_i h_O - h_f h_r$
	$D = h_i h_O - h_f h_r$		$M = D - h_r + 1 + h_f$

Fig. 5

Approximate formulas form some of the properties of transistor amplifiers, in the three basic circuit configurations, expressed in terms of the common-base h-matrix parameters. The resistors shown are external to the transistor.

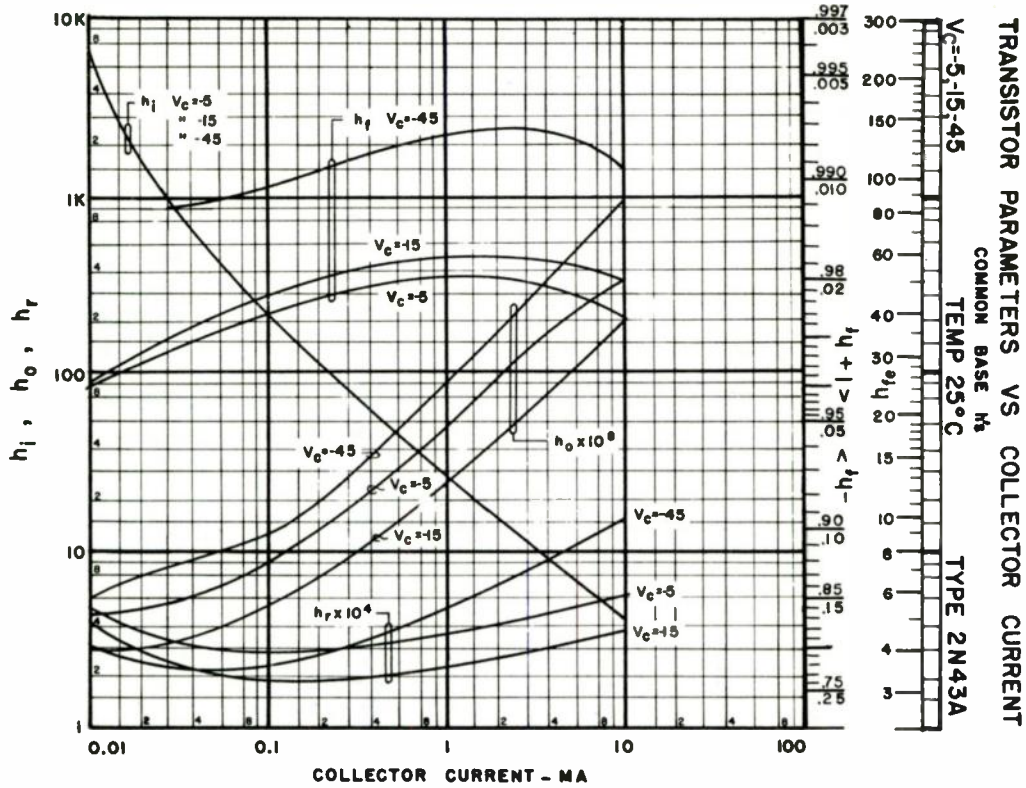

Fig. 6

The h-matrix parameters of the 2N43A transistor, illustrating the variation of each parameter with changes of collector current.

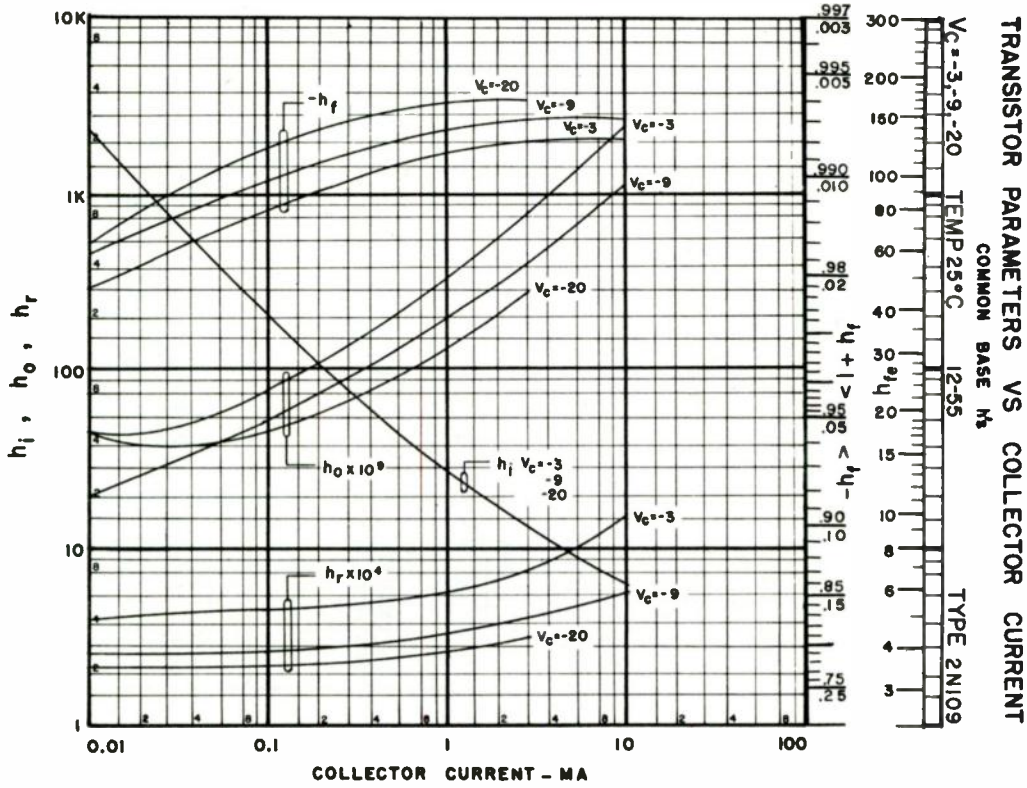

Fig. 7

The h-matrix parameters of the 2N109 transistor, illustrating the variation of each parameter with changes of collector current.

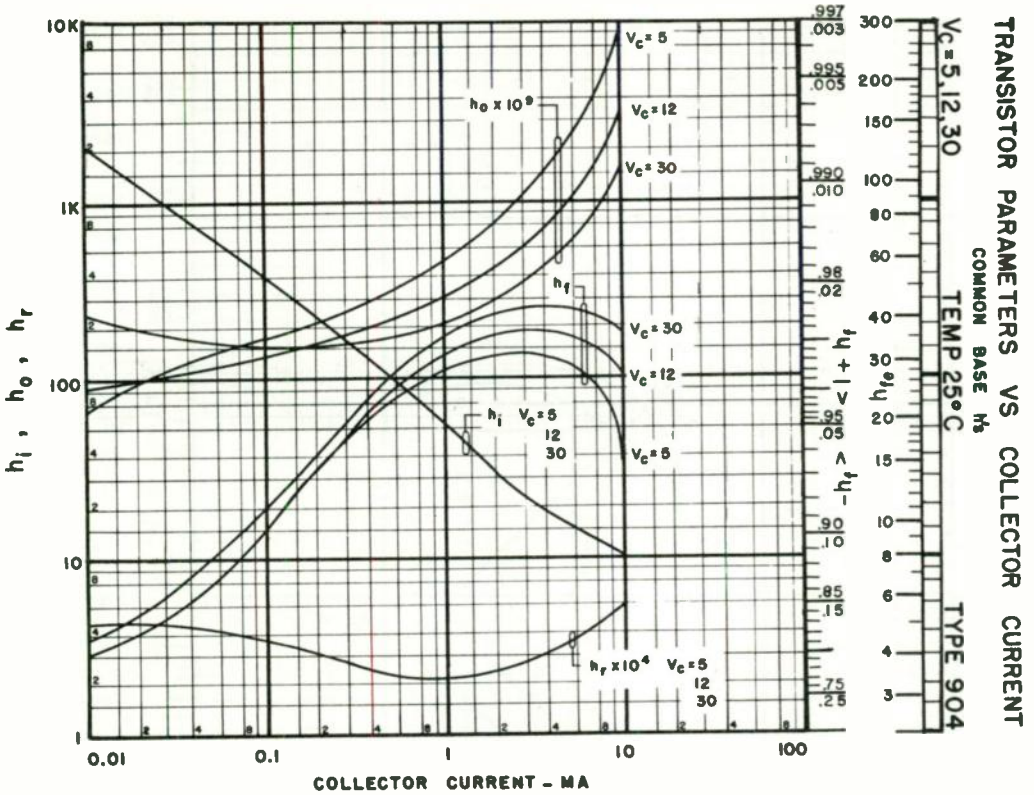

Fig. 8

The h-matrix parameters of the 904 transistor, illustrating the variation of each parameter with changes of collector current.

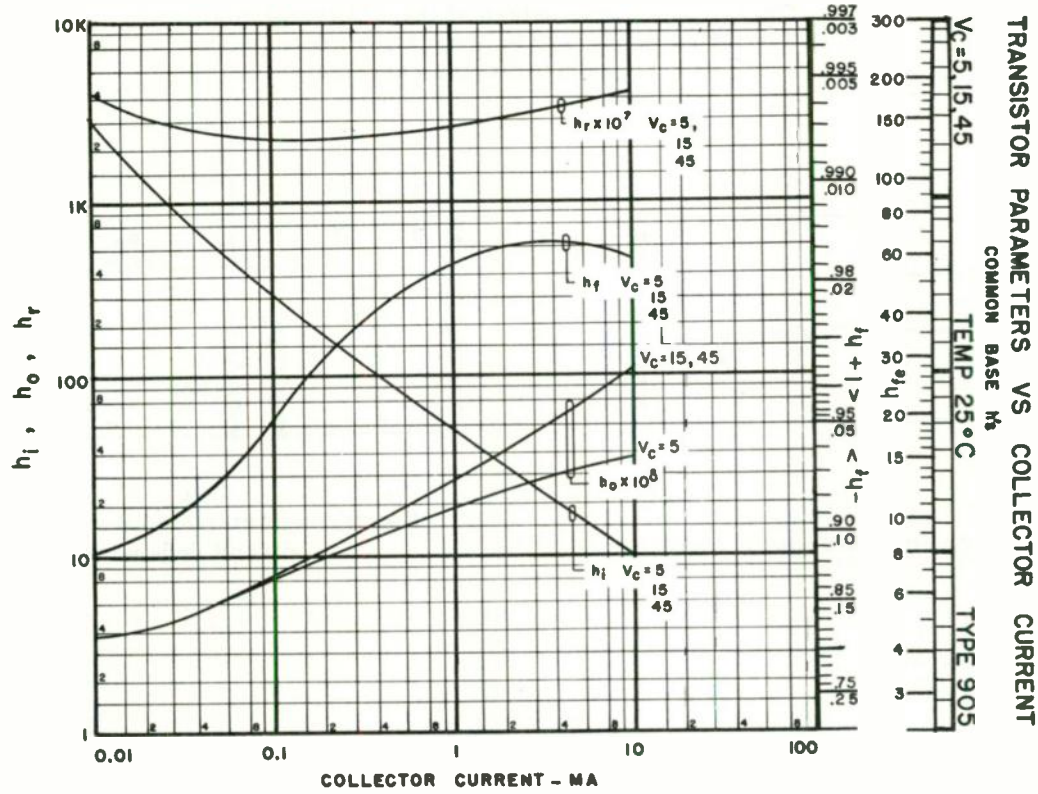

Fig. 9

The h-matrix parameters of the 905 transistor, illustrating the variation of each parameter with changes of collector current.

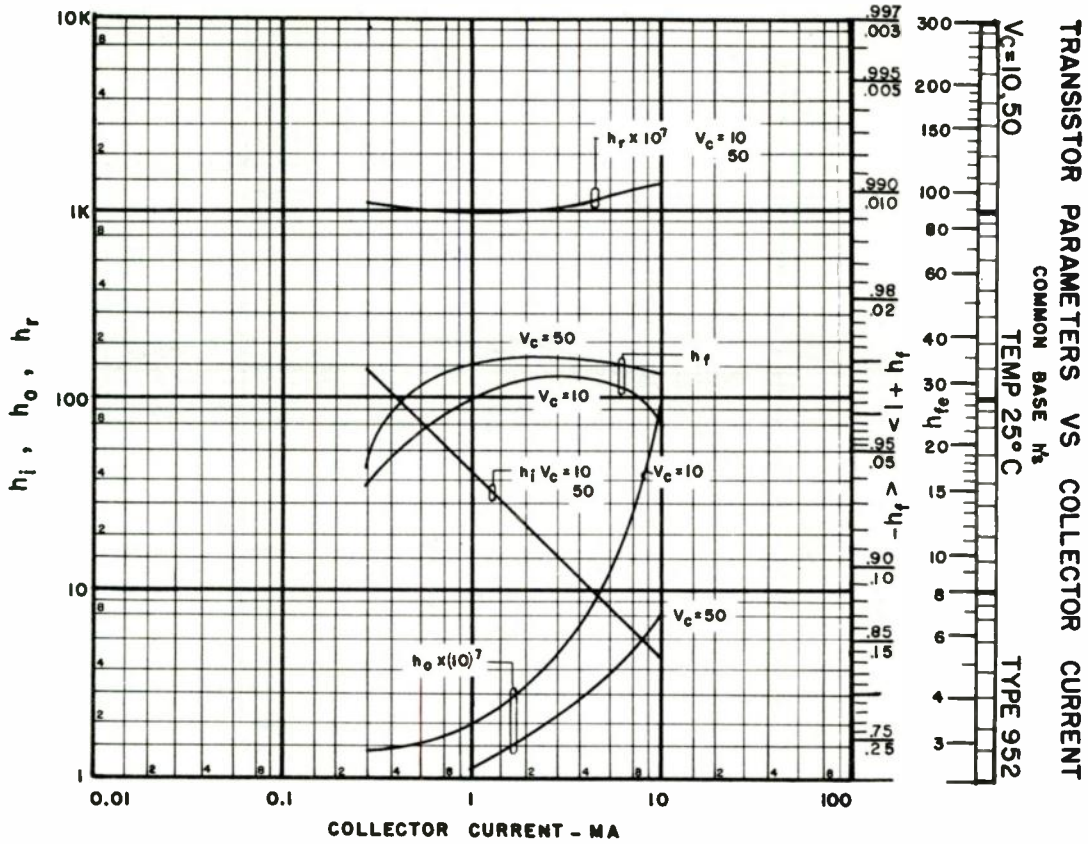

Fig. 10
The h-matrix parameters of the 952 transistor, illustrating the variation of each parameter with changes of collector current.

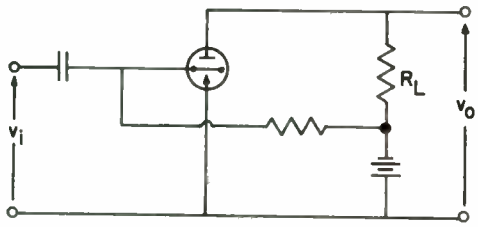

Fig. 11
The basic common-emitter amplifier.

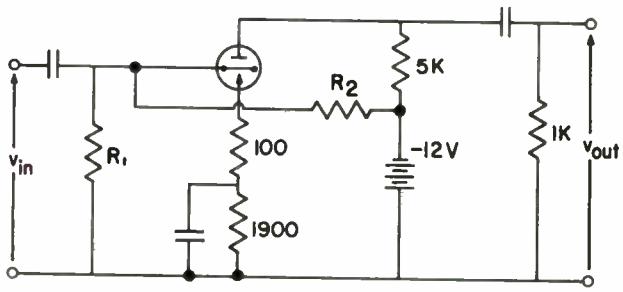

Fig. 12
Common-emitter amplifier with emitter circuit degeneration.

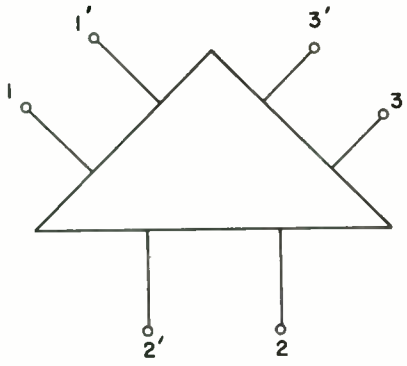

Fig. 13
The fundamental six-terminal network.

Fig. 16
The four-terminal network derived from the six-terminal network of Fig. 13 by shorting the 3′, 3 terminal pair.

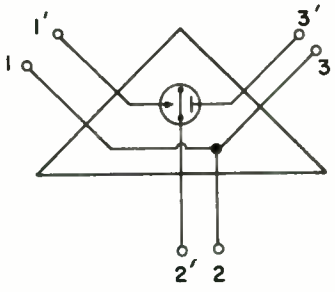

Fig. 14
The transistor as a six-terminal network. Note that the unprimed leads comprise a y-connection independent of the transistor leads.

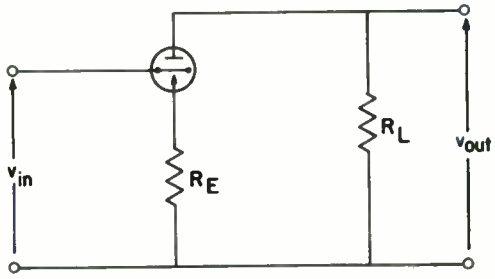

Fig. 17
A common emitter amplifier with an unbypassed resistor in the emitter lead.

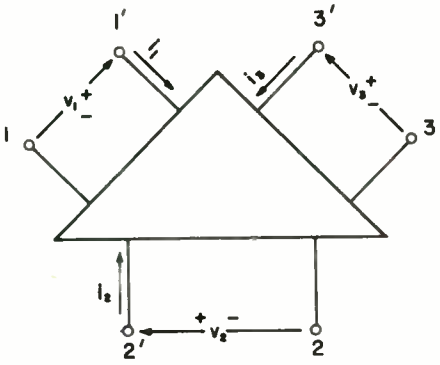

Fig. 15
Polarity conventions of the six-terminal network. The polarities indicated are all "positive."

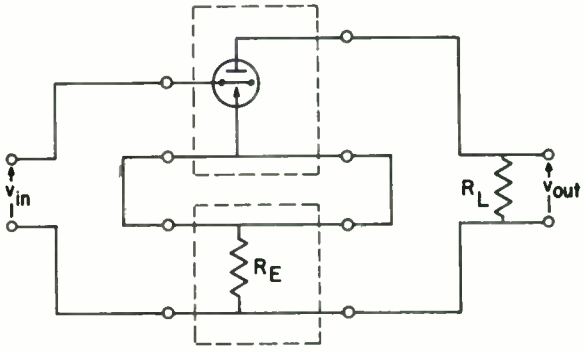

Fig. 18
The circuit of Fig. 17 redrawn to illustrate that it comprises two simple boxes in series. The z-matrix of the combination is equal to the sum of the z-matrices of the individual boxes.

AN AUDIO FLUTTER WEIGHTING NETWORK

Frank A. Comerci and Eliseo Oliveros
U. S. Naval Material Laboratory
Brooklyn, New York

Summary

Listener preference ranking of selected samples of programs containing many types of flutter are compared to measurements of the same flutter using a meter weighted with respect to flutter rate in accordance with the threshold of perceptibility. It is shown that the correct weighting curve varies with the level of flutter and modification should be made to the flutter meter in order to obtain objective rankings of various types of flutter which will agree with subjective rankings of program containing the same type of flutter.

Introduction

In a recent publication[1] it was shown that the effect of flutter on music program was similar to its effect on a 1000 cps tone and it was proposed that a flutter meter, incorporating a flutter rate weighting network based on flutter perceptibility thresholds for tone and music program, coupled with a well damped root-mean-square indicating meter could be used to provide a realistic measurement of flutter or "flutter index". In the experiments reported herein, such a meter was built and flutter index measurements of many varieties of flutter were compared with subjective quality rankings of three types of program containing the same flutter.

Flutter Index Meter

An available flutter meter was selected which contained a low impedance output section for operating an oscillographic recorder. A filter and a standard "VU" meter were connected to this output. The "VU" meter was selected as an indicating instrument in order to have a standard damping characteristic. Differences between "VU" meter readings (rectified average over a standard time period) and thermocouple meter readings (root-mean-square over a non standard time period) on complex flutter waveshapes were found to be small enough to be neglected. The sensitivity of the flutter index meter was as shown in Figure 1 and was adjusted so that the meter gave a reading of 100 percent for a flutter amplitude of 2% peak at a flutter rate of 3 cps. For the low flutter rates where the meter tended to follow the instantaneous flutter amplitude rather than indicate an average, the average peak swing was used as the reading since it was felt at these low flutter rates a peak measurement was more realistic than an rms measurement.

Subjective Rankings

The ranking technique employed was the Listener Preference test described in the previous paper. This test consisted of paired comparisons by a group of judges on program samples containing many variations of flutter. One flutter variation representing that least perceived was used as a standard to which each of the other variations was compared and judged as being "much worse"-"worse"-"same"-"better"-or "much better". The judgements for each program were then quantified for each judge, assigning a number of rank to each judgement category for each judge. The average number of rank assigned by the group of judges for each flutter variation was then taken as the "ranking score".

Flutter Generation

The flutter was introduced into the program material by means of the Material Laboratory Flutter Generator described in the previous article which used a magnetic head mounted to a loudspeaker cone to generate the flutter and also by means of a tape recorder which had a low flutter content when operating without a fly wheel, introducing the desired flutter by varying the frequency of the power source used to power the synchronous driving motor. The former was found to be wanting for flutter rates below 5 cps but ideal for the high flutter rates whereas the latter was ideal for the low flutter rates but wanting at the high rates. The latter system also made it possible to duplicate the type of flutter found in equipment by driving the motor by means of the amplified signal from a 60 cps recording as played back on the particular equipment. Since two different flutter generators were used, the experiments were divided into two parts for any differences other than flutter between the two generators might have influenced comparisons. In the first experiment, approximately 10 second passages of piano, military band, and speech program were selected from recordings of live local F.M. broadcasts. Piano and band were selected as being more susceptible to the effects of flutter. These selections together with a 20 second sample of a 3000 cps tone, which was recorded on the same recorder used to record the program, were spliced together at the center of a 1200 ft

reel of tape. The selections were then played back on the flutter generator, adding the flutter as required and rerecording on another recorder to obtain samples of fluttered program for use in the subjective tests and samples of tone for use in obtaining flutter measurements. Since the 3000 cps samples of tone had undergone the same operations as did the program, the flutter on these samples was the equivalent of that introduced in the program. Flutter oscillograms obtained from the tone samples are shown in Figure 2 to indicate the complexity and range of flutter variations used in this experiment. The program samples were spliced together to permit A-B comparisons between each flutter variation and the standard variation for each program. Program randomization was not employed in this experiment and for each comparison the standard was presented first. In the second experiment approximately 10 second passages of piano, band, and speech program were used. The method of introducing flutter was similar to experiment one except that the special recorder was used. In the first experiment, the particular flutter variations used were selected to give a representative sampling of flutter rates from 4 to 100 cps and amplitudes which were judged to provide a range from non-perceptible to maximum perceptibility. In this second experiment 20 single rate flutter variations were chosen with amplitudes randomly chosen to provide equal increments of perceptibility. Ten additional variations were randomly selected to contain a combination of high and low flutter rates with amplitudes judged to provide equal increments of perceptibility. Ten additional variations were representative of actual projector, disc playback, and tape recording equipment. Representative oscillograms are shown in Figure 3. The samples of fluttered program when spliced for the subjective comparisons were arranged in a statistically random fashion with respect to type program, flutter variation and presentation of standard.

Listener Preference Tests

For the Listener Preference tests, 18 judges all male ranging in age from 23 to 40 years were located in an acoustically soft listening room. The program comparison tapes were played back through a triaxial loudspeaker system to the group which was located about 20 feet from the speaker along the length of the room. The response of the overall system from initial program recording to final presentation to the judges was essentially that of the loudspeaker which ranged from approximately 40 to 15000 cps with only minor peaks and dips in response. The harmonic distortion for simusoidal signals from 100 to 10000 cps representing the amplitude of the program peaks was less than 1½ percent while the signal to noise ratio was about 45 db. Inherent flutter in the overall system was about 0.3% peak at a flutter rate of 6 cps. Amplitude variations in the order of seven percent peak were random in nature and introduced by the magnetic tape recording processes. Any amplitude variation which might have been caused by the flutter generators could not be detected in the electrical signal. Listener preference ranking scores were computed for each of the three programs for each experiment. Results were expressed in percent of the maximum score obtained. Finally, the listener preference tests of the second experiment were conducted for the following different room conditions, frequency response ranges, and sound levels and compared to ascertain any significant effect of these conditions on the listener preference rankings.

Condition A (Used for Listener Preference Test 1 and 2)

An acoustically soft listening room about 100 ft. long, 20 feet wide and 10 feet high. The walls and ceiling were polycylindrical and covered with acoustic tile. The floor was rug covered concrete.

Condition B

A diffuse reverberation chamber with polycylindrical walls and ceiling of poured concrete. The floor was poured concrete but flat. The chamber was about 20 feet long, 20 feet wide and 10 feet high. The reverberation time in the absence of the judges was about 5 seconds at 1000 cps.

Condition C

A room about 20 feet long, 15 feet wide and 12 feet high having flat brick surfaces on which were hung removable panels of acoustic tile randomly spaced over the wall surface. The floor was rug covered. The reverberation time of this room was about 0.5 seconds at 1000 cps.

Condition D

Same acoustic conditions as C but the frequency response of the system was restricted to the range 300 to 3000 cps.

Condition E

Same acoustic conditions as C but peak program level was reduced by about 10 db to 80 db.

Condition F

The judges were presented the program at a level of 60 db (program peaks) through high quality earphones having a range from about 40 to 8000 cps.

RESULTS

The flutter index measurements and listener preference ranking scores for the thirty flutter variations used in Listener Preference Test 1 are shown in Table 1 along with peak to peak flutter readings which were determined from flutter oscillograms for each flutter variation. Comparison of the ranking scores with the peak to peak flutter measurements, as expected, shows that little relationship exists between them. An appreciable relationship between the listener preference ranking scores and the flutter index measurements did exist.

The flutter index measurements and listener preference ranking scores for the forty flutter variations used in Listener Preference Test 2 are shown in Table 2 along with peak to peak flutter readings which were determined from the flutter oscillograms. Again, little relationship exists between the ranking scores and peak to peak flutter but an appreciable relationship exists between these scores and the flutter index measurements. When the average preference scores for piano and band were plotted against flutter index readings for each test, it was noted that the points seemed to indicate two straight line relationships, one for low flutter rates and another for high flutter rates, shown as A and B respectively in Figure 4. When the listener preference ranking scores for speech were plotted against flutter index, the same two straight line relationships were indicated. However, in the case of speech there was a scattering of points on that side of the lines which signified good quality but an excessive flutter index. This was expected, for it was known that large amounts of flutter at flutter rates below 5 cps could not be detected in speech. The weighting curve used in the flutter meter was considered applicable to music only but it was felt that it could also be applied to speech since any resulting flutter index measurements would always be on the safe side.

On examining the two straight line relationships it was noted that practically all of the points indicating the line B on Figure 4 were associated with a flutter rate between approximately 10 and 25 cps and amplitudes greater than 1% peak. This was thought to be due to either the particular room acoustics under which the listener preference tests were performed or a non linearity in the relationship between the effect of flutter and its amplitude for this flutter rate range. Further experiments showed that the room acoustics, at least for the recorded program used, had only a minor effect on the results of the listener preference tests. Therefore, the discrepancy was attributed to non linearity. It is conceivable, that in detecting flutter at flutter rates above 10 cps, human factors differing from those used at flutter rates below 7 cps come into play.

To correct for the above would require a new extended experiment to determine the exact relationship existing between the flutter perception and amplitude for various listening conditions. However, as an immediate means for obtaining a realistic measurement of flutter, a simple expedient was considered. As mentioned, the excessive ranking scores or more accurately stated, the low flutter index readings, occurred only when the flutter exceeded 1 percent. It would then only be necessary to measure the average unweighted flutter for flutter rates above about 10 cps. If the 1% peak level (0.7% r.m.s. level) were not exceeded then the flutter index meter having the weighting curve of Figure 1 would be satisfactory. If the 1% level were exceeded then the weighting curve would have to be modified. Fortunately in Listener Preference Test 2 enough sinusoidal flutters of known amplitude were included to permit an adequate estimate of the proper modification to the weighting curve.

A flutter index meter was subsequently designed which incorporated the two weighting networks with an automatic electronically operated switch. The two weighting curves employed are shown in Figure 5. Curve A represents the active weighting characteristic for the switch open position. Curve B represents the active weighting characteristic for the switch closed position. The operation of the automatic switch was controlled by the unweighted flutter signal as shown by its operating characteristics in Figure 6. The switch actuating circuit operated on a rise time-constant of 0.1 sec and a decay time-constant of 0.25 sec.

Flutter index readings obtained with this modified flutter index meter for the flutter variations of both listener preference tests are compared with the average listener preference ranking scores for piano and band in Figure 7. The flutter index measurements are tabulated in Table 3. The relationship is considerably improved. The relationship for speech was similarly improved.

The piano and band ranking scores of the flutter variations used in Listener Preference Test 2 for the six types of listening conditions are listed in Table 4 and show that the differences in listening conditions had small effect on the subjective ranking.

Conclusion

A flutter index meter having the characteristics of the modified flutter meter used in these experiments will provide a reading that will adequately predict the subjective ranking score which would be obtained were that flutter introduced in program samples and included in a Listener Preference test similar to that employed herein. Thus, such a meter will provide a realistic measure of flutter in program material.

Discussion

The various types of flutter employed in this experiment were representative of all the amplitudes and waveforms encountered in actual recording equipment over flutter rates from 0.5 to 100 cps. It might be expected that flutter rates above 100 cps might be encountered. Recently, flutter rates as high as 3000 cps are being observed in magnetic tape recorders. In view of this, it would have been interesting to extend the experiments to these flutter rates. Unfortunately, the flutter generators available could not produce adequate flutter amplitudes above flutter rates of 100 cps. Besides, previous observations indicated that judgements of flutter perceptibility in program for this range were erratic. It has been shown by H. Schecter[2] that in the range above flutter rates of 100 cps flutter perceptibility thresholds for tone can be used to predict the masking curves for the ear. It therefore would appear that perceptibility of flutter for such rates would be alien to the perceptibility of noise and could be included in a noise measurement (noise behind the signal).

It should be noted that in a few of the flutter variations the peak flutter amplitude varied periodically with time, for example observe types 9 and 16 in Figure 2. For this type of variation, the effect on the listener seemed to be connected with the average amplitude of the flutter over about a two-second time period. It also seemed to be a function of how the large amplitude periods coincided with the program peaks. Since, in obtaining flutter index readings, the average peak swing of the indicating instrument was used to indicate the flutter index, the flutter index readings tended to be too high relative to the corresponding listener preference score. Such a reading applies a margin of safety for that type flutter.

In a recent British publication[3] a flutter meter with a peak indicator and a flutter weighting network which peaks at flutter rates between 5 and 10 cps was proposed for obtaining realistic flutter measurements. This contradicts the results of the experiments reported herein. Another flutter meter was built using the above proposed weighting network. An oscillographic recorder was used as an indicator from which the peak weighted amplitudes for all of the flutter variations of Listener Preference Test 2 were obtained. The corresponding ranking scores were compared with these readings but little correlation was obtained. Most of the variation appeared to be due to the different weighting network but it was felt that some also resulted from the use of a peak indicator. A concrete explanation for the contradiction can not be advanced at this time.

In order to compare the results of the present experiments with those of the previous experiments the listener preference ranking scores of the latter for flutter rates from 0.5 to 5 cps and amplitudes up to 5 percent peak were replotted in the form of equal ranking score contours as shown by the solid lines of Figure 8. On this curve were plotted 43 of the 70 flutter variations employed in the present experiments, indicating in circles the appropriate ranking scores obtained. The remainder of the 70 flutter variations were not included since they either duplicate observations that are shown or their amplitudes and rates could not be determined adequately. The ranking scores, indicated at the plotted observations, are related to the contour lines. It should be noted that most of the ranking scores between 25 and 30 percent fall on or below the threshold curve, all the ranking scores of about 33 percent fall near the LP-30 line etc. until all ranking scores between 80 and 100 percent fall above the LP-80 contour line. This shows agreement between the previous and present experiments. The dotted lines on this figure represent an extension of the equal ranking score contours to flutter rates above 5 cps as estimated from the results of the present experiments. These extended contours, by their squeezing together above 10 cps, suggest the non-linearity experienced for the flutter rates between 10 and 25 cycles per second. It is obvious that further experiments are required to obtain an adequate measure of this non linearity.

References

1. Frank A. Comerci "Perceptibility of Flutter in Speech and Music" Trans IRE PGAU-3 pp 62-70 May-June 1955.

2. H. Schecter "Perceptibility of Frequency Modulation in Pure Tones" Doctoral Thesis, Mass. Inst. Tech.; 1949.

3. A. Stott and P.E. Axon "The Subjective Discrimination of Pitch and Amplitude Fluctuations in Recording Systems" Proceedings I.E.E., Paper No. 1874R, Sept. 1955.

NOTE: The opinions or assertions contained in this paper are the private ones of the authors and are not to be construed as official or reflecting the views of the Navy Department or the Naval Service at large.

Table 1

Flutter Index Measurements and Listener Preference Ranking Scores for Listener Preference Test I

Flutter Variation No.	Flutter Measurements Peak to Peak Flutter %	Flutter Index	Listener Preference Ranking Scores (% of Max. Score) Piano	Band	Speech	Aver-Piano & Band
1	4.0	55	59	41	20	50
2	2.5	55	61	59	38	60
3	6.2	67	100	97	89	98
4	3.5	49	75	83	70	79
5	3.0	49	62	77	66	70
6	2.7	57	51	56	60	54
7	5.6	84	82	97	89	90
8	2.4	52	51	55	59	53
9	5.7	43	63	57	45	60
10	5.0	55	86	88	84	87
11	2.5	31	49	44	50	47
12	4.0	52	44	59	34	52
13	5.0	61	66	86	60	76
14	4.0	39	32	48	36	40
15	1.5	25	28	22	25	25
16	8.5	55	85	76	60	81
17	4.4	58	62	74	87	68
18	8.0	58	65	71	82	68
19	1.2	23	25	19	25	22
20	1.8	41	12	9	22	11
21	3.5	54	33	42	39	38
22	3.6	47	48	59	59	54
23	5.5	61	93	97	100	95
24	2.7	38	29	27	30	28
25	2.7	25	53	40	57	47
26	3.7	43	41	50	69	46
27	1.0	26	20	14	15	17
28	3.3	54	69	85	84	77
29	3.5	26	34	23	26	29
30	7.5	58	91	100	87	96

Table 2

Flutter Index Measurements and Listener Preference Ranking Scores for Listener Preference Test II

Flutter Variation No.	Flutter Measurements: Peak to Peak Flutter (%)	Flutter Measurements: Flutter Rate (cps)	Flutter Measurements: Flutter Index	Listener Preference Ranking Scores (% Max. Score): Piano	Band	Speech	Aver-Band & Piano
1	6.6	0.5	90	93	93	39	93
2	7.6	0.5	97.5	89	94	47	92
3	2.0	0.75	31	65	19	39	42
4	3.0	1	55	43	47	47	45
5	7.6	1	100	97	100	48	99
6	4.6	1.5	97	93	88	33	91
7	2.6	2	55	36	54	47	45
8	3.0	3	60	43	44	49	44
9	4.4	3	85	87	86	53	87
10	6.0	4	87	91	100	52	96
11	1.6	6	20	39	34	41	37
12	5.4	6	55	98	98	44	98
13	0.8	8	10	26	23	44	25
14	1.5	10	18	35	28	38	32
15	2.4	5	32	39	41	34	40
16	5.6	10	45	88	92	84	90
17	7.0	15	48	100	100	100	100
18	3.6	20	32	64	83	69	74
19	5.6	20	40	77	99	86	88
20	5.3	25	36.5	93	90	87	92
21	8.6 4	0.5 12	95	100	100	92	100
22	6.0 2.0	0.75 27	96	87	98	73	93
23	1.0 0.2	1 12	20	32	27	35	30
24	3.6 2.0	2 9	90	57	78	49	68
25	2.6 0.8	2 24	75	74	44	44	59
26	4.0 2.0	3 24	88	86	89	54	88
27	1.0 0.5	4 21	20	34	33	32	34
28	4.4 3.0	4 18	68	94	95	62	95
29	3.4 1.4	5 18	43	75	73	58	74
30	4.8 2.0	6 15	56	98	83	65	91
31	-	-	10	35	32	43	34
32	-	-	55	90	94	84	92
33	-	-	35	39	54	46	47
34	-	-	25	25	39	46	32
35	-	-	60	53	59	46	56
36	-	-	45	46	43	41	45
37	-	-	25	21	27	47	24
38	-	-	28	37	44	31	41
39	-	-	25	30	25	49	28
40	-	-	40	31	25	31	28

Table 3

Flutter Index Measurements Obtained with Modified
Flutter Index Meter for Listener Preference Tests I and II

Experiment	Flutter Type	Flutter Index	Flutter Type	Flutter Index
I	1	-	16	70
	2	-	17	95
	3	120	18	85
	4	77	19	23
	5	70	20	35
	6	58	21	65
	7	98	22	63
	8	59	23	115
	9	55	24	35
	10	95	25	65
	11	50	26	60
	12	55	27	25
	13	85	28	80
	14	65	29	25
	15	33	30	115
II	1	80	21	130+
	2	95	22	120
	3	35	23	25
	4	45	24	87
	5	120	25	80
	6	100	26	100
	7	55	27	25
	8	65	28	98
	9	95	29	70
	10	102	30	94
	11	30	31	15
	12	98	32	95
	13	12	33	48
	14	30	34	35
	15	42	35	45
	16	93	36	45
	17	116	37	25
	18	75	38	35
	19	95	39	25
	20	83	40	40

Table 4

Comparison of Listener Preference
Ranking Scores for Various Listening Conditions

Flutter Variation No.	Listening Condition A Piano	A Band	B Piano	B Band	C Piano	C Band	D Piano	D Band	E Piano	E Band	F Piano	F Band	All List. Cond. Aver.
1	93	93	95	97	92	100	100	100	92	89	94	100	95.4
2	89	94	94	94	96	97	100	97	100	98	96	99	96.2
3	65	19	55	28	40	19	43	19	52	21	46	24	36.0
4	43	47	55	54	57	50	73	48	56	56	64	59	55.2
5	97	100	83	94	100	100	100	100	100	100	100	100	97.8
6	93	88	100	97	100	100	96	100	100	97	93	95	96.6
7	36	54	54	49	28	46	31	57	40	50	36	49	44.2
8	43	44	48	41	49	38	47	42	61	43	30	44	44.2
9	87	86	96	81	89	86	100	94	96	85	90	82	88.5
10	91	100	91	93	100	100	100	100	98	100	88	100	96.8
11	39	34	39	25	29	25	39	32	40	25	31	30	32.3
12	98	98	100	100	100	100	100	100	100	100	92	100	99.0
13	26	23	28	23	29	27	30	26	21	24	34	26	26.4
14	35	28	29	26	18	26	29	33	33	31	33	30	29.3
15	39	41	62	55	44	51	44	36	43	57	42	39	46.1
16	88	92	98	84	100	100	100	97	100	100	85	97	95.1
17	100	100	96	93	100	100	100	100	96	100	100	100	98.8
18	64	83	71	79	82	81	98	95	92	89	42	68	78.7
19	77	99	87	96	100	97	100	100	94	100	68	91	92.4
20	93	90	96	77	98	91	96	93	95	93	79	83	90.3
21	100	100	100	100	100	100	100	100	100	100	100	100	100.0
22	87	98	92	87	94	100	100	100	100	97	80	97	94.3
23	32	27	27	30	22	24	29	27	19	30	31	37	27.9
24	57	78	78	76	66	83	69	90	91	83	69	83	76.9
25	74	44	92	63	84	52	100	60	91	41	80	39	68.3
26	86	89	88	92	97	96	100	100	100	100	74	95	93.1
27	34	33	35	33	32	31	30	31	34	25	38	31	32.3
28	94	95	100	90	100	100	100	100	100	100	90	96	97.1
29	75	73	96	77	83	82	100	83	87	83	54	73	80.5
30	98	83	100	81	92	91	100	89	100	92	79	86	90.9
31	35	32	28	31	43	24	37	24	38	20	48	24	32.0
32	90	94	100	86	96	100	95	100	92	100	95	90	94.8
33	39	54	36	48	33	56	35	52	39	49	29	44	42.8
34	25	39	26	36	25	36	17	30	21	26	27	30	28.2
35	53	59	36	46	63	59	56	59	55	64	54	65	55.8
36	46	43	84	43	50	39	56	42	52	40	63	40	49.8
37	21	27	25	31	25	32	17	31	22	24	30	30	26.3
38	37	44	44	39	28	26	32	32	33	38	28	31	34.3
39	30	25	29	27	44	29	26	28	27	26	34	26	29.3
40	31	25	41	32	30	18	34	30	25	24	33	26	29.1

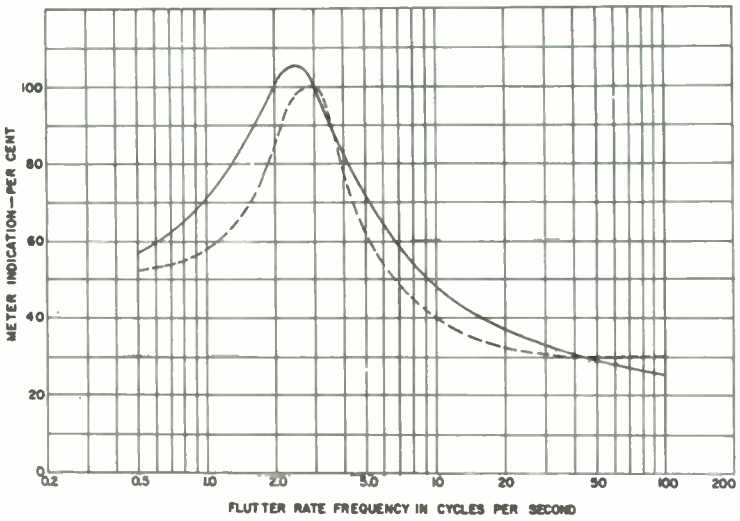

Fig. 1
Sensitivity vs. flutter rate for material
laboratory flutter index meter
Input flutter 2.0% (Peak)
_____ measured sensitivity
- - - - - - - design objective

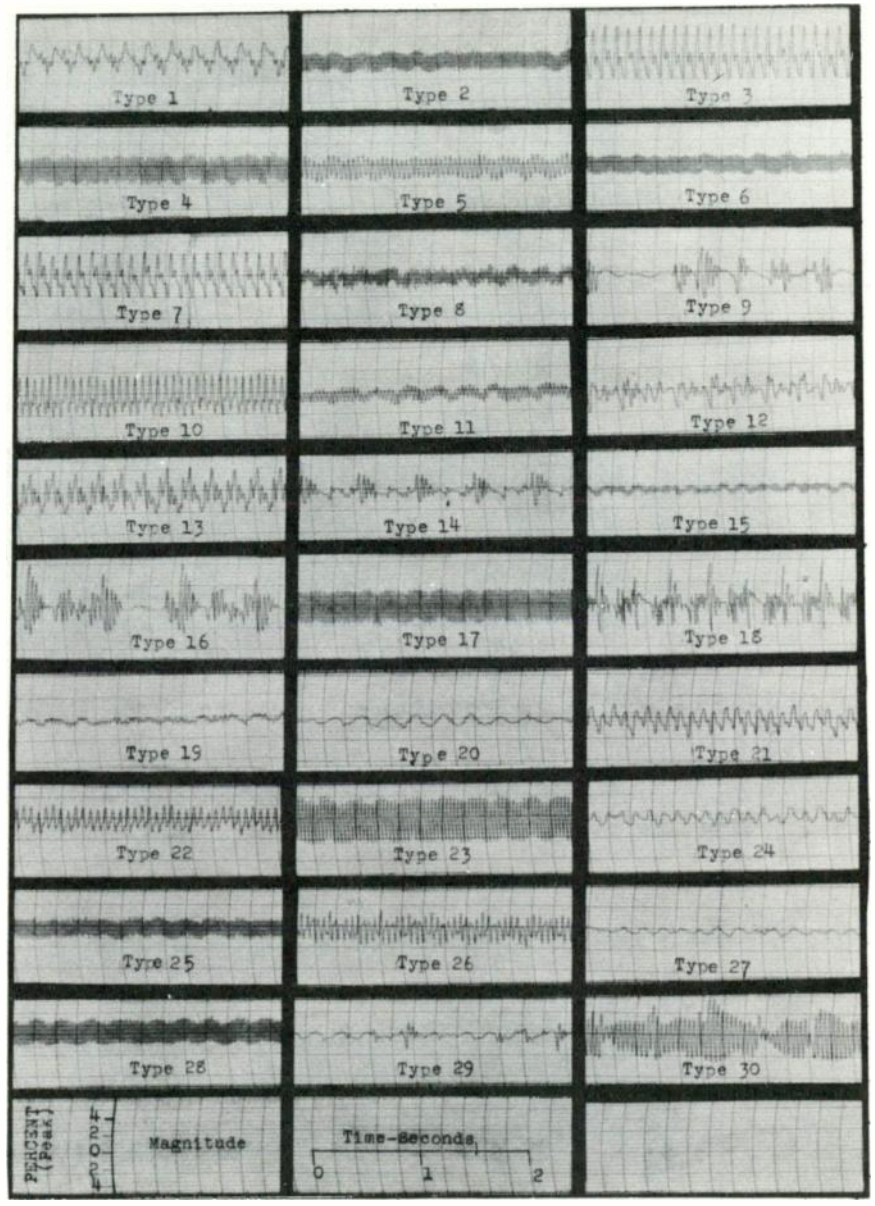

Fig. 2
Oscillograms for flutter variations used in
listener preference test I (Photo L16711-1)

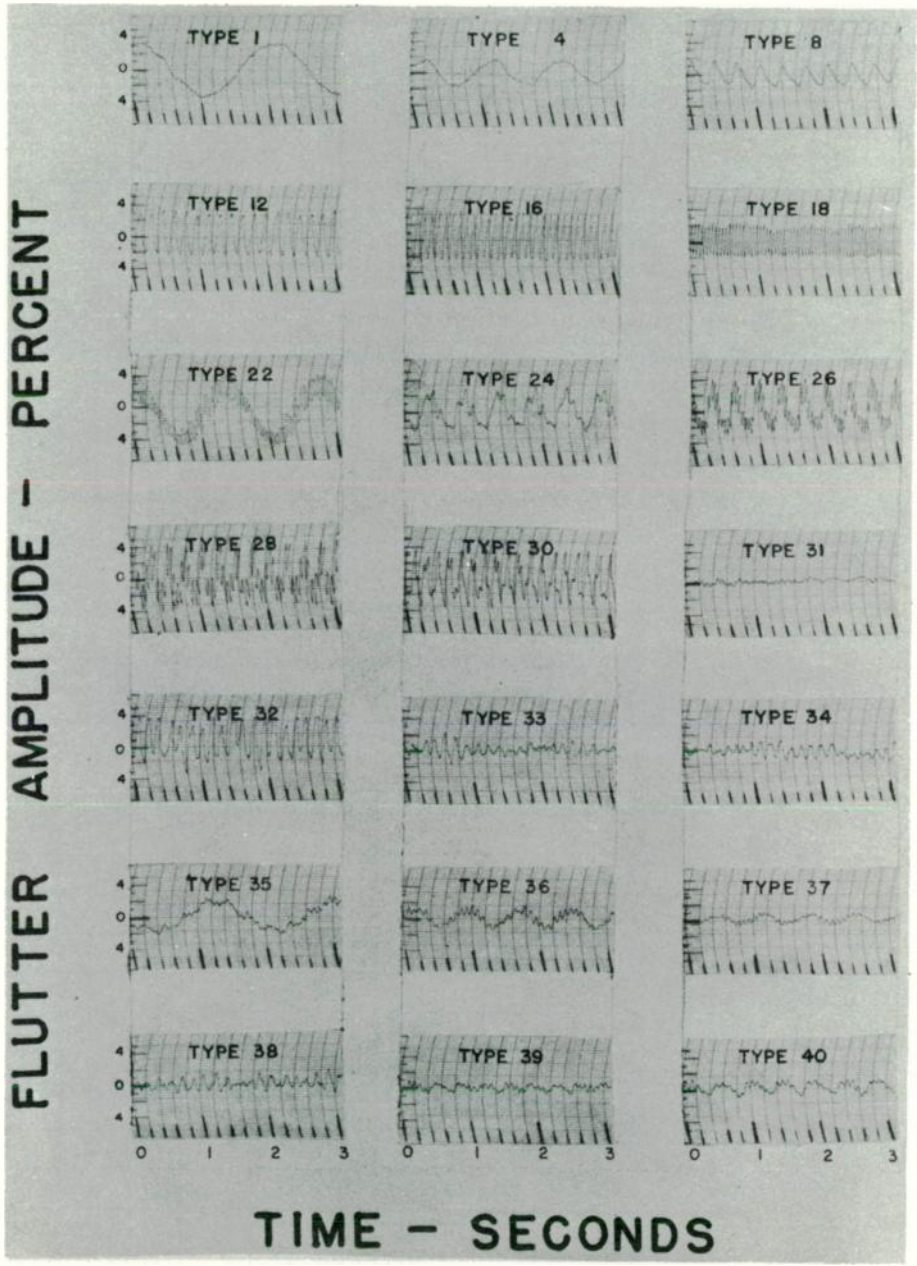

Fig. 3
Oscillograms for more complex flutter variations used in listener Preference Test II.
(Photo L16711-2)

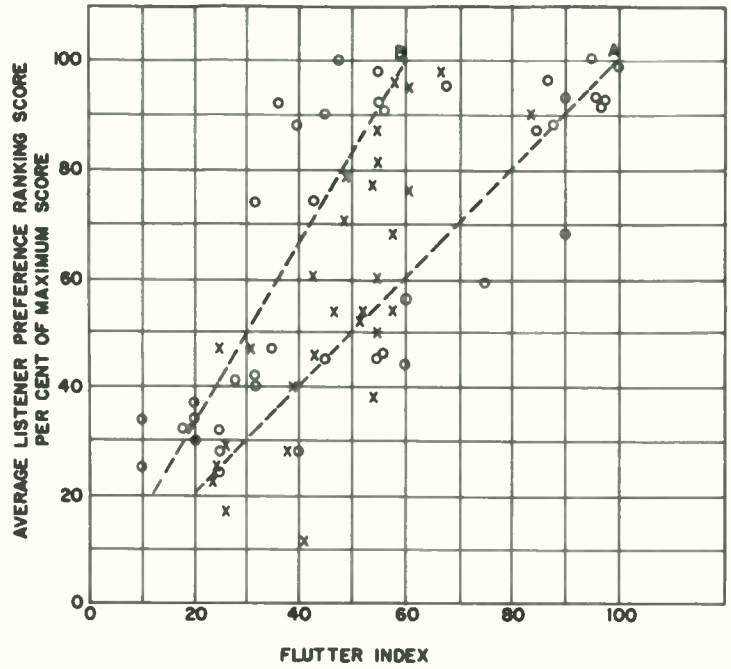

Fig. 4
Average listener preference ranking scores for piano and band programs vs flutter index. Includes data from Listener Preference Tests I and II. X listener experiment 1 O experiment 2.

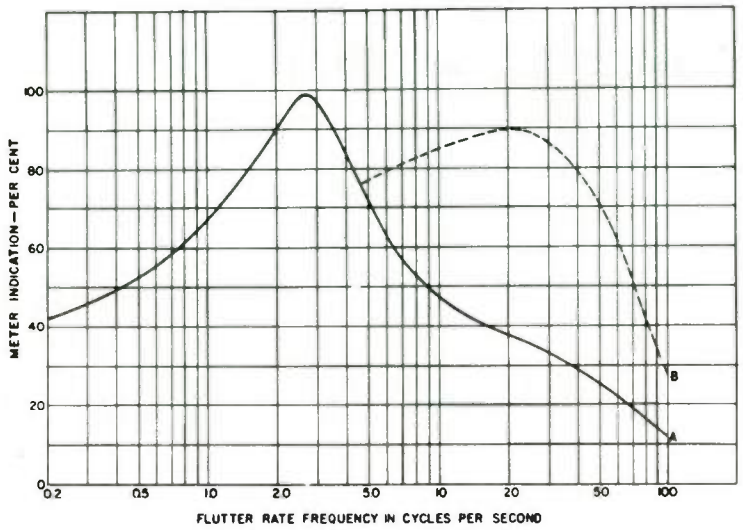

Fig. 5
Sensitivity vs flutter rate for material laboratory modified flutter index meter. Input flutter 2.0% (Peak). Curve A - Sensitivity for switch open position. Curve B - Sensitivity for switch closed position.

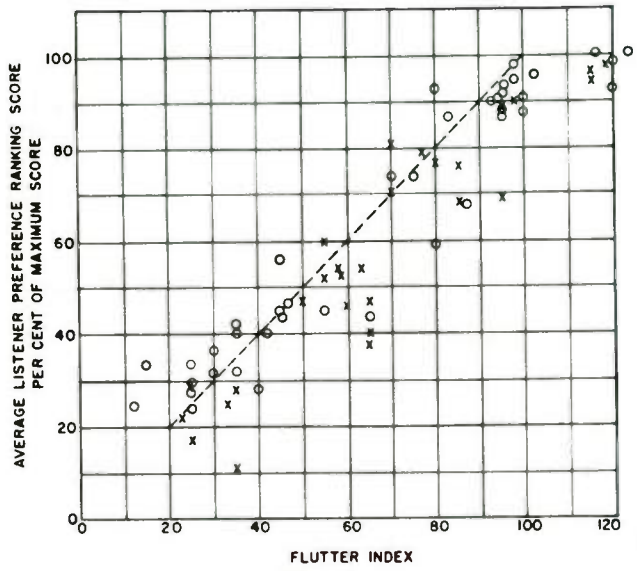

Fig. 7
Average listener preference ranking scores for piano and band program vs. modified flutter index. Includes data from Listener Preference Tests I and II
X Experiment 1 O Experiment 2.

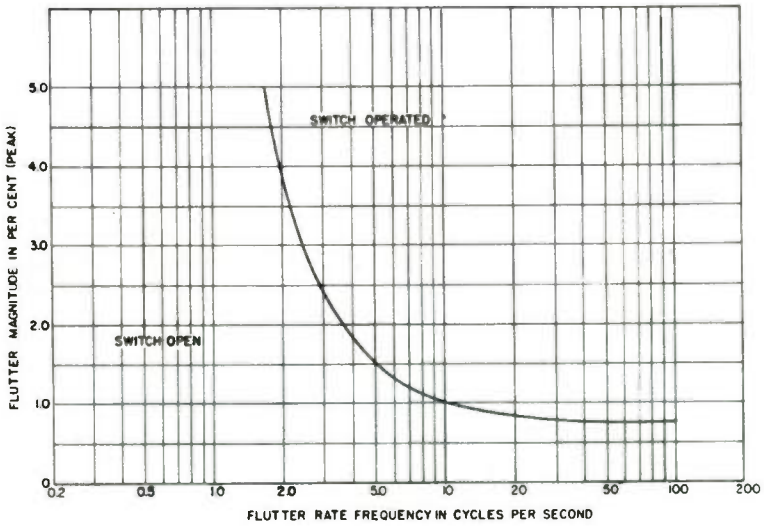

Fig. 6
Operating characteristic for automatic electronic switch of material laboratory modified flutter index meter.
Switch actuating circuit rise time constant 0.1 sec.
Switch actuating circuit decay time constant 0.25 sec.

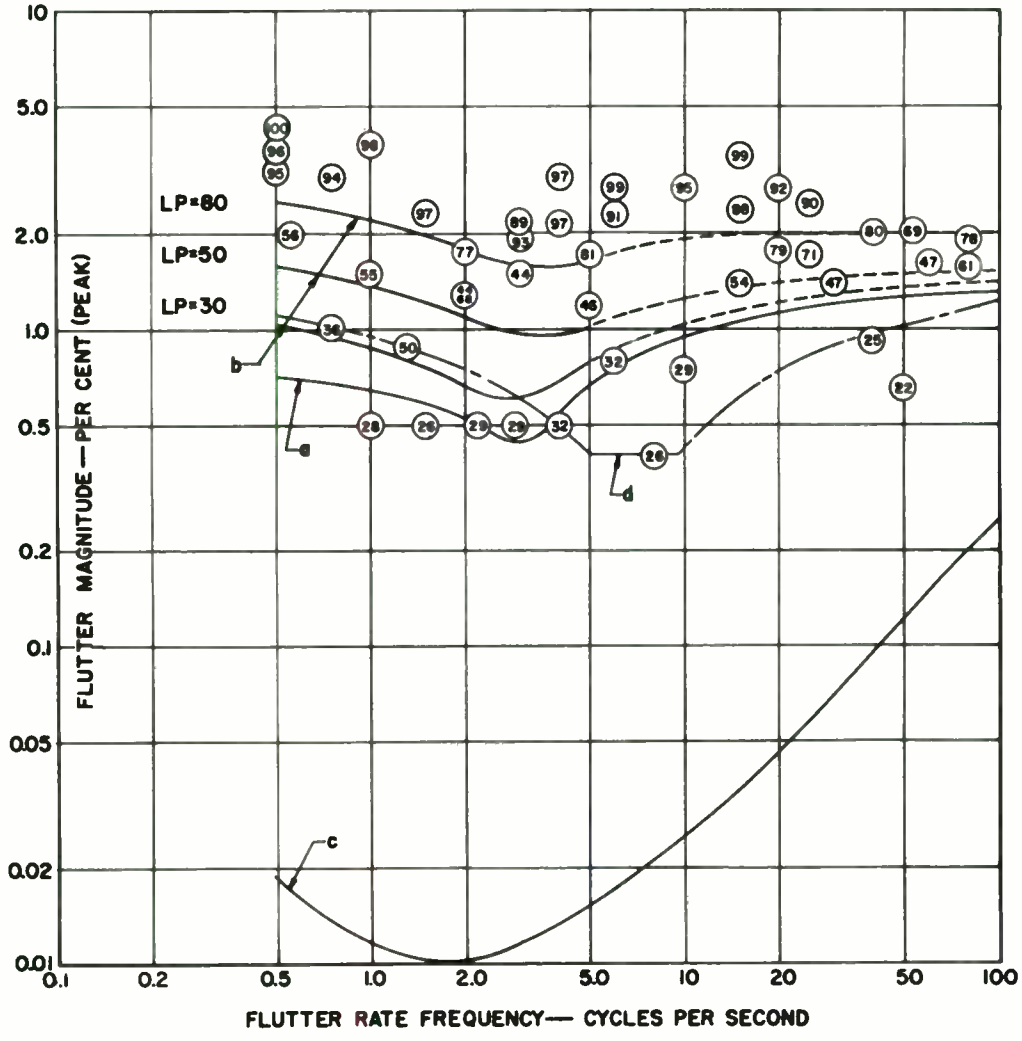

Fig. 8
Comparison of listener preference ranking scores with results of previous experiments.
a - Flutter threshold for recorded piano program (Material lab) b - Contour lines for equal listener Preference ranking scores c - Flutter threshold for 1000 cps tone in reverberant auditorium (Bell telephone labs) d - Stott and Axon flutter threshold for piano. Encircled numbers represent ranking scores obtained in experiments 1 and 2.

A FLUTTER METER INCORPORATING SUBJECTIVE WEIGHTINGS

M. A. Cotter
Consumers Union of the U.S., Inc.
Mount Vernon, N. Y.

ABSTRACT

An instrument is described which incorporates flutter rate weighting networks and utilizes a true rms indicating meter. Another feature is an aperiodic fm detector utilizing a pulse counting technique, which permits using a wide variety of carrier frequencies for flutter measurement, as well as direct frequency (or medium) speed indication. The rms indicating meter incorporates a control response damping characteristic. The instrument shows little aging drift and good stability to calibration. The unit can be readily constructed from standard components.

A SIMPLIFIED METHOD FOR THE PERFORMANCE MEASUREMENT OF MAGNETIC TAPE RECORDERS

J. B. Hull
Ampex Corporation
Redwood City, California

Introduction

Magnetic recording has become one of the most useful and versatile tools in the audio field. Recording studios almost universally use tape for recording material to be processed onto discs. Broadcast stations utilize tape for delayed program operation, split programming, on-the-spot recording, and as a convenience facility for storing material to be released either in modified sequence or at some later time. Although widespread use is made of tape machines in other fields such as computer networks and instrumentation, the primary emphasis in this paper is in the audio field.

Advances in engineering design and in manufacturing processes have made possible machines of greatly improved characteristics over those made a few years ago. They are reliable, relatively simple and inexpensive to operate, and a large amount of recorded material can be stored in a relatively small space. Generally, the performance which can be obtained from a professional tape recorder exceeds that required in actual service.

In essence, the operator of a tape machine desires three qualities in the performance of his recorder: consistency of performance, equivalence of input and output, and interchangeability of tapes among his recorders and others like it.

In order to maintain this operational utility, careful performance checks must be made periodically on the machines in question. There are several approaches to the problem of performance checking, and two will be examined here: first, a method such as might be employed in the engineering laboratory, and second, a simplified technique derived from these laboratory procedures which minimizes the time and equipment requirements for the task.

Problem Statement

A tape recorder may be considered as a variable delay transmission network having both electrical and mechanical elements. The design of these elements is directed toward achieving a linear input versus output characteristic. The electrical characteristics should be such that frequency response from record amplifier input to the output of the playback amplifier through the tape should be uniform. Further, tapes recorded on one machine should be reproduced on other similar machines within the recorder performance specifications. To accomplish these objectives it is necessary to provide record and playback amplifiers having suitable equalization.

Although the mechanical elements are largely fixed by the design and manufacturing operations, the quality of the mechanical performance is reflected in the quality of the electrical output. For example, velocity variations in the transportation of the tape over the record and playback head appears in the output of the machine as flutter in the case of the relatively higher frequency variations or as a timing error in the case of the very slow variations.

To examine some of the characteristics of the network over which surveillance must be exercised, let us consider the case of record and playback amplifier equalization.

Figure 1 shows a typical record amplifier equalization curve with pre-emphasis at the higher frequencies to take advantage, first, of the decreased average program energy distribution in this frequency range, and, second, to compensate for head losses. The NARTB standard playback amplifier equalization curve is represented in Fig. 2. The 6 db per octave negative slope through the mid audio range, necessitated by the converse positive slope in playback head voltage versus frequency characteristic, is modified at the higher frequencies to compensate for decreasing head output voltage

due to gap effect and head losses, and to give a flat overall frequency response in conjunction with the record equalization.

The importance of the playback amplifier standard equalization curve should be emphasized here. If the record amplifier equalization is adjusted to produce a flat overall frequency response in conjunction with a particular playback equalization, then it is clear that the ultimate flux versus frequency pattern which is then recorded on the tape depends primarily upon this particular playback equalization, assuming that heads of fixed electrical characteristics are being used. Furthermore, the interchangeability of tapes between machines depends upon the flux pattern and hence demands we standardize on the playback equalization.

Testing Techniques

A typical arrangement such as might be used in the laboratory of the equipment required to check recorder performance is shown in Fig. 3. Provision is made for checking the playback and record equalization by means of an oscillator, a precision attenuator and a precision vacuum tube voltmeter. The record amplifier output level is set so that the magnitude of the distortion in the recorded signal does not exceed the selected specification value. Flutter is checked with a conventional flutter measuring bridge.

The physical layout of the equipment in the block diagram of Fig. 3 is shown in Fig. 4. The input and output measuring vacuum tube voltmeters, the input oscillator, and the precision attenuators for adjusting amplifier input voltages to those of the design center curves are shown to the left. The oscilloscope is used for observing the character of the amplifier noise as well as the input and output signal conditions. The standard recording level is set to specification limits with the distortion analyzer. Further adjustments which may be checked include overall frequency response curve of the recorder, the bias level setting for optimum record performance, the essential head position adjustments, as well as final record amplifier equalization setting so that, with the standard playback amplifier equalization curve, the recorder will record and play back essentially flat throughout the useful audio frequency range.

This approach requires a considerable amount of equipment and time to examine the various adjustments on a recorder as just outlined. The simplified method previously referred to eliminates the need for a large part of the equipment shown and reduces quite considerably the time required to test the recorder performance satisfactorily.

This simpler method mades use of the Standard Alignment tape. With this tape it is possible to check the head alignment, the output of the playback amplifier, the frequency response and thus the equalization adjustment of the playback amplifier, its signal-to-noise ratio, as well as to make an audible check on flutter, without the cumbersome equipment set up of Figs. 3 and 4. In fact, the Standard Tape may be looked on as a secondary measuring standard. Moreover, it eliminates the maintenance required on the test equipment which it replaces.

The information program contained on a typical Standard Alignment tape for recorders is shown in Fig. 5. Following a voice announcement identifying the tape and the speed at which it is to be played, a signal of short wavelength is provided for head azimuth adjustment. Head azimuth adjustment is done at the beginning to assure the accuracy of subsequent high frequency response readings. The next section on the tape is recorded at 250 cps at a reference level of -10 on the VI, which is used throughout the following frequency response section. This reference level is 10 db below the normal program level (zero on VI) in order to avoid the effects of tape saturation which would occur at the higher frequencies where the record equalization takes effect. Following is a series of frequencies covering the audio range for establishing the frequency response of the playback amplifier. These frequencies are recorded to include standard record amplifier equalization, so that the output reading of the playback amplifier will be constant with frequency, provided its equalization is correct. It is important to note that the performance of the record and playback heads are also being checked. The final section on the Standard Tape is recorded at the standard program level of 1% distortion (zero on VI). Unusual deviations from the normal range of equalization adjustment, head azimuth or settings are sufficient evidence to warrant further investigation.

Returning to Fig. 1, the contrast between the laboratory set up and the simplified approach using the Standard Alignment tape, one oscillator, and one vacuum tube voltmeter (heavy outlines) is emphasized. The simpler procedure is

essentially outlined in the program on the tape. When this program has been accomplished, the playback section of the recorder is properly checked and the oscillator is then used to complete the alignment by setting the record bias level, record head azimuth, and record equalization in that order for flat overall frequency response.

The requirements for a machine on which Standard Tapes can be produced are rather stringent. As an example of the mechanical problems involved, continuous certainty of accurate tape guiding is essential to accurate azimuth control. In this respect, a constant tension tape supply is also mandatory. The record amplifier must have extraordinarily stable gain and equalization characteristics. In actual production each tape is made individually, thus giving the greatest practical quality control over the azimuth, recorded level and frequency response of the signals.

Conclusion

The increasing use of tape recorders in the broadcast, studio, motion picture and professional audio fields reflect the effectiveness of these recording techniques. As such, it is important to maintain this equipment to secure the quality of performance which is inherent in today's professional machines. By using the Standard Tape approach, the time and equipment required to satisfactorily maintain magnetic recorders in the field, are simplified. The more frequent checks which are consequently permissible will then assure a greater possibility of realizing the inherent excellent performance, flexibility and usefulness of today's high quality magnetic tape recorders.

Bibliography

1. "A Report on Five Years of Service Dealings with Ampex Customers", H. VanChilds, unpublished Ampex monograph.

2. "Equalization Considerations in Direct Magnetic Recording for Audio Purposes", R. H. Snyder, IRE - PGA, March 1956

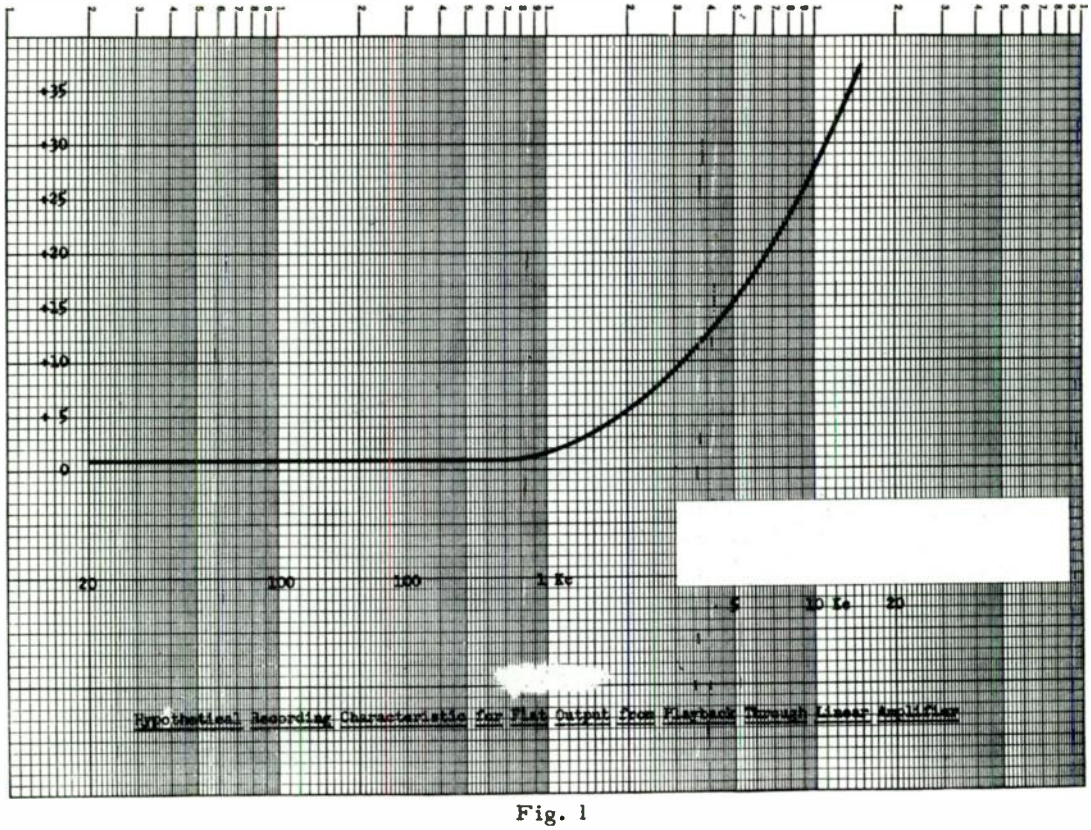

Fig. 1
Typical record equalization curve.

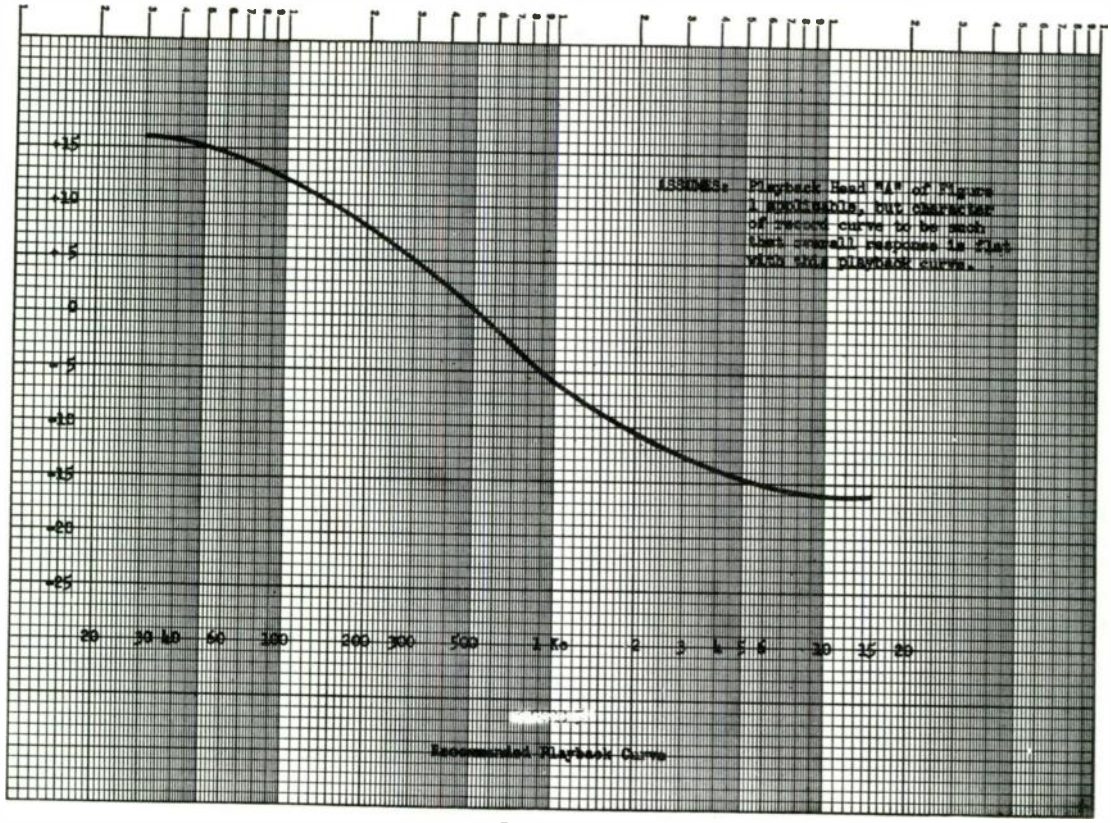

Fig. 2
Standard playback equalization curve

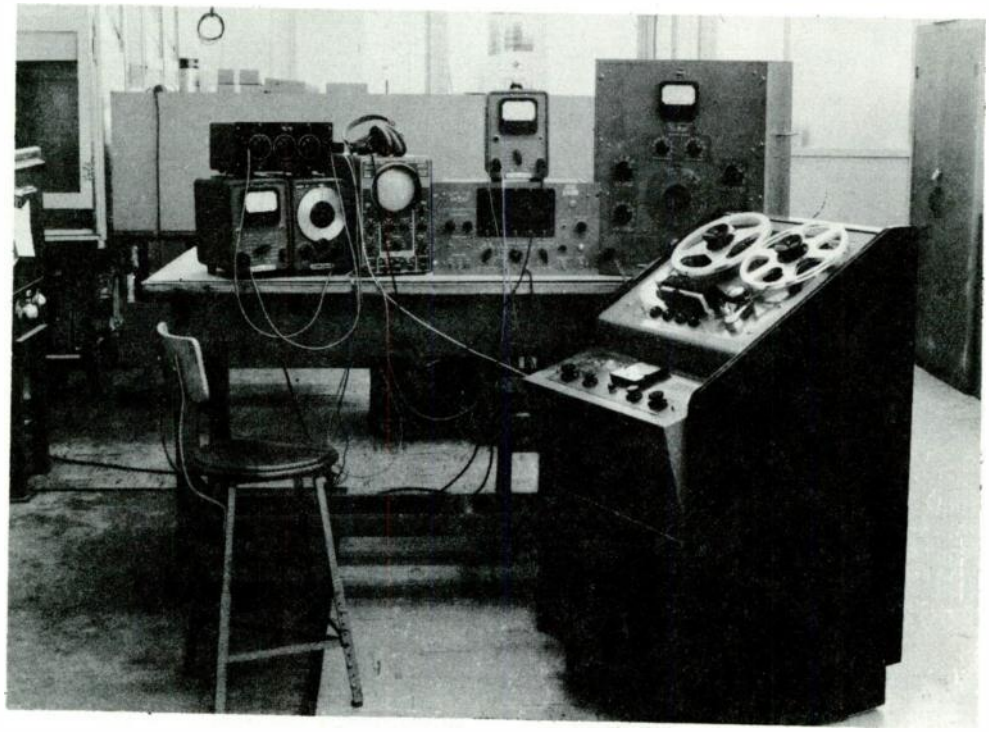

Fig. 3
Equipment layout for
overall performance test

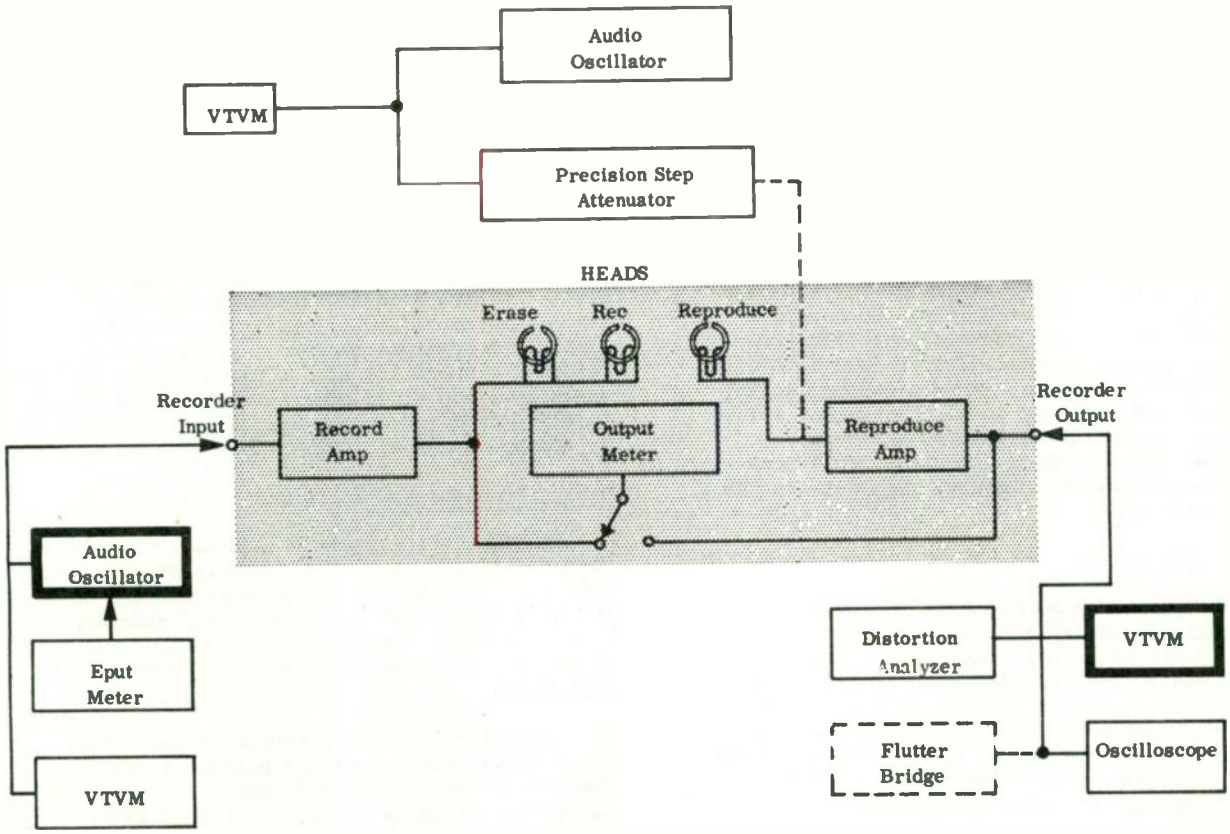

Fig. 4
Physical arrangement of equipment for
overall performance test

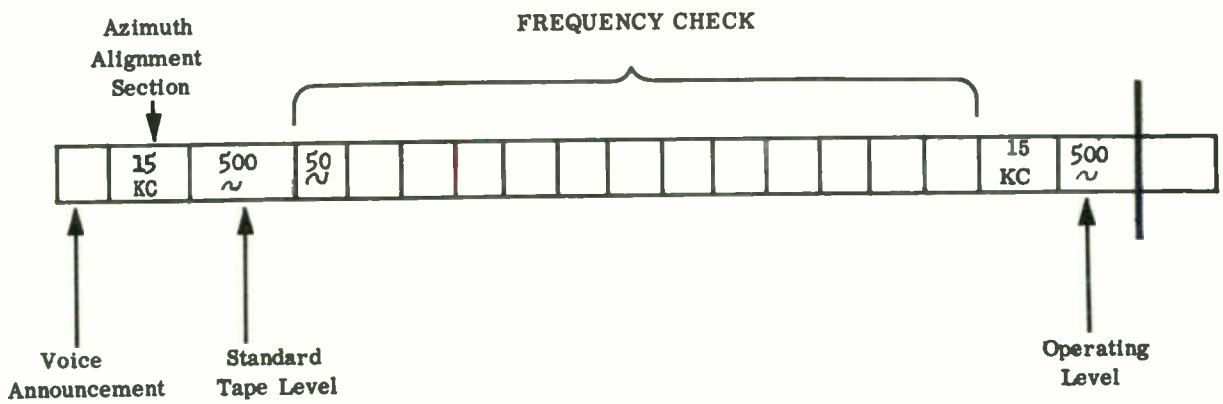

Fig. 5
Standard alignment tape information program

A 3000 WATT AUDIO POWER AMPLIFIER *

Alexander B. Bereskin
Professor of Electrical Engineering - University of Cincinnati
Consulting Engineer - The Baldwin Piano Co.

Introduction

A number of successful design variations of the Bereskin Power Amplifier[1] have been produced since the circuit was conceived. These have included various power and frequency ranges, in particular a 3000 watt unit which presented a number of problems leading to what are believed to be interesting solutions. It is the purpose of this paper to discuss these problems and their solutions and to present experimental test data on the completed unit.

Basic Circuit

Figure 1 shows the basic circuit of the Bereskin Power Amplifier. In this circuit two beam power tubes are connected in push-pull with their cathodes at common ground potentials. The screens are fed from any suitable power supply which need not be derived from the plate power supply. The screen and plate supply voltages may therefore be chosen independently to best suit the particular application.

The dual triode acts as a direct coupled phase inverter and driver supplying enough bias and drive for Class B_1 operation of the beam power tubes. Class B operation of the output tubes requires that the output transformer primaries be bifilarly wound in order to avoid the conduction transfer notch. A feedback winding, closely coupled to the bifilar primary and to the secondary, and statically shielded from them, is connected in series with the input to the grid of the left hand section of the dual triode. Good coupling between the bifilar primary and the secondary is assured by dividing the primary into two sections and sandwiching the secondary between these two sections.

This type of circuit has produced stable operation with 40 db of feedback, but this amount of feedback requires an excessive amount of driving voltage so that a value closer to 25 db is generally used. Due to the large amount of feedback used, the circuit is relatively insensitive to screen and plate supply ripple and regulation. The input signal may be either transformer or impedance coupled to the phase inverter-driver. Resistance-capacitance coupled input has been found to be relatively unsatisfactory due to the large dc resistance introduced in the grid circuit of the input triode. Grid current flow in this resistance tends to produce dc bias unbalance in the output tubes.

An appreciable amount of capacitance exists between the bifilar wound primaries of the output transformer. This capacitance tends to limit the high frequency power delivering capacity of the amplifier. This undesirable effect of the primary interwinding capacitance is reduced by operation at low plate signal voltage and high plate signal current. The capacitance itself can be reduced by approximately one third by transposing the bifilar winding at each turn.

Design Problems and Solutions

The specifications for the power amplifier proper required that it be capable of delivering 3000 watts in the frequency range between 400 and 4000 cycles per second with a distortion not to exceed 10%. The amplifier developed was able to deliver the required power with less than 2% distortion.

Investigation and analysis of available tubes showed that a pair of 4-1000A tubes operated Class B_1 Push-Pull would be capable of delivering slightly in excess of 3000 watts within the rated plate and screen dissipation if operated with 5 kv plate supply voltage and 1.25 kv screen voltage.

Information of this type is not usually available in the tube data supplied by the manufacturer. In order to develop the permissible peak plate currents without positive grid voltage drive it is necessary to operate the tubes with screen voltages considerably in excess of the values specified for Class AB_2 and B_2 operation. This is generally permissible if the various insulation and power dissipation limitations are not exceeded.

Insulation limitations must be determined either from manufacturer's data or by test. For this particular tube EIMAC specifies in pamphlet Number 3 "Pulse Service Notes" that the 4-1000A tube may be operated with 2.5 kv screen voltage and 15-30 kv plate supply voltage in pulsed operation. While the operation involved here is not of the pulsed variety, the insulation available is believed to be entirely adequate for the purpose.

The determination of plate and screen dissipation requires transposition of the available plate and screen characteristics to values corresponding to the desired value of screen voltage. This can be done if it is remembered that the voltage field pattern and the current distribution will not be altered if all interelectrode voltages are either raised or lowered

by the same relative amount. The current values, however, will take on new values in accordance with the 3/2 power law[2]. (EIMAC suggests that the use of the 4/3 power provides more accurate information.) If an adequate amount of feedback is used then it can be assumed that a sinusoidal input signal will result in sinusoidal plate current and plate voltage variation.

The manner in which the deliverable power can be computed is shown in Table I. In this table the first two columns were obtained from the e_{c_1} = 0 v, e_{c_2} = 1 kv data supplied by the manufacturer. Columns 3 and 4 represent computed data for e_{c_1} = 0 v, and e_{c_2} = 1.25 kv. Column 3 was obtained by multiplying the values in column 1 by 1.25. Column 4 was obtained by multiplying the values in column 2 by $1.25^{4/3}$ = 1.347. Column 5 represents the maximum ac power that can be developed in Class B_1 Push-Pull operation for e_{c_2} = 1.25 kv when $e_{b_{min}}$ and $i_{b_{max}}$ correspond to the values in columns 3 and 4 respectively and a plate supply voltage of 5 kv is used.

Maximum average plate dissipation, with sine wave signal, will occur when the plate is driven 2/3 of the way to zero volts, corresponding to a peak ac signal voltage of 3333 volts. For the condition of row 2 in TABLE I this results in a peak plate current of 1.27 amperes and an average plate current, for the two tubes, of .805 amperes. The dc input power is therefore 4025 watts while the ac plate power developed is 2115 watts. The maximum average plate dissipation is therefore 1910 watts. The condition of row 1 would not supply the required 3000 watts of output power while the conditions of rows 3 and 4 would have plate dissipation conditions exceeding the rated value of the tubes.

Maximum screen dissipation occurs at maximum drive. TABLE II shows the manner in which the information can be set up to compute the

TABLE I

Power Delivering Capacity Calculations
(E_{bb} = 5 kv, E_{c_2} = 1.25 kv)

E_{c_2} = 1 kv, e_{c_1} = 0 v		E_{c_2} = 1.25 kv, e_{c_1} = 0 v		
e_b (volts)	i_b (amp.)	e_b (volts)	i_b (amp.)	W_{max} (watts)
600	.930	750	1.252	2660
800	1.130	1000	1.520	3040
1000	1.270	1250	1.710	3210
1200	1.340	1500	1.805	3160

TABLE II

Maximum Signal Performance Calculations
(E_{bb} = 5 kv, E_{c_2} = 1.25 kv, $e_{b_{min}}$ = 1 kv, $i_{b_{max}}$ = 1.52 amp.)

At operating value of E_{c_2} (1.25 kv)				At nearest available curve value of E_{c_2} (1.0 kv)				At operating value of E_{c_2} (1.25 kv)	
θ (degrees)	e_b (volts)	Composite i_b (amp.)	Tube i_b (amp.)	e_b (volts)	Tube i_b (amp.)	e_{c_1} (volts)	i_{c_2} (amp.)	e_{c_1} (volts)	i_{c_2} (amp.)
0°	1000	1.520	1.520	800	1.130	0	.350	0	.471
22.5°	1310	1.405	1.405	1050	1.043	-17	.120	-21.2	.161
45.0°	2180	1.072	1.072	1745	.798	-44	.040	-55.0	.054
67.5°	3470	.581	.581	2780	.432	-78	.015	-97.5	.020
90.0°	5000	0	.100	4000	.074	-140	0	-175	0

expected screen dissipation and other important quantities assuming sufficient feedback is used to force a cosine variation of plate current and plate voltage.

The value of zero signal tube plate current was arbitratily chosen at .100 ampere to produce 50% of rated plate dissipation. This represents a reasonable compromise between severity of Class B bias and quiescent plate dissipation.

Fourier analysis applied to the data of TABLE II yields the following information:

I_b = .980 ampere

I_{c_2} = .118 ampere

Screen dissipation = 148 watts

Plate circuit input power = 4900 watts

AC power developed = 3040 watts

Plate dissipation = 1860 watts

Plate efficiency = 62%

This last tabulation indicates that the operating conditions chosen will yield the required power output within the plate and screen dissipation ratings of the tubes chosen. Of course the correct operating conditions are rarely obtained on the first choice and a few incorrect operating conditions may have to be investigated before the correct one is determined.

There is no dc voltage between the two primaries but an instantaneous peak voltage of 4000 volts appears between adjacent points of these windings at full signal. Commercially available polyvinyl chloride, Teflon, and Kel-F insulated wires have been found to have adequate insulation strength for this purpose. Polyvinyl chloride insulated wire is not satisfactory because of its high dielectric constant (6.5), which would produce a high primary interwinding capacitance and thereby interfere with the high frequency power delivering capacity, and its high power factor (0.10) which would produce excessive insulation temperature rise. Both Teflon and Kel-F had acceptable dielectric constant and power factor. Kel-F insulation had the advantage of higher dielectric strength, listed as high as 2500 volts per mil, high resistance to cold flow, and lower cost. At the time of this development polystyrene foam insulation was being discussed in the literature but was not commercially available. This insulation would have a marked advantage from the point of view of dielectric constant which would approach 1.00. Its other characteristics would require further investigation.

The wire used for the bifilar primaries was #22 (7-30) wire with .014" wall of Kel-F insulation. Twisted samples of this wire were tested with 20 kv peak 60 cycle power without breaking down. The manufacturer specifies that 100% of wire of this type with .008" wall is subjected to an Insulation Flaw ("Spark") Test with an impressed voltage of 7500 volts rms. Samples of the .008" wall wire must also pass the manufacturer's test of a four hour immersion in tap water, with the wire ends left out of the water, with a subsequent application of 5000 volts rms for one minute between the conductor and the tap water. All of these tests represent appreciably greater dielectric stress than that encountered between the two adjacent wires of the bifilar winding. No trouble has been experienced due to the lack of insulation in the bifilar winding.

Preliminary calculations indicated that the high frequency power delivering capacity would begin to fall off at frequencies slightly below 4 kc so it was decided to take advantage of the reduction in primary interwinding capacitance obtained by transposing the bifilar winding at every turn. Subsequent performance tests showed that the high frequency power delivering capacity specifications would have just barely been met without this refinement but were quite adequately met with the refinement.

The output transformer was designed to be used with two Moloney MA-306 grain oriented C cores. The winding buildup for this transformer is shown in Figure 2 and the complete circuit diagram is shown in Figure 3.

In order to supply the grid driving voltage required by the 4-1000A tubes without introducing excessive grid circuit resistance, the double triode was replaced with two 6AU6 tubes. This provided the additional convenience of being able to provide dc balance by adjustment of the 6AU6 screen voltages. The choke in the impedance coupled input is a Thordarson T20C51 choke modified by full interleaving of the laminations. The voltage limits of the plate and screen supply voltages are also shown in Figure 3.

Performance

The effect of various amounts of feedback on the residual hum and on the full signal input required is shown by the curves in Figure 4. Operation of this amplifier was stable with the maximum possible feedback of 30 db corresponding to the full seven turns in series. A single feedback turn corresponding to 13 db provided an adequate hum level 57 db below 3000 watts and only required 8.7 volts input voltage for 3000 watts output. The remaining tests were performed using the single turn feedback winding.

The 1 kc Power Loss and Distortion Characteristics are shown in Figure 5. The plate dissipation curve in this figure was obtained by

subtracting the transformer losses from the total plate circuit losses. The plate dissipation exceeds the rated value by 2% in the 1.4 kw output region while the screen dissipation remains below the rated value up to full power output. Residual Hum and Distortion remains at about 0.8% over most of the operating region rising rapidly to 1.4% at 3000 watts output. Additional reduction in the residual hum and distortion could have been obtained by using more feedback but the performance was already much better than that required by the specifications.

The Power Delivering Capacity of the amplifieris shown in Figure 6. At each of the frequencies shown in this figure the input was adjusted to produce 2% distortion in the output. The amplifier is capable of delivering in excess of 3000 watts within the plate and screen dissipation ratings of the tube over the required frequency range of 400 to 4000 cycles per second.

The Frequency Response Characteristics are shown in Figure 7. The upper curve in this figure is the 2% distortion power delivering capacity plotted to a db scale. The lower curve is the Low Level Frequency Response Characteristic obtained by maintaining constant input voltage while varying the frequency. This characteristic deviates by less than 1 db from the middle frequency response over a frequency range of 100 to 38,000 cycles per second. The low frequency peak in response is due to series resonance between the input capacitor and the modified T20C51 choke.

Figure 8 is a photograph of the completed amplifier, exclusive of power supplies, showing the chassis arrangement of the various components and the blower used for forced draft cooling of the tubes and transformer. The bottom of the chassis was enclosed and the blower provided positive air pressure inside the chassis. The air was allowed to escape through the air system sockets for cooling the 4-1000A tubes and through suitably located holes for cooling the transformer.

A characteristic of this type of amplifier is that the transition from very low power level to very high power level is made in a single step. The relative size of the two 6AU6 tubes used to drive the two 4-1000A tubes is clearly seen in Figure 8.

The transformer, complete with mounting hardware, weighs 26.5 pounds while the complete amplifier shown in Figure 8 weighs 54.5 pounds.

Only one unit of the amplifier under discussion was required. If another unit had been required certain minor modifications would have been introduced in the transformer construction. The primary and secondary turns would be increased by approximately 40% and the primary wire size would be changed to #24 (7-32) with a .014" wall of Kel-F insulation. The secondary wire size would have been changed to #10 Heavy Formvar. The changes indicated should reduce the 1 kc - 2% distortion core loss from 204 watts to 114 watts while increasing the copper loss from 20 watts to 40 watts. The increase in copper loss is not serious and the decrease in core loss is highly desirable. The increase in turns should move the low frequency end of the power delivering capacity curve to the left so that this curve would cross the 3000 watt level at about 280 cycles per second. The increase in number of turns would tend to increase the primary interwinding capacitance but this would be overcome to a large extent by the reduction in the wire size so that the high frequency power delivering capacity would not be expected to change appreciably.

If the specifications had called for operation at considerably lower frequencies than those required, the transformer would have been designed with a much larger magnetic path cross-section. Modifications in the number of turns and wire size would also have to be made.

The amplifier developed satisfied all of the design specifications and showed very good correlation between design data and final performance.

Bibliography

1. "A High-Efficiency High-Quality Audio-Frequency Power Amplifier" by A. B. Bereskin, Transactions of the IRE Professional Group on Audio, March-April 1954, pp. 49-60.

"High-Efficiency High-Quality Audio Power Amplifier" by A. B. Bereskin, Convention Record of the IRE 1954 National Convention, Part 6 - Audio and Ultrasonics, pp. 18-24.

"Fifty Watt Amplifier for High-Quality Audio" by A. B. Bereskin, Electronics, October 1954, pp. 160-164.

2. Eimac Tube Reference Data on 4-65A Tube, pp.6.

* The 3000 watt audio power amplifier was developed under government contract AF33(616)-2320.

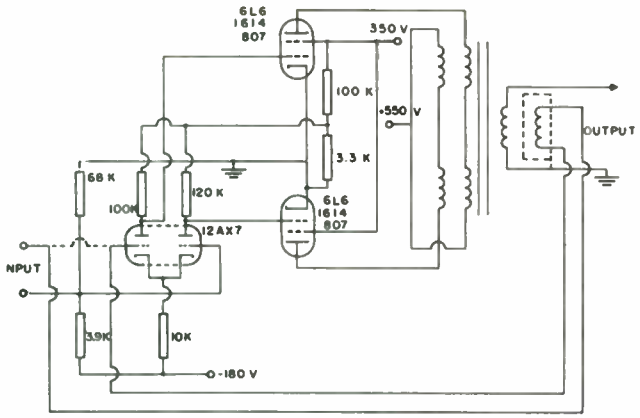

Fig. 1
Basic Bereskin power amplifier circuit.

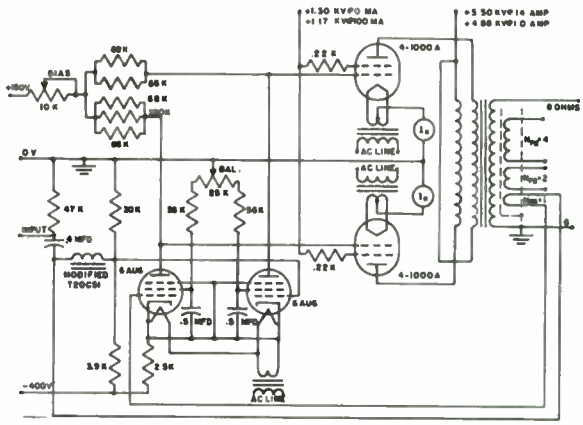

Fig. 3
3000 watt audio power amplifier.

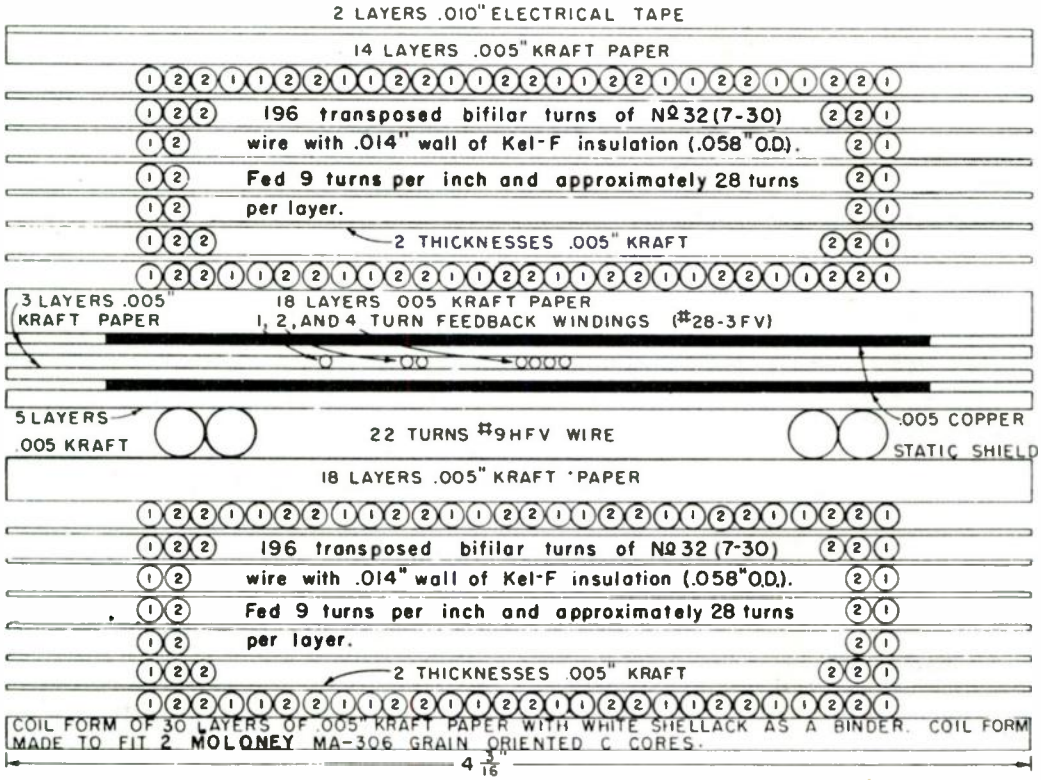

Fig. 2
Output transformer coil buildup for 300 watt audio power amplifier. (Note: Proper proportions on a vertical scale only.)

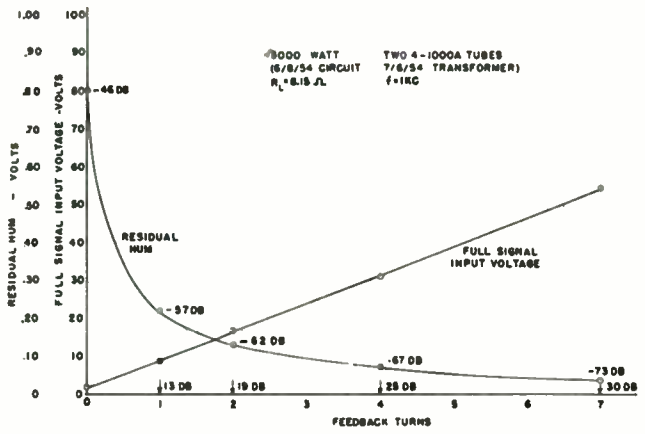

Fig. 4
Feedback analysis characteristics.

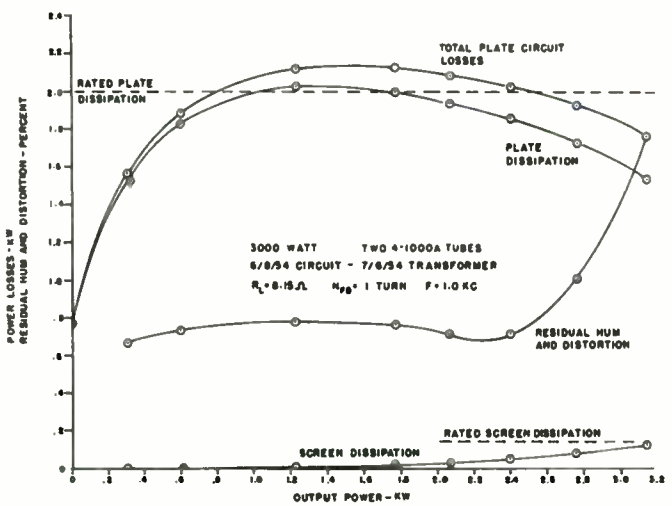

Fig. 5
Power loss and distortion characteristics

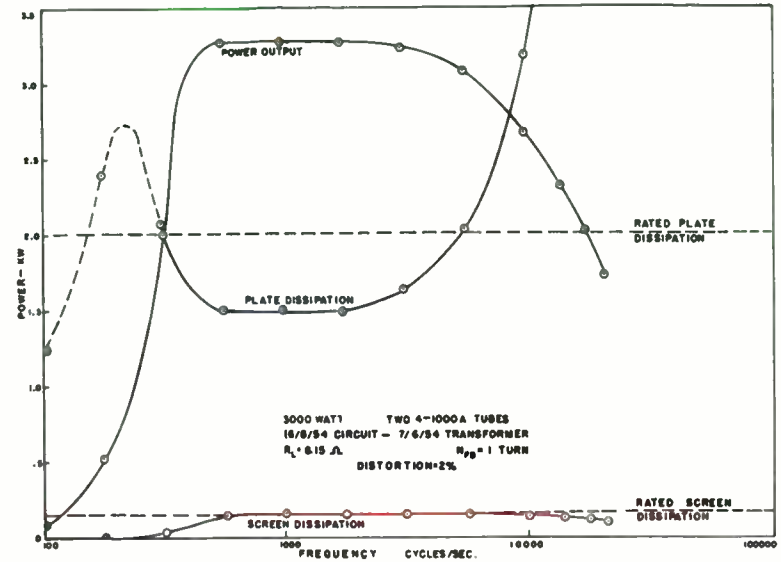

Fig. 6
Two percent distortion power relations.

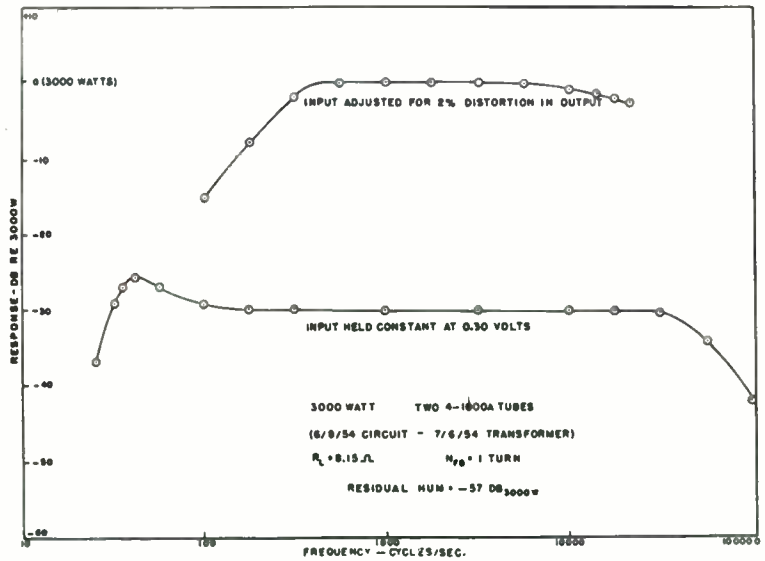

Fig. 7
Frequency response characteristics.

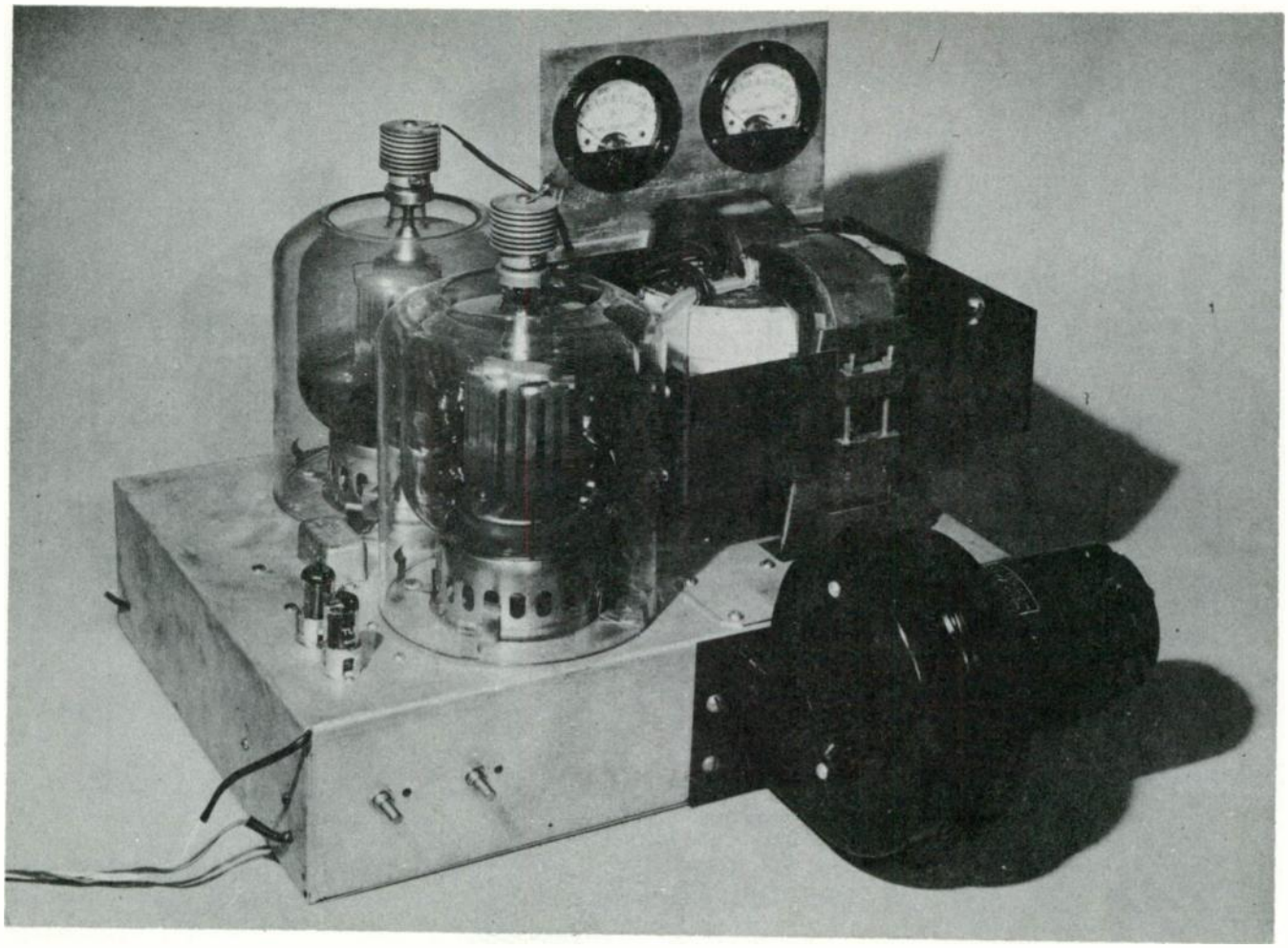

Fig. 8
A 3000 watt audio power amplifier.

HIGH-GAIN ANTENNA ARRAYS FOR TELEVISION BROADCAST TRANSMISSION USING A SLOTTED RING ANTENNA

by

Andrew Alford and Harold H. Leach
Alford Manufacturing Company, Inc.

Summary.

The paper deals with high gain antenna arrays, both directional and omnidirectional, which utilize a slotted ring antenna. The theory of operation of the slotted ring antenna and the various parameters that can be used to control the frequency range of operation as well as the impedance characteristics are discussed.

Several applications of the slotted ring antenna in commercial television broadcasting including the use of high gain omnidirectional slotted ring antenna arrays with low power transmitters to achieve authorized ERP's are shown.

The variety of horizontal patterns obtainable by directionalizing the slotted ring antenna with relatively simple structures are discussed. Measured horizontal patterns are included showing patterns which conform to the 10 db rule of the FCC for this country as well as several special patterns with extremely high gains and with considerably deeper nulls.

- -

The object of this paper is to describe a type of antenna which has been found useful in television broadcast transmission, both as an omnidirectional and a directional radiator of horizontally polarized waves. Its particular merit is that it allows one to obtain relatively high gains with a relatively simple feeding arrangement. For example, an array with an RMS power gain of 20 requires only five feed points.

The antenna can best be understood by considering a balanced transmission line shunted by a number of small loops or rings. It is possible by arranging the separation and cross-sectional area of the rings to substantially increase the phase velocity at which a high frequency wave is propagated along the transmission line. Figure 1 shows such a loaded transmission line which has been short-circuited at one of its ends and is fed with a balanced signal generator at the other. The standing waves which are set up along the line have an apparent wavelength λ_a which is normally larger than the free space wavelength. When the number of rings along the balanced transmission line is of the order of twelve per free space wavelength and the diameter of each ring is of the order of 0.14 λ (where λ is the free space wavelength) the apparent wavelength λ_a will be approximately twice the free space wavelength.[1]

If the arrangement shown in Figure 1 is fed at the center through a length of transmission line as shown in Figure 2 and short-circuited at both ends, then a wave propagates from the center feed point towards each of the two short circuits. The reflections from these short-circuited ends set up a standing wave and the difference of potential between the conductors of the balanced transmission line is distributed approximately as shown by the dotted line. The phase of this difference of potential is substantially constant over the entire length of the line for the spacing from the center feed point to either short circuit is only approximately 0.4 apparent wavelengths. It is possible then to feed cophasally with one feeder a loaded transmission line of this kind having a total span between short circuits of some 1.5 free space wavelengths. This unit is known as a half bay.

The potential which exists between the balanced conductors causes circumferential currents to flow in the shunting rings. Since the potential, and hence the currents, are very nearly cophasal, the overall behavior of the loaded line is similar to that of an array of closely stacked loops. This fact results in a substantial concentration of the power radiated by the rings in the direction of a plane passing through the halfway point along, and perpendicular to, the balanced conductors. The current which flows in each ring is a maximum at a point opposite to, and equidistant from, the balanced conductors while the minimum value of current occurs where the ring is joined to these conductors. The radiation pattern, then, of the rings in the plane of the rings is not quite an exact circle, but is rather an oval with slight maxima along a diameter which passes through the point of maximum current and with slight minima at approximately right angles to this diameter.

Since the potential on each ring at the point of maximum current is essentially zero, these points may all be joined to an electrically conductive common member without distorting the radiation pattern of the array. Further, since the potential increases gradually from zero on both sides of these neutral points, supporting masts of adequate size may be used without substantially affecting the operation of the antenna.

Such an antenna has been made for television broadcast transmission. As may be seen from Figure 3, it consists of a series of slotted rings mounted on a channel. Two rods are mounted to the rings, parallel to each other, one along each side of the open portion of the rings, to form a slot and to act as the balanced transmission line. The rings are lenticular in cross-section with the long axis in the plane of the rings so that the wind resistance of the structure may be as low as possible.

A portion of a slotted ring antenna is shown in Figure 4, mounted on a supporting mast. In order that a larger vertical aperture could be excited with a single external transmission line feeder, a feeding arrangement was developed which utilizes a portion of the rods and channel as an outer conductor to propagate an approximately coaxial TEM mode to the center of the slot in conjunction with an exposed inner conductor. It was then possible to mechanically join two half bays together, which were fed in the center through a coaxial tee. The overall length of a so-called bay then was approximately 3.4 free space wavelengths with substantially the entire aperture excited essentially cophasally with a single external rigid coaxial transmission line feeder.

The exposed inner conductor is an extension, through a large teflon coaxial end seal, of the coaxial tee inner conductor. It passes through a portion of the rings to the center ring of each half bay and is there connected to one side of the ring. Various inner conductor diameters are possible but the relatively small inner conductor presently used offers two distinct advantages. It is sufficiently small not to alter the distribution along that portion of the antenna through which it extended as compared to the remaining half which contained no inner conductor and yet, in conjunction with the rods, channel and slotted rings, it presented a characteristic impedance which resulted in a substantial improvement of the impedance versus frequency characteristic of the antenna; i.e., made the antenna more broad band.

If, at the center ring, the exposed inner conductor were connected to the neutral point of the ring (the point of attachment to the channel) the impedance seen would be that of a few ohms. If, instead, the exposed inner conductor were connected to a point on the center ring just to one side of but adjacent to the slotted portion, the impedance seen then with the components and spacings presently used would have a real component of the order of magnitude of 70 ohms. The center ring, therefore, in conjunction with the bar which joins the exposed inner conductor to the ring can be made to act as a transformer which is capable of transforming the real component of the slot impedance from approximately 70 ohms as an upper limit to a few ohms, if desired, as a lower limit.

A typical slot impedance when the point of attachment has been properly chosen is shown in Figure 5. Through the use of a relatively high impedance (approximately 160 ohm) line section made up of the exposed inner conductor and its effective outer conductor, and further by controlling the length of this line section (slightly over one apparent wavelength) this slot impedance is transformed to the relatively small circle of impedances shown on the same figure.

The frequency range of operation of the antenna is controlled to some degree by adjusting the spacing between, and the size of, the rods. Since the phase velocity of propagation is equal to $1/\sqrt{LC}$, increasing the diameter of the rods or decreasing the spacing between rods will decrease the phase velocity. To maintain a constant apparent wavelength, the center of the operating frequency range must also be decreased. In this manner the same antenna may be tuned to operate in several different television channels. The change of rod spacing and/or diameter also changes the slot impedance of course, and this must be compensated for by a slight movement of the point of attachment, on the center ring, of the exposed inner conductor.

The slotted ring antenna has several properties which are desirable for television broadcast transmitting antennas:

(1) It radiates almost pure horizontally polarized waves and its horizontal radiation pattern is essentially omnidirectional

(2) Because of its relatively large components, including the teflon seal, it can handle high power

(3) It is relatively insensitive to snow and ice formations because of the relatively low slot impedance

(4) The antenna exerts a relatively low shear and overturning moment and yet is extremely rugged

(5) Finally, it can be easily stacked to achieve quite high gains with only a few feed points and therefore an extremely simple interconnecting harness.

When the antenna is stacked vertically to achieve higher gains, rigid 3-1/8" coaxial teflon transmission line is used to make up the interconnecting harness. So that an input VSWR over the assigned six megacycle band may be guaranteed without necessitating the complete assembly and testing of the entire array at the factory, a common principle of interchangeable manufacturing is applied; i.e., maximum input VSWR's are assigned to each of the various components of the system in such a way that even if all reflections were to add in phase at some point in the frequency range of operation, the resultant input VSWR of the system would be less than 1.10. The individual bays are tested and compensated

separately to a maximum VSWR of 1.06. The entire interconnecting harness is then assembled and terminated in matched low power precision loads. A maximum VSWR limit of 1.02 is assigned to the complete harness. A typical impedance plot on an expanded Smith Chart for a typical harness is shown in Figure 6.

Since the supporting masts are not perfectly rigid and often deflect considerably under hurricane winds, and because of the differential coefficient of thermal expansion between the copper transmission line and the steel mast, careful design of the interconnecting harness and its supports has been an important part of the reliability of the stacked arrays. Through the use of double 90° elbows for connecting the feeders to the individual bays and through the use of sealed coaxial expansion joints, the interconnecting transmission line harness is allowed to deflect with the supporting mast without undue stress.

A five-bay omnidirectional slotted ring antenna array with a gain of approximately 20 has been built and installed in Washington, North Carolina, for Station WITN (TV). In conjunction with a 20 kilowatt transmitter, it radiates an ERP of 316 kilowatts. A field intensity radial as measured on this installation by Mr. Raymond Rohrer of Jansky & Bailey, Inc. is shown in Figure 7A. In order to determine the effects of the terrain, if any, and for comparison purposes, similar radials were measured on a nearby station which also radiated an ERP of 316 kilowatts with a higher power transmitter and a lower gain antenna. The measured field intensity radial for a corresponding direction on this installation is shown in Figure 7B. Both of the measured curves follow fairly closely the predicted curves calculated from the FCC (50,50) curves. Further, there is a remarkable similarity between the two measured curves in their slight deviations from the predicted curves. As closely as could be determined, the gain of the WITN five-bay antenna was found to be the value predicted from model measurements.

The calculated vertical beam width, based on measured half-bay patterns, at the half power points of the five-bay array is 2.9° as compared to approximately 3.6° for the lower gain antenna of the adjacent station. Measurements of the close-in fields for the two stations were also recorded and the instantaneous values of field strength measured are plotted in Figure 8 for the two stations as a function of distance from the respective towers.

Although the fundamental horizontal radiation pattern of the slotted ring antenna, even when mounted on a supporting mast, is essentially circular as described above, the antenna lends itself to achieving a variety of directional horizontal patterns through the addition of relatively simple beam shaping members. Several types of beam shaping members have been used, depending on the application and requirements of the various directional antennas.[2]

For television broadcast transmission, these beam shaping members have taken the form of relatively small rectangular bar stock of various lengths attached directly to each alternate active ring of the antenna. Sufficient beam shaping members are then present along the slot so that the distribution of potential remains essentially unchanged as does the vertical radiation pattern of the antenna. Several different horizontal radiation patterns have been achieved in this manner. Three typical patterns have been shown in Figure 9, all of which conform to the so-called 10 db rule set up by the Federal Communications Commission. Further, all of these patterns are essentially circular except in one sector where they have a null or nulls which are no more than 10 decibels below the maximum. The maximum power gain of a directional antenna depends, of course, not only on its vertical aperture but on the directivity of the horizontal pattern as well. The increase in gain which is achieved in certain directions as a result of this horizontal directivity allows a given maximum ERP to be radiated with a fewer number of directional bays (i.e., a smaller vertical aperture) than with omnidirectional bays. The typical directional horizontal patterns shown have maximum gains which vary from approximately 5.6 to 7.2 per bay, depending on the particular pattern chosen, as compared with an RMS or omnidirectional gain of approximately 4.0 per bay.

The rings provided with beam shaping members act differently from simple rings in that a substantial portion of the current which normally flows in the ring is diverted into the beam shaping members. The horizontal radiation pattern of a modified ring is determined not only by the shape and the length of the beam shaping member, but by its point of attachment to the ring as well. Because the potential along the ring varies from a maximum on both sides of the slot to zero at the neutral point, the nearer the point of attachment of the beam shaping members to the neutral point of the ring, the smaller is the amount of current diverted from the ring. The less then is the deviation of the directional horizontal pattern from the primary horizontal pattern of the slotted ring antenna itself.

To calculate the horizontal pattern of the slotted ring antenna after the addition of the beam shaping members described above would mean either the solution of a difficult boundary value problem or the integration of measured current distributions along the various antenna elements.

Fortunately, it was found practical to determine the optimum method of achieving a desired directional horizontal radiation pattern by performing measurements on accurate scale antenna models. Agreement between the model studies and the full scale antenna measurements has been checked many times and found to be good.

Although not presently authorized in this country, nulls considerably deeper than 10 db have been investigated through model studies. While it is possible to achieve almost complete nulls with the beam shaping members described above, the nulls are ordinarily quite narrow. For those installations where it is desired to suppress the radiated signal over a considerable sector in order to protect the coverage area of an adjacent station, considerably broader nulls have been achieved through the use of two auxiliary but driven radiators in conjunction with the main antenna.

In 1948, a series of model measurements were made which showed that a null over 30 db down from the maximum could be radiated over an azimuthal sector of some 47°.3 Such a pattern is shown in Figure 10C. The main antenna consisted of a slotted cylinder with solid wings as the beam shaping members, as shown in Figure 10A. The horizontal radiation pattern of this antenna alone is as shown in Figure 10B. The voltage which is set up across the slot originates a wave which travels outward along the wings. When the wave arrives at the edge of the wings, some of the energy is reflected back towards the slot and some travels in such a way as to keep the ends of the electric lines of force normal to the sheet. It is the energy which travels around the edge that causes the back lobe.

The field near the edges can be considered as two Huyghens' sources which radiate in all directions. These two sources are in the same phase with each other and their contributions add in the direction of 180°. As one deviates from 180° there is a difference in path length between the radiations from the virtual sources. At some given angle, this difference is a half wavelength and there is a null. As the angle approaches 90° the field of the main slot becomes predominant with the smaller effects of the two edges superimposed. By properly choosing the magnitude but reversing the phase of the power fed to the two auxiliary driven antennas, and by the choice of the proper spacing, the horizontal radiation pattern of the driven antennas was made to track and cancel the patterns of the Huyghen sources fairly closely over a relatively wide sector.

An extremely high gain antenna has been modeled and tested for the Air Force Cambridge Research Center for possible use in forward scatter ionospheric propagation. It utilizes a slotted ring antenna to feed a series of stacked wire vees which are attached, at the narrow end of the vee, to the two balanced conductors along the slot and at the wide end to two auxiliary supporting towers as shown in Figure 11A. At upper band VHF television frequencies, a four bay array of this type would have a vertical aperture of some 75 feet. With 40 foot long wires and a vee included angle of approximately 25°, a maximum power gain over a dipole in free space of 250 can be achieved. In spite of the attachment of the stacked wire vees to the slotted ring antenna, the major lobe of the measured vertical pattern of a modeled half bay of this array was essentially the same as that of the slotted ring half bay alone. The horizontal radiation pattern of such an array is shown in Figure 11B.

References.

1. A. Alford, "Antenna," U. S. Patent No. 2,622,196; December, 1952
2. A. Alford, "Slotted Winged Cylindrical Antenna," U. S. Patent No. 2,611,867; September, 1952
3. A. Alford, "Slotted Winged Cylindrical Antenna," U. S. Patent No. 2,611,864; September, 1952

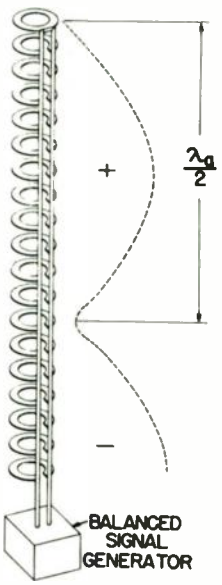

Fig. 1

Balanced transmission line loaded with shunt rings

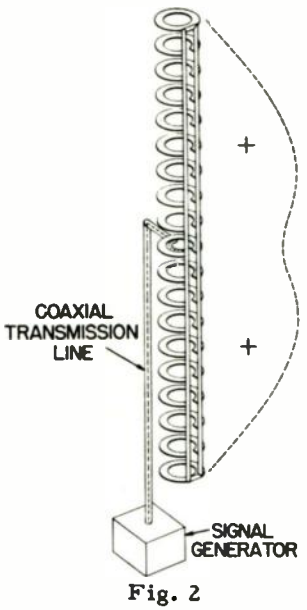

Fig. 2

Balanced transmission line loaded with shunt rings

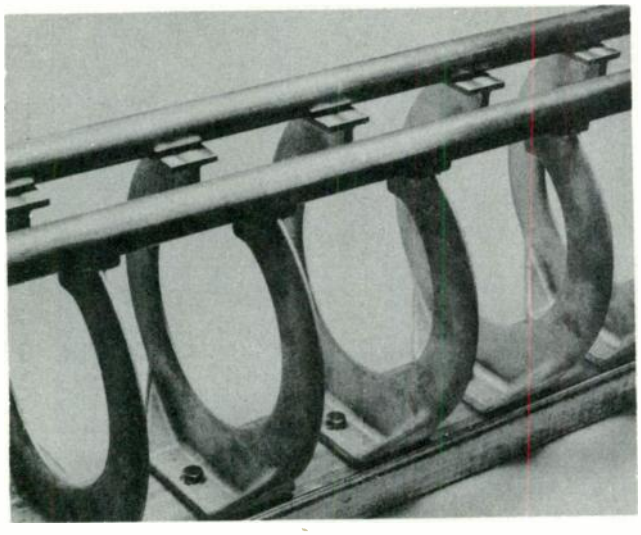

Fig. 3
Portion of a slotted ring antenna

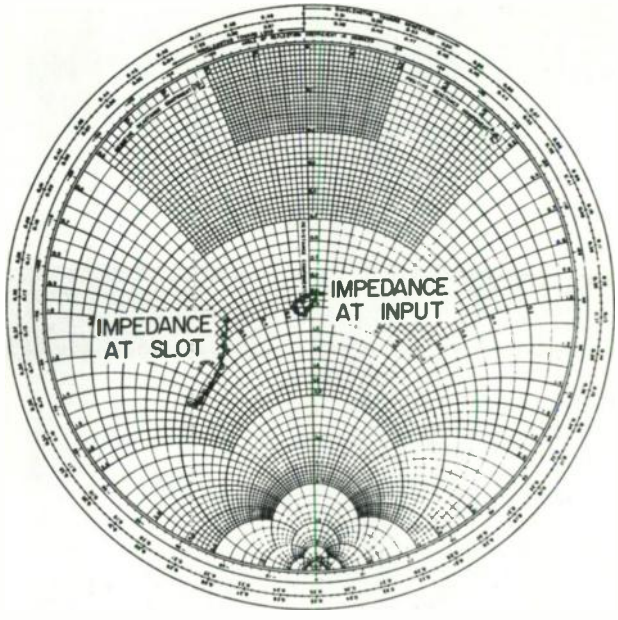

Fig. 5
Slotted ring antenna impedances

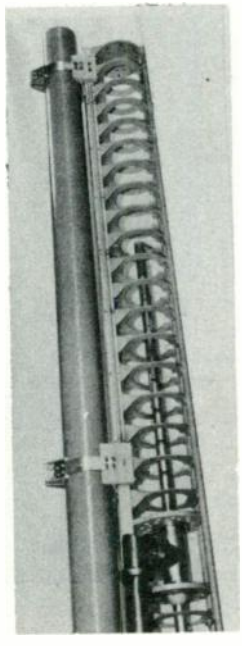

Fig. 4
Portion of a slotted ring antenna bay

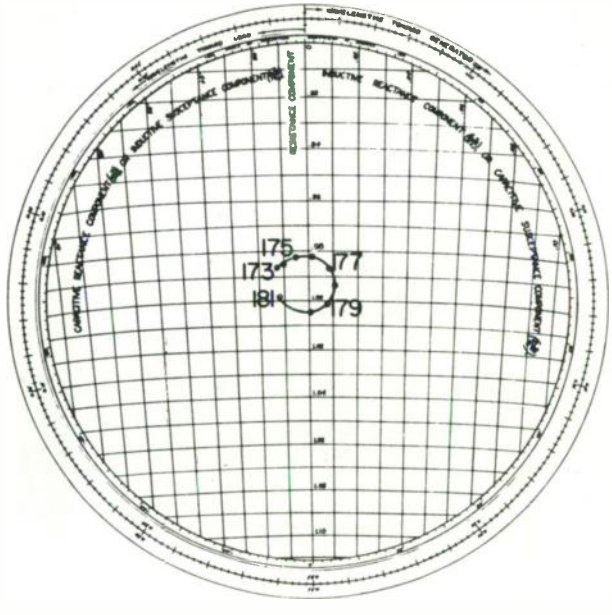

Fig. 6
Impedance of a typical interconnecting harness

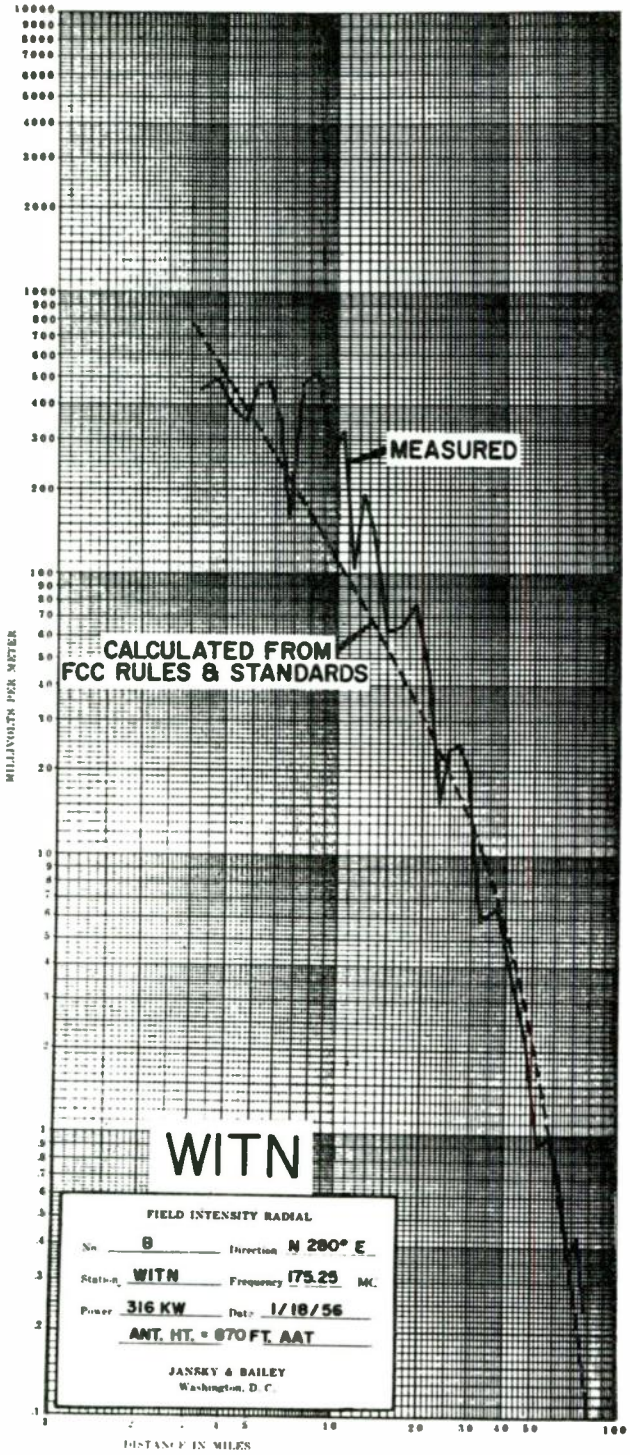

Fig. 7A
Measured field intensity radial for Station WITN

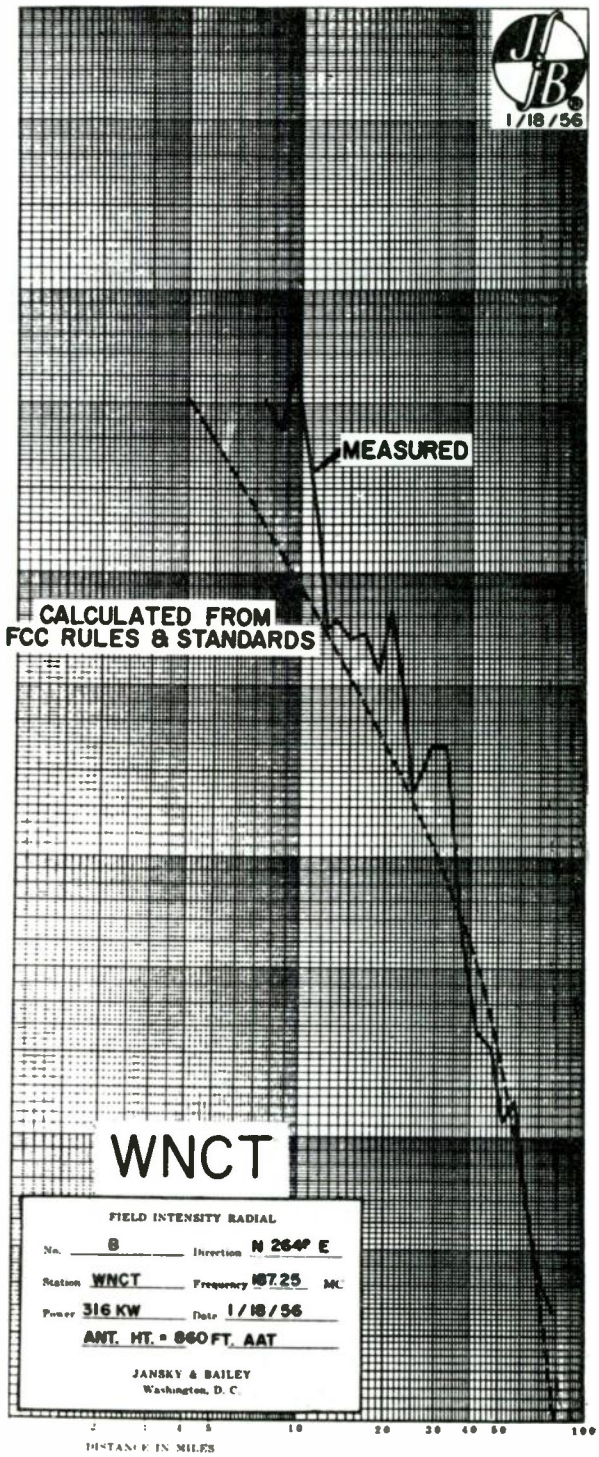

Fig. 7B
Measured field intensity radial for station WNCT

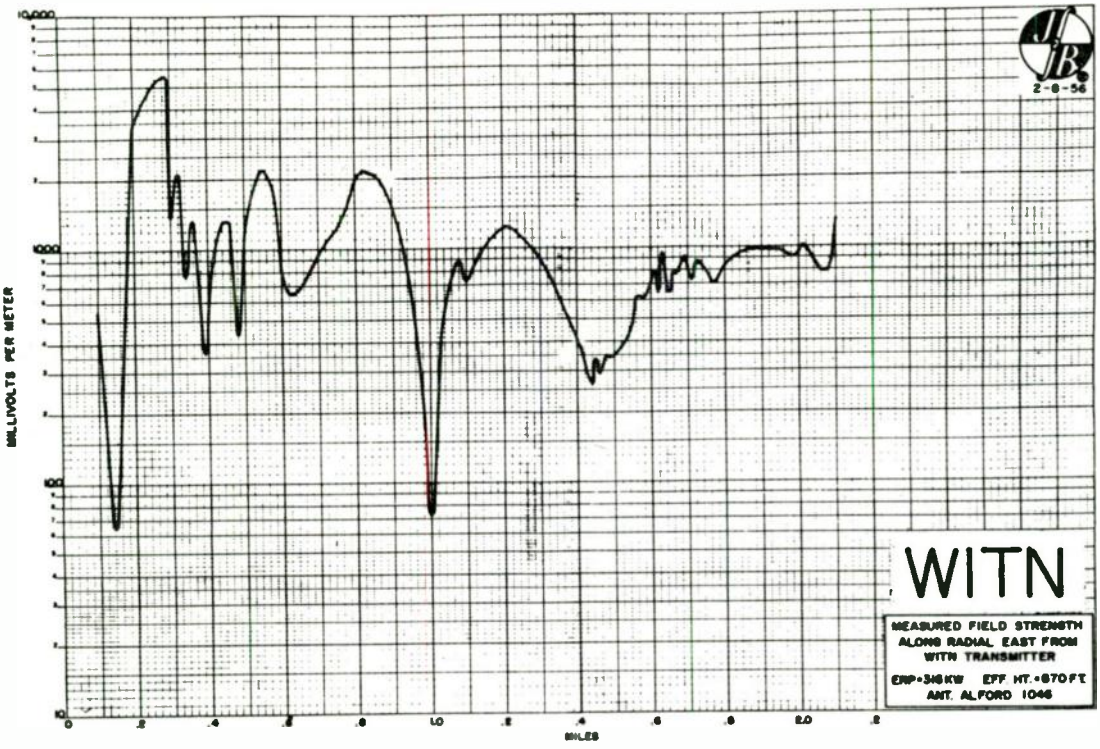

Fig. 8A
Close-in field measurements for Station WITN

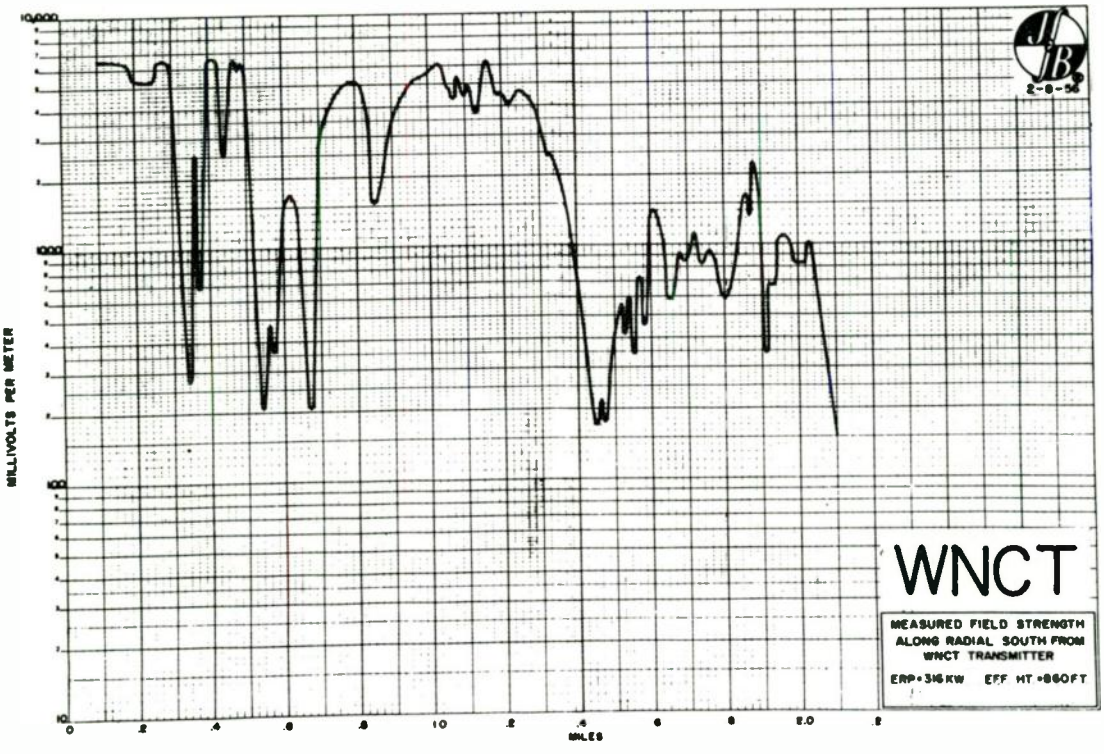

Fig. 8B
Close-in field measurements for Station WNCT

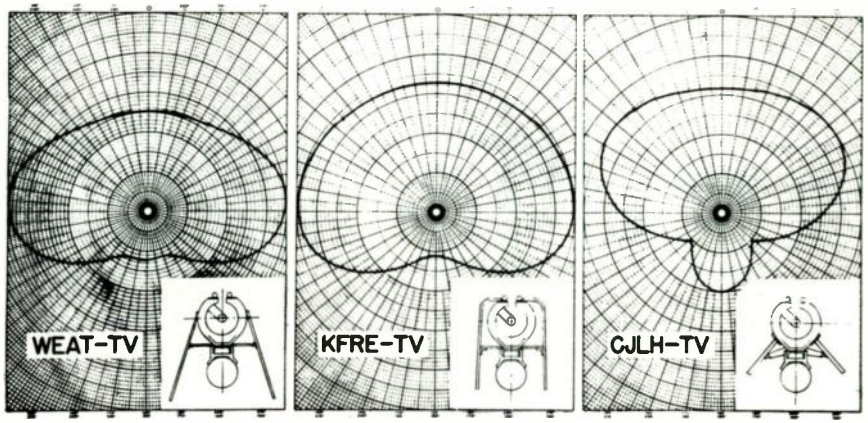

Fig. 9
Typical directional horizontal radiation patterns, relative field

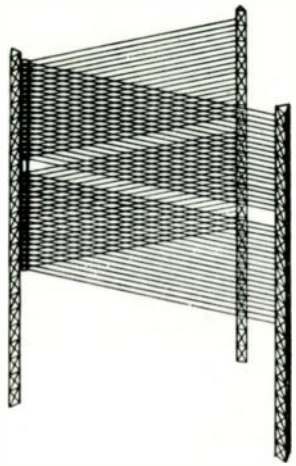

Fig. 11A
An extremely high gain directional antenna

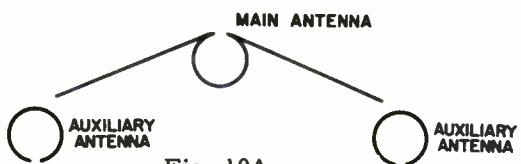

Fig. 10A
Wide angle null antenna

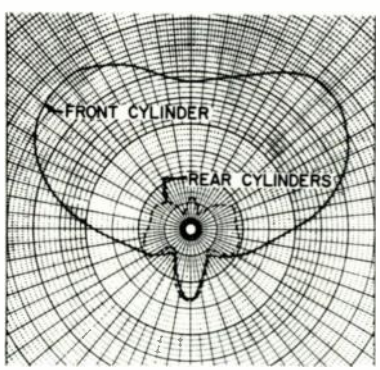

Fig. 10B
Horizontal radiation patterns of individual components, relative field

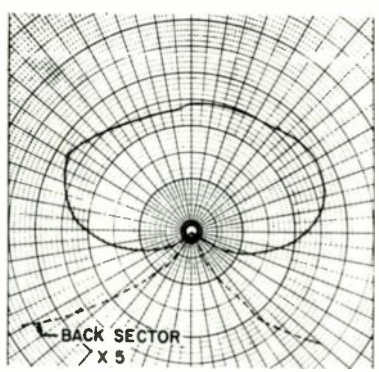

Fig. 10C
Horizontal radiation pattern of complete array, relative field

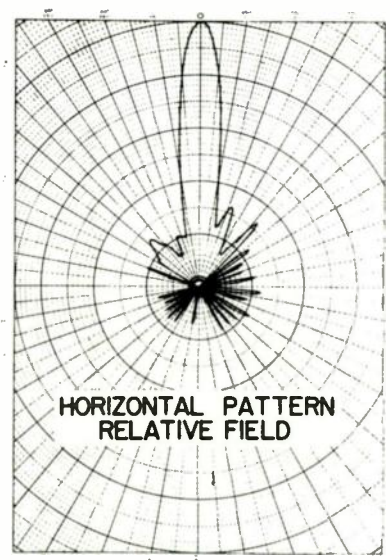

Fig. 11B
Horizontal pattern, relative field

SELF-DIPLEXING T-V ANTENNA

by
C. B. Mayer
P. M. Pan
General Electric Company

Introduction

The broadcast of television, consisting of the audio and video information on separate carrier frequencies, requires the use of two transmitters. All present-day transmitting systems use the same antenna for both signals. This requires the use of complex filter diplexing systems in order to isolate the two transmitters and get both signals onto a common transmission line.

The system which is described here eliminates the need for these complex filter systems. This is achieved by propagating the signals to the antenna in the form of two orthogonal transmission modes within the circular antenna mast, and then, by the use of a separate helical antenna for each signal. The two antennas are so arranged that in overlapping portions their windings are in the opposite sense, thus producing a cross-wound helix as shown in Fig. 1.

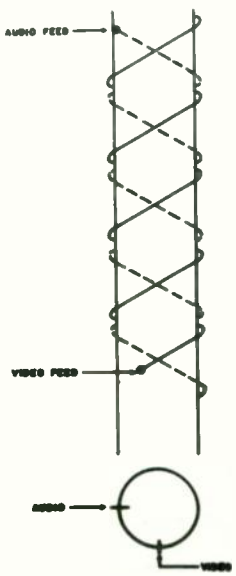

Fig. 1
Cross wound helix.

Since simplicity is the key to reliability of operating equipment, increased simplicity can result whenever a part of an operating structure is made to perform several functions simultaneously.

Using this principle, the original helical UHF-TV transmitting antenna, introduced five years ago, was the first to make large strides toward simplification. The number of feed points required for high gain antennas was reduced by a factor of about 15 to 1.

Now, further developments in the feed system again permit an increase in overall system simplicity. This results from increasing further the functions performed simultaneously by parts of the operating structure.

Present-Day Diplexing Schemes

In order to fully appreciate the significance of the development of this system, let us take a closer look at the transmitting systems in present use.

A typical system which is used by General Electric to meet the FCC specifications on sideband signal rejection and to perform diplexing action at UHF is shown in fig. 2b. (The system shown in Fig. 2a does not meet the specifications.) It consists of eight cavities and a number of hybrid rings. The cavities C_2, C_3 and C_4 are single-tuned cavities, while C_1 is a double-tuned cavity. (An analysis of such a system is shown in Appendix A.) The problem of

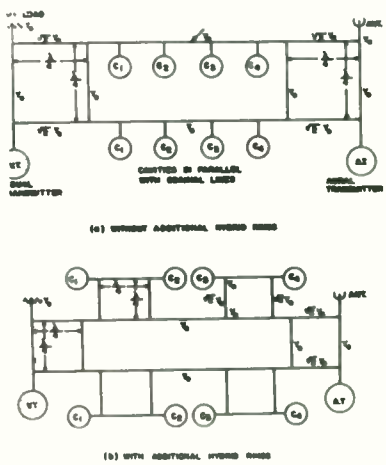

Fig. 2
Diplex - sideband filter system.

obtaining a particular Q and resonant frequency in each of these cavities, and maintaining sufficient stability in operation is not an easy one, to say the least. This becomes more apparent when we realize that the losses in each of these cavities is generally greater than 400 watts, and cooling must be required to prevent changes in resonant frequency and Q due to temperature rise. Other manufacturers might use fewer cavities, but the performance is not as good.

Another difficulty encountered with such a system is the phase error introduced in the signal by transmitting color television and thus the need for considerable phase compensation.

The cost of such a system as this is in excess of $10,000. Thus the need for an entirely new approach to the problem is apparent.

The system which is described here eliminates all this complexity with the exception of the video sideband filtering which may be done easily at low signal level.

This is accomplished, as we said above, by the use of two orthogonal transmission modes within a waveguide mast to provide almost complete isolation of the two signals within the waveguide. The signals are isolated on the outside of the mast by means of a cross-wound helical antenna using different windings for the two signals.

Excitation of the Two Modes and Cross Coupling Between Modes

Now, since the transmitter mast is usually a hollow pipe, it is convenient to use this as a circular waveguide and use two TE_{11} modes to propagate the signals. The transverse electric field pattern for these two modes is shown in Fig. 3. The size of the guide is chosen so that all other modes are beyond cutoff and will not propagate.

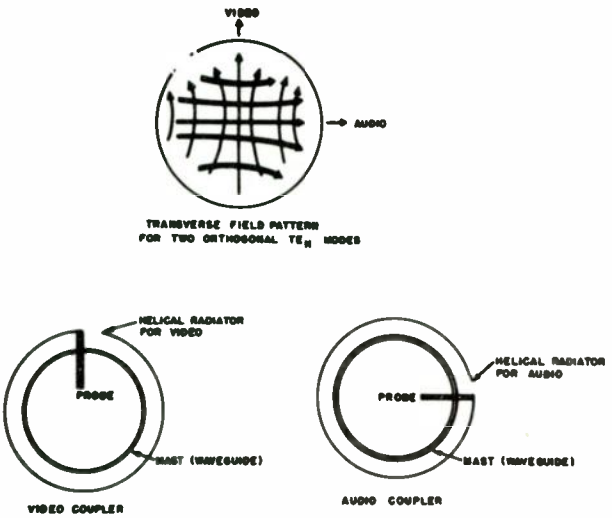

Fig. 3

We notice that these modes are identical except for the fact of the 90° rotation of the E vectors. This is particularly advantageous since the propagation constant for each signal will be the same. Also, since both modes are the same, the coupling to the antenna can be done in identically the same way and offer great simplicity.

Theoretically, there should be no cross coupling between modes if the waveguide mast is a perfect cylinder and the two modes are at 90° to each other. However, in practice the masts are not perfect so one might expect some cross coupling. Before starting on the experimental development, an analysis was made to determine to what extent the eccentricities found in a practical waveguide would cause cross coupling. (See Appendix B.) This analysis indicated that the amount of cross coupling that would be caused by waveguide imperfections was very small. Thus the first problem was that of devising a means of exciting these two modes in a manner which will isolate the two transmitters and have the necessary bandwidth requirements.

One method of exciting a TE_{11} mode in a circular guide is by a straight axial transformation from the fundamental or TE_{10} mode propagating in a rectangular guide. This mode we shall refer to as the axial mode. In our model, the wave impedance in the rectangular guide was slightly different from that in the circular guide, so a 1/4 wavelength transformer of rectangular cross section was placed between the two to perform the transformation. This does the job very nicely and is quite broadband.

A second method of exciting a TE_{11} mode in the circular guide, also from a rectangular waveguide carrying the TE_{10} mode, is to come directly in through the side of the circular guide. A short circuit is then placed 1/4 wavelength below the opening to propagate all the energy in one direction up the mast to the antenna. This mode we refer to as the "side mode".

These two systems may be combined very nicely into the dual mode transducer shown in Fig. 4.

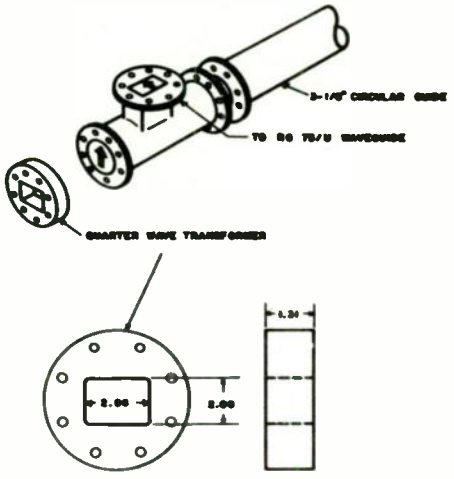

Fig. 4
Dual mode transducer.

The orientation of the "axial mode" is arranged so that its E vectors are at right angles to the "side mode". Under these conditions, the smaller cross sectional dimension of the quarter-wave transformer acts as a waveguide beyond cutoff to the "side mode", thus providing the short circuit necessary to send all the energy from getting back into the "axial mode" transmitter. This transducer provided better than 40 db isolation between the two transmitters when the circular guide was fed into a matched load.

One difficulty which arose with the transducer was a very high standing-wave ratio which occurred in the "axial mode" near the center of the band. This was due to the rather large opening in the side of the circular waveguide for the other mode. It was found that placing any sort of metallic bar across this opening would eliminate the discontinuity satisfactorily. In order not to disturb the impedance match of the "side mode", however, a resonant window was placed across the opening (see Fig. 5).

It was found that this resonant window, when placed in a matched rectangular guide, was very broadband. The VSWR is below 1.2 for a bandwidth in excess of 20 per cent. Thus, this represented a good way of preserving the match in the "side mode" and eliminating the discontinuity in the "axial mode" caused by the opening in the pipe.

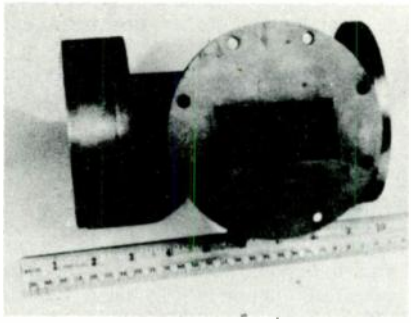

Fig. 5

Coupling the Energy to the Antenna

Having achieved the excitation of the two TE_{11} modes in our waveguide mast, the problem of coupling the energy to the antenna was taken up. Probe coupling appeared to offer the best solution. Consider again the transverse electric field pattern for the two modes shown in Fig. 3. If a probe is inserted into the field in the vertical direction as shown, it will couple only to the video signal and, if it is inserted in the horizontal direction as shown, it will couple only the audio signal.

The initial probe design was scaled from a similar probe coupling system used at X-band. The proven design is shown in Fig. 6. The

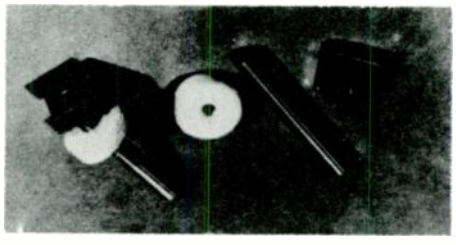

Fig. 6
Probe coupling devices.

threads on the inside and outside of the teflon washer enabled the positioning of the washer and the depth of the probe to be made independently. The trapezoidal-shaped connector is screwed onto the end of the probe and holds the helices.

A calculation of the probe and antenna impedance (see Appendix C) indicated that the match should be easily obtained.

100 Per Cent Coupling

In order to transfer all of the energy within the mast to the antenna, it is necessary to place a short circuit one-quarter wavelength beyond the coupling probe. (In this particular case, the choke short described in Appendix D was used.) Since, in our system, the two signals are not coupled out at the same point on the mast, it is necessary to have a device which will reflect the energy of one mode but transmit the other with a minimum of reflection.

To perform this function, a "dual mode filter" was devised. The principle applied here

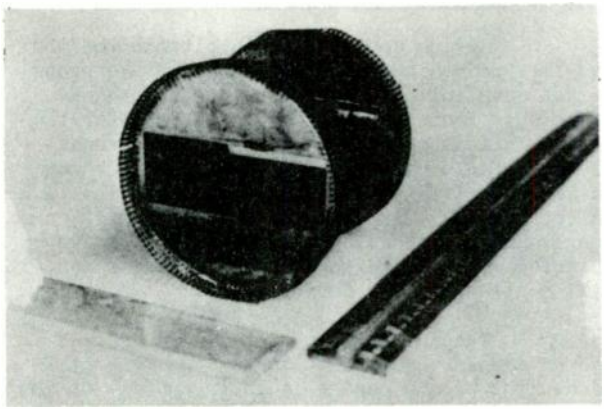

Fig. 7
Dual mode filter.

was to use a section of rectangular waveguide one-half wavelength long. The dimensions are such as to present a matched impedance for the one mode (thereby transmitting it on through) while presenting a waveguide beyond cutoff to the other mode thereby acting as a short circuit. A photograph of this device, using finger tip connectors, is shown in Fig. 7. Experiments showed that this type of connector was good enough for the purpose. It is important to bear in mind that the connector should contact the waveguide at all points evenly or cross coupling will occur between the two modes. The choke short is by all means much superior.

Tests which were run, using a helical antenna of 2-1/2" pitch and diameter of 3-7/8", indicated that 100 per cent of the energy could be coupled from the guide to the antenna with sufficient bandwidth using this type of coupling.

50 Per Cent Coupling

In order to extend the antenna to multiple bays, it must be possible to couple out less than 100 per cent of the energy at various points along the guide. In particular, the next to the last bay must couple 50 per cent of the energy.

When the probe depth was adjusted to couple out half the power from the guide, the VSWR turned out to be about 2.0 over a fairly wide frequency band.

Since a power split at the probe would produce an input impedance of $Z_o/2$ (see Fig. 8)

Fig. 8
Impedance matching for probe.

and since an impedance mismatch of 2:1 causes a VSWR of 2.0, this appeared as the obvious cause. Thus moving back towards the generator, the correct distance, the mismatch was tuned out satisfactorily by means of a capacitance probe screwed in through the side of the guide, parallel to the coupling probe. Measurements showed that this caused very little cross coupling to the other mode.

Extension to any Per Cent Coupling

From the results obtained in the 50 per cent coupling case, the extension to any per cent coupling using the same basic procedure appears straightforward. The amount of power coupled to the antenna is adjusted by means of the probe depth and the mismatch caused by the power split

is eliminated by a capacitive probe at the correct distance from the coupling probe toward the generator.

Antenna

It should be noted here that the development model was scaled to 3000 mc for experimental convenience.

The antenna which was used to continue the isolation of the two signals on the outside of the mast, and thereby complete the self-diplexing system, was an extension of the basic helical antenna.

To understand this, let us review briefly the theory of operation of the basic single-bay helical antenna shown in Fig. 9.

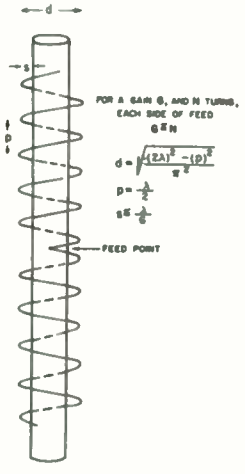

Fig. 9

Two traveling waves are launched along the helices at the feed point. Each helix acts very much like a single wire above a ground plane (the mast). The spacing between the mast and the helix is such that there is a considerable amount of radiation per turn. In the practical design, each helix is about five turns. Each turn is an integral number of wavelengths so that the currents at a given azimuthal angle are in phase. A high gain antenna is achieved by stacking a number of such single-bay antennas along a mast.

Use of the Basic Single Helix Antenna for Self-diplexing

The first attempt at a self-diplexing antenna was to use a single helix and to feed the two signals by means of probe coupling at opposite ends of the helix as shown in Fig. 10.

Fig. 10
Single wound helix (signal at each end).

It was hoped that sufficient isolation would result between the two feeds due to the radiation loss to produce a practical solution. However, the isolation obtained was only 13 db at one point in the band which was not sufficient. But this can be improved to 20 db by using mode suppressors.

The "Bifilar" or Parallel-wound Self-diplexing Antenna

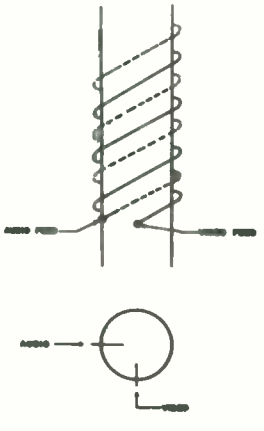

Fig. 11
Parallel wound helix.

Another method of obtaining isolation is to use two separate "basic" helical antennas arranged so that their windings run parallel to each other as shown in Fig. 11.

An attempt was made to feed the two signals at the same point along the mast, but it was found that considerable cross coupling was introduced between the two probes inside the guide due to higher order modes. However, considerable improvement was obtained over the single helix type when the feeds were displaced in a manner similar to Fig. 10. The isolation achieved with this scheme on a two-bay antenna ranged from 18 to 26 db over the operating band. This can be further improved by mode suppressors.

The Cross-wound Helix Self-diplexing Antenna

It was felt that further improvement might be obtained if the windings of one of the antennas were reversed, thus producing a cross winding in the overlapping portion of the aperture between the feed points. Figure 12 shows

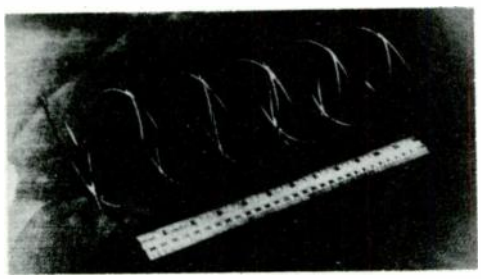

Fig. 12
Cross wound twin helices.

a set of the helices before mounting on the mast. A physical picture of why this might be so is obtained if we again consider the fact that the antenna acts as a single wire above a ground plane. This is equivalent to a two-wire transmission line. In the case of the bifilar or parallel winding scheme, this is analogous to two parallel transmission lines running side by side for many wavelengths. Thus, one might expect to get considerable coupling between them. However, the case of the cross-wound helix is analogous to two transmission lines which cross each other at an angle of 30 to 40°, and one would expect very little transfer of energy from one line to the other.

A two-bay cross-wound self-diplexing helical antenna was built (see Fig. 13), and the anticipated improvement was achieved. The isolation between the two signals now ranged from 23 to 38 db over the operating band. Isolation of 30 db can be achieved by using mode suppresors.

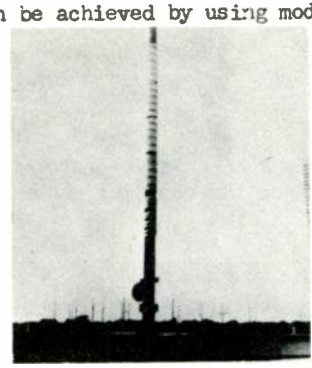

Fig. 13
Complete assembly two-bay self diplexing antenna.

Since 20 db of isolation is sufficient for this application, the cross-wound helical antenna does the self-diplexing job very nicely.

Antenna Patterns

Having obtained the isolation necessary to complete the self-diplexing of the two signals, the one remaining question is whether or not the antenna patterns are very much changed by the use of the cross winding.

Basic Helical Antenna

Let us first take a look at the patterns normally achieved with the basic 3λ mode helical antenna.

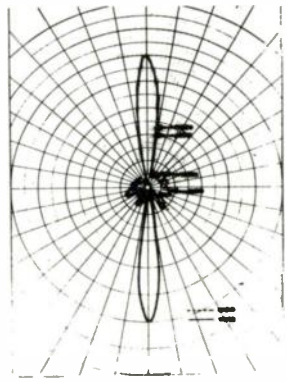

Fig. 14
3 λ mode G.E. 2 bay helical antenna relative voltage pattern.

Vertical Pattern. The vertical pattern for a basic two-bay helical antenna is shown in Fig. 14. The energy is concentrated in the horizontal plane due to the size of the vertical aperture. The beam width achieved is about 8-1/2° - 9°.

Horizontal Pattern

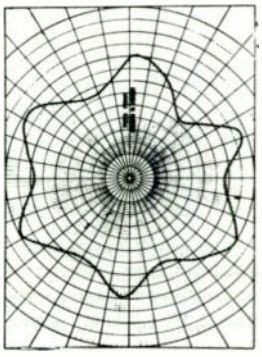

Fig. 15
Horizontal pattern 3λ mode 2 bay G.E. helical antenna relative voltage.

1. Cyclic Effect - The horizontal pattern of the basic helical antenna as shown in Fig. 15 is not quite as straightforward as its vertical pattern. In general, there appears a cyclic effect of about ±1-1/2 db. The number of cycles is equal to 2 times the number of wavelengths per turn.

2. Deep Null - A single deeper null also appears at one point in the pattern. The cause of these variations in the horizontal pattern is due to two modes propagating on the helix.

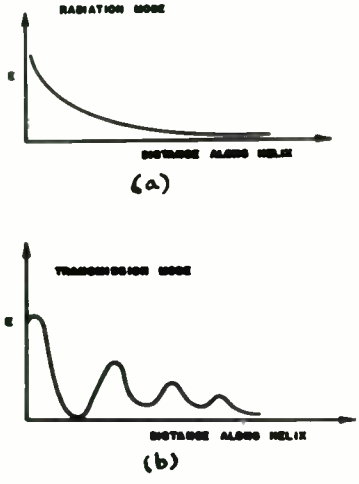

Fig. 16

The first of these modes is the radiation mode[3] which has a well behaved distribution as shown in Fig. 16a. This is the desired mode. The other mode, the transmission mode, shown in Fig. 16b is not so well behaved, and causes the deep null and cyclic effect.

Considerable success has been achieved in eliminating the deep null and reducing the cyclic effect by means of mode suppressors. These are described in a General Electric Report TIS No. R55ELP142.

Cross-wound Helical Antenna

Vertical Pattern

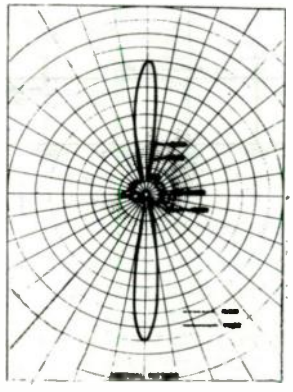

Fig. 17
3λ mode cross wound self-diplexing 2 bay helical antenna relative voltage.

The vertical pattern of a two-bay model cross-wound self-diplexing antenna is shown in Fig. 17. It is seen to be essentially the same as that of the basic helical two-bay antenna. The vertical beam-width is 8-1/2 to 9 degrees.

Horizontal Pattern

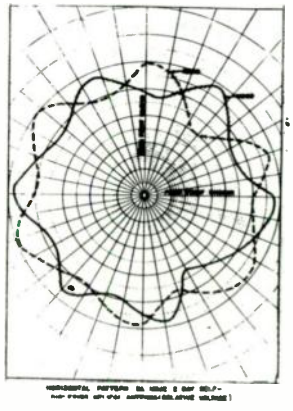

Fig. 18
Horizontal pattern 3λ mode 2 bay self-diplexing helical antenna (relative voltage).

The horizontal pattern shown in Fig. 18 shows the same cyclic effect and deep null found in the basic antenna, which indicates that the two antennas are acting nearly independent of each other due to the cross winding.

Over-All Performance

Isolation

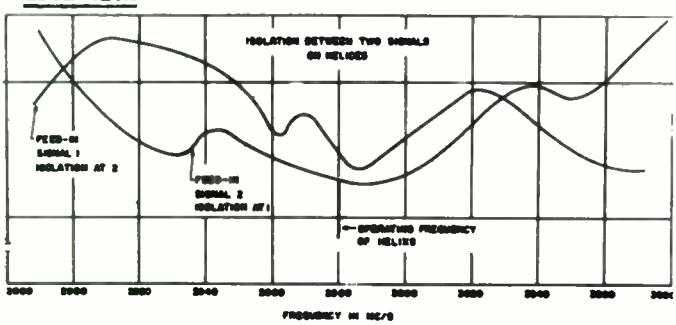

Fig. 19
Two bay cross-wound diplexing helical antenna.

The over-all isolation achieved for the two-bay model constructed using the cross-wound antenna is shown in Fig. 19. It is seen that the minimum isolation is 23 db near the center of the band and ranges above 30 db elsewhere in the band.

VSWR and Bandwidth

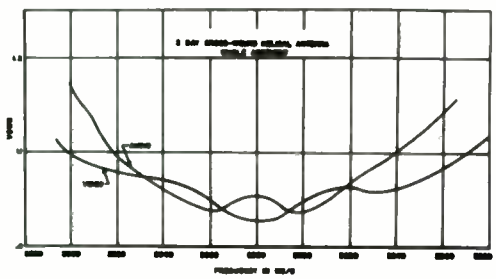

Fig. 20
Input VSWR vs. frequency.

The VSWR for the two-bay cross-wound self-diplexing antenna, fed by the dual mode transducer and probe coupling, is shown in Fig. 20. While this is not quite as good as the coaxial fed basic helical antenna, it is felt that further improvement could be achieved by careful design and additional matching.

Conclusions and Summary

We have seen that UHF television transmission requires the use of elaborate filter diplexing schemes when using a single antenna to transmit audio and video signals. The cost of these systems is in the order of $12,000. However, we have shown here that, by the use of two orthogonal transmission modes within the hollow antenna mast and a cross-wound helical antenna, it is possible to produce a self-diplexing antenna system which eliminates the need for these complex and costly filters. The system described here is a two-bay model. The extension of this model to high gain multiple bay systems appears quite feasible.

Appendix A

Diplexing System for TV Transmitters

In order to use the same antenna both for the video and audio signals in the present television transmission, a diplexing system must be used. One typical example is shown on Fig.A-1

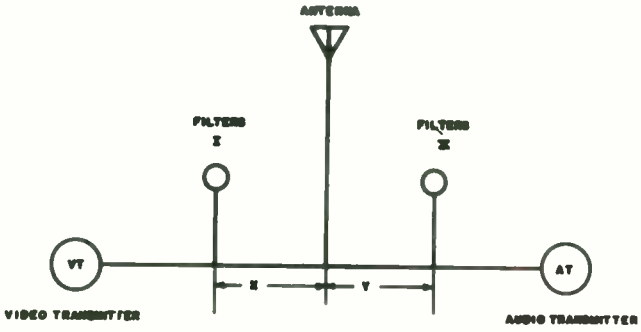

Fig. A-1
T.V. diplexing.

Filters I will reject all the audio signals, while filters II will reject all the video signals. Because of the FCC specification on sideband isolation, bandwidth and signal levels, the filters must have very high Q and at the same time be broadbanded, so as to meet the requirements.

The new approach used nowadays is the filterplex as shown in Fig. A-2.

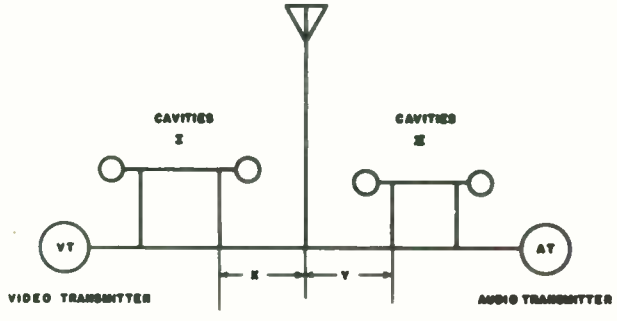

Fig. A-2
Filterplex for T.V. diplexing.

It introduces hybrid rings. Proper cavities are placed in the legs of the hybrid rings. The ideal operation of the square hybrid ring with matched loads was analyzed by a number of workers.

This analysis obtains the voltage relationships when the ideal hybrid is fed from a matched generator and terminated with two mismatched loads and one matched load.

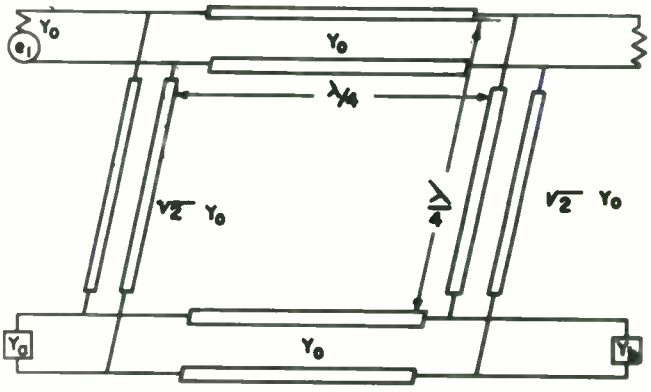

Fig. A-3

It is assumed that the arms of the hybrid are exactly one-quarter wavelength long. The circuit can be analyzed by replacing the admittances Y_a and Y_b with matched loads and voltage generators e_a and e_b. These generators will be adjusted in magnitude to produce the proper voltage and current relations on the output terminals.

For example, consider the arm with admittance Y_a, the incident voltage is 1, and the reflected voltage is Γ_a which is the voltage reflection coefficient.

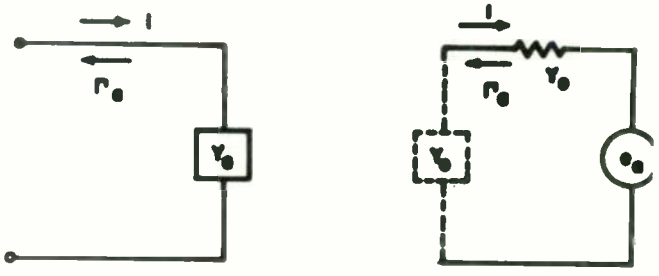

Fig. A-4

The generator e_a must then be

$$e_a = 2\Gamma_a \qquad \text{(A-1)}$$

where

$$\Gamma_a = \frac{Y_o - Y_a}{Y_o + Y_a} \qquad \text{(A-2)}$$

The effect of each voltage generator on the circuit is determined from the "superposition" method. Two generators are short circuited, then only one generator is in operation, with matched loads on the other three arms.

The sketch following shows the system of equivalent generators with the direction of propagation indicated.

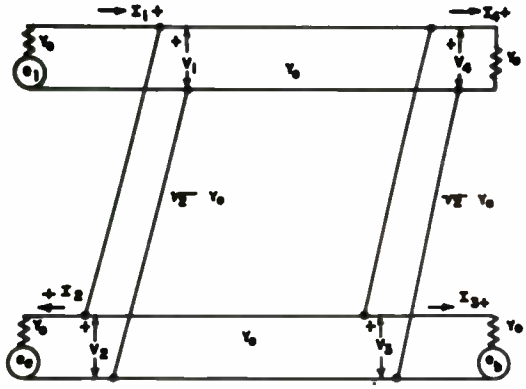

Fig. A-5

A table below shows the voltages with their directions due to each of the generators:

	OPERATION OF e_1		OPERATION OF e_a		OPERATION OF e_b		HYBRID RING OPERATION	
e_1	2		0		0		2	
e_a	0		$-j\sqrt{2}\Gamma_a$		0		$-j\sqrt{2}\Gamma_a$	
e_b	0		0		$-\sqrt{2}\Gamma_b$		$-\sqrt{2}\Gamma_b$	
DIRECTION	+	−	+	−	+	−	+	−
V_1	1	0	0	$-\frac{\Gamma_a}{2}$	0	$\frac{\Gamma_b}{2}$	1	$\frac{\Gamma_b-\Gamma_a}{2}$
V_2	$\frac{-j}{\sqrt{2}}$	0	0	$-j\frac{\Gamma_a}{\sqrt{2}}$	0	0	$\frac{-j}{\sqrt{2}}$	$\frac{-j\Gamma_a}{\sqrt{2}}$
V_3	$-\frac{1}{\sqrt{2}}$	0	0	0	0	$\frac{-\Gamma_b}{\sqrt{2}}$	$-\frac{1}{\sqrt{2}}$	$-\frac{\Gamma_b}{\sqrt{2}}$
V_4	0	0	$j\frac{\Gamma_a}{2}$	0	$j\frac{\Gamma_b}{2}$	0	$j\left(\frac{\Gamma_b+\Gamma_a}{2}\right)$	0

Fig. A-6

The resultant voltage diagram is shown below.

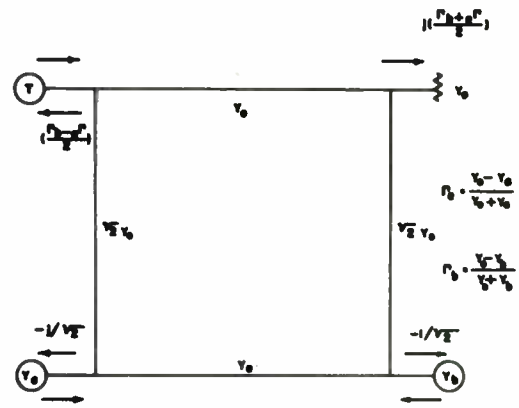

Fig. A-7

From the characteristics of the cavities, such as 'Q', the response of the diplexing system of TV transmitters can be obtained.

Appendix B

Decoupling Due to Orthogonal Modes in Circular Waveguide

To analyze the coupling of the two orthogonal TE_{11} modes in the circular guide, due to the irregular shapes of the guide, it is necessary to have the polar equation of an ellipse centered on the axis of the waveguide. This is given by

$$r = b\sqrt{1 - \frac{e^2}{2}(1 - \cos 2\theta)}$$

where r = radius of circular guide

b = semi-minor axis

e = eccentricity of the ellipse

For small eccentricities ($e \ll 1$) this reduces to

$$r = b\left(1 + \frac{e^2}{4}\cos 2\theta\right) \qquad \text{(B-1)}$$

and, therefore,

$$r_{max} - r_{min} = \frac{be^2}{2} \approx \frac{Re^2}{2} \qquad \text{(B-2)}$$

where R is the mean radius of the cross section.

To obtain the propagation constant for TE_{11} waves polarized along the major and minor axis of the ellipse, we proceed as follows: a potential type function is introduced from which the field components may be obtained by differentiation.

$$\Pi = \bar{U}(r, \theta) \exp j(\omega t - \beta Z) \qquad (B-3)$$

where Z is the axial direction of the waveguide

$$\beta = \frac{2\pi}{\lambda_g}$$

λ_g = guide wavelength

and $\bar{U}(r, \theta)$ gives the transverse field pattern. For TE_{11} mode, it is of the form

$$J_1(K r) \exp j\theta \qquad (B-4)$$

For an exactly circular boundary, K and thence β can be found by applying the boundary conditions. For a slightly non-circular boundary, we shall find that there will be two new values of K, differing slightly from the old value. The two new β values give rise to a slow rotation as they progress along the waveguide.

The boundary conditions that the tangential electric field or normal magnetic field vanish are expressed as

$$\frac{d\bar{U}}{dn} = 0 \qquad \text{or } \nabla\bar{U} \cdot \vec{n} = 0$$

where $\vec{n}$ is the direction of the normal. For a circular guide, n is the radial direction; but for non-circular cases, there will be an angular component involved. To derive the appropriate expression, refer to the Fig. B-1 where C and D are areas of the unperturbed and perturbed circular cross-sections respectively. C' is concentric with C.

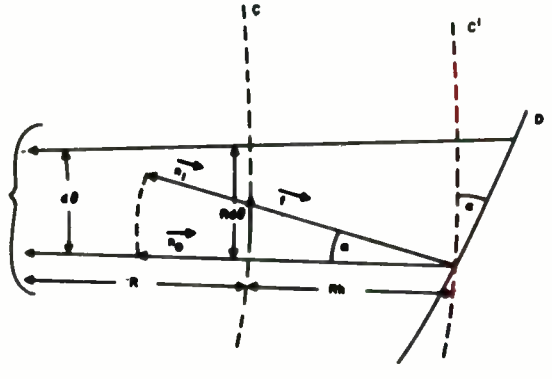

Fig. B-1

The equation of the cross-section is given by

$$r = R\left[1 + h(\theta)\right]$$

where R is the radius of the original circular cross-section, and h is a small variable which describes the new contour.

For changes in the separation constant K, as shown in equation (B-4), K is introduced to represent the small change. Therefore, for TE_{11} mode it is

$$J_1(K r) \exp j\theta$$

To get an expression for h, it is expressed in Fourier series

$$h = \sum_{n=1}^{\infty} (a_n e^{jn\theta} + a_n^* e^{-jn\theta}) \qquad (B-5)$$

and

$$h = \sum_{n=1}^{\infty} (A_n \cos n\theta + B_n \sin n\theta) \qquad (B-6)$$

Since $|a_2| = 1/2\sqrt{A_2^2 + B_2^2}$

we have

$$K = \pm K/2 \frac{K^2R^2 + 1}{K^2R^2 - 1}\sqrt{A_2^2 + B_2^2} \qquad (B-7)$$

The propagation constant of β is related to K through the familiar expression

$$\beta = \frac{2\pi}{\lambda_g} = \frac{2\pi}{\lambda}\sqrt{1 - (\lambda/\lambda_{c.o.})^2}$$

$$= \frac{2\pi}{\lambda}\sqrt{1 - \left(\frac{\lambda KR}{2\pi R}\right)^2} \qquad (B-8)$$

Since the cut-off wavelength

$$\lambda_{c.o.} = \frac{2\pi R}{KR}$$

$$\therefore \quad |\delta\beta| = \frac{K^2R^2}{2\beta}\,\frac{K^2R^2 + 1}{K^2R^2 - 1}\sqrt{\frac{A_2^2 + B_2^2}{R^2}} \qquad (B-9)$$

For example, a 11-1/2" circular guide, whose major axis - minor axis = 20 miles, equation (B-2) gives e = 0.059. For the TE_{11} mode, KR = 1.84 and at 680 mc β = 0.169/in

$$\delta\beta = .577\sqrt{A_2^2 + B_2^2} = .577\,\frac{e^2}{4}$$

$$= 4.85 \times 10^{-4} \text{ /in.}$$

For decoupling of X db

$$X \log \cot \delta\beta Z \qquad (B-10)$$

Therefore, the decoupling is obtained.

Appendix C

Calculation of Probe and Antenna Impedance

An approximation to the impedance of the probe may be made by assuming that the currents in the probe return to the guide through the capacitive reactance between the end of the probe and the guide walls.

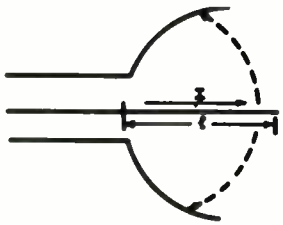

INPUT IMPEDANCE TO THE PROBE IS

$$z = \frac{V}{I} = \frac{\int_{LOOP} \bar{E} \cdot \overline{dl}}{I} \cdot \frac{1}{j\omega c} \cdot \frac{\int_0^{\ell} \bar{E} \cdot \overline{dl}}{I}$$

Fig. C-1

The current, I, along the probe, produces an electric field intensity ${}_1\bar{E}$, and the charge at tne end of the probe produces an electric field intensity ${}_2\bar{E}$.

The input impedance to the probe is

$$Z = \frac{V}{I} = \frac{\int_{loop} \bar{E} \cdot \overline{dl}}{I} \qquad (C\text{-}1)$$

$$= \frac{1}{j\omega c} - \frac{\int_0^{\ell} {}_1\bar{E} \cdot \overline{dl}}{I}$$

Thus, the probe impedance is the sum of its own capacitive reactance (which excites no modes) and the impedance due to a current element of length ℓ. The real part of the impedance is given by the second term.

The real power we can find by integrating the fields across the entire guide. The real part of the voltage is given by

$$\int_0^{\ell} \bar{E} \cdot \overline{dl}$$

The power is given by

$$P = \int_{SURFACE} \bar{E} \times \bar{H} \cdot dA \qquad (C\text{-}2)$$

$$\bar{E} = E_\rho = \frac{j\omega\mu}{\rho} \left(\frac{\lambda_c}{2\pi}\right)^2 H_o J_1\left(\frac{2\pi\rho}{\lambda_c}\right) \sin\varphi$$

$$\bar{H} = H_\theta = \frac{j\beta}{\rho} \left(\frac{\lambda_c}{2\pi}\right)^2 H_o^2 J_1\left(\frac{2\pi\rho}{\lambda_c}\right) \sin\varphi$$

$$\bar{E} \times \bar{H} = \frac{\omega\mu\beta}{\rho^2} \left(\frac{\lambda_c}{2\pi}\right)^4 H_o^2 J_1\left(\frac{2\pi}{\lambda_c}\right) \sin^2\varphi$$

$$dA = \rho\, d\varphi\, d\rho$$

$$\bar{E} \times \bar{H} = \omega\mu\beta \left(\frac{\lambda_c}{2\pi}\right)^4 H_o \int_{\rho}^{\rho+\ell} \int_0^{2\pi} \frac{1}{\rho^2} \left[J_1\left(\frac{2\pi}{\lambda_c}\right)\right]^2 \sin^2\varphi\, d\varphi\, d\rho$$

Thus the real part of the probe impedance may be written

$$Z_{(real)} = \frac{V^2_{(real)}}{P_{(real)}} = \frac{\left[\int_o^{\ell} \bar{E} \cdot \overline{dl}\right]^2}{\bar{E} \times \bar{H} \cdot da} \qquad C\text{-}3$$

Now E_ρ and H_θ are given by

$$\bar{E} = E_\rho = \frac{j\omega\mu}{\rho} \left(\frac{\lambda_c}{2\pi}\right)^2 H_o J_1\left(\frac{2\pi\rho}{\lambda_c}\right) \sin\varphi$$

where θ and ϕ are the angle in the transverse plane about the axis of the cylinder

λ_c is guide cut-off wavelength

H_o is the peak H field intensity

ω is the angular radian excitation frequency

$$\bar{H} = H_\theta = \frac{j\beta}{\rho} \left(\frac{\lambda_c}{2\pi}\right)^2 H_o^2 J_1\left(\frac{2\pi\rho}{\lambda_c}\right) \sin\varphi \qquad (C\text{-}5)$$

Thus

$$\bar{E}_\rho \times \bar{H}_\theta = \frac{\omega\mu\beta}{\rho^2} \left(\frac{\lambda_c}{2\pi}\right)^4 H_o^2 J_1\left(\frac{2\pi}{\lambda_c}\right) \sin^2\varphi \qquad (C\text{-}6)$$

Also

$$dA = \rho\, d\varphi\, d\rho \qquad (C\text{-}7)$$

Substituting C-6 and C-7 into C-2 yields

$$P_{real} = \omega\mu\beta \left(\frac{\lambda_c}{2\pi}\right)^4 H_o \int_0^{\rho} \int_0^{2\pi} \frac{1}{\rho^2} J_1\left(\frac{2\pi}{\lambda_c}\right)^2 d\rho \sin^2\varphi\, d\varphi \qquad (C\text{-}8)$$

Using C-4 and assuming the probe to be oriented in the direction where $\sin\varphi = 1$, we have

$$V_{real} = j\,\omega\,\mu\,H_o \left(\frac{\lambda_c}{2\pi}\right)^2 \int_{\rho-\ell}^{\rho} \frac{1}{\rho} J_1\left(\frac{2\pi\rho}{\lambda_c}\right) d\rho \qquad (C\text{-}9)$$

Substituting C-8 and C-9 into C-3 and simplifying we obtain

$$Z_p = \frac{2}{\pi} \frac{\ell}{\rho_o} Z_o \qquad \text{(C-10)}$$

for an assumed probe depth of 7/8", ρ_o this becomes

$$Z_p = 26.5 \text{ ohms} \qquad \text{(C-11)}$$

Calculating the impedance of the coaxial section at the exit to the guide for the chosen dimension, we get 50 ohms.

The impedance of the helix was calculated as 350 ohms. However, the feed sees two helices in parallel, so that the impedance is

$$Z_h' = \frac{350}{2} = 175$$

For a match, it is desired to have

$$Z_c = (Z_p Z_n)^{1/2}$$

$$Z_c = 69 \text{ ohms}$$

The calculated value was about 50 ohms, indicating that the match should be easily obtained and that it may be adjusted by changing the probe depth.

Appendix D

Choke Short

A choke short is used at the end of the waveguide to insure the perfect 100% coupling. The choke is a conventional $\lambda g/4$ short.

This choke short has a VSWR of 1.15 over the bandwidth of ± 10%. A choke short not only reflects most of the energy to let the last probe pick it up, but it will also serve as a good short all around the guide, so that no cross coupling between modes will result.

References

1. H.G. Smith, "High-Gain Side Firing Helical Antennas for Ultra-high-Frequency Television Broadcasting", Communication and Electronics.

2. C.E. Nelson, "Loop and Probe Coupling to Waveguides", General Electric Advanced Engineering Program Notes, Feb. 1954.

3. J.D. Kraus, "Antennas" - McGraw-Hill, 1948

4. H. Poritsky, "Propagation of EM Waves Along Helices", Research Laboratory, General Electric, TIS 52RL652.

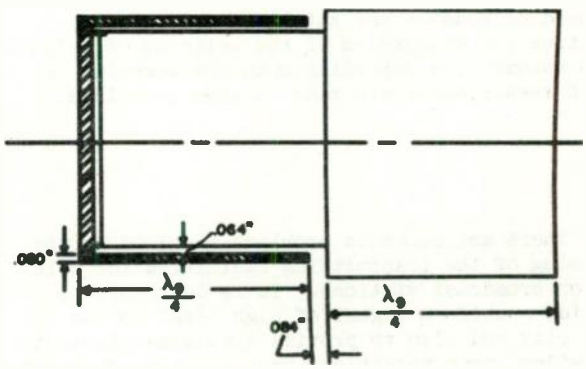

Fig. D-1
Choke short.

TELEVISION FIELD STRENGTH MEASUREMENTS - A TOOL IN TRANSMITTING ANTENNA PLANNING

Raymond E. Rohrer and Oscar Reed, Jr.
Jansky & Bailey, Inc.
Washington, D. C.

Summary

Extensive experience with field strength measurements is useful in the planning for television transmitting antenna systems, and station transmitter plant location. Measurements made on stations located in various types of terrain show a difference in the slope of the curves depicting the ratios of decile to median values. The results show some correlation with transmitting antenna height and antenna gain. The importance of providing for relatively uniform signal level over urban areas is illustrated. Field strength measurements can also be used to determine areas in need of booster and satellite transmitting stations. A discussion of the validity of height-gain assumptions depending upon the terrain over which measurements are made is also contained.

There are numerous problems involved in the planning of the transmitting facilities for television broadcast stations. It is desirable to provide a uniform signal of high level to the main city and also to provide a useable signal to the widest area possible. Such a desire dictates the combination of maximum effective radiated power and antenna height above average terrain. An ever increasing number of commercial television stations operating in the VHF band are utilizing a combination of maximum power and height as evidenced by the fact that as of March 12, there were 52 commercial VHF stations authorized to operate with maximum height and power. There are presently a total of 407 commercial VHF stations operating and authorized. Of the remaining 355 authorized VHF stations, 9 have applications pending requesting maximum height and power. There are 93 UHF commercial stations in operation.

The desire for maximum height and power and the attendant increase in antenna supporting tower height and antenna gain has been accompanied by a number of problems. It is necessary to choose a transmitter location which will allow the station to provide the widest coverage possible and also a uniform signal to the main city. This choice of site is somewhat dependent upon the type of transmitting antenna used since some of the high gain antennas have undesirable nulls in their vertical radiation patterns and care must be taken so low signal strength resulting therefrom does not occur in populous areas. Care must also be taken so that the main city does not lie in a shadowed area due to terrain obstacles. It is also desirable to select a transmitter location which will allow line-of-sight to as large an area as possible within the normal service area.

Numerous field strength measurements have been made on television broadcast stations since 1948 with the majority having been made on stations in the VHF portion of the spectrum. These measurements have been made in various sections of the country and for various frequencies and combinations of power, antenna height and antenna type. The field strength measurements made in various sections of the country show the effects of terrain on the propagation of television signals. Since television coverage contours are determined on the basis of the percentage of receiving locations and time, it is necessary to analyze these measurements by the use of statistical methods. The results and analysis of these measurements allow us to better determine the type and location of future transmitting antenna systems.

Field strength measurements made on four typical stations in various parts of the United States show different characteristics depending on the type of terrain traversed. Two of the stations were operating with effective radiated powers of approximately 28 kilowatts and antenna heights of 500 feet above average terrain. One station operated on Channel 10 and the other operated on Channel 13. Both stations employed six-bay superturnstile transmitting antennas. The third set of measurements were made on a Channel 12 station operating with an effective radiated power of 12 kilowatts and an antenna height of 850 feet. These stations are located in three different types of terrain. The measurements made on a fourth station operating on Channel 3 along the coastal plain region of the Atlantic Coast show somewhat different characteristics.

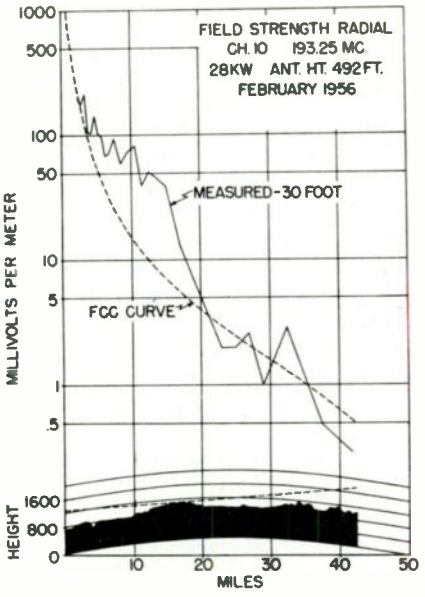

Fig. 1
Channel 10 Field Strength Radial

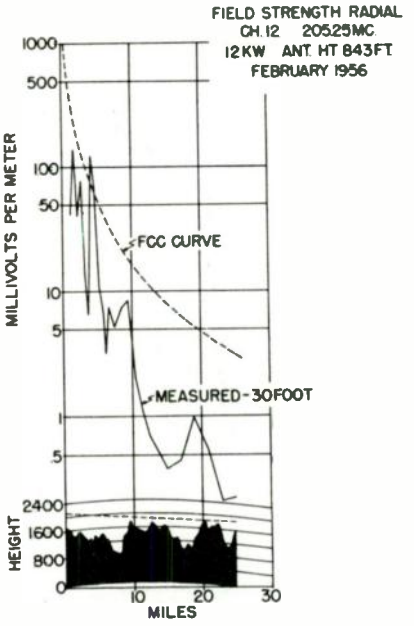

Fig. 2
Channel 12 Field Strength Radial

Fig. 1 shows one of the analyzed field strength radials for the Channel 10 station. The analyzed curve represents the measured median field strength adjusted to a receiving antenna height of 30 feet. The calculated curve is based on the methods outlined in the Technical Standards of the Federal Communications Commission. The terrain profile for the path is shown at the bottom of the graph in order to correlate the received fields with the terrain roughness. This set of measurements was made in semi-rough terrain and the measured fields are generally equal to or larger than the calculated fields for the greater part of the first 36 miles. Beyond this point, the measured fields fall below the calculated fields. In this case, the end of the measuring route is more than 300 feet below line-of-sight.

Fig. 2 shows an analyzed field strength radial for the Channel 12 station which is located in a rough area in the northeastern part of the United States. In this case the measured fields are almost entirely below the calculated values. Also, most of the measuring route is at least 300 feet below line-of-sight. Fig. 3 contains the field strength and terrain data for a typical radial for the Channel 13 station in the Midwest. The measured fields are generally equal to or greater than the calculated fields along this radial even though the end of the measuring route is approximately 600 feet below line-of-sight.

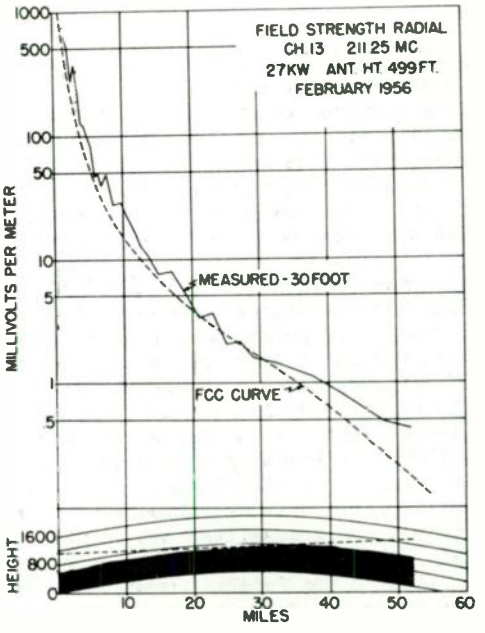

Fig. 3
Channel 13 Field Strength Radial

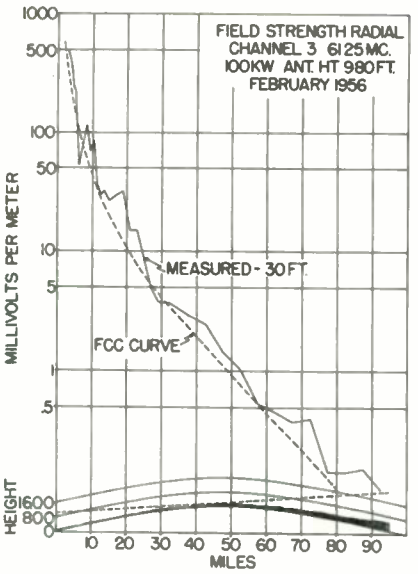

Fig. 4
Channel 3 Field Strength Radial

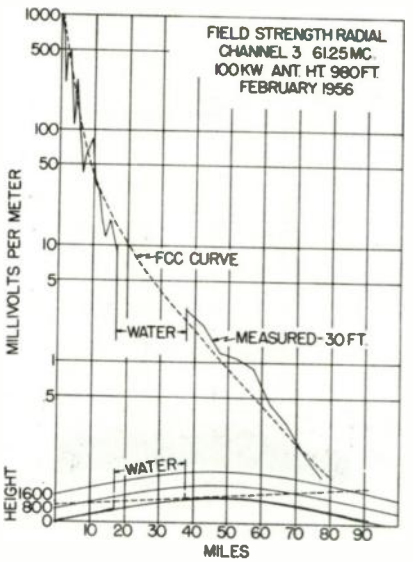

Fig. 5
Channel 3 Field Strength Radial

Fig. 4 is a field strength radial for a Channel 3 station operating in the coastal plain area. This station operates with a six-bay superturnstile antenna with an effective radiated power of 100 kilowatts and an antenna height of 980 feet above average terrain. The average measured curve is somewhat above the Federal Communications Commission curve for the entire radial. At a distance of 57 miles, 10 miles beyond the radio horizon, the measured signal and the Federal Communications Commission curve are equal. Beyond this point the measured signal is progressively greater than the Federal Communications Commission curve. It can be seen that the terrain is relatively flat out to 50 miles and then begins to rise. At 90 miles the measuring route is 1600 feet below line-of-sight. Fig. 5 is another radial for the Channel 3 station. In this case the terrain is approximately the same elevation from the transmitter out to the end of the radial. The measured field strength curve averages close to the Federal Communications Commission curve and falls below the FCC curve beyond 70 miles.

In addition to the disparity between the measured and theoretical median fields, consideration should be given the percentage of potential viewers who would be able to receive a useable signal. This factor leads to the statistical analysis of field strength measurements to determine signal levels exceeded for various percentages of locations. Experience has shown that the relationship between the median value and the decile values (values exceeded at 10 and 90 per cent of the locations) varies with the type of terrain and also the distance from the transmitter.

Analysis of numerous field strength measurements made on Frequency Modulation and Television stations, indicate that the disparity between measured and theoretical fields generally increases as the frequency increases and also as the terrain becomes more rugged. These factors should be considered, along with the Television Technical Standards of the Federal Communications Commission, when planning the type and location of television transmitting antennas.

The calculated curves shown on Figs. 1, 2, 3, 4, and 5 were determined using the standard methods outlined in the Television Technical Standards of the Commission. The measured contours are based on mobile field strength measurements made at a height of 8.5 feet above ground. This measured data has been converted to equivalent field strength at 30 feet by applying a linear height-gain relationship. It is necessary to apply this "correction" factor since the Commission uses 30 feet as the height of the standard receiving antenna. There is considerable doubt as to the realization of such a relationship, particularly in rough and mountainous terrain where evidence to the contrary exists. Results of certain height-gain measurements outlined herein lead to this conclusion.

In order to determine more fully the effects of frequency and terrain on the propagation of signals in the VHF band of television frequencies, studies have been made of field measurements on selected FM and TV stations. These measurements were made on FM and TV stations using the same transmitting site in an area of relatively smooth terrain and also in an area of rough terrain.

Field strength measurements have been made in a midwestern city at a broadcasting installation which includes an FM and a TV station. The measurements were made on an FM station operating on 97.1 megacycles with an effective radiated power of 53 kilowatts and an effective antenna height of 430 feet. The transmitting antenna was an RCA Type BF-14D four-section pylon radiator. Sets of TV field strength measurements have also been made on three different transmitting installations employed by this station which operates on Channel 10 (192-198 megacycles). The first set was made when the station used a six-section superturnstile antenna with an effective radiated power of 28.4 kilowatts and an effective antenna height of 485 feet. Further measurements were made when the station employed a twelve-section superturnstile antenna with an antenna height of 451 feet and an effective radiated power of 220 kilowatts. The final measurements were made with an effective radiated power of 219 kilowatts and an effective antenna height of 710 feet. The station employed a twelve-section superturnstile antenna modified to give null fill-in when the final set of measurements was made.

The second group of field strength measurements was made at a broadcasting installation in a city in the northeastern section of the United States. The measurements were made on an FM station operating on 100.5 megacycles with an effective radiated power of 12 kilowatts. Measurements were made when the station was operating with an effective antenna height of 800 feet. The TV station operates on Channel 12 (204-210 megacycles) from the same site. Measurements have been made on the station under a number of different operating conditions. The station first operated with a six-section superturnstile antenna with an effective radiated power of 12 kilowatts and an effective antenna height of 850 feet. Further measurements were made when the station was operating at 250 and 166 kilowatts with effective antenna heights of 820 and 1200 feet, respectively.

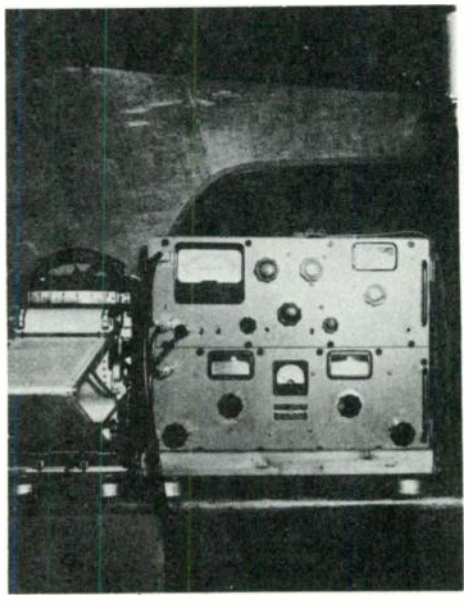

Fig. 6
Field Strength Measuring Equipment

The field strength measurements used in connection with this study were made using commercial field strength meters. The meters were installed in a field car with a tape recorder geared to the speedometer drive, driving the chart at a speed of four inches per mile to obtain a continuous recording of field strength versus distance along eight routes running radially outward from the transmitting antenna. Fig. 6 shows the equipment mounted in the field car. A non-directional horizontally polarized antenna is mounted above the center of the car positioned to place it 8.5 feet above ground. The car and measuring equipment were calibrated as a unit, using the basic calibration of the manufacturer. Fig. 7 shows the field car and the antenna in place for making measurements.

Fig. 7
TV Receiving Antenna and Field Car

The field strength chart recordings were analyzed using a special Chart Analyzer developed by Jansky & Bailey, Inc. The individual charts were broken down into various sectors for the purpose of analysis. The sectors were established every half mile from 1 to 7 miles, every mile from 7 to 14 miles, every 2 miles from 14 to 30 miles and every 5 miles from 30 miles to the end of the measurements. It is possible, using the Chart Analyzer, to obtain the signal exceeded for 10, 50, and 90 per cent of the distance within each sector.

It is believed that the relationship of the 10, 50, and 90 per cent values is a very important tool in the study of field strength measurements and their relationship with frequency, power, antenna height, antenna gain and terrain features. The Federal Communications Commission recognized the relationship between the 10, 50, and 90 per cent values when they issued the "Third TV Freeze Report" on March 24, 1951. This report contained a curve for converting the median field for 50 per cent of the locations and 50 per cent of the time to a field for "L" per cent of the locations by the application of a proper factor. For VHF stations this curve indicated that the field at 10 per cent of the receiving locations in a given area could be expected to be 11 db larger than the median field. Likewise, the expected field at 90 per cent of the locations was indicated to be 11 db smaller than the median field.

Studies have been made of the data obtained at the two aforementioned installations in order to determine what effects, if any, the frequency, power, antenna height, antenna gain and terrain have on the 10, 50, and 90 per cent relationship. The data for each condition was analyzed to give the 10, 50, and 90 per cent values of field strength for three representative sectors along each radial. These sectors were from 2 to 3 miles, 5.5 to 7 miles and 20 to 28 miles. The ratios of the 10 to 50 per cent and 90 to 50 per cent values of field strength were obtained for each sector.

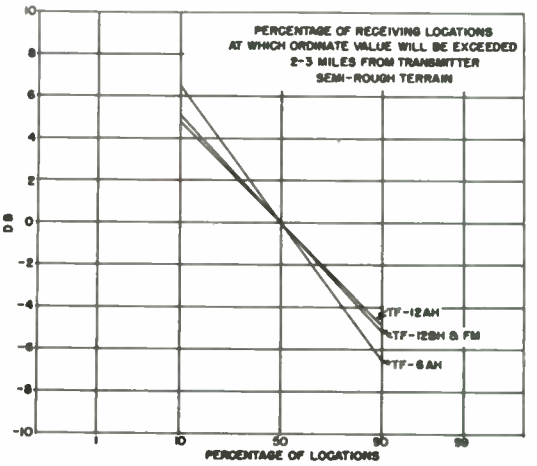

Fig. 8
Median-Decile Relationship in
Semi-Rough Terrain 2-3 Miles

Fig. 8 shows the relationship between these values for the sector 2 to 3 miles from the station located in semi-rough terrain. The difference between the fields exceeded at 90 per cent of the locations from the various antennas is approximately 1.5 db with the maximum difference being between the conditions when the station was operating with the TF-6AH and TF-12AH antennas. An average value of 5.4 db can be assumed for the difference between the decile and median values. Fig. 9 is a similar plot for the sector from 5.5 to 7 miles from the station. In this case the maximum difference is 1.0 db. The average for the decile values (10 and 90 per cent) for this case is 4.7 db. The data regarding the sector from 20 to 28 miles is shown on Fig. 10. The values for all four conditions are approximately equal and decile values of 5.8 db would average these conditions. The decile values obtained for these three sectors are all substantially less than the value of 11 db which is given in the Commission's curve. There is a difference of only 1.1 db between the average decile values for the three sectors so it is difficult to detect any major effect on the

decile values for this installation due to frequency, power, antenna height or antenna gain.

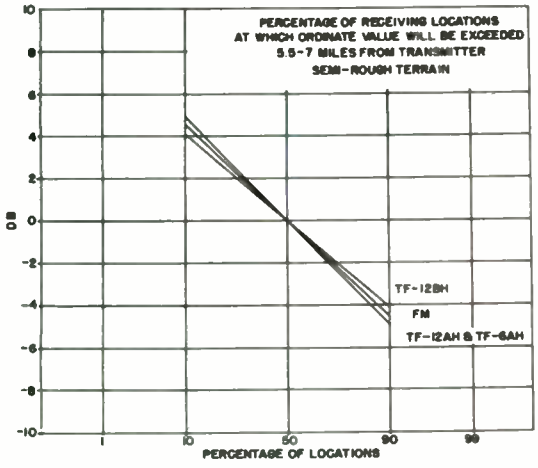

Fig. 9
Median-Decile Relationship in
Semi-Rough Terrain 5.5-7 Miles

The data regarding the Channel 12 station, which is located in rough terrain, was also analyzed to determine the median and decile values. Fig. 11 contains the data for the sector from 2 to 3 miles from the site. In this case, the curves for the fields from the FM and the high gain television antennas are identical. The decile values for the six-bay television antenna differ by only 1 db from the decile values for the other operations. The curves shown on Fig. 12 are for the sector from 5.5 to 7 miles from the transmitting antenna. The maximum difference between the decile values is 1.5 db with the maximum being between the TF-6AH antenna values and the Federal and FM antenna values. This set of curves shows a slight effect of antenna height and antenna gain on the slope of the curves but is so small that it can be neglected. The curves shown on Fig. 13 for the 20 to 28 mile sector also exhibit a difference in the slope of the curves depending on the height and gain of the antenna. In this case the decile values approach more nearly the originally postulated 11 db departure from the median. The relationship of the received fields from the antennas with the higher gain and higher effective height result in curves which have less slope (lower decile values) than the low gain television antenna. The FM antenna though, results in received fields which exhibit characteristics similar to those exhibited by the fields from the Federal antenna. The fields for all three of the sample sectors for this installation showed the same characteristics relative to the various types and heights of antennas.

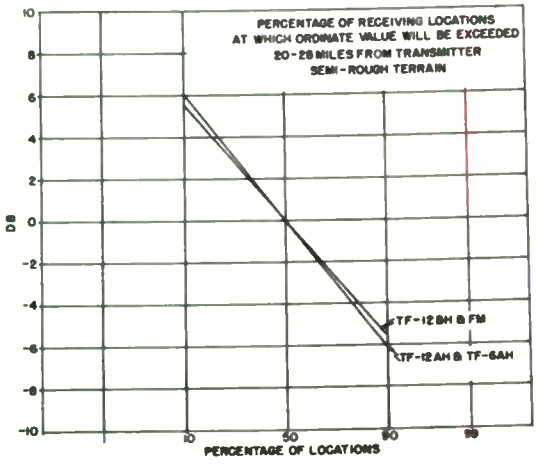

Fig. 10
Median-Decile Relationship in
Semi-Rough Terrain 20-28 Miles

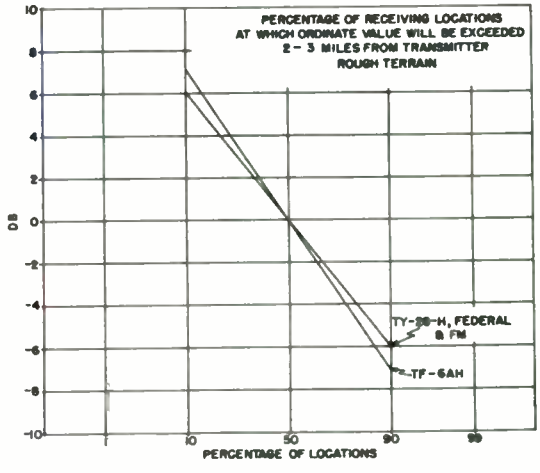

Fig. 11
Median-Decile Relationship in
Rough Terrain 2-3 Miles

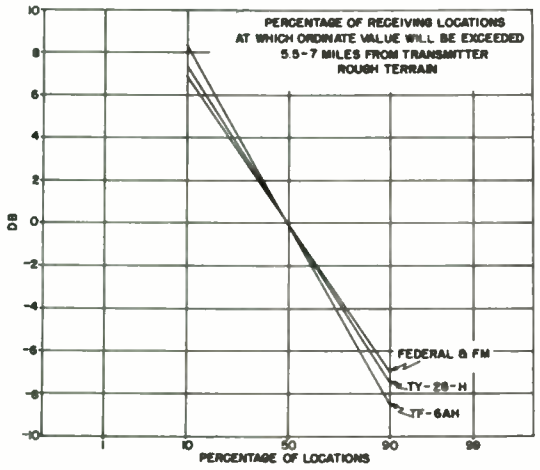

Fig. 12
Median-Decile Relationship in
Rough Terrain 5.5-7 Miles

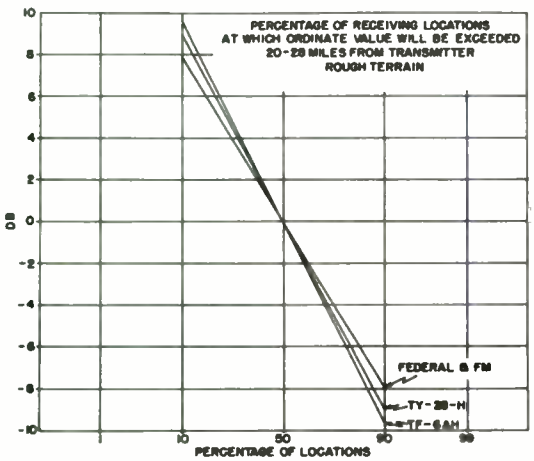

Fig. 13
Median-Decile Relationship in
Rough Terrain 20-28 Miles

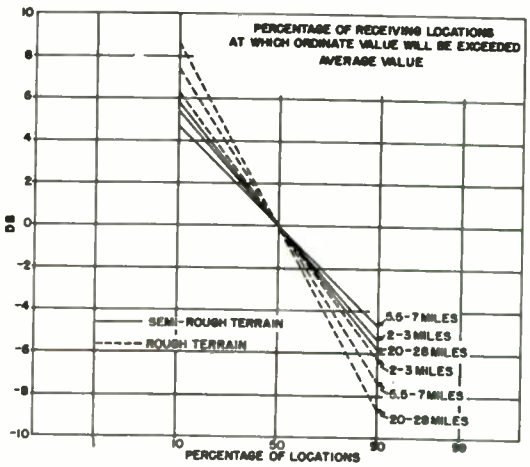

Fig. 14
Composite Median-Decile Relationship

In order to make a direct comparison of the decile values for the various sectors for the two types of areas, the individual values have been averaged for the respective sectors and these averaged curves are shown on Fig. 14. These curves show the decile values for the installation in the rough terrain to be larger than the values for the installation in the semi-rough terrain. The curves for the rough terrain installation also show more divergence between the values at 2 to 3 miles and the values at 20 to 28 miles. The values are increasing with distance from the transmitter for the rough terrain installation while the values for the semi-rough terrain installation exhibit a random characteristic. The values for the 2 to 3 mile sector for the semi-rough terrain installation are approximately the average of the 5.5 to 7 mile and 20 to 28 mile sector values. This would indicate that in smooth or semi-rough terrain the relationship between the 10, 50, and 90 per cent values remains relatively constant regardless of the distance from the transmitting antenna. In the case of installations in rough terrain, the relationship between the decile values and the median value varies with the distance from the transmitting antenna - exhibiting a greater difference as the distance increases. The decile values obtained at these two installations are all lower than the value obtained from the "Third Report" of the Commission. It is interesting to note that measurements made on a station in smooth terrain yielded decile values of about 3 db which are less than those shown on Fig. 14. A considerably larger number of measurements in various types of terrain must be analyzed before a comprehensive conclusion can be reached regarding the complete relationship of the decile values.

It is also important in the planning of television transmitting antenna installations to provide as uniform a field as possible to the main city to which the channel is assigned. Field strength measurements made along a number of routes in a city serve to indicate the variations of received signal and also serve to detect any areas of low signal due to the vertical nulls in the radiation pattern of the transmitting antenna. The measurements can be analyzed to determine the variability of the signal over the entire city. An example of such an analysis is shown on Fig. 15 which contains curves obtained for two different conditions of operation for a typical high

band VHF station. In this case, field strength is plotted versus percentage of receiving locations. It will be noted, while we are accustomed to think in the simplified terms of the median value, it should nonetheless be kept in mind that for this particular set of circumstances including frequency, type of terrain, and city characteristics, signal peaks of the order of twice the median value will frequently be experienced and what is more important, signal minimums of the order of one-half the median value will occur over a substantial area.

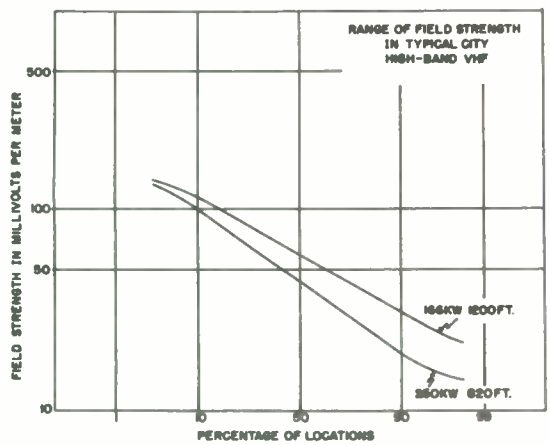

Fig. 15
Field Strength Distribution in
Typical VHF City

The received field from the transmitting installation having the most height was more uniform than the field from the other installation. The antenna employed with an antenna height of 1200 feet had the nulls filled in to a greater degree than the antenna which was used with a height of 820 feet. The variation between the 10 and 90 per cent field strength values was 3.2 to 1 or 10.1 db for the 1200-foot installation and 5.9 to 1 or 15.4 db for the 820-foot installation. The practical result of this increased null fill-in was to increase the strength of received signal to the city and also to remove the areas of low field strength which existed with the 820-foot operation. For the 820-foot installation a narrow band of low field strength, approximately 10 millivolts per meter, was measured over an arc within the city. Within this region, there were numerous complaints from viewers who were troubled with ghosting problems. The four to five per cent of the locations within this area are very important to the station since it is these people who call and write the station complaining of these problems. Numerically speaking this percentage can represent a large number of people. Field studies showed regions of very high field strength, 100 millivolts per meter, contiguous to these areas suggesting the possibility that reflections from buildings in the high signal areas cause the ghosting in the low signal areas. After the completion of construction of the new 1200-foot operation, measurements showed these areas of low signal to be eliminated. Also, the contiguous areas of extremely high and low field strengths were eliminated.

Field strength measurements, similar to the aforementioned, made in various urban areas within the coverage area of the station can serve to indicate cities which are in need of satellite or booster installations in order to provide the desired service from the particular station involved. The field strength measurements can be used to locate the areas of lowest signal and it is desirable to locate the satellite or booster station so that it provides the maximum signal to these areas.

A number of field strength measurements were made for various receiving antenna heights at several locations within the coverage area of a typical VHF station in semi-rough terrain. The measurements were made using the calibrated dipole antenna mounted on top of a supporting structure which yielded five different heights. Fig. 16 shows the dipole antenna in the 30-foot receiving position.

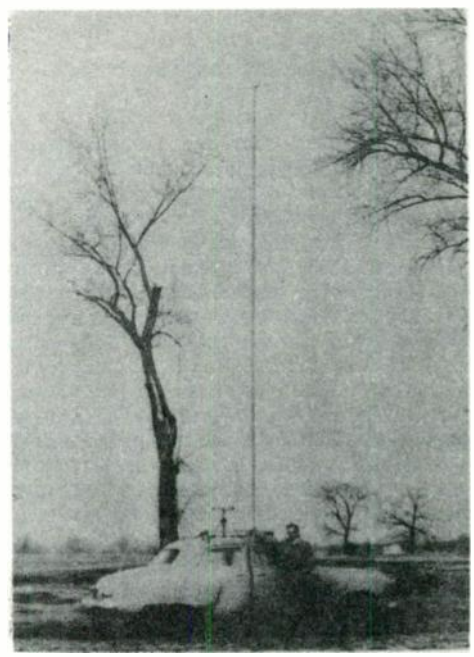

Fig. 16
Receiving Antenna for 30-Foot Measurements

Four measuring points were selected on each of two radials and a series of measurements with progressively greater receiving antenna height were made at each location. Fig. 17 contains curves of height-gain experienced versus receiving antenna height. Since the normal measuring and recording height for this equipment is 8.5 feet, the field measured at this height is the reference field. The theoretical linear height-gain curve is shown for reference purposes.

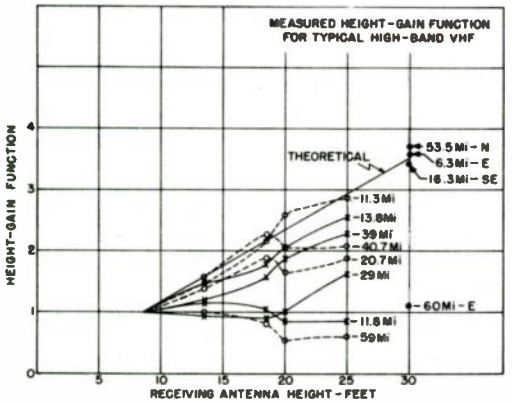

Fig. 17
Measured Height-Gain Function

The solid curves represent measurements made on one radial along which the terrain was gently rolling. At the distance of 11.8 miles from the transmitter there is a terrain discontinuity where the measuring route crosses a creek. The measured field strength at various heights at a point in the shadow of this discontinuity indicated a height-gain of approximately unity, even though the land dropped off only of the order of 25 feet. The next set of measurements made at 13.8 miles on this radial was in the clear and the resulting height-gain locus approached the theoretical relationship. The location at 29 miles was partially obstructed and no gain was experienced with increasing height until the antenna cleared the obstruction. The final point on this radial was in a region where there were no abrupt terrain discontinuities but the gain obtained at 25 feet was still less than theoretical.

The other radial selected for these tests traversed both smooth and rough terrain. The first set of measurements made at 11.3 miles yielded a height-gain relationship which closely approximated theoretical. The remaining three locations were in locally unobstructed locations but the intervening terrain was rough. This condition became very severe at 59 miles as can be seen by the measured curve which shows the measured field strengths at 18.5, 20 and 25 feet to be lower than those measured at 8.5 and 13.5 feet.

In order to further study the effects of terrain on the height-gain relationship, a series of field strength recordings were made for short sectors in four different areas. These recordings were made at 8.5 and 30 feet and were analyzed to determine the median values for each set. These measurements were made over sectors which varied in length from 0.4 to 1.6 miles. The measurements made at 6.3, 16.3 and 53.5 miles yield gain figures which show good correlation with the theoretical figure of 3.53. These measurements were made in areas in which the local terrain was flat and the intervening terrain was gently rolling. The route for the fourth measurement was along a path perpendicular to the radial from the station and about 500 feet from an intervening ridge having a height of approximately 50 feet above the road. At this location, negligible height-gain was observed.

A possible reason for the difference in the results obtained by the two methods is the fact that one set represents measurements made at specific locations while the other set comprises median values obtained over distances from 0.4 to 1.6 miles. The spot method gives a representation of what can happen at an individual receiving location while the recording method results in a value which might be expected to exist for the average location.

Where it was possible to obtain good unobstructed measuring locations for both spot and mobile measurements in terrain which was not particularly rough, good correlation was noted. However, where the terrain is rough, gains with antenna heights were not experienced and it was apparent that roughness of either a general or a localized nature produced this effect. The cumulative effects of these discontinuities is very evident in the shaping of the slope of the field strength versus distance curves. Each discontinuity takes its toll in attenuation for the total path, and the relative number and severity of these, directly influences the distance to which the signal is propagated. Further studies of this type should be made for all types of terrain and various frequencies in order to obtain more information regarding the effect of terrain on received signals at various receiving antenna heights.

A NEW MONITOR FOR TELEVISION TRANSMITTERS

Charles A. Cady
General Radio Company
Cambridge, Massachusetts

Summary

This paper will describe the development of a complex monitor that provides the means for testing and measuring several characteristics of modern television transmitters. The advent of color television has made it desirable to review the monitoring techniques employed to date for monochrome television, and to introduce additional methods of measurement, as for example, the measurement of incidental f-m noise on the visual transmitter, in the presence of normal video (am) modulation.

In developing such an instrument, many new concepts were introduced as a result of investigations in diverse fields. Studies in crystal oscillator stability were made to obtain an inexpensive and reliable oscillator with long-term stability of 5 parts in 10^{-7}. The precise temperature control required led to the development of a small enclosure maintaining constant temperature within a few hundredths of a degree, without the requirement of elaborate control circuits.

The instrument must operate over a wide range in input frequencies, from 50 to 900 Mc, necessitating investigations in the field of low-noise frequency multipliers employing both tubes and crystal diodes. New types of discriminators have been used to solve the problems of linearity and sensitivity for modulation detection, and for sensitivity and stability for metering purposes.

The entire device has been assembled into a package of novel design which provides high heat dissipation in a relatively small volume without forced-air cooling and provides maximum access to all parts.

Introduction

The introduction of color TV broadcasting has imposed new and more exacting requirements upon the equipment used to monitor TV transmitters. In addition to the requirement of increased accuracy in the measurement of transmitter frequency, several new measurements are about to become a matter of station routine. Accordingly, a new TV transmitter monitor has been designed to provide for these changes. Many new features, both mechanical and electrical, are included which provide the operator with a convenient means of making these measurements.

A discussion of a TV transmitter monitor can properly begin with a review of the signal upon which it is expected to operate. Figure 1 shows the frequency spectrum of a standard TV channel. The relative positions of the visual and aural transmitter carrier frequencies are shown. In order that we may measure various functions of these two carrier frequencies, we place a master reference frequency 150 kc below the aural transmitter carrier frequency. By heterodyne action, we may then obtain two IF output frequencies.

A 150-kc IF frequency is obtained, which contains the signal information present on the aural (fm) carrier. Another IF frequency is obtained at 4.35 Mc, which contains the signal information present on the visual (am) carrier.

The 150-kc IF signal (fm) passes through a limiter amplifier to a pulse-counter discriminator operating at 150 kc center-frequency. The output of the discriminator is shown on the lower right. As the aural carrier frequency changes with respect to the master-reference frequency, the 150-kc IF frequency also changes by the same amount. Thus, the d-c output component can be used to operate a d-c meter calibrated in deviation of the aural transmitter frequency from its assigned channel frequency. The a-c components in the range of 30-15,000 cycles comprise the audio modulation (fm) of the aural transmitter.

The 4.35-Mc IF signal (video-modulated) will be used in two ways, first in the measurement of the visual transmitter frequency; and secondly, in the measurement of residual fm (noise) on the visual transmitter, as will be shown later. Frequency metering circuits at low frequencies are convenient and stable, hence the 4.35-Mc IF signal is heterodyned with another crystal oscillator, offset by 1750 cycles. This action is illustrated in the left center portion of Figure 1. As the visual carrier frequency changes, a linear change in (audio) frequency is obtained from a discriminator,

which is centered at 1750cycles. The d-c output of this discriminator is used to operate a d-c meter calibrated directly in terms of the (±) frequency deviation of the visual transmitter carrier frequency from the assigned channel frequency.

Figure 2 shows the block diagram of the principal circuits used. The two transmitter inputs are heterodyned with a common master-reference frequency. The 150-kc (fm) system is shown on the center right, and provides for the frequency and modulation monitoring of the aural (fm) transmitter. On the center left is the 4.35-Mc IF system, the second conversion step, and low-frequency meter discriminator, providing for the frequency measurement of the visual transmitter.

This arrangement has been in use for some years in previous monitors and may be readily recognized. The advent of color TV broadcasting has made it desirable, however, to provide additional measurements. For example, FCC frequency tolerances impose limits on the visual transmitter, and also on the difference frequency. It thus becomes desirable to provide a measurement of the aural transmitter carrier frequency, and a direct indication of the difference frequency. This can be done by the addition of a detector to recover the (4.5-Mc) difference frequency, an IF amplifier, and a converter to produce an output of 150 kc. At this point, the signal can be applied to the existing IF system. Since this includes complete audio monitoring facilities, the result is a complete Intercarrier Monitoring System, shown to the right in Figure 2.

The output of the first mixer is nominally 4.5 Mc, or intercarrier frequency, and contains the modulation products of both transmitters, i.e., video (am) and sound (fm). If we are to monitor the aural functions in a manner analogous to sound recovery in an "intercarrier" type of TV receiver, we must first remove the unwanted video components. This is accomplished initially by having a band-pass IF system, centered at 4.5 Mc and thus effectively removing directly-detected video components in the first mixer output. After passing through a fast-response, 4.5-Mc limiter, the 4.5-Mc IF signal is subsequently converted to 150 kc in a second conversion by heterodyning with a 4.35-Mc local crystal oscillator. The resultant signal may then be passed to the IF limiter-amplifier system. This IF (150-kc) system has an input band-pass characteristic as shown. High-frequency video components are thus attenuated and any remaining amplitude-modulation components are reduced by the limiters.

Several advantages accrue from this additional measurement. Note that we are measuring the difference frequency by reference to an independent crystal oscillator and thus provide for a measurement independent of the original system. Since we are deriving the sound from an intercarrier system, correlation of extraneous noise, etc., as experienced on "intercarrier TV sets", is now possible. In the new monitor, this mode of operation is available by turning a selector switch.

Another measurement has recently become significant, particularly in color TV. This concerns the direct measurement of the residual f-m noise existing on the video carrier in the presence of normal video modulation. To the left in Figure 2, additional facilities are shown. In using the existing 4.35-Mc IF system, we find that additional amplitude-limiting is necessary to remove the effects of the normal amplitude video modulation. Bandwidth requirements are based upon the elimination of all video components within the audio range, and also the 4.5-Mc beat frequency due to intercarrier spacing. It is, however, necessary to avoid "ringing" in the tuned circuits due to phase shifts, which would appear as residual noise in the discriminator output.

In the interest of sensitivity, a simple tuned-circuit discriminator operating at 4.35 Mc is used. Since this system will only be used to measure residual f-m noise and will not be called upon to accept full modulation deviation, the discriminator does not have to be as elaborate as the one used for fidelity measurements of the (fm) aural transmitter. In the absence of a reference (100% mod) f-m calibration, an external a-c voltage is used to match the stabilized discriminator output level to permit calibration of the noise meter. In actual use, measurements of -50 to -60 db below 100% mod (25 kc) residual f-m noise on the visual transmitter carrier were made while standard color programs were in progress.

Since this measurement of residual f-m noise on the visual transmitter carrier is continuously available, it is possible to monitor this characteristic continuously, using an external Distortion and Noise Meter. The transmitter operator can thus instantly recognize overmodulation due to excessive (negative-white) modulation. Since the carrier frequency component will momentarily go to zero in the presence of full negative-peak video modulation, a burst of audio noise will appear in the discriminator output. Thus, during normal video modulation conditions, a continuous level of -50 to -60 db may be indicated by the Distortion and Noise Meter. Sudden appearance of noise bursts above this level are a warning to the operator of excessive negative-video modulation.

The same effect is experienced with color TV operation, where it is recognized that certain saturated colors may modulate the transmitter to 100%, unless prevented from doing so by limiting controls in the video input system.

Tests made, indicate that no noticeable difference exists between monochrome and color TV operation in the measurement of residual f-m noise on the aural transmitter carrier frequency.

Details of Operation

Having outlined the objectives of this equipment, a closer look at the individual circuit detail is in order. Basic to the operation is the generation of the master-reference frequency, which is accomplished in the R-F Section.

R-F Section

Figure 3 shows the general form of this part of the monitor. A quartz crystal, operating in the region of 5-7 Mc, is used to drive a buffer amplifier and then a single frequency doubler stage. From this point, two individual frequency-multiplier chains are used to develop a signal in the fundamental range of both the aural and visual transmitters. A dual system is employed in order to isolate the individual mixers used with the visual and aural transmitters. In this manner, cross modulation is avoided, and coupling between transmitters through the monitor itself is minimized.

The upper illustration shows the UHF arrangement. The final multipliers in this chain are germanium crystal diodes, which generate frequencies in the 470-890-Mc range, where conventional receiving-type tubes become increasingly difficult to handle. 9005 diode mixer tubes are used and feed directly to 6BE6 tubes used, in this case, as IF amplifiers.

The lower illustration shows the VHF arrangement which is similar to the above with the exception that the 6BE6 tubes now function as mixers, and the crystal diode multipliers are omitted.

Aural IF System

The aural IF system is shown on Figure 4. Here successive amplifier-limiter stages are used to convert the frequency-modulated 150-kc output of the aural mixer into a square wave of constant amplitude. To insure complete freedom from the effects of amplitude variation in the measurement of residual f-m noise, -80 db below 100% modulation signal level, a high degree of limiting is necessary. The first three amplifier stages, plus the two diode limiter stages are used for this purpose. The fourth (dual) stage establishes the exact magnitude of both positive and negative peaks of the square wave. The lower tube (6CL6) is driven between saturation and cutoff. Positive excursions are thus equal to the regulated plate supply voltage. A 6J6 tube is used to clamp the negative peaks, with its grid maintained at a fixed potential with respect to the regulated supply voltage. Negative cathode swings below this critical voltage cause conduction through the tube thus limiting any further negative excursion. In this manner both positive and negative peaks are basically determined by the regulated plate-voltage supply.

The fifth, or output stage (dual), consists of an upper tube (6CL6) acting as a modified cathode follower to provide a low-impedance source for the purpose of driving the discriminators. A lower tube (6CL6) is used in lieu of a cathode resistor. The combination provides a low-impedance source for both positive and negative excursions of the square wave.

The output of this section is thus a frequency-modulated square wave of constant amplitude.

Discriminators

It has been found advantageous to operate a center frequency meter directly from the discriminator output signal, without any intermediate d-c amplifiers, by use of a novel differential system. This is shown on Figure 5.

The input (150 kc - fm) signal is shown on the left. A simple pulse counter arrangement forms one-half of the circuit. The capacitor C_1 is charged once per cycle, through the diode connected to ground, and then discharged into the larger capacitor C_2 on the alternate half cycle. Consequently, a voltage E_2 appears across this capacitor C_2. This voltage increases linearly with frequency.

To the right is shown a series LRC circuit. This low-Q circuit is series resonant at a relatively low frequency, and in the region of 150 kc the potential across the capacitor C is inversely proportional to frequency. C_3 and the two associated diodes constitute a charge-discharge circuit, wherein the charge is transferred from C_3 to C_4, and the voltage across the latter is thus inversely proportional to frequency.

E_1 and E_2 are two opposed d-c voltages which vary in accordance with changes in frequency as shown on the lower diagram. The d-c meter current, I_3, is the difference between I_1 and I_2. Thus, at 150 kc, the operating center frequency, I_3, becomes zero and will change to plus or minus as the center frequency is shifted. A zero-center d-c microammeter (100-0-100 μa) is calibrated to read -3, 0, +3 kc and used to indicate carrier frequency deviation from the assigned center frequency.

Since this d-c meter is grounded at one side, external recording devices or meters are readily connected. Also, since the system is symmetrical, about a zero center, minor changes in the amplitude of E_{in} are balanced out at

center scale. In this discriminator, symmetry and stability are emphasized, to provide a stable meter circuit capable of a full-scale resolution of ±3/150, or ±2% (of the 150-kc center frequency), and possessing a long-term stability better than 200 cycles, or 0.133% of the operating frequency.

To recover the audio signal, emphasis is placed upon discriminator linearity and freedom from noise. Consequently, the pulse-counter discriminator shown in Figure 6 is used. The upper illustration shows a simple pulse counter in general use. Such a device is inherently linear, but it suffers from low sensitivity and requires extensive filtering to remove the high-amplitude IF pulses that appear in the output. By the relatively simple expedient of balanced operation, the fundamental of the IF frequency can be balanced out in a coupling transformer in the circuit as shown below. In this case, the transformer serves the dual purpose of low-pass filter (with a 30-kc cut-off) and that of a coupling device. It is not quite a simple transformer, however, since it must provide a flat audio response from 30-30,000 cycles at low distortion, maintain good balance, have low-input capacitance, and be very well shielded between primary and secondary; nevertheless, its cost can be held to a small part of the equivalent filter network that would be necessary with an unbalanced discriminator. With the circuit shown at the bottom, a transformer has been designed which will give one volt audio output with less than 32 millivolts of IF appearing on the secondary side. Thus, to achieve a final signal-to-noise ratio of -80 db, we require about 50 db of additional audio filtering. Owing to the balanced arrangement, most of the residual IF appears as second harmonic, which further simplifies the filter problem.

Positive or negative modulation-peak response is obtained by reversal of the transformer polarity.

Audio System

The audio signal is passed directly to a preamplifier which includes an active filter network, as shown in Figure 7 at the top. For convenience in transmitter testing, a switch is provided to establish reference levels of 100% modulation equivalent to 25- and 50-kc deviations.

Three separate audio functions are provided. On the lower left is shown the output cathode follower, which includes a 75-μsec de-emphasis network. An audio output for both aural monitoring and fidelity measurement is thus provided.

In the center is shown the semi-peak-response diode voltmeter (left half of tube) and the d-c amplifier used to drive a d-c meter, indicating modulation. The time constants are so chosen that the diode circuit has a rapid charge and slow discharge. Overall dynamic response, including meter ballistics, conforms to existing FCC regulations requiring a fast upswing and slow return of the modulation meter.

To the lower right may be seen the over-modulation indicator. The 12AT7 tube is arranged as a monostable multivibrator. In the quiescent state the left half is biased at cut-off, with the right half conducting due to its positive grid bias. A positive signal peak, in excess of the bias voltage setting on the MOD. PEAKS dial, will momentarily trip the left half of the tube into conduction. The resultant negative pulse is transferred to the grid of the right half and momentarily stops its conduction. A positive pulse is generated in its plate circuit which is used to trip the thyratron. A lamp in the thyratron anode circuit flashes, indicating a modulation peak. A-C bias is used to keep the thyratron at cut-off during quiescent periods.

Intercarrier

The preceding entire aural-monitoring system is operated directly from an intercarrier signal by adding the circuits shown on Figure 8.

A separate intercarrier mixer (6AL5) is used to derive a 4.5-Mc beat frequency between the aural and visual carriers. In general, the full monitoring output of the visual transmitter is applied directly to the diode, and residual leakage through the transmitter multiplexer provides enough aural transmitter carrier (-20-40 db) to give normal detection. By having the aural (fm) carrier the smaller of the two, the beat frequency output tends to be proportional to it rather than the amplitude-modulated visual carrier, and provides considerable amplitude limiting in the resultant IF output.

Because the IF output does contain both a-m and f-m components, severe filtering and limiting is necessary. The former is obtained in the band-pass characteristics of the three tuned amplifiers, as shown. The low frequency end of the video modulation spectrum is effectively removed. The f-m components of the aural transmitter modulation are retained, and care must be exercised to avoid introducing phase modulation in the successive stages.

A local crystal oscillator (4.35 Mc) is used to convert the IF signal in the 6BE6 mixer tube to 150 kc. Here again the constant amplitude local oscillator is made much smaller than the 4.5-Mc intercarrier amplitude applied to the mixer to produce effective amplitude limiting. At this point, we have a 150-kc IF (fm) signal which can be passed on to the (fm) system previously described. In this instance, the system will indicate the aural-visual

transmitter difference frequency directly; and the audio functions obtained will simulate those obtained on an "intercarrier"-type receiver.

Visual-Carrier Frequency

The frequency-metering section for monitoring the visual transmitter carrier frequency is shown in the upper portion of Figure 9. The output derived from the "visual" mixer is at 4.35 Mc and is converted to a low audio frequency (1750 c) in the 6BE6 mixer tube by heterodyning it with an offset crystal oscillator.

In the interest of meter-circuit stability, this low audio frequency is used, since there is no fm present which would require wider bandwidths. The limiting amplifiers and diode clipper are used to develop a constant-amplitude square wave; and an output cathode follower drives a conventional pulse-counter discriminator and meter, calibrated to read +1500 cycles about a zero center. Since the actual audio frequency is 1750 + 1500 cycles, a guard band of 250 cycles (x2 between image response) is provided, and a bias voltage equivalent to 250 cycles prevents initial deflection until this frequency (or higher) is reached.

Although this measurement of the visual-carrier frequency requires dual conversion, the second (or interpolating reference) oscillator contributes an additional error barely visible on the meter scale. The meter circuit itself has a stability of 2%, or 35 cycles, at the zero-center point.

Visual-F-M Noise

For the purpose of monitoring the residual f-m noise on the visual transmitter, the same 4.35-Mc IF signal is used, and the circuits shown in the lower portion of Figure 9 are added. The problem here is to separate the residual f-m noise components occurring within the band of 30-30,000 cycles from the unwanted broadband a-m video components.

One IF amplifier-limiter stage is included in the R-F Section previously described, and this signal then feeds the three cascaded limiter amplifiers as shown in Figure 9.. A conventional tuned-circuit discriminator is used to derive the residual f-m noise components, which are then fed to an external Distortion and Noise Meter for measurement.

In this instance, advantage is taken of the high sensitivity provided by this type of discriminator. Since the residual noise signal will be -40 db or more below reference modulation (100% = 25 kc) or 2.5 kc or less, bandwidth and linearity requirements are not severe. The absence of an f-m calibrating reference requires an external (60 cycle) signal to standardize the external Distortion and Noise Meter against the fixed output level obtained from this discriminator. (This is not shown in Figure 9.)

Power Supply

The power supply is shown in Figure 10. Requirements for this instrument were such that existing rectifier tubes were not readily adaptable, being just beyond ratings for many types and inefficiently loading others. Selenium rectifiers might have been used, but uncontrolled temperature environmental conditions are problematical and require extreme derating. Series-regulator tubes have rather large heater-power dissipations, and are wasteful of plate power as well. In an effort to reconcile these conflicting requirements, investigation led to the development of a thyratron-regulated plate supply. Here the rectifier could be made to serve the dual purpose of rectification and control. In the event of failure, replacement is easy, obtained directly from normal tube stocks maintained by the station operator.

The rectifier is a full-wave system, employing two 2D21 thyratrons. Regulation is obtained by means of a d-c voltage applied to the thyratron control grids, together with a phase-shifted a-c voltage which improves the thyratron grid-control characteristic. A voltage-reference tube (5651) and a d-c amplifier (12AT7) are used to develop a d-c control voltage, inversely proportional to the output d-c voltage.

Note that the ripple filter is placed in the negative (ground) lead, rather than more conventionally in the positive lead. This was done specifically to remove all ripple frequencies from the d-c control circuits, including the d-c reference tube, amplifier, and the grid-cathode circuit of the thyratrons. In this arrangement, the entire control circuit operates without interference due to stray a-c voltages being induced in the control system. To insure this, the RC network (shown at the extreme right) is used as a filter around the d-c amplifier circuit.

The ripple frequencies now appear on the transformer secondary winding. It is a relatively simple matter to isolate this individual winding by means of electrostatic shielding, and the generation of stray a-c fields, which might cause interference within the monitor itself, is localized in one place, i.e., the power transformer which is shielded.

Precision Temperature-Controlled Crystal Oven

The "heart" of any frequency measuring device is its master-reference frequency. To maintain this as stable as possible against changing ambient temperatures requires a precision temperature-controlled enclosure. Such

devices have been made in many forms and sizes. Reduced size and close control with low heater power all imply low heat loss. Since this implies exceptional insulating qualities, a Dewar Flask (vacuum bottle) is a natural choice.

These devices are commercially available in relatively few sizes and shapes, hence the problem becomes one of building the proverbial "ship-in-a-bottle". Consequently, a likely size and shape bottle was selected, and a crystal and associated parts were arranged to fit inside.

Figure 11 shows the arrangement used. An outer aluminum cylinder encloses the entire unit for mechanical protection. Since the internal elements must remain in a fixed position when the vacuum flask is removed, these components are mounted upon a Balsa wood plug. (Literally, this is the equivalent of the bottle "stopper".)

With this arrangement, the Balsa-wood mount may be affixed to a panel and a thermometer inserted from the front to show the internal temperature. Two frequency-adjusting capacitors are available from the panel by extension shafts brought out from two internal air capacitors.

Since the major heat loss is through the Balsa-wood mount (i.e., the vacuum flask "stopper"), the main heater winding is wound upon an aluminum disc, which is then mounted directly against the inside of the Balsa-wood plug. A thin-wall aluminum tube attaches directly to this disc and serves to distribute the heat toward the inner part of the vacuum flask. Since the heat loss is greatest near the mouth of the vacuum flask, the heat source is thus concentrated at this point.

The quartz crystal itself is mounted in a modified 9-pin tube socket, located well inside the vacuum flask, at a point of minimum heat loss. Small-diameter wires connect the crystal to its series air capacitors, and are brought out through the heated aluminum disc thereby tending to compensate for the heat losses due to conduction along the wires.

Control Circuit

The temperature-control system is based upon the operation of a sensitive mercury-column thermostat, which is used in a very simple on-off heat-control circuit. An "anticipator" heater is wound around the "bulb" of the thermostat which effectively minimizes "overshooting" of the controlled space temperature with ordinary changes in both heater power and external ambient temperature.

The simple control circuit used is shown in Figure 12. Current is flowing through the heater winding during the normal conduction period of the thyratron. When the mercury-column contacts close upon a rise in temperature, an a-c bias is applied to the thyratron grid to stop conduction. Because of the very low peak-power requirements (3.8 watt, maximum), a small 2D21 thyratron is used.

This control system successfully eliminates problems usually found due to "contact resistances" in low-current thermostat circuits, and "sticking" relays as well. Resistances fully protect the sensitive mercury-column thermostat for accidental burn-out due to shorts or grounds in the circuit.. Moreover, the system will operate with more than a megohm contact resistance developing in the thermostat itself.

Figure 13 illustrates the dynamic control characteristics obtained with the unit. The upper chart is made from a recording of the temperature of the quartz crystal mounted within the vacuum flask, while the lower chart shows the external ambient temperature. Note that when the external ambient temperature was suddenly changed from 24 to 48°C within a period of 10 minutes, the internal temperature rose by +.04°C and then nearly recovered its control point within 45 minutes. The dynamic response of the unit was not fast enough to follow this extremely rapid shift in external ambient. Fans were used during the test to assure rapid air circulation around the outside of the vacuum flask.

On the second rapid change in ambient temperature from +48 to +2°C in a period of 10 minutes, the internal temperature dropped by -.075°C and then recovered to its normal control point in about 90 minutes.

These rapid changes in external ambient were made to illustrate the dynamic response of the device and are not likely to occur in normal use where air flow is less violent and physical mountings provide additional shelter. Fluctuations in ambient temperatures at rates which are likely to be encountered in normal environments do not show significant shifts in the oven-control temperature. For most purposes the oven controls within a few hundredths of a degree, for any slowly varying ambient temperature between 0 and +50°C, and for any fluctuation in input power caused by line-voltage changes from 105-130 volts.

Mounting

This monitor has been designed to meet the environmental conditions found in a TV transmitter room. Accordingly, it is intended to be rack-mounted, as shown in Figure 14, and is provided with slides to enable it to be withdrawn from the front of the rack. A locking device holds it in place when extended out in front of the relay rack, and a tilting mechanism provides access to all parts. All controls,

cables, connectors, etc., are reached with the instrument extended on its slides, as shown in Figure 15, and all maintenance can be performed from the front of the rack. It is not necessary to go around to the rear of the rack or cabinet.

When pushed back into its normal position, the monitor provides an unobstructed path for cooling air to pass completely through from top to bottom. Thus, cabinet racks provided with vertical air flow will not be blocked off and overheat.

All necessary test facilities have been built into the monitor. A switch, located directly behind the easily removable front panel (which now serves mainly as a dust cover) connects a meter into various circuits of the monitor for checking purposes. With the panel in position, only "authorized" controls are available. By turning four hand fasteners, the panel is removed disclosing the test switches, input-level controls and adjustments. Parts identification and signal tracing diagrams have been plainly marked on the two vertical-mounted chassis. All tubes project into the open space between the vertical front chassis, located directly behind the panel and the rear vertical chassis. Thus, most of the heat generated by the tubes is dissipated directly into the high-velocity air stream passing through the center of the instrument. Consequently, no blowers are necessary to dissipate the 265 watts of a-c power used by the monitor.

Bibliography

1. Cady, C. A., "Type 1170-A F-M Monitor for Broadcast and Television Services", General Radio Experimenter, October 1947.

2. Cady, C. A., "FM Monitor has Pulse-Counter Discriminator", FM and Television, December 1947, p. 18.

3. Cady, C. A., "Frequency and Modulation Monitor for TV and FM", Teletech, February 1948, p. 44.

4. Cady, C. A., "Measuring Noise Levels on Frequency-Modulated Transmitters", General Radio Experimenter, August 1949.

5. Lewis, F. D., "Harmonic Generation in the U-H-F Region by Means of Germanium Crystal Diodes", General Radio Experimenter, July 1951.

6. Lewis, F. D., "Ultra-High-Frequency Television Monitor", Proceedings of the National Electronics Conference, 1951.

7. Clapp, J. K., "Notes on the Design of Temperature Control Units", General Radio Experimenter, August 1944.

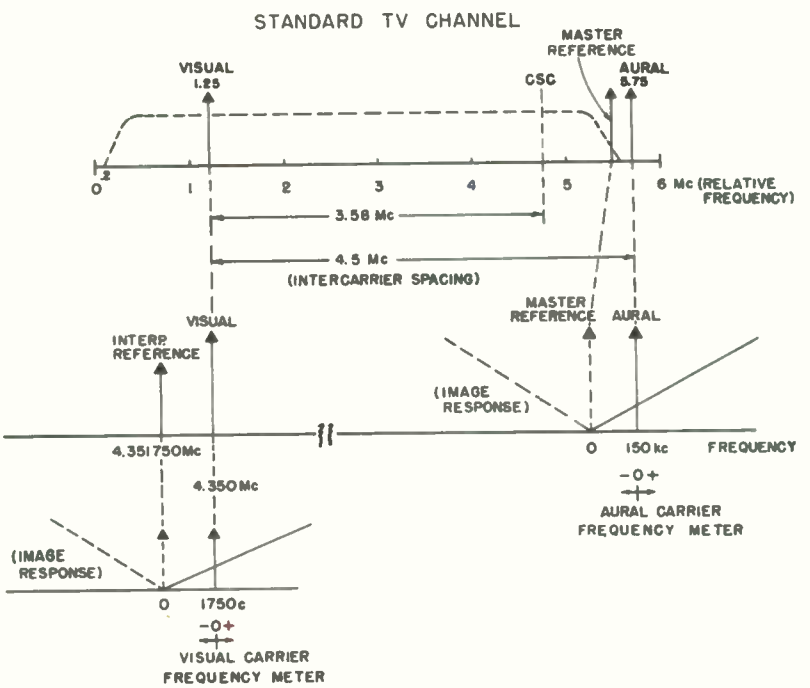

Fig. 1
Principles of operation for frequency-measuring circuits.

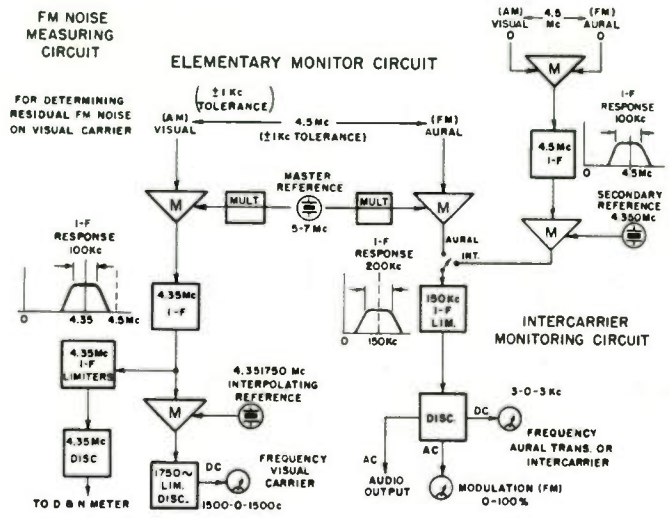

Fig. 2
Elementary monitor circuits.

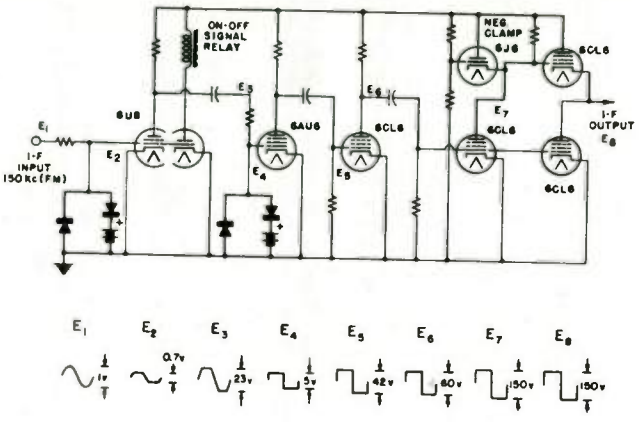

Fig. 4
Elementary schematic of aural IF section.

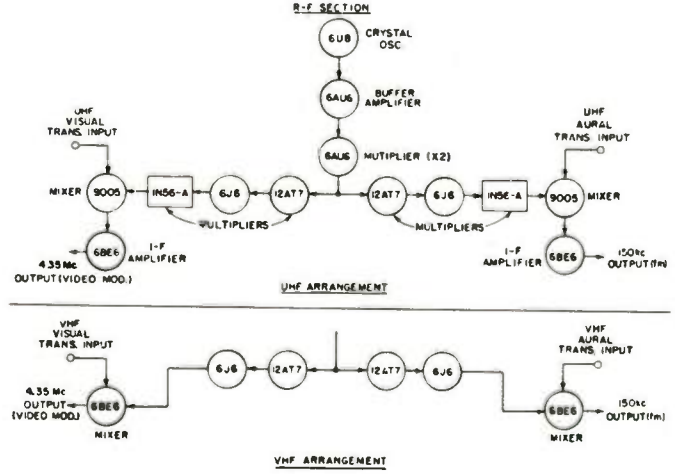

Fig. 3
R-F sections.

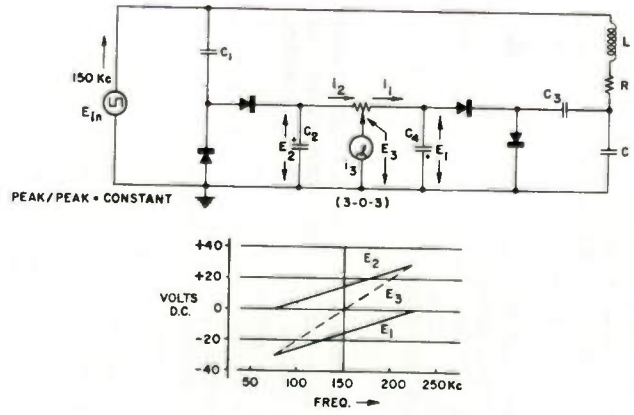

Fig. 5
Balanced discriminator as used for center frequency meter.

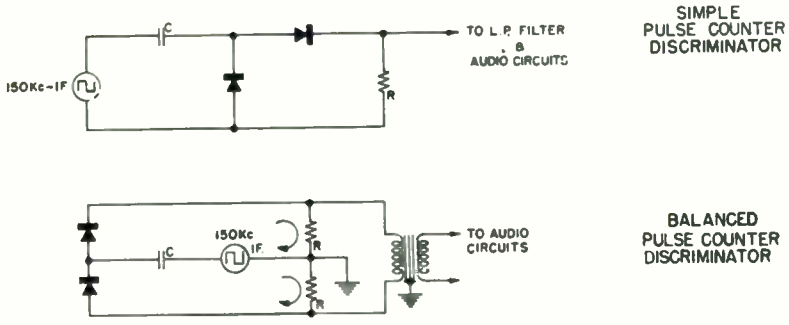

Fig. 6
Pulse-counter discriminators.

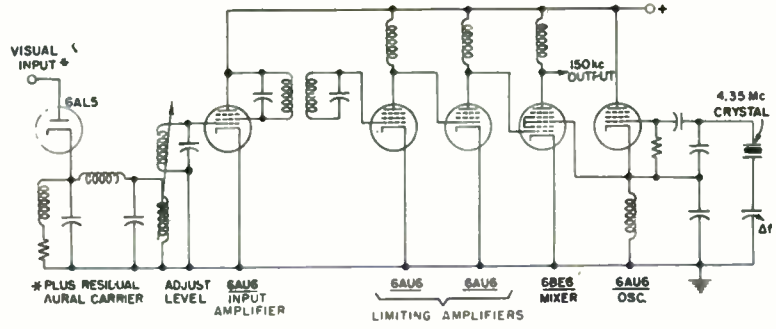

Fig. 8
Elementary schematic of intercarrier monitoring system.

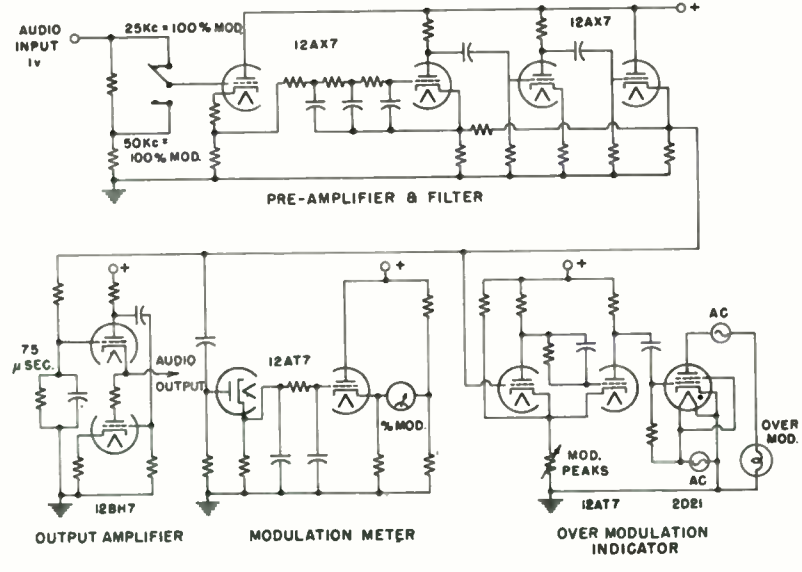

Fig. 7
Elementary schematic of audio circuits.

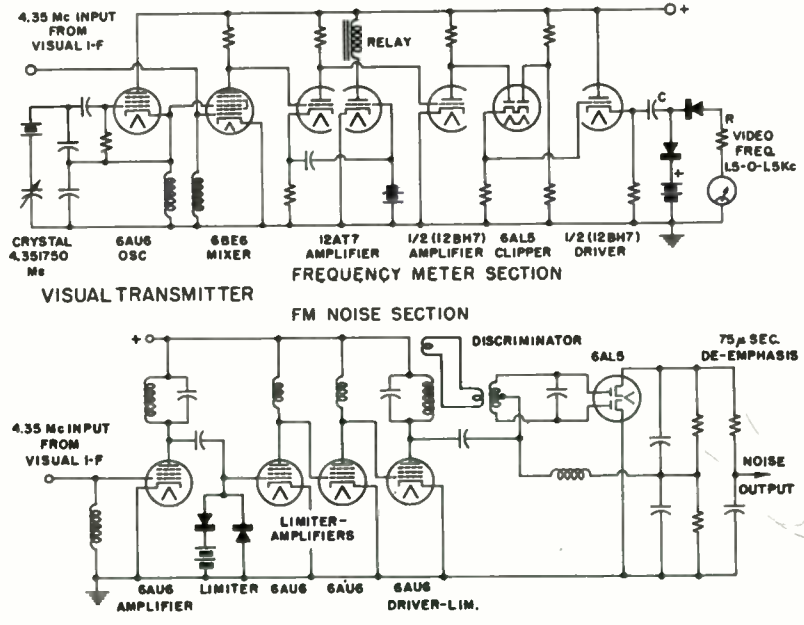

Fig. 9
Visual transmitter, frequency-meter and F-M noise sections.

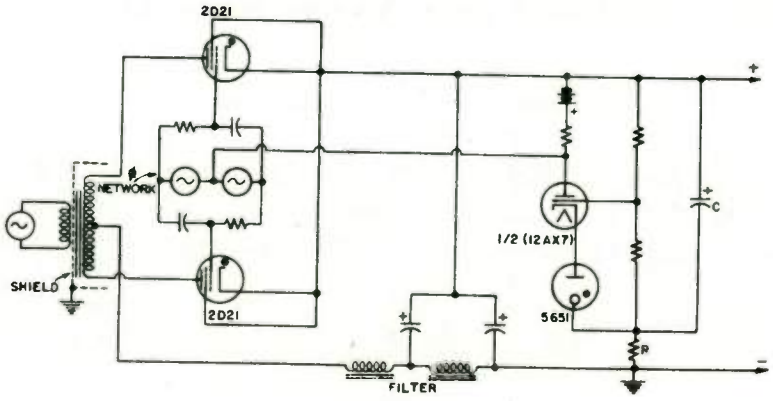

Fig. 10
Elementary schematic of regulated thyraton power supply.

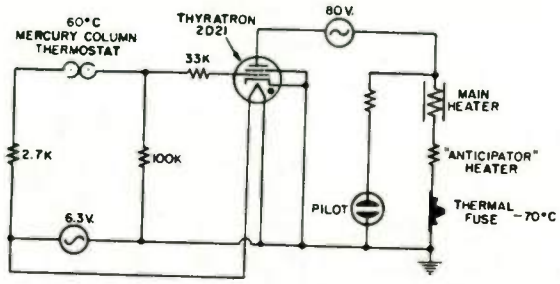

Fig. 12
Elementary schematic of control circuit for crystal oven.

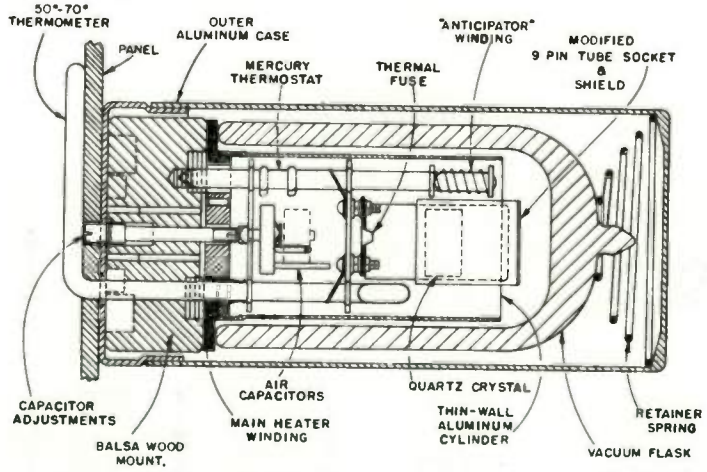

Fig. 11
Precision temperature-controlled oven.

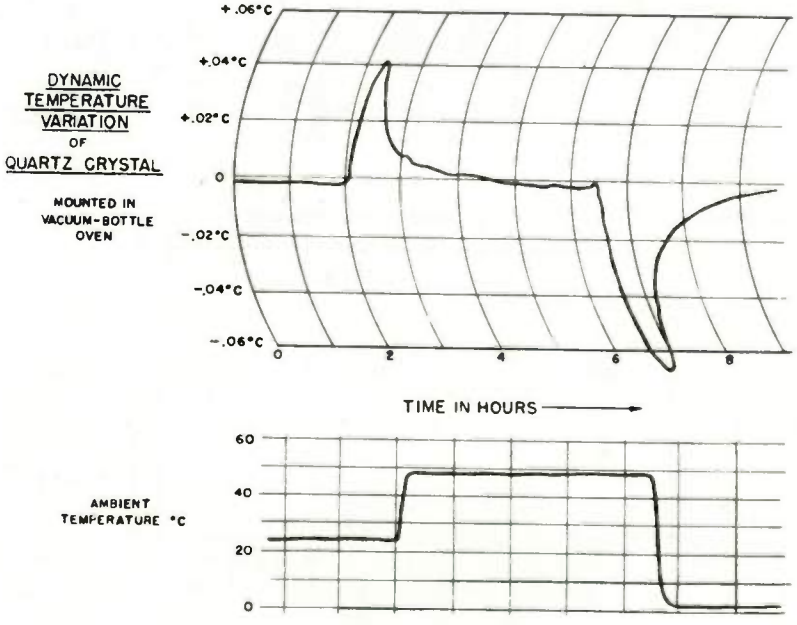

Fig. 13
Control characteristics of precision temperature control.

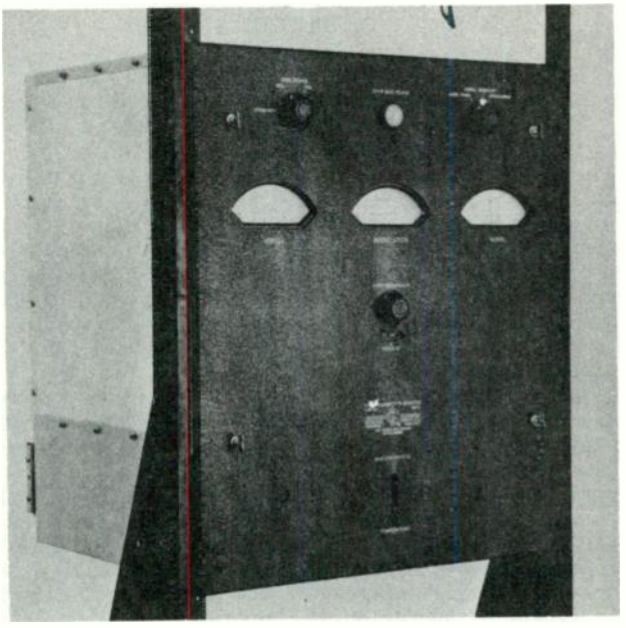

Fig. 14
Panel view of monitor.

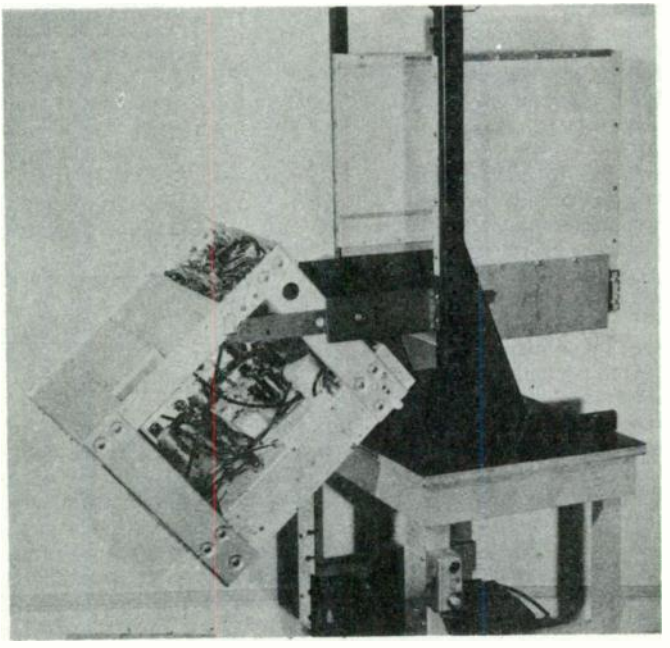

Fig. 15
View of monitor showing access to
interior sections.

A PACK TYPE TELEVISION SYSTEM

William B. Harris
Defense Electronic Products Division
Radio Corporation of America
Camden, N. J.

Introduction

A Television Equipment unhindered by cables and designed for man-carried operation offers complete portability and maximum flexibility. The United States Signal Corps, recognizing the military potentialities of such a device, awarded RCA a contract for development of a Pack Type Television System. While details of military applications for this equipment may not be discussed, it takes little imagination to visualize possible uses, among them artillery fire observation and reconnaissance of enemy territory.

Because of the rugged field conditions under which the equipment has to function, every effort was directed toward achieving a high degree of reliability, stability, and simplicity of operation. The features which make this equipment effective for the Military also recommend its use for special commercial broadcast applications. Its complete portability permits penetration of area inaccessible to standard television equipment enhancing on-the-spot coverage of sports, disasters, and special events.

System Description

The complete system consists of a Roving Station, a Receiving Station, and a Processing Station. Figure 1 is a block diagram of the system.

The Roving Station consists of a vidicon camera weighing 8 pounds and a back pack unit weighing 47 pounds. The camera is equipped with a pistol grip handle for hand carry operation, but facilities for triped mounting are also included. A pack board is used to distribute the weight of the back pack unit evenly thereby minimizing inconvenience to the wearer. A 525 line, 30 frame interlaced picture can be transmitted over a half mile range. Arrangements are made for bypassing the transmitter and sending video over five hundred feet of RF-59/U coaxial cable. Two hour operation is possible without recharging the batteries. Figure 2 shows the Roving Station in operation.

A television receiver, 10 inch monitor, and power converting equipment, all capable of vehicular mounting, comprise the Receiving Station. A switch on the receiver panel provides selection of either the RF input or any one of four video inputs.

The Processing Station is made up of a TG-12A Field Sync Generator, a modified TA-5D Stabilizing Amplifier and power supply, and a battery charger. All of these are portable. The first two units remove the non-standard synchronizing signals from the received signals and reinsert RETMA standard sync locked in phase with the original. The battery charger in addition to charging the batteries is capable of operating the Roving Station from a 115 volt, 60 cycle source.

The entire system has been designed to withstand the shock and vibration incident to portable and vehicular use.

All equipment will function properly at temperatures from +20 to +125°F., relative humidities up to 90%, and altitudes up to 10,000 feet above sea level. Splash-proof construction of the Roving and Receiving Stations assures that operation will not be impaired by long periods of exposure to rain or snow.

When the RETMA resolution chart is viewed, the received picture quality is as follows.

a. Horizontal limiting resolution in excess 350 lines.

b. Correct reproduction of eight steps in the horizontal and vertical gray scales.

c. Horizontal and vertical linearity such that no point is displaced by an amount more than 2% of picture size.

d. Shading such that the chart background is an even gray.

e. Ringing less than 5% of reference white.

Equipment Description

Roving Station

A block diagram of the Pack Unit and Camera is shown in Figure 3. The hand carried camera features a vidicon pick-up tube, selection of which was dictated by size limitations and circuit simplicity. The deflection and focus coils chosen are of the type used in the RCA TK-21 Film Chain. Regulation of the focus current is obtained by drawing through the coil a portion of the plate current of the first three video stages which are current regulated. The conventional alignment coil normally used to correct for discrepancies in vidicon gun alignment and shading has been replaced by a two ring permanent magnet. This produces a rotatable transverse field in the vicinity of the vidicon gun.

The video pre-amplifier employs a cascode amplifier with a high mutual conductance 417A triode as the ground cathode portion and one section of a 6111 dual triode as the grounded grid portion. The output stage of the pre-amplifier utilizes the other section of the 6111 tube as a cathode follower. The pre-amplifier has a gain of 50.

The Camera contains a kinescope viewfinder providing the operator with a means of monitoring system operation. The 2 inch kinescope is viewed through a magnifier lens for which a light shield is provided. Kinescope deflection and signal amplifier circuits are mounted on a sub chassis in the Camera.

Placement of all operating controls is such that they may be adjusted without interrupting the flow of video information. Recessed knobs are located along the top of the camera for fingertip control of focus, target, beam, and video output for the vidicon circuits and of focus and brightness for the viewfinder. A 6 foot cable connects the camera to the Pack Unit.

All circuits and components in the Pack Unit are grouped according to function on a miniaturized rack and panel assembly. The front and rear panels are easily removable providing ready access for servicing. This unit contains the following plug in assemblies; sync generator, vertical deflection chassis, horizontal deflection chassis, video amplifier, and RF chassis. The video signals from the camera pass over the cable to the pack unit and are coupled into a three stage video amplifier of conventional design. The overall video bandwidth is 5.5 megacycles. A keyed feedback clamping circuit maintains the grid of the last video stage at black level for blanking reinsertion. A control is provided for adjusting for optimum "set-up". A diode clipper provides for clean blanking output. To produce a picture with sharp edges generally requires reinserted blanking be wider than camera blanking. The slightly trapezoidal shape of the blanking pulses suggested a relatively easy means of accomplishing this objective. The pulses are amplified before reinsertion and the gain of the amplifier adjusted so the width at clipping level is greater than the width at vidicon cutoff level.

A crystal controlled, amplitude modulated transmitter operating at 360 megacycles provides the RF link for the system. It features two watts peak power output and a bandwidth of 10 mc at the 3 db down points. A 60 megacycle third overtone oscillator, a buffer amplifiers and a doubler stage comprise the exciter section of the RF chassis. In the oscillator circuit a coil is used to tune a Pi network the output capacity of which excites the buffer amplifier. This circuit does not favor the crystal fundamental frequency thus reducing the possibility of 20 megacycle operation with maladjustment of the tuning. The oscillator uses the triode section of a 6U8 tube and the buffer uses the pentode section. The frequency is doubled to 120 mc in a 5686 pentode stage. The frequency is then tripled to 360 mc in a grounded grid circuit using a 5893 pencil triode. The final amplifier also uses a 5893 pencil triode in a grounded grid circuit.

The tripler plate circuit and the final amplifier plate and cathode circuits all use tuning elements of the coaxial line type since this approach is most convenient for the frequencies involved. The plate lines of both tripler and final amplifier are a quarter-wave length long. The decision to employ cathode modulation dictated the selection of lines a half-wave length long to tune the cathode of the final amplifier. Modulation is applied at the midpoint or low impedance point of the cathode line thus reducing the capacity presented to the modulator. In cross-section the lines are about 11/2 inches square for the outer conductor and 3/8 inches diameter for the inner conductor. When properly loaded by the antenna, the efficiency of the final amplifier is 45%. The output from the plate tank is loop coupled to a coaxial transmission line which feeds the transmitting antenna.

The modulator stage serves a dual purpose. In addition to cathode modulating the transmitter, it functions as a video line amplifier for cable link operation. A switch is provided on the top of the pack unit for selection of either mode of operation. The signals from the video strip are amplified by a 6CL6 pentode to a level sufficient for 100% modulation of the final amplifier. Diode clamping at the grid of this stage is employed to restore the DC component of the video signal. White clipping occurs when the negative white signals go beyond the cutoff point of the modulator. Sync mixing is accomplished by applying the sync signals to the screen-grid of the modulator. Video from the modulator plate is supplied to the viewfinder signal amplifier during both transmit and cable operation.

A vertical quarter wave antenna and a ground plane comprise the transmitting antenna. This assembly is mounted on an aluminum tube long enough to allow the ground plane consisting of 4 rods to clear the operator's head. The antenna and ground rods are constructed of flexible steel to prevent breakage when going through underbrush. The flexible steel rods are declined 22 degrees from the horizontal in order to match the transmitter output circuit without recourse to transformer sections. Another desirable effect of this is the lowering of the radiation angle. The antenna is omnidirection in the horizontal plane. The VSWR is less than 1.2 over the frequency range of 335 megacycles to 365 megacycles.

The sync generator provides the system with composite sync, composite blanking, and horizontal and vertical drive pulses. A block diagram is shown in Figure 4. In the interest of conserving power and reducing complexity, a simplified sync signal is used. This sync, represented in Figure 5, varies from stand in two ways; by the absence

of serrations, equalizing pulses, and front porch, and by the sync and blanking pulse widths.

Eight dual triodes are used in the sync generator. A crystal controlled Miller Oscillator operating at 31.5 kilocycles provides the master frequency for this system. Buffer stages isolate the oscillator from the count down circuits. Two stabilized monostable multi-vibrators are used for counting from the master frequency down to a field rate of 60 cycles. Their counting ratios are 25:1 and 21:1 respectively. These count down circuits exhibit a high degree of independence from tube characteristics, supply voltage variation, and temperature changes.

The output from the 21:1 counter is a negative pulse, 840 micro-seconds wide, from which both vertical sync and blanking are derived. To obtain vertical sync the pulse is differentiated and drives a zero biased amplifier far beyond cutoff. The output of this amplifier is a positive 350 micro-second pulse which is applied to the sync mixer and to the vertical deflection chassis as a drive pulse. The sync mixer circuit consists of two triodes connected in series, one of which operates as a cathode follower, the other as a conventional amplifier. The 15.75 kilocycle sawtooth from the 2:1 blocking oscillator is shaped in an R-C circuit and applied to the other section of the sync mixer. The resultant pulse is 4.5 micro-seconds wide . The horizontal and vertical pulses are combined in the output circuit of the mixer. A series clipping circuit assures flat topped horizontal and vertical pulses of equal amplitude. The output cathode follower supplies composite sync signal.

The blanking system is similar to the sync system just described. The output of the 21:1 counter which has correct width for vertical blanking is applied directly to a zero biased amplifier. The mixer, clipper, and cathode follower output stages are identical to those used for the sync circuits except that RC circuits are designed for blanking pulse widths.

The output of the 2:1 counter is used directly for Horizontal drive.

The deflection circuits are more or less conventional in design, however, special emphasis was given to keeping size and power consumption to a minimum.

The horizontal deflection system is similar to that used in television receivers. It was necessary to exercise special care in the choice of components in order to meet the linearity requirements of the system. The horizontal drive pulse is amplified and shaped to produce a 5 micro-second pulse of sufficient amplitude to trigger the sawtooth generator and to provide drive for the feedback clamping circuit in the video chassis. The sawtooth voltage is also coupled to the grid of a 5763 output tube which together with a 6X4 damper and a miniature output transformer provides deflection power for the vidicon. A portion of the output is rectified by a selenium rectifier to furnish a negative bias for the vidicon. A 5785 subminiature high voltage rectifier supplies 2000 volts from the horizontal flyback to operate the kinescope viewfinder.

Vertical deflection power is derived in a conventional manner. A sawtooth initiated by the vertical drive pulse is amplified and drives the vertical output stage. The output is transformer-coupled to the vertical deflection coils. A sawtooth voltage is developed across a resistor connected in series with the deflection coil and applied to the cathode of the sawtooth amplifier. This feedback loop assists in meeting the linearity requirements of the system.

Viewfinder deflection circuits employ two subminiature dual triodes which are located in the camera. The vertical feedback voltage is amplified in a cathode coupled amplifier to the level required for kinescope deflection. The voltage pulse appearing across the horizontal deflection coil charges a capacitor through a resistor and silicon diode. The capacitor discharging through the resistor provides a sawtooth voltage which is applied to a cathode coupled amplifier similar to that used for vertical deflection.

Primary power for the Pack and Camera units is furnished by five silver-zinc, rechargeable batteries connected in series. They furnish the 30 amperes at 6.7 volts required for the Roving Station. Since the equipment must operate for two hours without interruption, 60 ampere-hour cells are used. An essentially flat discharge characteristic contributes to system stability. The batteries are mounted in a removable tray permitting a change of batteries to be made rapidly. The weight of the battery supply is 9 pounds.

A dynamotor is used to convert the 6.7 volts to the 150 and 260 B + voltages. The dynamotor is extremely small, weighing only 4 pounds. Extensive filtering in both the primary and output leads is employed to prevent dynamotor noise from appearing in the picture. All power supply components are located in the bottom of the Pack Unit.

Receiving Station

The equipments comprising the Receiving Station, Figure 6, are normally mounted in an Army jeep and can be operated while the vehicle is in motion. A portable inverter converts the 24 volts DC from the vehicle power source to 115 volts, 60 cycles for the Receiving Station equipment.

The receiver which picks up off-the-air signals from the Roving Station is also capable of accepting cable inputs from four additional equipments. Selection between these inputs is provided for by means of a switch on the front of the receiver panel. The receiver consists of an RF unit, an IF unit, a distribution amplifier,

and power supplies.

The RF unit converts the 360 mc signal received by the antenna to a 30 mc I.F. signal. Lumped constant L-C tuning elements are used in the RF unit. The antenna is coupled to the cathode of a grounded grid RF amplifier utilizing a 417A triode. A copper strap connected from the cathode to ground is broadly resonant with the input capacity of the 417A at 360 mc. A push-pull oscillator using both section of a 6101 tube operates at 330 mc. Good frequency stability is obtained by employing a high Q tank circuit with loose coupling to oscillator and mixer grids. A second 417A serves as a mixer. The RF and oscillator voltages are parallel-fed to the grid. The last stage of the RF unit is an IF amplifier using a 6CB6 tube.

In order to obtain the required IF band width, stagger tuned, triple stages are employed using nine 5654 pentodes. The tuned frequencies are 23.8, 30, and 37.8 megacycles. The output from the last triple tuned stage is amplified by a broadband 6AN5 stage and then rectified by a diode detector. The diode detector is directly coupled to two 6CL6 video amplifiers. One operates as a cathode follower and delivers the composite video signal to the distribution amplifier. The second amplifies the video signal and applies it to a sync separation circuit. The DC cathode voltage of this circuit is proportional to the average value of the video signal. This is applied to the control grid of the AGC rectifier. The horizontal sync appearing across the plate resistor of the sync separator is amplified and then applied to the plate of the AGC rectifier. AGC voltage is developed across the load resistor. Since the AGC tube only conducts for the duration of the horizontal sync pulse, the system exhibits a high degree of noise immunity.

The receiver has a gain of 105 db, a noise figure of 10 db, and a bandwidth of 10 megacycles at the 3 db down points.

The distribution amplifier supplies video to the Display Unit and to four 75 ohm terminated lines. A series amplifier, a cathode follower, and a series-parallel output stage comprise the distribution amplifier. The series amplifier consisting of 2 tubes in series provides for high current gain. The cathode follower isolates this amplifier from the high input capacity of the output stage thus preserving the high frequency response. The video response is flat from several cycles to 5 megacycles rolling off to the 6 db point at 15 megacycles. The gain of the amplifier is 2.5.

The receiving antenna is a directive, high gain yagi antenna with a beam width of 35° at the 3 db down points. A weather proof antenna rotator with provisions for mounting on a Military vehicle is included with this antenna.

The Display Unit is a commercial ten inch monitor ruggedized and repackaged for Military use.

Processing Station

The primary purpose of the Processing Station is to process the signal received from the Roving Station to conform to RETMA standards for monochrome television. An RCA TG-12A Field Sync Generator and a Processing Amplifier perform this function. The Processing Amplifier consists of a TA-5A Stabilizing Amplifier modified to accept blanking reinsertion and provide a simplified sync output. The Processing Amplifier strips the simplified sync from the received video signal and feeds it to the Sync Generator. Here the Genlock circuits lock the local sync to the remote sync. The new sync signals are mixed with the original video signals in the Processing Amplifier. Standard blanking signals, wider than pack unit blanking, are supplied for reinsertion in the Processing Amplifier.

The Sync Generator, Processing Amplifier and its power supply are each mounted in individual carrying cases.

Conclusion

The system described in this paper has been evaluated by the United States Signal Corps in simulated field operations. The results of their evaluation revealed that stability and picture quality have not been sacrificed for portability. The equipments met all the rigors of field conditions without impairment of operating effectiveness.

Acknowledgment

The development of the equipment described here was performed under Signal Corps Contract DA-36-039-sc-64651.

The author wishes to express his appreciation for the assistance and suggestions furnished by engineers of the Commercial Electronics Products Division and the RCA Laboratories Division during the development of this system.

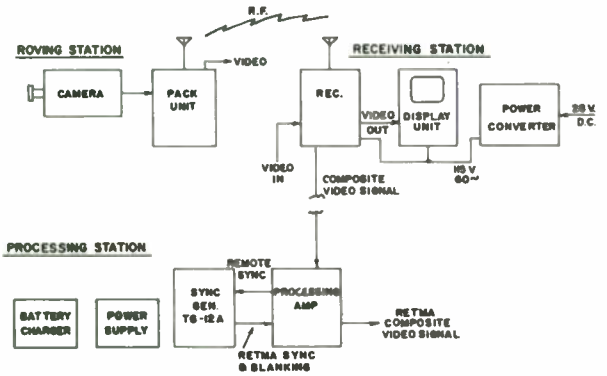

BLOCK DIAGRAM
OF
PACK TYPE TELEVISION SYSTEM

Fig. 1
Block diagram of pack type television system

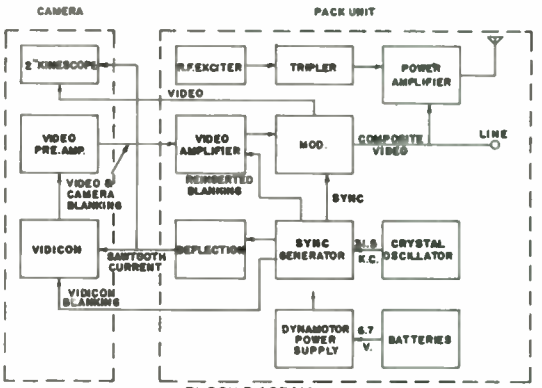

BLOCK DIAGRAM
OF
PACK UNIT AND CAMERA

Fig. 3
Block diagram of pack unit and camera

Fig. 2
Roving station in operation

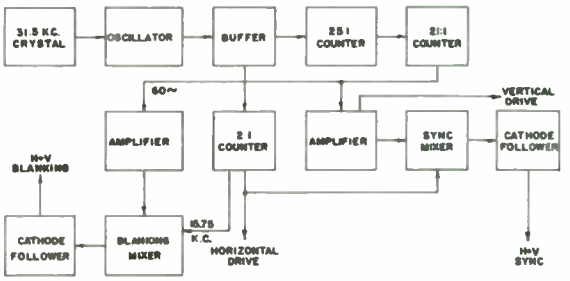

BLOCK DIAGRAM
OF
SYNC GENERATOR

Fig. 4
Block diagram of sync generator

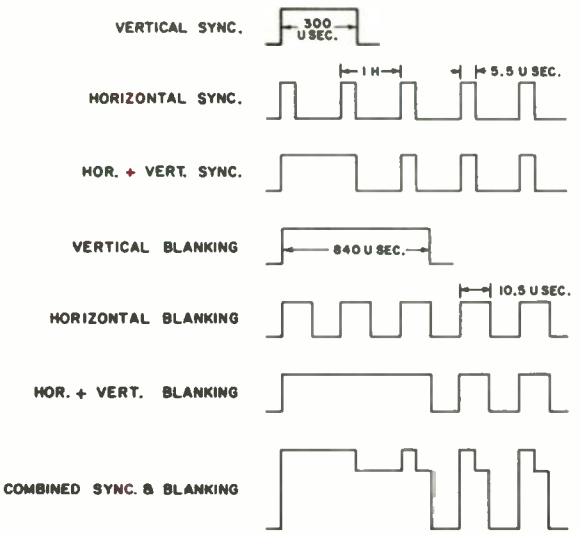

Fig. 5
Sync generator wave forms

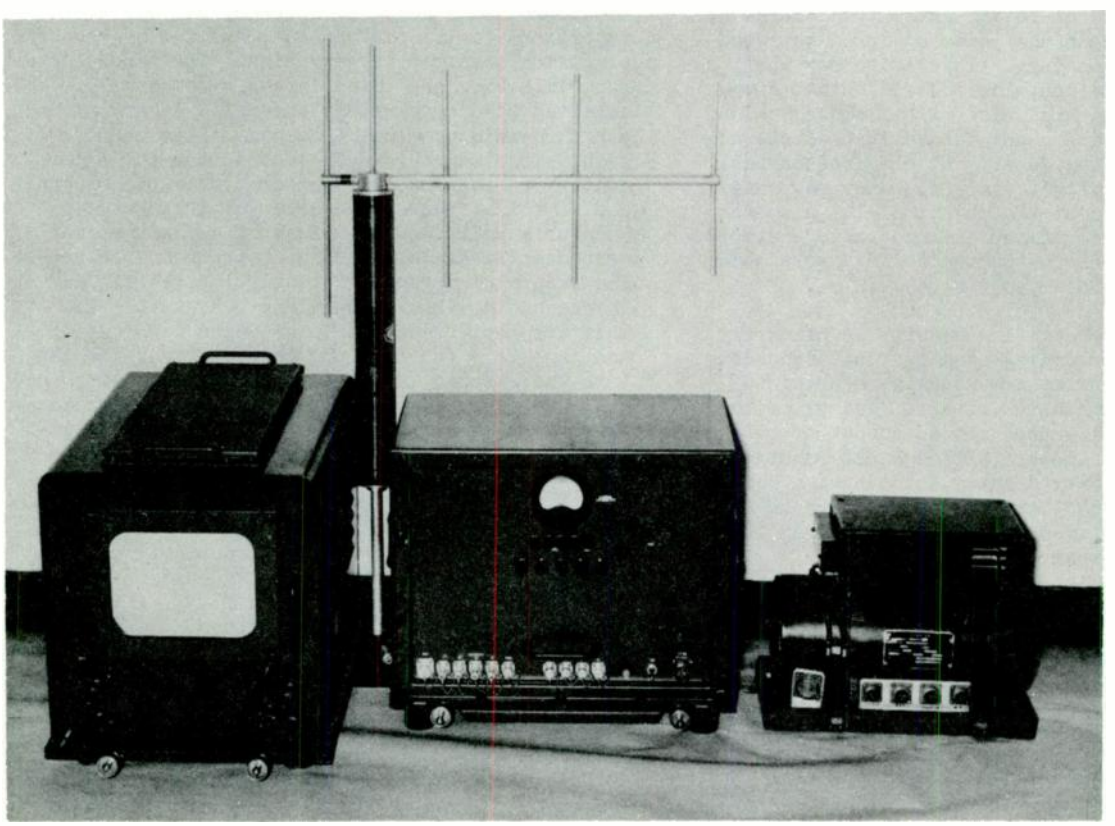

Fig. 6
Receiving station

EQUALIZATION CONSIDERATIONS IN DIRECT MAGNETIC RECORDING FOR AUDIO PURPOSES

Ross H. Snyder
James W. Havstad
Ampex Corporation
Redwood City, California

In this paper, the authors explain the purpose of equalization in direct magnetic recording for audio purposes, and explore the limits which are imposed by the medium and by the nature of the information to be recorded. A specific recommendation is made of a particular method of equalization.

Fundamentals

In this discussion we will confine ourselves to the relations which exist between the magnetic recording medium and the magnetic heads with which it functions, as these affect frequency response and signal-to-noise ratio in a magnetic audio recorder. The discussion assumes that high frequency bias is optimum in level, that its waveform is substantially sinusoidal, and that its frequency is approximately six times the highest audio frequency of interest.

A pattern of magnetic flux is produced on tape by passing it across a magnetic recording head, which subjects it to a magnetic field which varies in accordance with the impressed audio signal. As a crude approximation, the magnetic flux density on the tape is proportional to the current in the coils of the recording head, and the voltage across the terminals of the playback head is proportional to the rate at which the playback head scans the lines of force surrounding the magnetized tape. This is to say that, as a first approximation, the voltage output from the playback head will rise with frequency along a slope of 6 decibels per octave if the tape assumes constant flux density at all frequencies. It is also to say that flat frequency response would be obtained at the output of the playback amplifier if it contained an integrating network, and if the current in the record head were made constant with respect to frequency.[6]

Since recorded flux density is primarily dependent upon recording head current, recording characteristic curves are usually referred to current, rather than to voltage. And since in practical circuitry the voltage output of the playback head is linear (although not constant) with respect to flux density throughout a considerable portion of its bandpass, playback characteristic curves are usually referred to voltage, rather than current.

Practical Operating Conditions

It is necessary to modify the approximations given in several ways. The curve of voltage-response, even of a theoretically perfect reproduce head, peaks at an upper mid-range frequency, and then declines, due to the approach of "gap null," when playing a tape of constant flux density. Self-demagnetization of the magnetic particles occurs at short wavelengths.

In contrast to gap null and self-demagnetizing effects, which depend upon wavelength, certain losses dependent upon frequency are inherent in most practical recording head designs, the most important being hysteresis and eddy current losses. If the tape is to be recorded with constant flux density at all frequencies, a certain level of high frequency pre-emphasis must be added to the record current characteristic to compensate for these effects. Simple "constant current" in the recording head will usually not produce a tape of constant flux density.

Recording and Reproducing Heads

Certain compromises which must be made in designing recording heads in order to accommodate high currents need not be considered in the design of reproducing heads. The configuration of the reproducing head is, however, of very great importance to its performance, and the degree of precision involved is very high. The record head gap width, for one thing, appears to be well selected at approximately one-mil. A narrower gap than this provides inadequate bias penetration, since the thickness of the magnetic tape coating rapidly becomes comparable to the record gap if this is under one-mil, yet a larger gap than this will result in loss of definition and consequent degradation of high frequency response. The record head can efficiently impress signal images on the tape of wavelength as little as half its gap, since the information recorded on the tape is a function of the field to which the tape was exposed immediately prior to leaving the gap; the tape, then, remembers only what it last "saw." A one-mil recording head gap will satisfactorily record half-mil wavelengths, although the playback gap must be substantially less than a half-mil if it is to produce useable output at the frequencies corresponding to such wavelengths. Thus, one-quarter-mil gaps are routinely used in high quality magnetic reproducing heads.

Reduction of the gap width of the reproducing head to less than half the shortest wavelength to be handled must reduce the useful output, and usually to reduce the signal-to-noise ratio, if the gap depth is held constant. Or, the gap depth may be reduced so that additional turns of wire may be added to compensate for the reduction in useful output, thus maintaining good

signal-to-noise, with the result that the useful life of the head is reduced. Head life, frequency range, and useful output are mutually opposed parameters, no one of which may be changed excepting at the expense of one or both the others. A reasonable choice among these design parameters can result in the head which is responsive to half-mil wavelengths, with sufficient output for 60 decibels of signal-to-noise ratio or more, and for useful life in excess of fifty-million feet of tape.[5]

Figure 1 illustrates the frequency response of a reproducing head of negligible electrical losses, when playing a tape which has been recorded with constant flux density at all frequencies. The increased area under the curve of response for the quarter-mil gap head indicates the possibility of obtaining useful output at half-mil wavelengths, provided the reproducing characteristic or the record characteristic or both are suitably modified. This corresponds to an upper useful bandpass of 15,000 cycles at the 7½ inch per second tape velocity. Indefinite extension of frequency response is not possible, because the response curve becomes vertical and its output zero at that frequency which corresponds to a recorded wavelength equal to the gap size of the reproducing head.

Selection of Record-Reproduce Characteristics

In establishing satisfactory pre-emphasis and post-emphasis curves for use with direct magnetic recording for audio purposes, two extremes are possible. Figure 2 shows the recording characteristic which would be necessary in order to obtain flat overall output if the playback amplifier were compensated to a constant 6 decibel per octave declining slope, at 7½ inches per second. Figure 3 illustrates the playback curve which would be necessary with a theoretically perfect head of quarter-mil gap, if the recording characteristic were flat with respect to current and frequency, modified upwards in the higher frequencies only to compensate for such electrical losses as may exist in the recording head.

Neither of these curves is satisfactory. In the extreme of incorporating all compensation in the record process, overloading of the tape may readily occur with signals of normal intensity from ordinary audio sources, at the higher frequencies. On the other hand, if all of the compensation is applied in the playback circuit, high frequency hiss becomes exceedingly prominent.

If we are to lean in one direction or the other, in making our selection somewhere between these options, it may well be in the direction of lower hiss and greater likelihood of occasional high frequency overloading. This philosophy is urged, because the direction in which the audio art is moving is toward microphone and loudspeaker equipment of smoother and flatter high frequency performance, in which range the preponderance of noise products are concentrated. As loudspeakers of smoother and more extended high frequency performance become available, hiss in the reproduction becomes more and more prominent, and since it is present at all times it is the major source of objection by users. We are also justified in leaning away from hiss because of the graceful overload characteristic of magnetic recording.

It remains, then, to determine what shape we may reasonably assign to that curve which describes maximum useful (that is to say, substantially undistorted) output across the audio spectrum while yet keeping hiss components well down. Even at economy tape speeds, this curve must surely have a slopewhich is no steeper than that of the average spectral distribution of energy in typical program material, and should probably have substantial dynamic reserve to accommodate at least the large majority of infrequent high frequency peak energies which may be encountered.

It is conventional to construct magnetic tape recorders which are capable of operation at more than one tape velocity. Logically, then, one of these tape velocities might well be selected in accordance with the physical capabilities of the medium so as to accommodate even the greatest extremes of peak energy which may be encountered in unusual program material, for use in the original recording of high quality material, and for its preservation for long periods of time. For such exacting purposes, a higher tape velocity is appropriate, and the increased medium costs are not inappropriate for the purpose.

On the other hand, one or more economy tape velocities are certainly needed, one of which may well be selected to accommodate wide range high quality material, with the sacrifice only of the ability to record the most extreme peaks of unusual high frequency energy. The 7½ ips velocity, it may be shown, is well adapted to this purpose. Even lower velocities are appropriate when a limitation of the bandbass[2] to, say, 8 or 10 kilocycles may be accepted, and when a somewhat narrower dynamic range is anticipated.

Figures 4 and 5 illustrate the U.S. NARTB playback and recording curves, which are recommended for the first two purposes mentioned.

In Figures 6 and 7 lie the data upon which justification is sought for the record and reproduce curves of Figures 4 and 5. The curves describing maximum useful output and accumulating noise are absolute measurements, made on a machine whose performance for audio purposes is limited by tape characteristics alone, and not by limitations inherent in the machine. (Ampex Model 350, full-track, 7½ - 15 ips.) This is to say that the inherent electrical noise in the amplifying system is less than that originating from a tape in motion, and whose amplifier overload point is substantially higher than that which occurs as the result of the approach of

tape saturation, the electronics thus contributing negligibly to distortion at the upper dynamic limit. The curve of peak energy[7] is arbitrarily attached to the figure at maximum level, in order to illustrate the likelihood of overload at any frequency under gain conditions such that peaks in the mid-range touch but do not exceed the maximum useful (substantially undistorted) record level on the tape. This curve is derived from an extensive study of typical original and first-copy tapes recorded by major American recording companies, and supplied to us by their courtesy, and from a series of especially prepared original recordings of orchestral music, which were deliberately recorded far below normal level in order to register all peaks without "clipping" due to the approach of tape saturation. Energy maxima from all these fell at or below the curve shown. This curve is in substantial agreement with the data of Sivian, Dunn, and White[1] excepting in the region 3 to 8 kilocycles, where our studies confirm the presence of somewhat higher energy levels in the program material selected, which is believed to be representative of a change in both musical taste and manner of orchestration and performance since the Sivian, Dunn, and White studies of the late 1920's. The average energy curve[3] shown is also derived from the Sivian, Dunn, and White papers[1] and is similarly applied to the figures. It will be seen from Figure 6 that unusually high peaks of infrequent occurrence may be expected to saturate the tape at the 7½ ips velocity if the gain is adjusted so that mid-range peaks exactly touch the upper limit of recordability. In exchange for this relatively infrequent hazard, which is entirely controllable if "needle banging" is avoided on program material of unusual high frequency content, we continuously benefit by the highly desirable noise characteristic described on the figure. It is apparent that the high frequency noise energy output of the tape-machine combination is substantially below that of normal or "white" noise, which would describe on the figure a curve ascending at the rate of 3 decibels per octave throughout the spectrum. Since this is the characteristic "hiss" of any transmission device which is sufficiently refined so as to be limited by random noise products, it may be seen that the curve achieves the highly desirable condition of continuous relative quietness in exchange for the controllable hazard of rare tape overload. In Figure 7 it may be seen that the 15 ips curve provides about equal overall signal-to-noise ratio, and substantially no likelihood of tape overload at the frequency extremes.[4] Desirable as this may be, the industry still needs more signal-to-noise ratio. In recent experiments,[10] in which the music of a live symphony orchestra was compared immediately with stereophonic reproduction of itself, the limitation upon realism was tape hiss, not distortion or frequency response irregularities. This was true even though the perhaps extravagant 30 ips speed was used, enabling the playback curve to decline constantly at 6 db per octave. If even at this extreme of available signal-to-noise ratio (70 db or more) hiss is still the limiting factor upon faithful reproduction, we hold there can be no substantial ground for favoring a 7½ ips curve which offers 6 or more decibels less signal-to-hiss ratio than the U.S. NARTB curve. A curve such as that recommended by the CCIR must be regarded as leading us toward a degradation, not an improvement, in international standards of performance.

The ultimate test of the acceptability of the U.S. equalization curves is in the analysis of the experience of those who use them.[8]

During the five years since these curves were standardized, user reports of difficulties over noise have approximately equaled those over the occurrence of "splatter," substantiating the original engineering estimate that the 7½ ips curve chosen was a good compromise between these conflicting extremes. There is a tendency now, toward a preponderance of complaints over noise, which, in our belief, indicates that the original compromise erred, if at all, in the direction of too little high frequency pre-emphasis; certainly the increasing need for less noise does not point to less pre-emphasis, and the U.S. NARTB curves, which have been described here, are in realistic agreement with the needs of the recording industry. The only foreseeable reason for changing the standard to one of lower pre-emphasis would be the result of large improvements in tape coatings. The peak-output versus noise of the tape itself, at short wavelengths, must be improved before such a change could reasonably be contemplated. The U.S. manufacturers of recording tape are continuously investigating the possibility of such improvements. Experiments with higher output tapes have been made, but none thus far have produced a coating of substantially greater output capability at short wavelengths.

APPENDIX I

Measurement Methods

The equipment used to derive the curves on maximum signal and noise spectra included an Ampex Model 350 (7½ - 15 ips, full-track), the necessary instrumentation, and a tape of "centerline" characteristics. Recording tape varies considerably in output capability, in maximum output versus wavelength characteristic, in bias requirement, and in noise.[9] We are indebted to the Minnesota Mining and Manufacturing Company, to Reeves Soundcraft Corporation, to Audio Devices, Inc., and to Orradio, Inc., for their unlimited cooperation in submitting samples of their various tapes, and of separate runs of manufacture, which has enabled us to establish a "centerline" of performance from tape in each of the characteristics mentioned above.

"Maximum useful output" was established in two ways. First, the tape was completely saturated with signals whose frequency included the entire spectrum, and the maximum fundamental tone which could be derived from the saturated signal was measured. Second, the departure from linearity

of output versus input was measured at 400 cycles at that level of tape magnetization at which the r.m.s. total of distortion products equaled 3%. It will be seen that, in a device of limited overall bandpass, total distortion measurements at frequencies whose harmonics would considerably exceed the upper bandpass of the instrument would be meaningless, and artificially high. Therefore, the "maximum useful output" curve describes that level at which the non-linearity of the machine's transfer characteristic is equal to that found at 400 cycles at 3% distortion.

Noise measurements were made in accumulating half-octaves, beginning at 33 cycles. The highest noise figure shown, at 15 kilocycles, is the measured total of noise products in the band 30 to 15,000 cycles.

It will be seen that overall signal-to-noise ratios described by the figure are somewhat in excess of published specifications on the equipment. This reflects conservatism on the part of the manufacturer, for the ratios indicated are in no way artificially weighted. The equipment was aligned, the bias adjusted, and the equalization circuitry set precisely according to instructions in the published manual. The machine is considered in every way typical, and the results obtainable on most machines whose design is refined to the point where performance limitations are imposed by the tape.

APPENDIX II

Design Considerations In The Construction Of Equipment To Record And Reproduce The Curves Described

Among the other considerations upon which the curves were selected was that of the desirability of using curves which are readily reproducible with comparatively simple circuitry. Since the interchangeability of tapes among different machines depends most heavily upon uniform adherence to the flux densities in the tape implied, primary emphasis was placed upon the establishment of a playback curve which is of readily reproducible characteristics. The coincidence which permitted the establishing of identical curves for the reproduction of both 15 and 7½ ips tapes was a happy one, and the curve may be reproduced with simple resistance-capacitance components. The record circuitry is the point at which such complications as may be required should be concentrated, in our opinion. This gives the manufacturer who wishes to adhere to the standard curve the option of constructing comparatively inexpensive record circuitry, at the expense of the widest possible range, if this is appropriate to the grade of equipment contemplated. That is to say, a 7½ ips machine whose upper frequency response may be limited to 10 kilocycles can be constructed with electronics of gain adequate only to realize the equalization up to that frequency, and the more costly elements needed to extend the record curve to 15 kilocycles may be omitted yet the machinery still be capable of producing tapes which will play back "flat" up to the upper frequency limit selected through playback equipment adhering to the standard curve. In equipment of still less cost, where the record circuitry cannot incorporate the elements necessary even for the steep rise to a low upper frequency limit, and where less "roll-off" of the playback circuit is thus necessarily imposed in order to match the simpler record equalization, it is still a comparatively simple matter to incorporate sufficient range of "tone control" in the equipment to give the recommended playback curve. By this means, such a machine could be used to play back "flat" professionally recorded tapes which are more and more becoming available for sale, while yet retaining the ability to play self-recorded tapes satisfactorily. The professionally recorded tapes, in this case, would, of course, exhibit less noise in the output.

APPENDIX III

Bibliography

1. "Absolute Amplitudes and Spectra of Certain Musical Instruments and Orchestras," L. J. Sivian, H. K. Dunn, and S. D. White, Journal of the Acoustical Society of America, January, 1931, Pages 330 to 371.

2. "Hearing, The Determining Factor in High Fidelity," Harvey Fletcher, Proceedings of the Institute of Radio Engineers, June, 1942, Pages 266 to 277.

3. "Auditory Patterns," Harvey Fletcher, Reviews of Modern Physics, December, 1940, Pages 47 to 65.

4. "Why the NARTB Curve for Magnetic Tape?" W. E. Stewart, Radio and Television News, June, 1955, Pages 40 etseq.

5. "Magnetic Recording--A Report On The State Of The Art," W. T. Selsted and R. H. Snyder, Transactions of the Institute of Radio Engineers Professional Group on Audio, September - October, 1954, Pages 137 to 144.

6. "Instrumentation For Magnetic Recording Research," Naval Research Laboratory Report S-3448, April, 1949 (unclassified) 47 pages.

7. "Analysis of Spectral Energy Distribution In Certain Orchestral Tape Recordings," George A. Brettell, unpublished Ampex monograph.

8. "A Report on Five Years' Service Dealings With Ampex Customers," H. Van Childs, unpublished Ampex monograph.

9. "Non-Uniformity of Magnetic Recording Tapes," J. Leslie, unpublished dissertation presented March 28, 1955, to National Convention of Audio Engineering Society, Los Angeles

10. "An Experiment in Immediate Comparisons Between Live Symphonic Music and High Quality Reproductions," W. T. Selsted and R. H. Snyder, unpublished Ampex monograph, March, 1956.

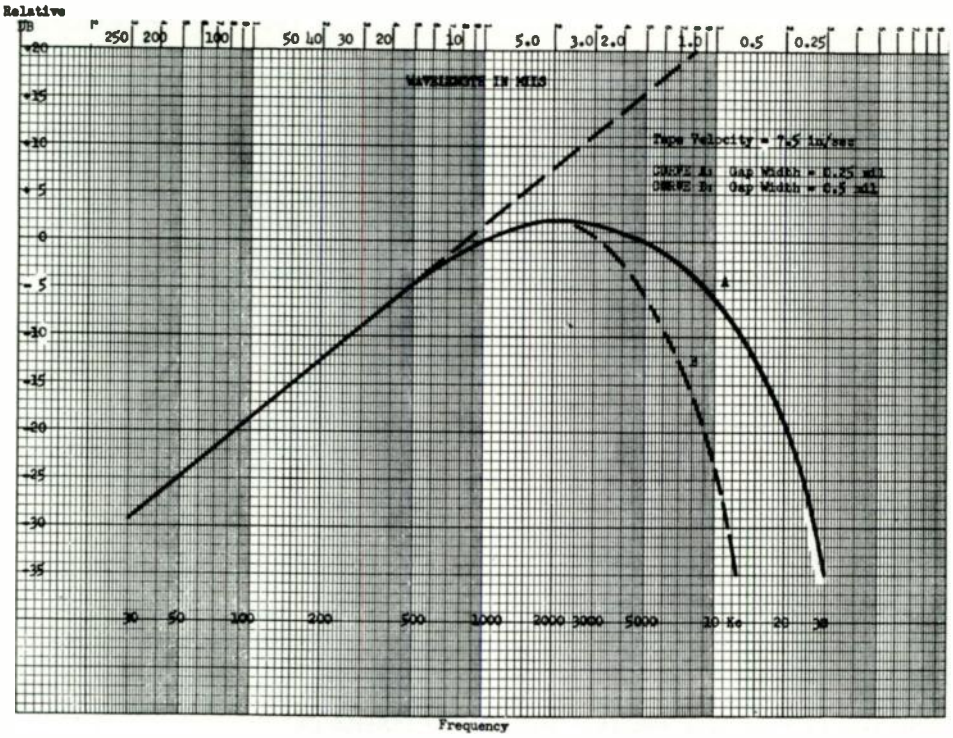

Fig. 1

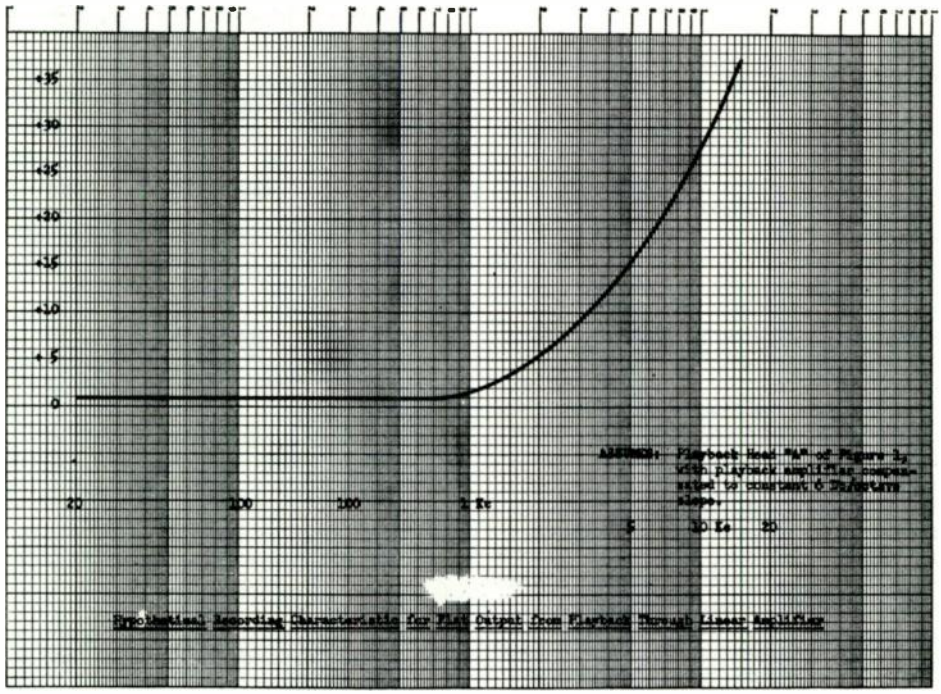

Fig. 2

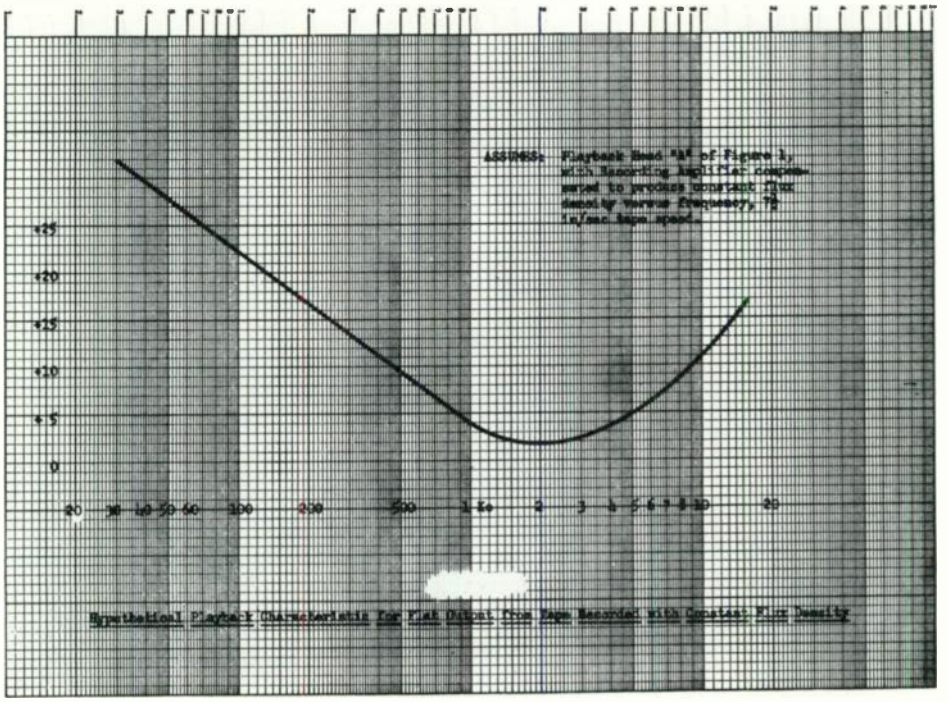

Fig. 3

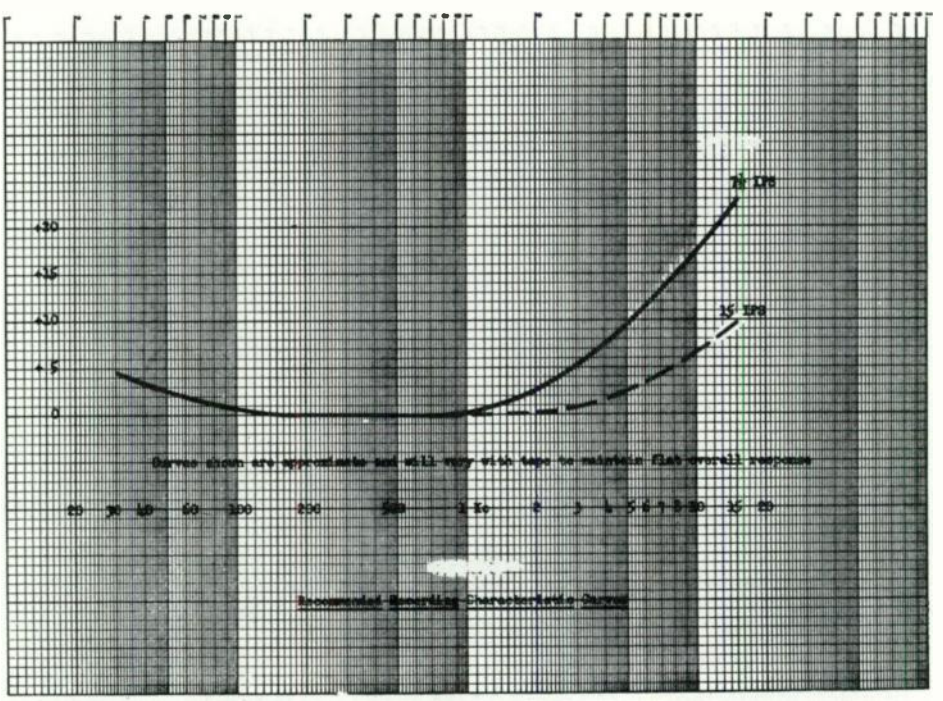

Fig. 4

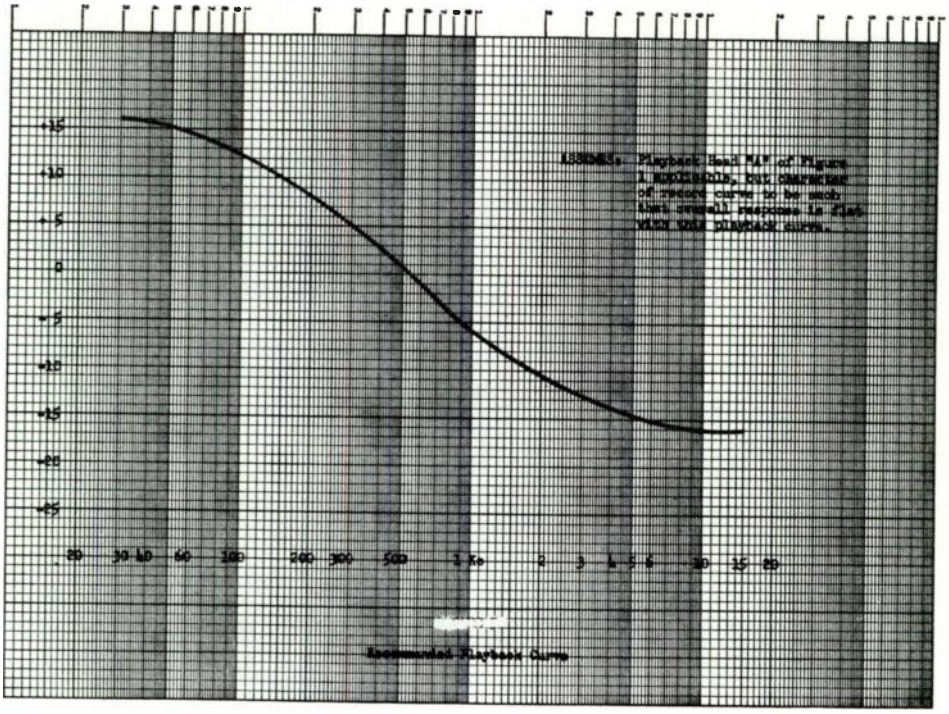

Fig. 5

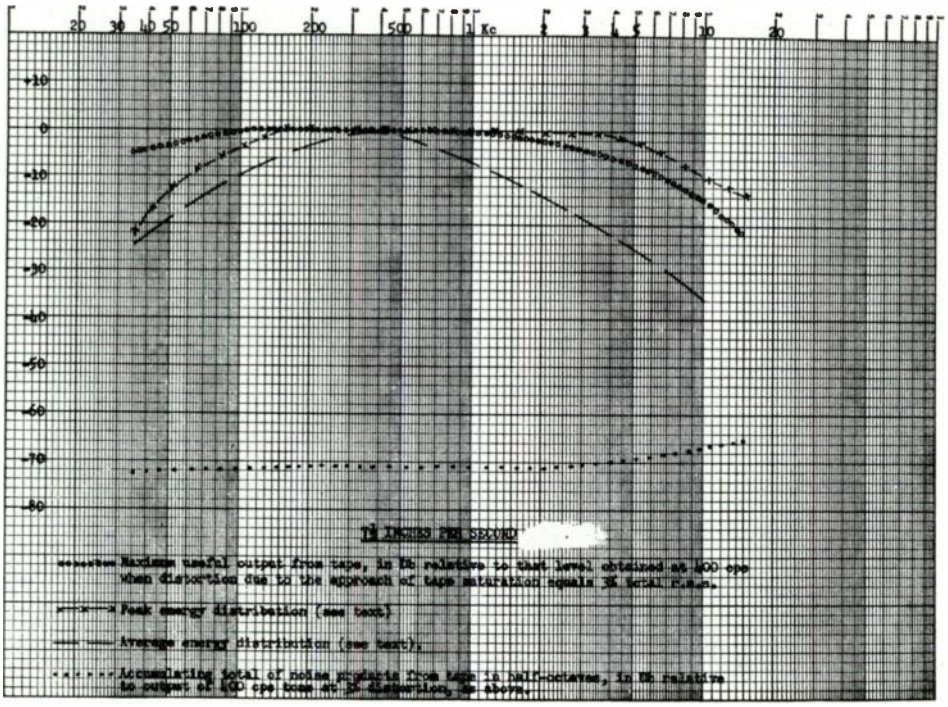

Fig. 6

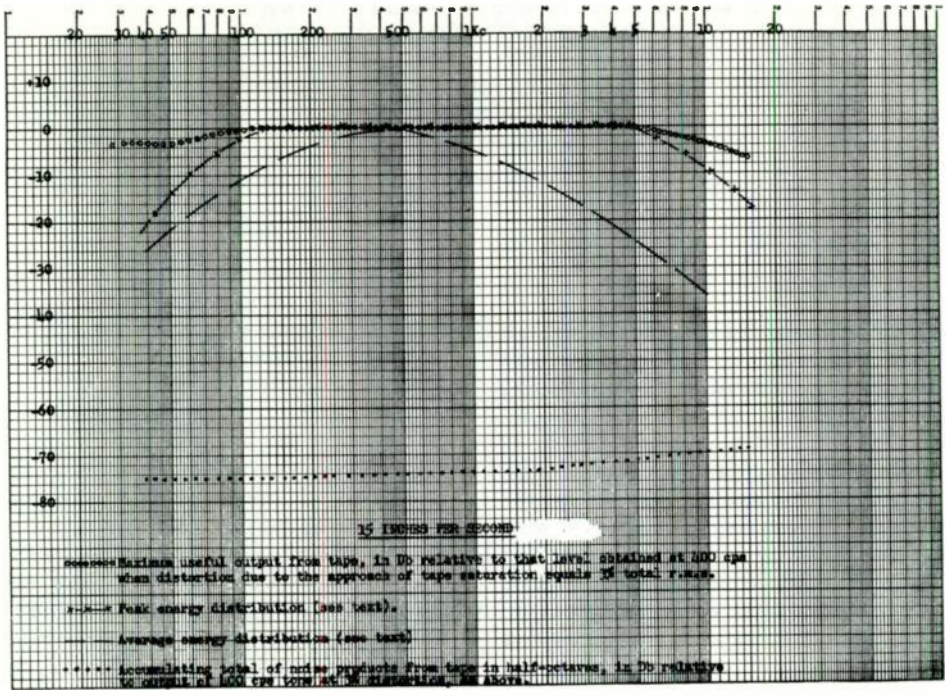

Fig. 7

DESIGN OF A HIGH FIDELITY 10 WATT TRANSISTOR AUDIO AMPLIFIER

by
Robert P. Crow
Robert D. Mohler
Motorola, Inc.

Introduction

Since the recent availability of relatively high power junction transistors, considerable effort has been put into development of audio amplifiers with outputs of 5 watts and higher. The push-pull class B amplifier provides the best utilization of the transistor's well-known capabilities of high efficiency and low standby drain.[1,2,3] It is the purpose of this paper to consider this type of amplifier and its problems, along with a practical design of a 10 watt unit. While much of the work presented in this paper is based on operation from so-called "12 volt" sources, which are being used extensively for automotive and other applications, the general considerations and results will apply, or can be adapted, for other supply voltages. Also, while the characteristics and other transistor data presented are specifically for the 2N176, manufactured by Motorola, there are a number of other units available that are similar. The 2N176 is an alloy PNP transistor with the collector junction directly connected to a copper mounting base which acts as an initial heat sink. The unit has a collector dissipation rating of 10 watts with a mounting base temperature of 80°C.

Basic Design Considerations

Although characteristics and design considerations of large signal transistor amplifiers, including push-pull class B types, have been considered at length in many publications, and will not be repeated in detail in this paper, a few points should be reviewed. As is well known, transistors can be used as power amplifiers with three basic connections, the common base, common emitter, and common collector, which have characteristics analogous to the three basic tube connections, the common or grounded grid, common cathode, and common plate or cathode follower. In considering characteristics of these three basic transistor connections, several points should be kept in mind. Among the important class B amplifier design considerations are the abilities to provide good power gain and low output distortion, which generally requires linear gain characteristics. In addition, because of the fact that in a class B circuit the two halves work independently on each half cycle, the ability to provide and maintain equal gains for each half, is necessary. There are obviously other factors too, such as efficiency, cross-over distortion, or transients, temperature stability, and size of circuit components.

Power Gain

It is generally true in high level amplifier designs that the required load impedance is determined not by the output impedance characteristics of the amplifying device, but rather by the required output volt-ampere swing, the output power for class B sine wave conditions then being given by 1/2 the peak voltage times the peak current. Most transistors have characteristics, as will be shown later, that approach the ideal in that a reasonably linear current-voltage swing can be extended from nearly zero voltage drop on one end to nearly zero current, or cutoff, at the other end. As a result, an approximation for optimum collector load resistance, R_L, for a class B amplifier is given by the ratio of collector (supply) voltage, E_C, over the peak collector current, or in terms of sine wave output power: $R_L \cong E_C^2/2P_{out}$. The actual value of R_L will, of course, always be somewhat lower in order to allow for the losses in the transistors, output transformer, and bias circuit. This above relation is essentially independent of the transistor connection.

A comparison of transistor power gain versus load resistance and output power for the three basic connections can be made. Figure 1 shows such a comparison for a typical 2N176 transistor. The power gain shown is the ratio of maximum "undistorted" output over the input power required to produce this output, thereby taking into account any effects of non-linearity. The load resistance is that presented to the individual transistors and for a conventional push-pull class B circuit would be 1/4 the collector-to-collector load. The power output shown is the maximum "undistorted" output directly from the transistor and is, of course, a function of supply voltage, which in this case is 14 volts, the fully charged voltage of the "12 volt" systems. As is well known, and can be seen from this figure, the common emitter connection provides the highest gain, although it drops, rapidly at low loads and high power levels. The common base connection, while starting at low powers in

second place, ends up at the bottom with almost useless gain at 20 watt and higher levels. As a result it cannot be seriously considered for high power amplifiers unless relatively high supply voltages are used. The gain of the common collector, while starting at the lowest value, does not fall as rapidly as that of the other two connections with increasing power output.

Although the common emitter gain exceeds the common collector gain throughout the load range shown by these curves, the advantage of the common emitter circuit rapidly disappears at high power levels. When the effects of unbypassed emitter circuit resistance are taken into account, the gain of the common collector circuit can actually exceed that of the common emitter circuit at high power levels. Such emitter circuit resistance is needed for temperature stabilization and cannot be bypassed in a class B circuit. Temperature compensation in the base circuit can be used over a limited temperature range but is not a complete substitute. In the common collector circuit, the output transformer winding resistance, which is in series with the emitter, can provide the necessary stabilization.

Collector Characteristics

The collector characteristic family for the 2N176 is shown in Figure 2. This family of curves is well adapted for common base amplifier use. It will be noted that relatively even spacing between emitter current lines is maintained to at least 2 amperes, indicating a high degree of linearity with this connection, if driven from a constant current generator.

Because the common emitter connection has the attraction of providing considerably more gain than the common base, this connection has been preferred in most applications. The "common emitter" collector characteristic family is shown in Figure 3. This curve shows the relationship between the collector-to-emitter voltage and the collector current for various fixed values of base current. It can be seen that the lines of constant base current are not uniformily spaced as are the comparible lines in the common base characteristic, but decrease in spacing with increasing collector current. This is further illustrated in Figure 4, a curve of small signal collector-to-base current, beta (β), versus collector current. This curve essentially shows the rate of change of the spacing of the constant base current lines of Figure 3 with increasing collector current. Ideally, β should be a constant and a high value over the whole range, but it can be seen that there is an appreciable drop-off, primarily due to the loss in emitter efficiency, at the relatively high current (density) levels.[4]

Circuit Linearity

One is not, however, restricted to providing a current generator for the input of either this or any other transistor connection; in fact, the more usual case is an approximate match to the transistor input. In order to better see the effects of driving generator impedance on linearity of output along with a more complete comparison of the three transistor connections, curves of the input-output relation using a simulated high power amplifier have been taken for the three cases. The same supply voltage (14 V) and load resistance (6 ohms) were used in each case, the combination being such that a maximum output of 10 to 15 watts could be realized, depending on circuit efficiency. Other reasonable values of voltage and load will not appreciably change the shape of the curves. Figure 5 shows the curves for the common base circuit. It can be shown that the test circuit conditions very closely simulate actual AC operation so long as high quality transformers are used. The two curves on this figure, as well as for the following figures, very closely approximate a constant voltage generator (R_g = O) and a constant current generator (R_g = 10 ohms in this case*), thus giving the limiting conditions as far as the effect of generator impedance is concerned. Any practical circuit conditions will give a curve between these two. To facilitate comparison, voltage has been normalized so that the values for both curves coincide at approximately the full current swing. As previously mentioned, and as seen on this figure, the characteristic for a constant current generator is very linear over the entire input excursion with the only departure from a straight line being a slight curvature at the higher current values. The constant voltage generator curve, however, is far from linear because of the change in input impedance with current, indicating that this is obviously not the way to drive this type of amplifier.

Figure 6 shows the curves for the common emitter connection. The curve with a constant current generator (R_g = 5000 ohms) supplying the base is seen to have considerable curvature throughout most of the current range and is the result of the drop-off in , shown in Figure 4; an integration of this factor (β) with respect to Ic produces the same curve. The constant voltage generator curve appears similar to the corresponding curve of the common base connection, but the curvature at both low and high levels of input is greater. Although not shown, a curve with R_g = 40 ohms follows the 5000 ohm curve closely except near the origin where it is similar in shape to the zero resistance case. For any value of R_g the common emitter has greater non-linearity than the common base circuit with a constant current gen-

erator.

The curves for the common collector circuit are shown in Fig. 7. It will be noted that, for all practical purposes, the constant current generator (R_g 5000 ohm) curve is identical with the corresponding one for the common emitter current, both having considerable curvature. However, for the constant voltage generator, (R_g = O), extremely linear characteristics are obtained. In fact, one has to look closely to see the slight hook at the origin and the very slight curvature near the peak. This non-linearity is, however, far less than for any other circuit condition.

Thus, the basic advantages of higher power gain and lower distortion of the common collector over the common base circuit indicate, along with other design factors, th at the common base circuit should be dropped from further serious consideration

Cross-Over Distortion

Along with large signal linearity considerations, the manner in which the two transistors work together in the cross-over region is important. The transition from conduction of one transistor to the other must be smooth and linear in order to eliminate cross-over distortion. As indicated in Figures 5, 6 and 7, circuits operating with constant current generators have the advantage that they are very linear in the region near the origin. Consequently, a true class B amplifier could be designed with little or no cross-over distortion, exclusive of any transformer leakage reactance effects.

Cross-over distortion can take on different forms depending upon the transfer characteristic of the transistor and the operating conditions. As can be readily seen, an attempt to design a true class B amplifier using a common emitter amplifier with a constant voltage generator (see Figure 6) would result in considerable distortion of the type shown on Figure 8(a). The transfer characteristic of this distorted wave is shown on the left.

In order to eliminate this distortion, it is common practice to supply a small bias current to each amplifier section, thereby overlapping the low gain regions near cut-off. The result should then be a linear transfer characteristic that will provide an undistorted output, as seen in Figure 8(b). If, however, an excessive amount of standby, or no signal collector current, is used, there will be an appreciable region where both transistors are operated at full gain, actually providing class A operation for low and medium signal levels. But at high levels only the one transistor is providing power and as a result of this type of transition, a discontinuity in the amplifier transfer characteristics occurs as shown in Figure 8(c). The resultant distortion of a sine wave is also shown.

So it appears that there is an optimum standby current for minimum distortion over the full range of signal level. The actual value depends on the particular circuit conditions, and is usually under 10% of the peak current, and in some cases may be less than 1%. The transfer, or input-output characteristics of an amplifier, as shown in Figure 8, can be presented on an oscilloscope, and such a presentation has been found to be an accurate and rapid way of adjusting stand-by current.

Transistor Matching

It is obvious that the two gain elements in a class B amplifier should be identical in characteristics or a distorted output will result even though the individual units may have linear characteristics. It is rather common practice to closely match transistors in order to eliminate or greatly reduce this distortion; while this practice may be acceptable in the laboratory, it is rather costly for production use. In order to illustrate the effects of mismatch, curves of distortion versus mismatch for the common emitter and common collector circuits, are shown in Figure 9. The mismatch between the two amplifier transistors is in terms of β, the predominant gain determining factor, with other parameters like h_{11e} essentially equal. Mismatch ratios up to 2:1 are shown as many transistor manufacturers are using this ratio as a production tolerance of The distortion is shown in terms of the two predominant harmonics, the second and third, in order that the mismatch effects may be better seen, the second harmonic being proportional to the unbalance and the third being primarily a function of transistor nonlinearities. Optimum driver impedance (20 ohms base-to-base) and standby current were used for the common emitter amplifier, and a practical low limit value of driver impedance (60 ohms base-to-base) and standby current were used for the common collector amplifier. The upper half of the Figure 9(a) shows the results with the full output of 10 watts. The effects of the unbalance can readily be seen by the large rise in second harmonic for the common emitter amplifier. The internal feedback of the common collector circuit, however, reduces the effects of transistor mismatch and results in much lower distortion. It will be noted though, that in the case of the com-

* The transistor input impedance is a fraction of an ohm over most of the current range, thus being small compared to 10 ohms.

mon emitter amplifier, the third harmonic is larger than the second even for the 2:1 mismatch, and the amount of distortion due to unbalance is not large in comparison to the distortion due to the high level signal. However, if the input of these amplifiers is decreased to provide 1 watt output, as is shown in 9(b), the third harmonic drops to much lower values, but for the unbalanced common emitter amplifier, the second harmonic remains at nearly the same high value as at 10 watts. Thus, even at relatively low power levels, the distortion from this amplifier is high unless matched transistors are used, whereas the common collector can tolerate a rather large variation in transistor parameters and still provide relatively low distortion in its output.

Even if the transistors of an amplifier are balanced under a given set of conditions, temperature and supply voltage variations produce changes in β and other parameters that are not necessarily equal. Changes in β with time, or aging, occur on most present-day transistors. Thus, even if initially accomplished, it is difficult, if not impossible, to maintain any good degree of balance between a pair of transistors.

Inverse Feedback

The use of inverse feedback loops for reducing distortion caused by non-linearities, cross-over, and unbalance with tubes and some transistor amplifiers is common. Its use has been considered and tried with a number of power transistors in an attempt to minimize or eliminate some of the above problems with the common emitter connection, but this method was found to have a basic limitation. The β cut-off frequency on the 2N176 is generally 10-20 Kc, and other units have been found to be comparable, or in some cases considerably lower. As a result, the associated transistor phase shift in the middle and high audio frequency ranges is relatively large (i.e. 45° at β cut-off frequency). It is apparent then that high frequency instability and/or oscillation will occur if more than a few db of feedback are used around two or more stages.[7] If the high frequency phase shifts of the transformers are taken into account, instability is a problem with feedback around even one stage. Attempts to tailor the amplitude-phase characteristics of the loop in known manners greatly reduces the band width. Although the transistor phase shift adversely affects the operation and stability of the common collector circuit it can be shown to be considerably more serious for the case of common emitter amplifier with an external feedback loop.

Common Collector Amplifier Design

It has been shown that the push-pull class B common collector amplifier has low distortion when driven by a zero internal impedance generator. This may raise the question of the advisability of attempting to design a practical amplifier with this requirement, however, the problem is not too difficult to solve. A common collector driver stage with its inherently low internal output impedance provides an excellent driving source. This driver stage may be either a push-pull class B or a single-ended class A stage and derives its low internal output impedance from the negative feedback inherent in this configuration. The common emitter amplifier has a high output impedance, but could be considered as a driver if sufficient voltage feedback were used to lower this internal impedance to an acceptable value. However, it would then have essentially the same gain as the common collector and would have the problems inherent in an external feedback path such as transformer phase shift, and feedback circuit losses. The schematic of a practical two-stage amplifier using a single class A driver stage is shown in Figure 10.

Calculations based on the common collector transfer characteristic for a constant voltage driving generator ($R_g = O$) and the proper value of no signal bias, give a value of harmonic distortion on the order of 1/4% for an audio output power of 10 watts, assuming realizable output transformer efficiencies and transistor collector efficiencies. Since the lowest practical value of driver source impedance, including driver transformer losses, is on the order of 10-15 ohms (40 - 60 ohms base to base in a push-pull stage), the acutal output stage distortion is on the order of 1/2 to 1% at this output level. In order to eliminate cross-over distortion due to the very small departure from linearity in the transfer characteristic near the origin, a no-signal bias of about 20 milliamperes per transistor is required. This bias current is about 1% of the peak collector current

The design of the transformers for the circuit shown in Fig. 10 is an important factor in determining the performance of the amplifier. Their design is considerably different than any associated with vacuum tube circuitry. Since the output stage is operating with very low no-signal stand-by current, the coupling between the two halves of this stage must be very good if switching transients are to be avoided. To accomplish this, the two halves of the secondary of the driver transformer T_2 and the two halves of the primary of the output transformer T_3 are wound bifilar. The associated high interwinding capacities would cause serious

trouble in vacuum tube circuits, but here they are of little consequence because of the low impedance levels. The coupling between the primary and secondary windings of these transformers is of less importance since no feedback need be applied around them. If a dual battery power supply is permissible, the output transformer can be eliminated and ideal coupling achieved by means of a modified circuit directly coupling the loudspeaker to the transistors.

The driver transformer represents the most difficult design problem since its losses appear directly as an increase in the effective driving impedance of the driver stage, thus increasing the distortion in the output stage. The total effective winding resistance of this transformer must be kept as low as is consistent with the necessary primary inductance and turns ratio. In addition, within this limit, it is desirable to make the secondary resistance as low and the primary as high as practical to aid in stabilizing the operating points of the driver and output stages. The resistance of the secondary is used together with R_3 and R_4 to form the base bias bleeder for the output stage. The resistance of the primary winding is used as an emitter resistor in the stabilization of the driver stage. To aid in maintaining the low driving impedance, the primary to secondary turns ratio of T_2 should be as low as possible. The lowest value that can be used is determined by the less-than-unity voltage gain of the common collector output stage and the desirability of having reserve driving power. With the same supply voltage for both the driver and output stages, the minimum primary to one-half secondary voltage step up ratio must be slightly greater than the voltage loss in the output stage. The total secondary to primary turns ratio will thus lie in the range of 2.5 to 3.

The power input requirement of the driver stage is much lower than that of the output stage, therefore, the current gain and input impedance excursions of the driver are less. Thus, while the design requirements of the driver input transformer T_1 are similar to those of the driver output transformer, T_2, they are not nearly as severe. The generator impedance seen by the driver (R_g in Figure 10) should be low with respect to the input impedance of the driver stage and this can be accomplished either by the use of inverse feedback around a common emitter stage or the use of a common collector stage preceding the driver.

Common Collector Amplifier Performance

An indication of the performance of an amplifier of the type just described is shown in Figure 11. This figure shows a curve of total harmonic distortion vs. power output for this two-stage amplifier, using standard production Motorola type 2N176 power transistors. Using experimental type transistors having less β fall-off at high collector currents,[8] the distortion at all levels can be considerably reduced. The schematic of a complete four-stage amplifier having the same characteristics is shown in Figure 12. A push-pull driver stage is used to eliminate direct current saturation effects in the driver output transformer, thus reducing the required transformer size. However, this does not otherwise effect the overall performance. The power gain of this amplifier is 65 db with 14.2 db gain in the driver stage and 13.5 db gain in the output stage. The frequency response is flat within one db from 30 cps to 20,000 cps. The intermodulation distortion at 10 watts output is 2.3%, measured by the SMPTE method using frequencies of 40 and 4000 cps mixed 1:1. The no-signal current drain with a 14 volt supply is 140 milliamperes and the total drain with a sine wave audio output of 10 watts is 1.3 amperes. The over-all, (4 stage) amplifier efficiency at 10 watts output is about 55%. The no-signal current drain can be considerably reduced by operating the driver stages class B, however, this results in a slight increase in distortion.

A small portable public address amplifier using the circuit of Figure 12 is shown in Figure 13. This unit, together with its associated microphone, loudspeaker and enclosure makes up a high quality portable public address system that will operate for several hours from its self-contained battery. This unit has a preamplifier suitable for a high quality dynamic microphone and incorporates a frequency response shaping network that gives the best over-all acoustic response with the associated speaker and enclosure. A small, sealed nickel-cadmium storage battery powers the amplifier and is mounted on the same chassis together with a built-in charger for recharging the battery from a 115 volt 60 cycle AC power source. A close-up view of the 2N176 power transistor used in this amplifier is shown in Figure 14.

Conclusion

Consideration of all the basic factors influencing the design of a low distortion class B power amplifier leads to three possible circuit configurations; the common base, the common emitter with inverse feedback, or the common collector. At high power levels the common base has lower gain and higher distortion than the common collector, thus it can be eliminated as a choice. The higher power gain of the common emitter configuration is very attractive, however, when the inherent high distortion is reduced to the level of the common collector configuration with sufficient feedback, the advantage of high power gain disappears and the difficulty of achieving this amount of

feedback remains. Thus, the common collector configuration remains as the first choice and has been shown to produce excellent results in a practical amplifier design.

Acknowledgements

The authors wish to acknowledge the assistance of L. S. Korch and R. E. Hulse in making many of the measurements and in constructing the amplifier model.

Bibliography

1. Transistor Audio Amplifiers, (book), R. F. Shea, John Wiley & Sons, Inc., New York, N. Y., 1955
2. Class B Operation of Transistors, K. E. Loofbourrow, Electronic Design, July, August, October 1955
3. Transistor Electronics, (book) Lo, Endres, and Zawels, Prentice Hall, Inc., Englewood Cliffs, N. J.
4. The Variation of Junction Transistor Current Amplification with Emitter Current, W. M. Webster, Proc., I. R. E., Vol. 42, June 1954, p. 914
5. Electrical Characteristics of Power Transistors, A. Nussbaum, Proc., I. R. E., Vol. 43, March 1955, p. 315
6. Some Aspects of the Design of Power Transistors, M. H. Fletcher, Proc., I. R. E., Vol. 43, May 1955, p. 551
7. A 20-Watt Transistor Audio Amplifier, H. C. Lin, RCA Laboratories LB-1012
8. Recent Advances in Power Junction Transistors, B. N. Slade, RCA Laboratories LB-1010

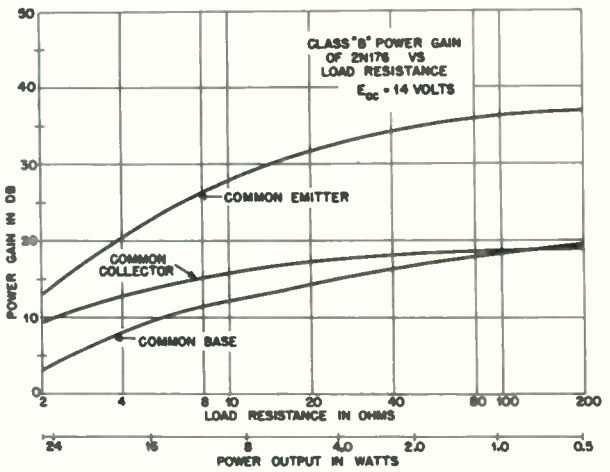

Fig. 1
Power gain vs load resistance

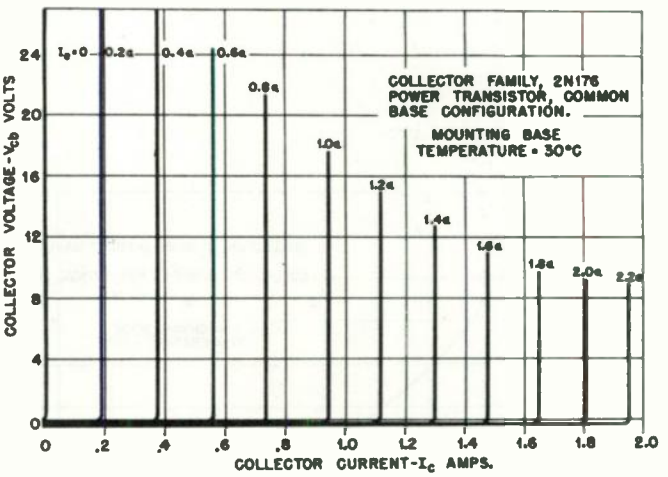

Fig. 2
Common base collector characteristics

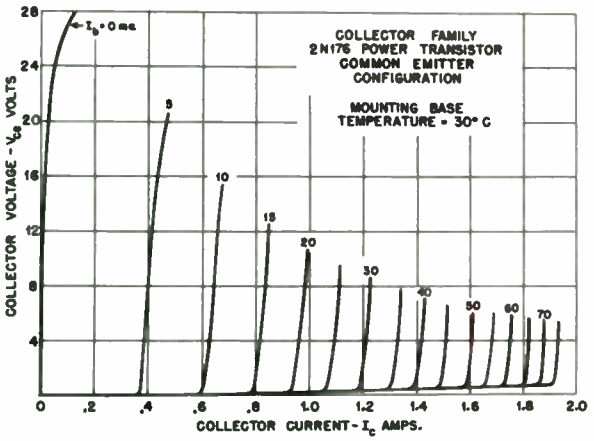

Fig. 3
Common emitter collector characteristics

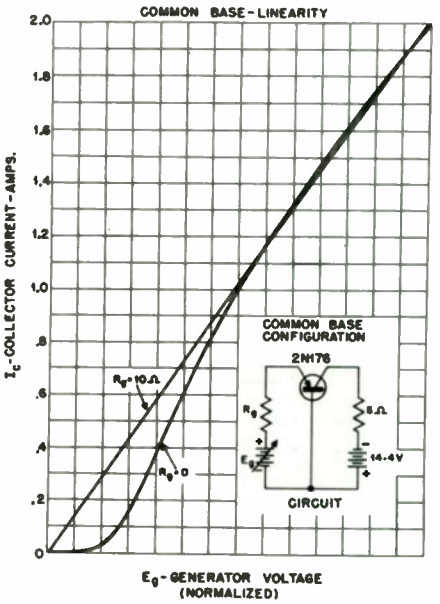

Fig. 5
Common base transfer characteristics

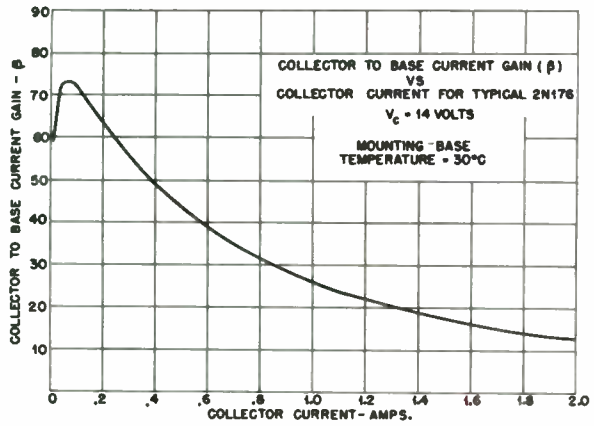

Fig. 4
Common emitter current gain vs
collector current

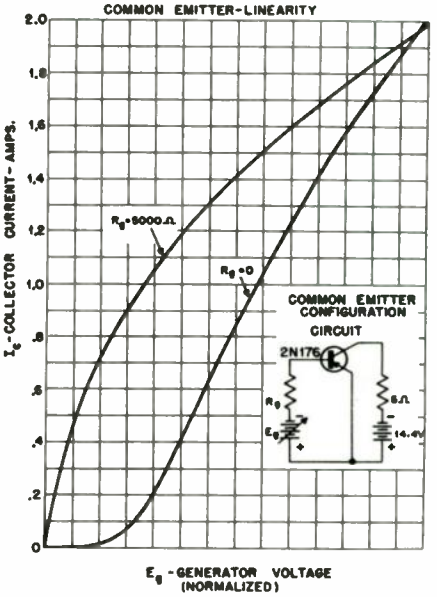

Fig. 6
Common emitter transfer characteristics

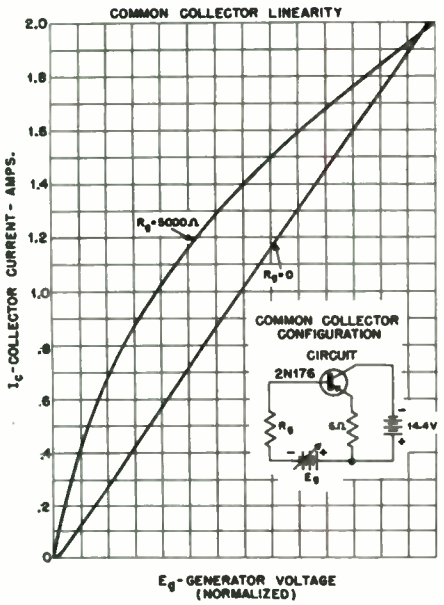

Fig. 7
Common collector transfer characteristics

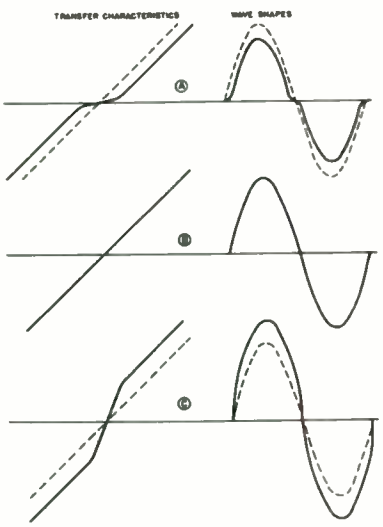

Fig. 8
Class "B" amplifier cross-over distortion

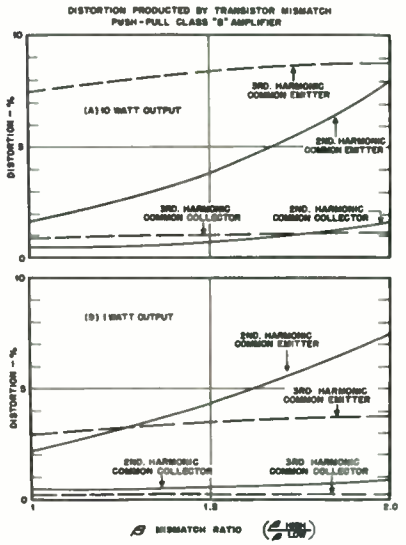

Fig. 9
Transistor mismatch effects on distortion

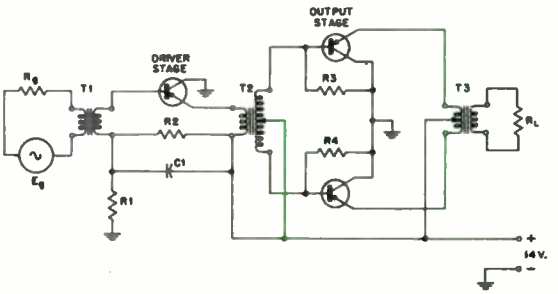

Fig. 10
Class "B" common collector power amplifier & driver

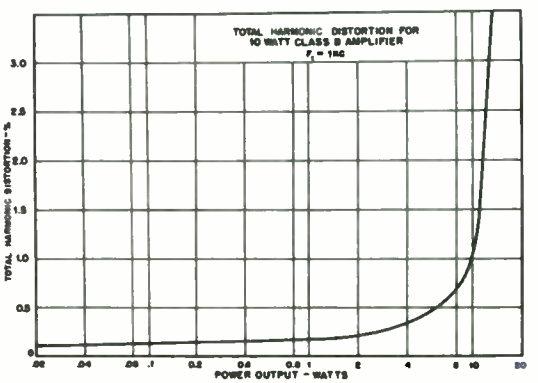

Fig. 11
Total harmonic distortion for 10 watt class B amplifier

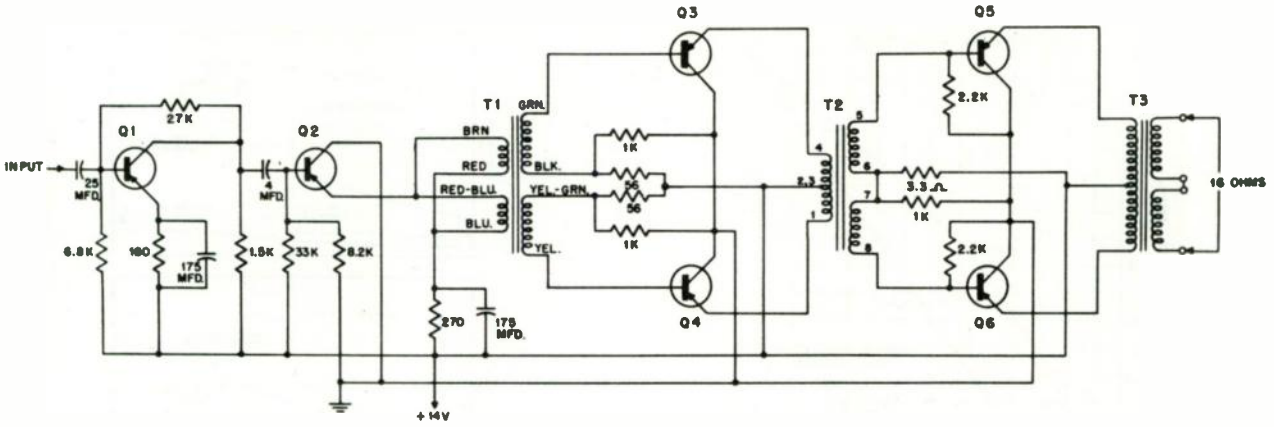

T1- INTERSTAGE TRANSFORMER (CHICAGO-STANDARD 24861)
T2- DRIVER TRANSFORMER (CHICAGO-STANDARD 25138)
T3- OUTPUT TRANSFORMER (CHICAGO-STANDARD 24246)

TRANSISTOR TYPES
Q1 - XN2
Q2 - XN6
Q3,4,5,6 - 2N176

Fig. 12
Transistorized high-fidelity 10 watt amplifier

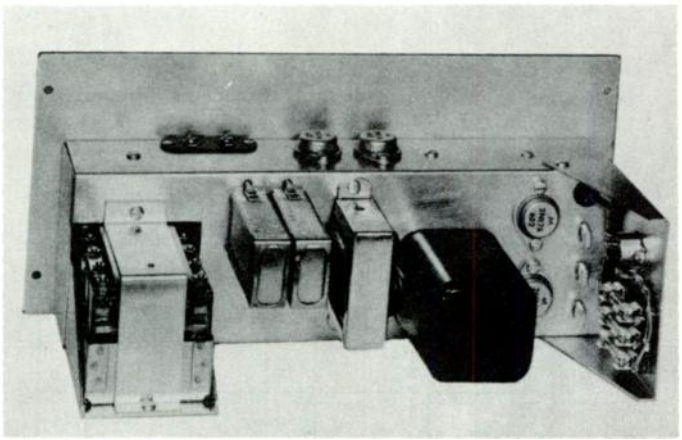

Fig. 13
10 watt transistor amplifier with battery supply

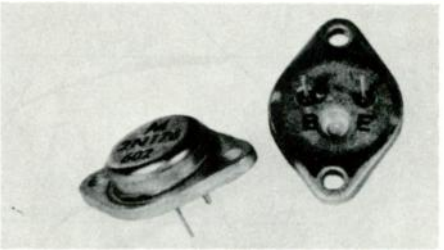

Fig. 14
2N176 power transistors

PERFORMANCE OF THE "DISTRIBUTED PORT" LOUDSPEAKER ENCLOSURE

Adelore F. Petrie
Audio Products Engineering
Television Department
General Electric Company
Syracuse, New York

Summary

There is a short discussion of the requirements of a loudspeaker enclosure followed by a description of the "Infinite Wall" type of baffle. Frequency response and power output curves are presented for a typical loudspeaker in the "Infinite Wall" baffle. A short description of the "Distributed Port" enclosure is given, followed by performance curves on three designs. A brief theory section containing impedance curves and electrical analogs is added for those who desire more detailed information.

* * *

The subject of loudspeaker enclosures is a very controversial subject. This controversy is due to the complexity of the subject and to its rather widespread interest among experimenters.

The complexity of the subject becomes apparant when analysis or synthesis of enclosures is attempted. First of all, it is necessary to work in three systems: Electrical, Mechanical, and Acoustical; and to make the necessary transformations from one system to another. As if this were not enough, enclosures which utilize back radiation result in a three terminal pair network: 1 input and 2 outputs.

This paper does not intend to provide sufficient information to design a "Distributed Port" loudspeaker enclosure, although readers schooled in acoustics can extract this information from the theory section. The great majority of readers will profit more from data which will allow them to correctly utilize the features of this system. For this reason, only a description of the performance of the enclosure will be given, along with sufficient theory for a clear evaluation of its performance.

Method of Attack

First, the necessity of loudspeaker enclosures and the criteria by which they should be judged will be explained. Next, the performance of a typical loudspeaker in a basic type of enclosure will be discussed. And last, a comparison will be made between the performance of the loudspeaker in a "Distributed Port" enclosure and that in the basic enclosure.

Curves showing the response and distortion of loudspeaker enclosures can be very misleading. For this reason, great care was taken in plotting the curves accompaning this article. Room effects were carefully eliminated; and hum, noise, and distortion were prevented from giving false readings on the frequency response plots. Less efficient loudspeakers and/or enclosures will obviously show less distortion in the output for the same power input. For this reason, distortion curves in this article are always plotted as a function of power output (sound pressure). The corresponding voltage input is merely shown to give an indication of driving requirements (amplifier output).

Requirements of a Loudspeaker Enclosure

There are three main requirements that any loudspeaker enclosure should fulfill:

1. Prevent interference between the front and back radiation from the loudspeaker.
2. Improve low frequency response.
3. Improve low frequency power handling ability.

Interference

A loudspeaker acts as a di-pole radiator. The sound coming from the back of the loudspeaker is 180° out of phase with the sound coming from the front. This means that there will be cancellations and additions at various frequencies when a loudspeaker is operated without some sort of baffle. The amount of cancellation or addition depends on the difference in distance which the sound has to travel when coming from the back and front of the loudspeaker, and the frequency involved.

In other words, a loudspeaker acts like the piston in an air pump. Without some sort of baffle around the piston (loudspeaker), the air displaced in front of the piston will merely circulate around to the back without building up any useful pressure. Figure (1) shows what happens to the low frequency response of a good 12" loudspeaker when it is operated without any baffle.

Response

It is desirable that the low frequency response of a loudspeaker system extend down to the lowest frequency that is contained in the program material normally fed into it. It is also necessary that the response be smooth so that tonal balance of the program is maintained. Sharp dips or peaks in response curves indicate points of high distortion and/or poor transient response. A gentle slope in bass response is permissable since this may be offset by additional bass boost in the driving amplifier. However, this boosting wastes power and may severely limit power output.

Power Handling Ability

It is not enough for a loudspeaker to have smooth response and wide range. Due to the fact that the ear is insensitive at low frequencies, a loudspeaker system must also have sufficient power handling ability to make the frequencies it reproduces audible to the listener. For example, sounds at 50 cycles per second must be 52 db louder than those at one thousand cycles per second in order to be heard. Therefore, it is necessary to check the low frequency acoustic power handling ability (sound pressure or intensity - not power input) of a loudspeaker system at a tolerable level of distortion to see if it is sufficient for the application.

Figure (2) shows the frequency and volume ranges of speech and music. The solid line indicates the limits of normal hearing. The upper boundary of the solid line indicates the level at which sound becomes painful. The lower boundary indicates the level below which sounds become inaudible. In order to be adequate, a reproducing system for music must be capable of the frequency and volume range included in the shaded area.

The acoustic power handling ability of a loudspeaker is limited by the maximum sound pressure that the loudspeaker can produce without running into distortion. At low frequencies, this pressure is determined only by the maximum distance that the loudspeaker cone can move before it is limited mechanically or magnetically. It makes no difference in this discussion whether the cone movement is limited by magnetic distortion in the flux gap or mechanical distortion in the cone suspensions. The important fact is that every loudspeaker has some definite maximum cone movement. Because the acoustic power handling ability depends only on cone excursion, it is interesting to note that the stiffness of the cone suspensions or the fundamental cone resonance of the loudspeaker has little effect on the power handling ability of the loudspeaker system (providing the linearity of the stiffness is the same).

The "Infinite Wall" Baffle

The previously mentioned interference problems may be completely eliminated by simply preventing the sound from the back of the loudspeaker from reaching the front. One means of doing this would be to mount the loudspeaker in a hole in a large wall, see Figure (3). This is known as an "Infinite Wall" type of enclosure. Because this is a simple enclosure which is comparatively easy to analyze, and actually may be realized in practice; it can be used as a standard of comparison when evaluating the performance of other types of enclosures.

Interference

With this type of baffle, obviously there is no interference between the front and back radiation - they are separated by a wall, infinite in size.

Response

The low frequency response of a loudspeaker in this type of baffle depends on the size of the loudspeaker, the efficiency of the loudspeaker, the damping factor of the amplifier driving the loudspeaker, and the low frequency resonance of the loudspeaker in the baffle. Figure (3) shows the response of a typical high quality 12" loudspeaker in this type of enclosure.[1]

This particular loudspeaker had a fundamental resonance of 60 cycles per second when mounted to the wall baffle. Note that this fundamental resonance was not apparent in the response curve. Instead of a resonant rise, the response was gently sloping off in the region around resonance. This is characteristic of all high efficiency loudspeakers when driven from a feedback amplifier or other low impedance source. The electromagnetic coupling is so great that the amplifier shunts the resonant circuit, causing it to be overdamped (low "Q"). This makes for good transient response, but requires some sort of compensation to bring the low frequency response up to where it should be.

Figure (4) shows the effect of efficiency on the low frequency response of a loudspeaker in an "Infinite Wall" type of baffle. The efficiency of this loudspeaker was varied by de-magnetizing it in steps and thus plotting a family of response curves.

Curves (a) and (b) show the over-damped case, curve (c) shows the critically damped case, and curve (e) shows an extreme under-damped case. Assuming the same type of construction, each time the high frequency response was reduced by 3db it was equivalent to reducing the magnet weight to one-half. This is the reason why loudspeakers of high efficiency often seem to lack bass response unless the bass end is compensated in some way (either in the amplifier or the enclosure).

Power Handling Ability

Figure (5) shows the acoustic power handling ability (P_a) of the above loudspeaker in the "Infinite Wall" baffle for five and ten percent harmonic distortion.[2]

Figure (5) also shows the corresponding electrical input to the voice coil (E_{vc}). Note that the power at higher frequencies is limited, not by distortion, but by the maximum heat dissipation rating of the voice coil.

- - -

[1] In order to eliminate the amplifier from this discussion, the frequency response curves shown in this paper are plotted with a constant voltage input to the loudspeaker.

[2] The average sound pressure that this same loudspeaker system can produce throughout a typical living room is approximately 3 db below the level shown here (which is measured 18" in front of the loudspeaker in a "dead" room).

Note also that the electrical input to the loudspeaker must be greatly reduced at very low frequencies to prevent driving the loudspeaker into severe distortion. Rumble coming from the turntable and/or the record will often drive a loudspeaker into distortion, even though the rumble itself is too low in frequency and amplitude to be heard by the listener. To eliminate this difficulty it is usually desirable to have a sharp cut off low frequency filter somewhere in the system.[1]

If the loudspeaker in figure (5) were less efficient it would handle more electrical input at low frequencies; however the maximum acoustic output at low frequencies would be the same, and due to lower efficiency, the maximum acoustic output would be less in the region where the power is limited by the voice coil dissipation.

The "Distributed Port" Enclosure

The "Distributed Port" enclosure is a reflex type of enclosure in which the back radiation is added to the front radiation at low frequencies. By this means it improves both the low frequency response and the power handling ability. It differs from most reflex enclosures in that the response and impedance characteristics are controlled by the addition of a specific amount of acoustic resistance.

Interference

There is no cancelling between the front and back radiation at high frequencies due to the fact that the reflex action has an inherent high frequency cut off of back radiation.

In the useful low frequency range a controlled amount of back radiation is added to the front radiation, increasing the output and power handling ability.

At very low frequencies (usually sub-audio) there is cancellation between the front and back radiation and air is merely pumped from the front to the back of the loudspeaker. This characteristic is common to all loudspeaker enclosures which utilize both front and back radiation, and makes it even more desirable to use a "rumble" filter such as mentioned above.

Low Frequency Response

Figure (6) shows the low frequency response of a typical high quality loudspeaker in three "Distributed Port" enclosures. Also shown, is the "Infinite Wall" response for comparison. Note the large increase in output and the smoothness of response at low frequencies, where the reflex action occurs. Adding the correct amount of damping in this design matches the impedance of the enclosure to that of the loudspeaker. This means maximum power output from the enclosure and broad-band response (low "Q"). Putting this damping in the form of a "Distributed Port" - a fixed number of holes spread over a definite area- assures the permanent accuracy of the damping.

Power Handling Ability

Figures (7), (8), and (9) show the acoustic power handling ability (P_a) of these same "Distributed Port" enclosures. Note the great increase in the undistorted sound pressure that these enclosures are capable of delivering at low frequencies. Note that, at some frequencies, the larger enclosures will handle less voltage input (E_{VC}) than the smaller ones, although the sound pressure (P_a) produced by the larger enclosures is greater. This is due to the fact that they are more efficient than the smaller enclosures at these frequencies.

Construction Data

The 6 cubic foot enclosure is available commercially as the GE A1-406 loudspeaker enclosure. Dimensions for constructing "Distributed Port" enclosures are given in figure (10), views (a) thru (c).

The A1-400 loudspeaker features a handsomely styled protective front plate, making the use of a grille cloth unnecessary in many installations. To take full advantage of this feature, the speaker should be mounted on the front surface of the speaker mounting board. If a grille cloth is required for styling purposes, the material used must not impair the transmission of high frequencies. Suitable materials are woven plastic or fabric, having a light porous weave. The grille cloth should be mounted in a manner which will not allow vibration of the cloth against the cabinet. When grille cloth is used, the speaker is attached to the rear surface of the speaker mounting board.

Use plywood at least ½" thick for the 3 and 6 cubic foot sizes and 5/8" thick for the 10 cubic foot size. Line back, bottom and one side of the 3 cubic foot enclosure with 1" of fiber glass or similar soft acoustic material. Line bottom and two back sides of the 6 and 12 cubic foot enclosures with 2" of fiber glass or equivalent. Glue all joints. Make front or back removable, if speaker is to be mounted on the inside surface of the mounting board. The 1 X 2 brace is to keep the speaker from setting up vibrations in the front panel, which will subtract from the low frequency output.

The shape of the enclosures may be altered to suit the needs of the user as long as the internal volume and the configuration of the front panel are maintained.

Loudspeaker Characteristics

The results presented in this paper are accurate only when the loudspeaker used has characteristics which are similar to those of the

- - -

[1] The GE A1-901 record filter is an example of such a filter.

GE A1-400 loudspeaker. However, the general characteristics indicated in this paper are typical of all loudspeakers and must be kept in mind when choosing or designing a loudspeaker, or enclosure, or associated equipment.

The important characteristics of the A1-400 "woofer" for enclosure design are given below:

Nominal Diameter	12 inches
Effective Cone Diameter	26 centimeters
Free air resonance	60 cycles/second
Mass of moving system (exclusive of air load)	25 grams
BL (Force Constant)	12,000,000 gauss cm.

Similar types are the GE 1201-A and 1203-A loudspeakers.

Using loudspeakers of larger diameter than 12" in these "Distributed Port" enclosures will, in general, improve the power handling ability but result in a poorer low frequency response. A smaller loudspeaker will give correspondingly better low frequency response and poorer power handling ability. A larger loudspeaker should not be used with the 3 cubic foot enclosure and a smaller loudspeaker should not be used with the 10 cubic foot enclosure.

Room Effects

It should be noted that the curves presented in this paper were taken under conditions which did not include reflections and resonances usually found in the listening environment. This is desirable because the effect of the room on the performance of a loudspeaker system is usually the same regardless of the system used. These same effects also color the music as the listener hears it when live performers are in the room, and therefore are not necessarily harmful.

Every hard object of appreciable size in a room sets up reflections. The most important objects to be considered at low frequencies are the walls, ceiling and floor. Standing waves are set up in a room at frequencies where the distance between parallel surfaces is equal to $\frac{1}{2}$, 1, $1\frac{1}{2}$, 2, etc. wave lengths. These standing waves always build up high pressure points at the walls which cause them. The impedance match between the loudspeaker and the room is best at these high pressure points. For this reason, the best place for a loudspeaker system is the corner of the room where all walls meet, and efficient coupling is made to all room resonances.

In most rooms, the only resonance which might be objectionable is the standing wave between the floor and ceiling which usually occurs between 60 and 80 cycles per second. Coupling to this resonance may be reduced by placing the loudspeaker enclosure in the corner, but off the floor (half way up the wall is best). This is usually objectionable appearance wise. An equally good solution is to damp the resonance by applying sound absorbing material to the ceiling. To absorb these frequencies may require padding up to 8" thick, or hung 8" below the true ceiling.

Figure (11a) shows the response of a 6 cubic foot "Distributed Port" enclosure placed in a corner of a live room. Curve (b) shows the response of a typical back loaded folded corner horn enclosure of equal size under the same conditions. This figure was originally made to answer those who feel that horn enclosures have a "corner" on response in the corner of a room. However, it shows very nicely the effects of room resonances on two different loudspeaker enclosures.

THEORY

In order to obtain a clear understanding of the performance of loudspeaker enclosures it is necessary to delve into the theory behind their operation.

Note. The equivalent circuits in this section show all of the elements as they appear when reflected back into the electrical impedance of a typical high quality 12" loudspeaker. The values given are approximate only, and are intended primarily to indicate the order of magnitude of the various elements.

Infinite Wall Baffle

Figure (12) shows the low frequency equivalent circuit of a typical high quality 12" loudspeaker when placed in an "Infinite Wall" baffle. (a) shows the circuit broken down into its electrical, mechanical and acoustical sections where:

- R_{vc} = Electrical Resistance of the voice coil.
- Z_m = Motional Impedance of the loudspeaker system.
- R_s = Mechanical Resistance of the cone suspensions.
- C_s = Compliance of the cone suspensions.
- M_c = Effective mass of the moving system.
- R_{a1} = Resistive component of the air load on the front of the cone.
- M_{a1} = Mass component of the air load on the front of the cone.
- R_{a2} = Resistive component of the air load on the back of the cone.
- M_{a2} = Mass component of the air load on the back of the cone.

The acoustic output is represented by the power in the radiation resistances (R_{a1}) and (R_{a2}). The cross over in the acoustical part of the diagram indicates that the back radiation is 180° out of phase with the front radiation. (b) shows the combined equivalent circuit. In this case there is no interference between the front and back radiation and therefore the phase considerations may be neglected. (c) shows the simplified circuit for equivalent output and response at low frequencies.

$$\left[R_{at}' = R_{at} \left(\frac{M_{at}}{M_T} \right)^2 \right]$$

Figure (13) shows the impedance curve of a loudspeaker with characteristics similar to those shown in the simplified circuit of Figure (12c). Well above resonance the motional impedance (Z_m) is low and capacitive (mass controlled). In this region the current flowing thru the output resistor is relatively constant, and therefore the frequency response in this region is flat. Well below resonance the motional impedance is again low, but inductive (compliance controlled). In this region, the current through the output resistance is reduced to $\frac{1}{4}$ each time the frequency is reduced to $\frac{1}{2}$ its original value. This causes the response well below resonance to slope off at approximately 12 db per octave. At resonance, the motional impedance is high and resistive. This causes a constant voltage to appear across the mechanical impedance in this region, which in turn causes the current thru the output resistance, and hense response, to slope off at the rate of 6 db per octave towards low frequencies. The extent of the region around fundamental resonance in which the loudspeaker is resistance controlled depends on its efficiency. This effect has already been shown in Figure (4).

Reflex Enclosure

Figure (14) shows the equivalent circuit of a loudspeaker mounted in a 6 cubic foot reflex enclosure where:

- R_{a1}' = Resistive component of the air load on the front of the cone (combined and simplified as above).
- C_v' = Compliance of the volume of air inside of the enclosure.
- R_{a2}' = Resistive component of the air load at the port as reflected back to the loudspeaker cone.
- M_p' = Total effective mass at the port as reflected back to the loudspeaker cone.

The total output is obtained by adding the power due to direct radiation (R_{a1}') and that due to port radiation (R_{a2}') as vectors. The crossed lines again indicate 180° phase shift.

It can be seen that the reflex enclosure is a high "Q" series resonant circuit shunting the mechanical impedance. At its resonance the enclosure presents such a low impedance that most of the output comes from the port of the enclosure (R_{a2}') and very little is supplied by direct radiation from the speaker (R_{a1}').

If there were some way to reduce the "Q" of the enclosure resonance, a better impedance match could be made to the loudspeaker, resulting in smoother response and greater output at enclosure resonance. The simplest means of doing this is to place some acoustic damping material across the port of the enclosure. The main problem here is mechanical: to add a controlled amount of acoustic resistance that will not change with time. The "Distributed Port" design is one accurate solution to this problem.

"Distributed Port" Enclosure

Figure (15a) shows the equivalent circuit of a 6 cubic foot "Distributed Port" enclosure where:

- C_v' = Compliance of the volume of air inside of the enclosure.
- R_p' = Damping due to distributed port as reflected back to the loudspeaker cone.
- M_p' = Mass due to distributed port as reflected back to the loudspeaker cone.
- R_{a2}' = Resistive component of the air load at the port as reflected back to the loudspeaker cone.
- M_{a2}' = Mass component of the air load at the port as reflected back to the loudspeaker cone.

Breaking up the port into a series of holes will introduce acoustic resistance, although it also increases the mass load. However, it is possible to compensate for the added mass by spreading the port over a larger area and thus reducing the air mass load a like amount. Figure (15b) shows the same circuit with the mass loads combined. $\left[R_{a2}'' = R_{a2}' \left(\frac{M_{a2}'}{M_p''}\right)^2\right]$

Thus, we have the same circuit as the reflex enclosure except that a controlled amount of resistance has been added.

Figure (15c) shows the complete equivalent circuit combined with the loudspeaker.

Figure (16) shows the impedance curve of a typical high quality 12" loudspeaker in a 6 cubic foot "Distributed Port" enclosure. Note that there are three resonances: Two high impedance shunt resonances separated by a low impedance series resonance. The low impedance resonance (which in this case appears at 50 cycles per second) is the enclosure resonance mentioned above. At this frequency the port output is 90° out of phase with the speaker output and the two outputs add as right angle vectors. Above enclosure resonance, the enclosure appears as a compliance (inductive in this analogy) and resonates with the mass at the speaker cone (70 cycles per second in this case). At this resonance the port output is in phase with the speaker output but considerably reduced in level; and serves to fill in the response between enclosure resonance and the frequency at which the speaker attains full output. Below enclosure resonance, the enclosure appears as a mass, and with the speaker mass resonates with the compliance of the speaker suspensions. At this resonance the port output is 180° out of phase with the speaker output, producing almost perfect cancellation. This resonance appears at 35 cycles in Figure (16).

The dashed line in Figure (16) indicates the impedance curve of a reflex enclosure. Note the change in impedance at enclosure resonance (50 cycles per second). This shows that the addition of damping in the "Distributed Port" design has reduced the shunting effect, and hence the "Q" of enclosure resonance.

Conclusions

1. Loudspeakers are capable of handling very little input at extremely low frequencies. If the full capabilities of a loudspeaker are to be realized, low frequency rumble and noise must be eliminated from a reproducing system.

2. High efficiency usually means less, rather than more bass response, unless a proper enclosure is used.

3. The use of a "Distributed Port" enclosure will improve the bass response and increase the low frequency power handling ability of moderately efficient loudspeakers similar to those mentioned in the text.

4. The use of a "Distributed Port" greatly complicates the design of an enclosure. However, this also makes it possible to optimize the design for range, response, or power handling ability in a given size.

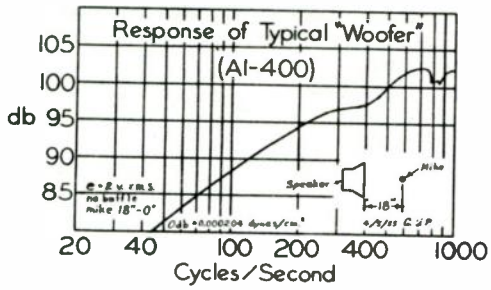

Fig. 1
Response of a typical high quality 12" loudspeaker without any baffle.

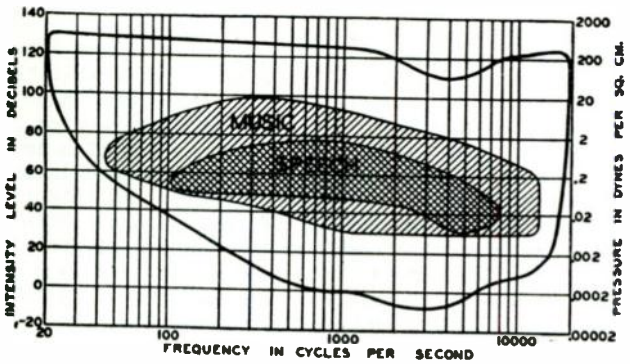

Fig. 2
Frequency and volume ranges of speech and music. The solid line depicts the boundaries of normal hearing, that is, the upper and lower limits of intensity and frequency. (From Bell Laboratories Record, June 1934.)

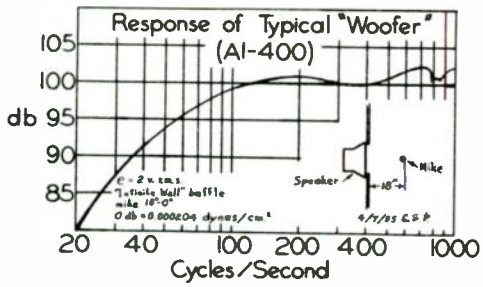

Fig. 3
Response of a typical high quality 12" loudspeaker in an "Infinite Wall" type of baffle.

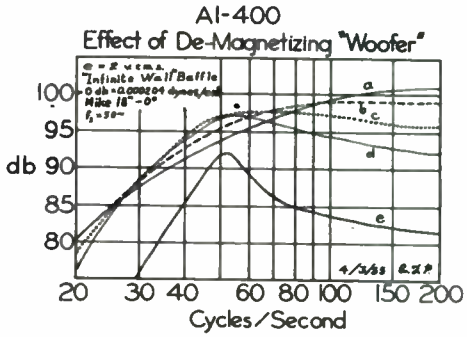

Fig. 4
Effect of magnet size on the response of a typical high quality 12" loudspeaker. (Made by de-magnetizing the loudspeaker in steps.)

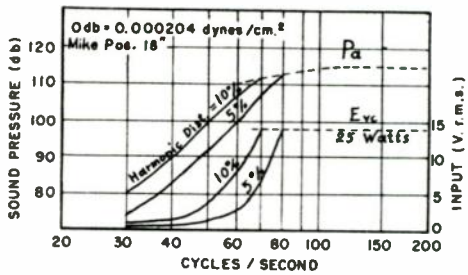

Fig. 5
Power handling ability of a typical high quality 12" loudspeaker in an "Infinite Wall" type of enclosure.

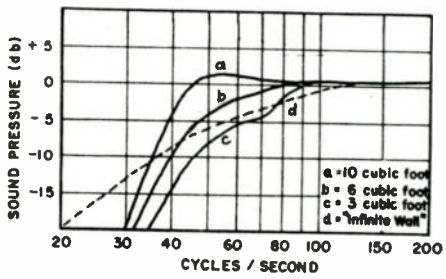

Fig. 6
Frequency response of a typical high quality 12" loudspeaker in several "Distributed Port" enclosures. "Infinite Wall" response shown for comparison.

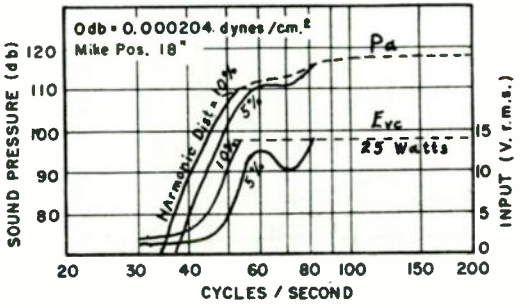

Fig. 7
The acoustic power handling ability of a typical high quality 12" loudspeaker in a 3 cubic foot "Distributed Port" enclosure.

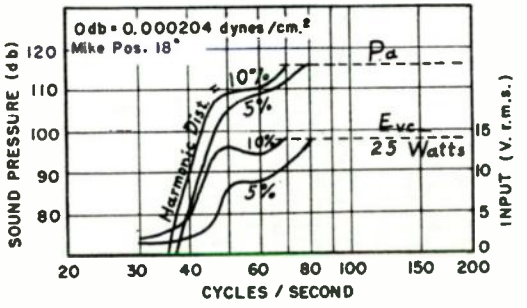

Fig. 8
The acoustic power handling ability of a typical high quality 12" loudspeaker in a 6 cubic foot "Distributed Port" enclosure.

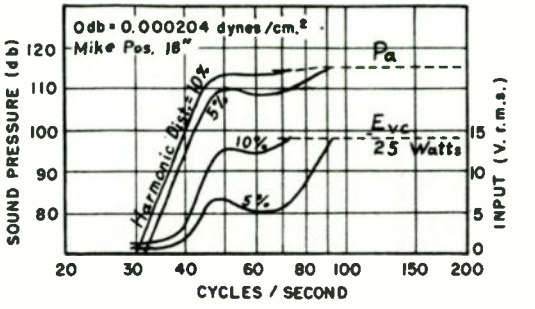

Fig. 9
The acoustic power handling ability of a typical high quality 12" loudspeaker in a 10 cubic foot "Distributed Port" enclosure.

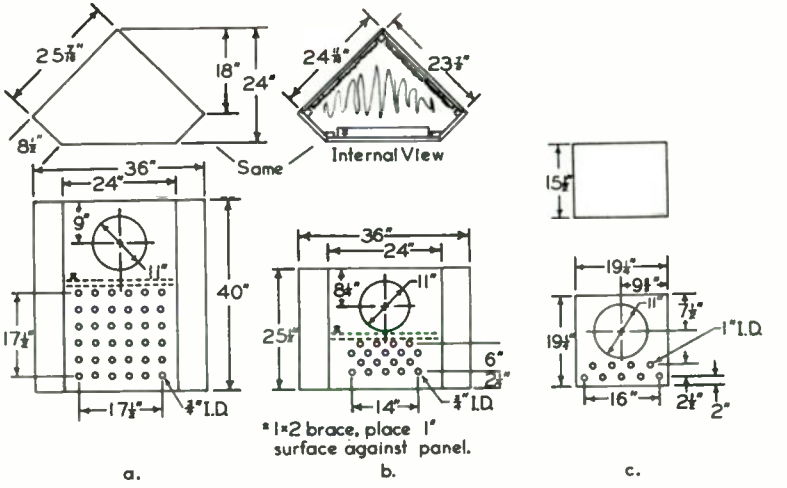

Fig. 10
Sketches of three "Distributed Port" enclosures:
(a) 10 cubic foot enclosure
(b) 6 cubic foot enclosure
(c) 3 cubic foot enclosure

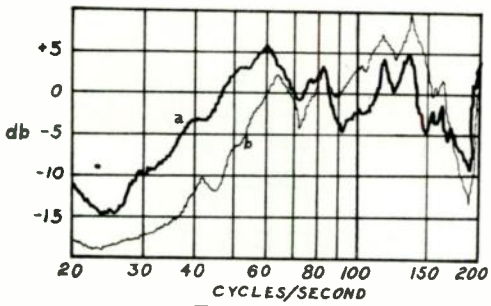

Fig. 11

(a) Response of a typical high quality 12" loudspeaker in a 6 cubic foot "Distributed Port" enclosure in the corner of a "live" room, illustrating the effect of standing waves and reflections on response. (b) Response of a typical back loaded folded corner horn enclosure of equal size under the same conditions.

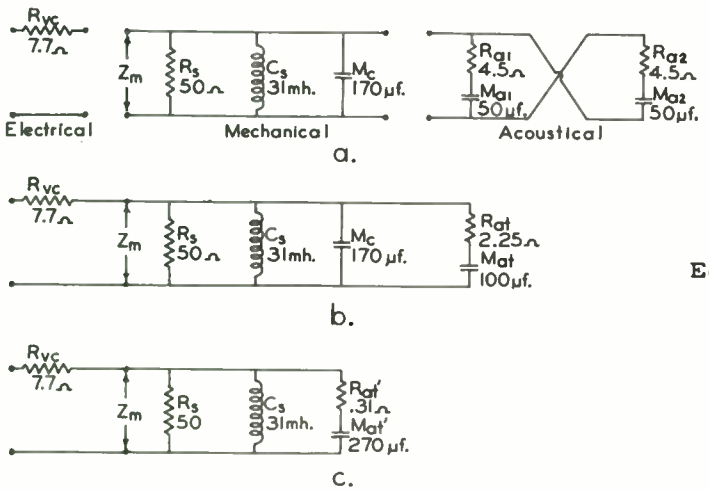

Fig. 12

The low frequency equivalent circuit of a typical high quality 12" loudspeaker in an "Infinite Wall" baffle. (a) Broken down into its components, (b) Combined, and (c) simplified.

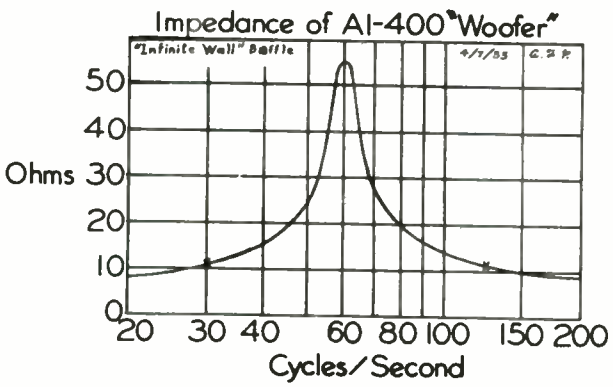

Fig. 13

Impedance curve of a typical high quality 12" loudspeaker in an "Infinite Wall" baffle.

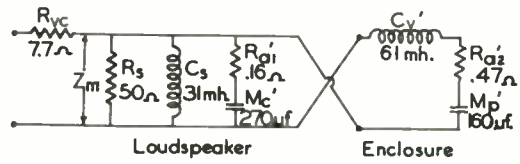

Fig. 14

Equivalent circuit of a typical high quality 12" loudspeaker in a reflex type of enclosure.

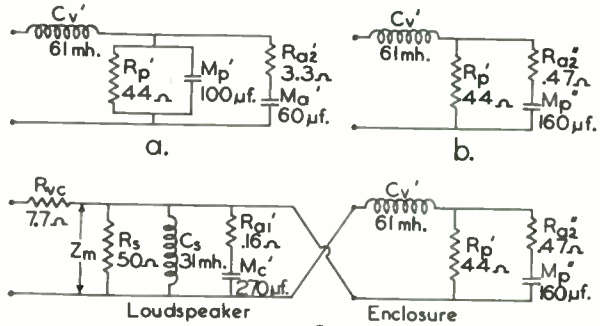

Fig. 15

Equivalent circuit of a "Distributed Port" enclosure. (a) Air load and port separated. (b) With mass loads combined. (c) Combined with the loudspeaker.

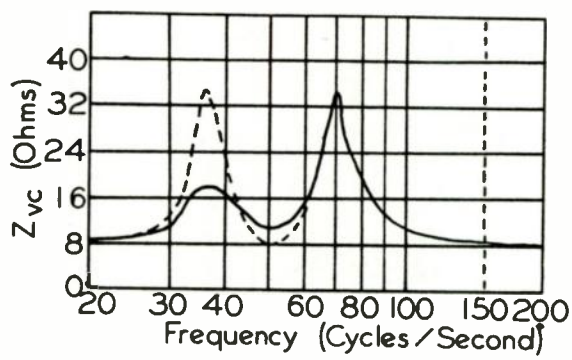

Fig. 16

Impedance curve of a typical high quality 12" loudspeaker in a 6 cubic foot "Distributed Port" enclosure. (Dashed line indicates impedance of similar reflex enclosure without damping).

A PHONOGRAPH SYSTEM FOR THE AUTOMOBILE

Peter C. Goldmark
CBS Laboratories, a Division of
Columbia Broadcasting System, Inc.
New York, N. Y.

As the automobile became one of the most prized and necessary possessions of almost every American family, the question was frequently asked why, with the amount of time spent driving, recorded music and speech is not available in the car?

The question is quite proper because driving nowadays in modern cars is so effortless that the driver's attention to road hazards is almost the only exertion required. It is a proven fact that listening to the radio while driving does not interfere with one's ability to drive safely; as a matter of fact it contributes towards the driver's alertness by preventing drowsiness. It would thus seem quite natural to provide the driver with a system of recorded sound, giving him a choice of programs most suited to the environment and his interests. Thus the CBS Laboratories and the Chrysler Corporation established a joint program in the area of recorded sound for the automobile with the purpose in mind of introducing to the motoring public this new medium if the result of the studies and subsequent technical development should warrant it.

The successful conclusion of this program has recently been announced to the public by the Chrysler Corporation. Under the name of "Highway Hi-Fi", Chrysler is making available in all their 1956 models (Imperial, Chrysler, De Soto, Dodge, Plymouth) a special automobile phonograph which is mounted under the dash and uses a 7" extra long playing record.

Prior to tackling this specific development by the CBS Laboratories, other methods were first examined. Everything else being equal, choosing a system already used in the home was considered to be a desirable goal. First the pre-recorded magnetic tape was investigated since it appeared to be the most logical system for the car. The tape, for instance, could meet such basic requirements as very long play - up to two hours per reel - if double track with a speed of 3.75"/sec. were used and if size of reel is of no consequence. The long, uninterrupted play is an important factor in the car because driving offers the opportunity to listen to entire musical works, books, stories for the young and grown-ups, travelogues, etc., and even the person who makes relatively short trips to and from his work (or shopping) can listen to recorded books or musicals, stopping the instrument when leaving the car and resuming listening when entering it again.

Another advantage of the tape system is that it can be made to resist without undue complications, shocks, jars and vibrations occurring in the automobile.

Unfortunately the tape system has many disadvantages. The cost of the magnetic tape itself, compared with the cost of record material, is much higher. The customary method of threading the tape would not be practical in the automobile, and so a self-threading cartridge with automatic take-up mechanism would be required for each individual reel of tape. The cost and the required storage space of these recorded works could then be quite excessive. There are still other disadvantages to consider. For instance, a particular section on a recorded tape would be quite difficult to spot unless some fairly elaborate and costly system were employed. Also the electrical output of the tape being low and requiring considerable equalization would necessitate the use of a pre-amplifier as part of the tape machine. Last but not least, the public has been accustomed to the use of records to such an extent that, unless some extremely foolproof and simple method were found to play tape, considerable inertia would be encountered from the very outset against large-scale use of tape.

The next medium which was investigated dealt with phonograph records. The 78 rpm type record is wasteful of speed, space and time, and so the 45 rpm record was considered next. Its small size (7" diameter) and availability, at least in the popular music field, made it seem attractive at first glance. However, further investigations revealed that from the point of view of the automobile driver the mere fact that this record can be played on his machine (if he has one) at home does not offset some serious disadvantages. The maximum playing time on the current 45 rpm

records is 8 minutes on each side (extended play) or 16 minutes per record.

Thus, to provide two hours' entertainment, almost 8 of these records would be required (7.5 exactly). This then calls for a record changer which has to be loaded with 7 or 8 records in their proper sequence, and for each hour the listener will get 7 or 8 interruptions. Clearly this is not desirable in a new system designed for many years to come. The manufacturing costs of putting two hours of program on 7 or 8 records would be of considerable extra expense to the ultimate customer and the storage of such stacks of records in the car represents a problem in itself. The space occupied by a record changer, even of the 45 rpm type, and its accompanying cost are undesirable features, too.

The next consideration was given to the standard long playing records which, as is known, turn at 33-1/3 rpm. The maximum playing time per side of a 12" LP record is approximately 30 minutes, and does not fully satisfy the playing time requirements for the automobile. Due to the large diameter of the record, it would be difficult to design a shock-proof player mechanism without undue size and cost and the storage problem also could be a difficult one.

It then appeared that the possibilities among the existing systems were exhausted and thus something entirely new and more suitable for the car had to be found. It would seem best to omit the trials and tribulations of the period of research that followed. The final outcome was a new record and record player, mated to each other, and described in the following.

The record is seven inches in diameter turning at 16.6 rpm and can carry up to 45 minutes of music, or one hour of speech, on each side. The 45 minutes of music playing capability was established on the basis that 96% of classical and semi-classical pieces have less than 45 minutes duration. The number of grooves per inch is approximately 550 (or twice as many as the conventional LP). The 45 minutes of playing time per side does not take variable pitch recording into account. Its use would provide further leeway in the recording of long musical works. Economically this new record represents by far the least expensive method of reproducing music. With a maximum of one-and-a-half hours of music, or two hours of speech, this seven inch record brings the physical manufacturing costs of music or speech reproduction to an absolute minimum. The basic design of the records is such that after complete mastery of the cutting and production techniques, they should give performance substantially equivalent to current LP records. In the following some theoretical considerations will be given which will serve to substantiate this statement.

There are many criteria which will influence the performance of a record, but among the important technical considerations one should consider the following three, which will determine its basic capabilities:

1. Frequency response
2. Signal-to-noise ratio
3. Tracing distortion.

There exists a close interrelation between these three items and the last one is particularly dependent on the dimension of the reproducing stylus.

Linear groove velocity and groove deviation (recording level) for a given reproducing stylus radius are the chief factors determining record performance.* The inside grooves of standard LP records for maximum playing time lie along a diameter of approximately five inches and represent a linear velocity of 8.64 inches per second. Tracing distortion, one of the determinants of record performance, is primarily a function of the minimum radius of curvature of the traced waves as recorded on the disc, and of the effective reproducing stylus radius. Distortion increases very rapidly when the effective stylus radius exceeds the minimum radius of curvature of the traced wave.

The minimum radius of curvature of the traced wave on the record can be expressed as:

$$r = \frac{\lambda^2}{4\pi^2 D} \qquad \text{.....(1)}$$

where λ is the wavelength of the recorded signal and D the peak-to-peak

---

*The Columbia Long-Playing Microgroove Recording System. P. C. Goldmark, R. Snepvangers, W. S. Bachman, Proceedings of the IRE, August 1949, pp. 923-927.

displacement of the groove (recording level). The wavelength λ as traced at any given point of the record is equal to the linear velocity V of the groove at that point, divided by the frequency F of the signal delivered to the recording stylus. Thus (1) can be written:

$$r = \frac{V^2}{4\pi^2 F^2 D} \qquad \text{.....(2)}$$

For minimum tracing distortion it is necessary that $r \geq r_{eff}$ where r_{eff} is the effective radius of the reproducing stylus tip and equals tip radius time $\cos \alpha/2$, where α is the total groove angle. For $\alpha = 90°$, $r_{eff} = \text{tip radius}/\sqrt{2}$. Thus the following relationship exists in place of (2):

$$r_{eff} = \frac{V^2}{4\pi^2 F^2 D} \qquad \text{.....(3)}$$

The new seven-inch records are designed for use of a 0.00025" reproducing stylus tip radius. For commercial phonographs with somewhat limited frequency response, 0.0003" tip radius is entirely adequate.

Using the expression for the effective stylus tip radius, the ratio of recording levels will be determined for the standard LP and the new XLP records for equal amount of tracing distortion. The ratio of groove displacement for the conventional LP (index 1) and the new records (index 2) will be determined by applying formula (3) to both types of records.

$$r_{1(eff)} = \frac{V_1^2}{4\pi^2 F^2 D_1} \qquad \text{.....(4)}$$

$$r_{2(eff)} = \frac{V_2^2}{4\pi^2 F^2 D_2} \qquad \text{.....(5)}$$

From (4) and (5) follows that:

$$\frac{D_2}{D_1} = \left(\frac{V_2}{V_1}\right)^2 \frac{r_{1(eff)}}{r_{2(eff)}} \qquad \text{.....(6)}$$

Now the inside grooves of the new records after 45 minutes playing time follow a diameter of 3.93 inches and V_2 will be $\pi \cdot d_2 \cdot 16.6/60$ or 3.42 inches/sec. For standard LP records 8.75 inches/sec. is the value for V_1 corresponding to an inside diameter of 5 inches; also

$r_{1(eff)} = .001/\sqrt{2} = .00071"$

and $r_{2(eff)} = .00025/\sqrt{2} = .00018"$

Thus $D_2/D_1 = .61$

Therefore, for equal amounts of tracing distortion the maximum groove displacement (recording level) for the new records should not exceed 61% of the standard LP records.

Actually a recording level of approximately 6 db below LP records is employed, corresponding to a 2.5 cm/sec lateral groove velocity standard at 1000 cycles/sec. Tests have shown that though the signal output from the new records is roughly one-half that of the LP records, the signal-to-noise ratio remains substantially the same. This is apparently due to the lower stylus force (2 grams) and the smaller contact area (.25 mil tip radius) as well as to the lower linear speed.

The use of low stylus force also results in reduced stylus wear even though the stylus pressure has theoretically increased. Life tests carried out with sapphire stylii on the new records showed less wear after the same number of hours playing time as the 1 mil radius stylii with 6-8 grams pressure, playing standard LP records. These paradoxical results could be explained by the "size effect" described in a paper of Professor F. V. Hunt.*

It may be interesting to determine what performance the new records are capable of at the maximum outside diameter of 6.626 inches in terms of the equivalent diameter of a standard LP record for equal amount of tracing distortion.

From equation (6)

$$.61 = \left(\frac{V_2}{V_1}\right)^2 \cdot \frac{r_{1(eff)}}{r_{2(eff)}} \qquad \text{.....(7)}$$

Substituting for V_2 ... $\pi d_2 \cdot 16.6/60$

and for V_1 ... $\pi d_1 \cdot 33.3/60$

where d_2 is the diameter of the outside groove of the new records and d_1 the diameter of the standard LP groove with

---

*F. V. Hunt, "On Stylus Wear and Surface Noise in Phonograph Playback Stylus", Journal of the Audio Engineering Society, Vol. 3, No. 1, Jan. 1955.

the same performance quality in terms of tracing distortion.

Now (7) can be expressed as:

$$\frac{d_2^2 \cdot 16.6^2}{d_1^2 \cdot 33.3^2} = .61 \frac{r_{2(eff)}}{r_{1(eff)}} = .152$$

$$\text{thus } d_1 = 1.28\, d_2 \qquad \text{.....(8)}$$

and for $d_2 = 6.625"$, d_1 will be 8.5".

Thus the tracing distortion in the new seven inch records during 45 minutes of continuous playing between the diameters of 6.625" and 3.93" will vary as the tracing distortion on standard LP records between the diameters of 8.5 and 5".

When recording speech, each side of the new records is capable of carrying one full hour or two hours per record. The inside grooves for one hour duration correspond to a diameter of approximately three inches. At that diameter, the linear groove velocity is decreased over the inside groove velocity for music and from (3) the frequency for which the minimum radius of curvature equals the effective stylus tip radius can be expressed as follows:

$$F = \frac{V}{2\pi} \sqrt{\frac{1}{D\, r_{eff}}} \qquad \text{.....(9)}$$

Now substituting for the linear velocity $V = \pi d \cdot 16.6/60$ inches/sec. where d is the groove diameter and rpm is 16.66, the resultant frequency will be:

$$F = 0.14\, d \sqrt{\frac{1}{D\, r_{eff}}} \qquad \text{.....(10)}$$

For equal maximum groove deviation D and effective stylus tip radius, the relationship of frequencies for 4" and 3" diameters will be

$$F_{(3")} = 0.75\, F_{(4")} \qquad \text{.....(11)}$$

Thus for speech records of one hour duration per side, the recording characteristic should be so modified that the amplitude excursions at frequencies above 2 or 3 kilocycles be limited to 3/4 of the values used for music recording at the larger inside groove diameter. In practice it was found that because of the natural lack of high frequencies in speech, the above conditions are fulfilled automatically and thus the standard recording characteristic can be employed.

The new 7" extra long playing records designed for automobile use cannot be played on existing home instruments. There are several types of home phonographs on the market which contain the 16-2/3 speed but the relatively heavy pickup arm and the 1 mil stylus radius are not suited for playing the extra fine grooves.

In the car these records meet all the necessary criteria mentioned earlier in this article. During a two hours' program only one interruption is required, namely to flip over the record, and thus there will be no need for a record changer. The required storage space for the maximum playing time is at a very minimum, as are the manufacturing costs. Fig. 1 shows a commercial pressing of one of the new records, with Tchaikovsky's Sixth Symphony on one side (42 minutes) and a series of Russian Dances on the other. Fig. 2 is a tabulation comparing some pertinent data of the various recorded music systems.

Because of the small size of the record, it was feasible to design a compact player which, with the cooperation of the Chrysler Corporation, was fitted into their 1956 series of cars. In its current form the player is mounted on a base which can slide in and out of a metal container mounted underneath the dash (see Fig. 3). When opening the door, the player can be pulled out a sufficient amount to drop a record onto the turntable (Fig. 4).

The pickup and arm device represent a radical departure from existing practice. The distance between the stylus and the vertical arm axis is only 3½". Between the vertical axis and the arm bearing there is a fluid of proper viscosity (30,000 centistoke) furnishing adequate friction to permit the arm to follow rapid torsional movements of the car, at the same time providing a virtually frictionless bearing for following the extremely fine groove pitch. Also this method helps to damp out arm resonance and vibration transmitted from the road and engine.

Inside the arm is a cartridge assembly which pivots around a horizontal axis and is carefully balanced so that

acceleration forces in a vertical plane are neutralized and will not displace the stylus from the groove. A small spring applies approximately 2½ grams force on the cartridge in the direction of the record, thereby assuring adequate tracking of the stylus in the groove. The arm assembly is also counterbalanced around its vertical viscously damped axis. This prevents the development of torsional forces around the vertical axis of the pickup arm which would produce acceleration components in a radial direction of the record.

To start the record, one presses a tab protruding from the left side of the pickup arm, thus disengaging the arm from its resting position, and moves the arm to the right until it hits a stop. Now the pickup is automatically set down on the lead-in spiral of the record, and the turntable starts to rotate automatically too. This mode of operation makes it possible for the driver, once familiar with his instrument, to place a record on the turntable and start playing it without having to take his eyes off the road. The record cannot be damaged by sliding the arm across it because the arm is rigid in a vertical plane and the only force exerted by the stylus against the record is the spring pressure of 2½ grams, which will not produce an audible scratch on the record.

The player mechanism is mounted on a specially designed rubber shock mount system which has a sufficiently low natural period to filter out harmful shocks and vibrations. The weight of the player unit is evenly distributed among the three suspension points and the lateral compliance of the shock mounts is also equal. As a result, forward or sideways jolts cannot be translated into torsional movement in the plane of the record, causing wow. The most vehement acceleration or deceleration of the car, or driving over bad road conditions, will not cause the stylus to leave the groove or create any audible effect.

A great deal of attention had to be paid to the constancy of speed. The possibility of wow has been eliminated by the type of drive applied to the turntable, and variations in speed due to supply voltage changes have been taken care of by the use of an AC induction type shaded pole motor and a 60 cycle vibrator which provides substantially constant turntable speed for primary voltage variations from 10.5 to 15.5 volts.

The player contains a half-inch high record storage compartment for six records (equal to a maximum of 12 hours listening), in the bottom of the player where a spring and pressure plate insure that the records will stay flat even under the maximum temperatures encountered in the car (such as when parked in the sun with windows closed). A separate storage compartment for an additional 25 records will also be made available.

The cartridge employed has been specially developed for this use in cooperation with Shure Brothers, and is of the ceramic type. The frequency characteristics of the cartridge are such that when playing the new automobile records through a flat amplifier, the resulting response will be substantially uniform between 50 and 10,000 cycles.

The output of the ceramic cartridge is sufficient to play it through the audio portion of the automobile radio without need of a pre-amplifier. The audio section of the automobile radios for all 1956 Chrysler Corporation cars have been modified to take advantage of the record player fidelity and are also provided with a five-prong jack for connecting to it the record player. The switch to change from radio to phonograph is located in the player unit and is also indicated in Fig. 5, which shows the circuit diagram of the car phonograph and one of the modified automobile radios.

In addition to the six records supplied originally, Columbia Records has released some additional 30 records with a wide variety of selections from symphonies and musicals to books and stories for grown-ups and children. The program possibilities for this new medium are almost endless; travelogues, spoken editions of magazines, educational records, etc., all will help to entertain the automobile driver and his passengers, and also keep restless children under control.

ACKNOWLEDGMENT

The author wishes to express his gratitude for the untiring assistance given him by his associates in the CBS Laboratories, especially John W. Christensen, Rene Snepvangers, Daniel Doncaster, Wilbur Clade and Thomas Broderick; by his associates in the Columbia Records Division, William Bachman, Al Ham, and Herbert Greenspon;

and in the Chrysler Corporation Engineering Division by Phil Kent and Robert Stinson. Special appreciation is due to James Conkling, President, and Goddard Lieberson, Executive Vice President of Columbia Records for their continuous encouragement and cooperation. I wish to thank Peter Goldmark, Jr., for his advice concerning elastic suspension and his helpful assistance during the many test drives.

Fig. 1

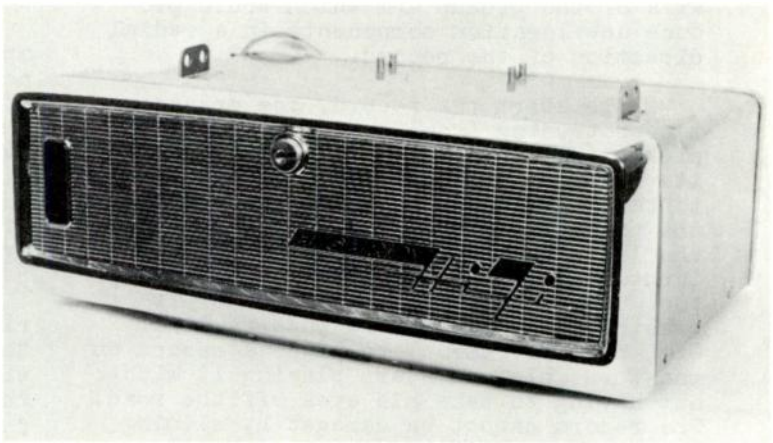

Fig. 3

Speed	Tape			Disc					
	3-3/4"** per Sec.	7-1/2" per Sec.	7-1/2" per Sec.	33-1/3 RPM-LP	33-1/3 RPM-LP	45 RPM Standard	45 RPM Extended Play	16-2/3 RPM Music	16-2/3 RPM Speech
Diameter	5" dual track	5" dual track	7" dual track	10"	12"	7"	7"	7"	7"
Playing time per side, minutes	30	15	30	15	30	4	8	45	60
Interruptions in two hours	3	7	3	7	3	29	14	2	1
Storage volume, 2 hours play, cu. in.	20*	39*	39*	59	42	72	36	4	3
Cost for 2 hours play	$17.90*	$27.80*	$25.90*	$11.80	$7.78	$13.35	$11.10	$2.60 to 6.55	$2.25 to 3.95

* Not in magazine
** Inferior Quality

Fig. 2
A comparison of recorded music systems.

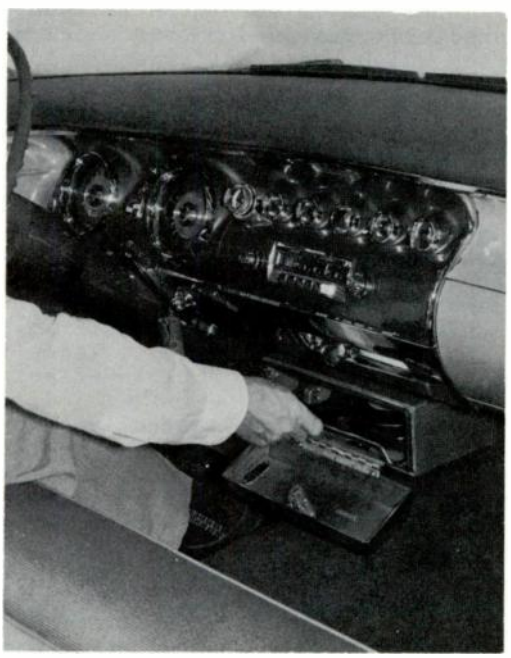

Fig. 4

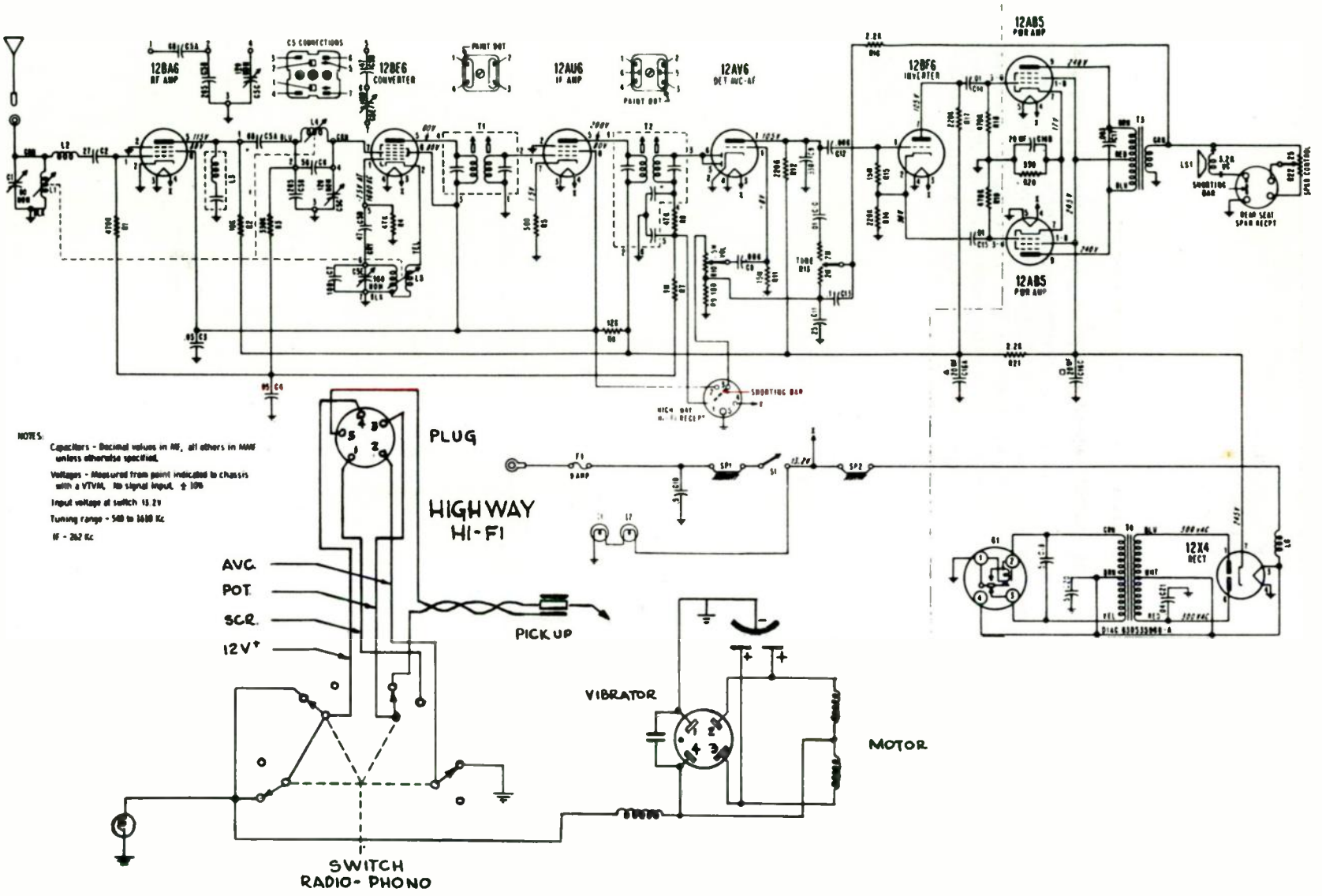

Fig. 5

A MAGNETIC TAPE SYSTEM FOR RECORDING AND REPRODUCING STANDARD FCC COLOR TELEVISION SIGNALS--GENERAL CONSIDERATIONS

H. F. Olson
RCA Laboratories
Princeton, N. J.

ABSTRACT

A system for recording and reproducing television signals by means of magnetic tape was described and demonstrated more than two years ago. Since that time further developments have been made as follows: a reduction in tape speed from 30 to 20 feet per second. An increase in resolution by the use of improved heads and the addition of a fifth channel for carrying the combined highs. Recording and reproducing a complete composite FCC color signal. An improved servo system for maintaining constant equivalent tape speed in recording and reproducing the television signal.

A MAGNETIC TAPE SYSTEM FOR RECORDING AND REPRODUCING STANDARD FCC COLOR TELEVISION SIGNALS--ELECTRONIC SYSTEM

W. D. Houghton
RCA Laboratories
Princeton, N. J.

ABSTRACT

The most important consideration in the selection of a system for producing FCC color signals, from information stored on magnetic tape, was the phase stability of the color carrier and burst components. In order to insure the desired stability in a practical field test system, the color carrier is not recorded on the type. Instead, the composite color signal is decoded into its simultaneous color components. These signals are then recorded on separate tracks on the tape. In reproduction, the simultaneous signals are applied to a different color carrier by standard encoding equipment.

A MAGNETIC TAPE SYSTEM FOR RECORDING AND REPRODUCING STANDARD FCC COLOR TELEVISION SIGNALS--THE MAGNETIC HEAD

J. A. Zenel
RCA Laboratories
Princeton, N. J.

ABSTRACT

A magnetic head, capable of recording and reproducing a complete video signal, or any similar wide band of frequencies, has been developed by the RCA Laboratories. The head is capable of resolving wavelengths considerably smaller, and at a rate considerably faster, than that which has been possible in previous magnetic recording practice. The basic unit has been incorporated in a multichannel head which has proven itself in three years of experimental video recording. RCA Laboratories heads were used by the RCA video tape recorder in the public demonstrations of December, 1953, and May, 1955. Mechanical and electrical problems concerning the basic unit, as well as those posed by the demands of the recording system, are discussed.

A MAGNETIC TAPE SYSTEM FOR RECORDING AND REPRODUCING STANDARD FCC COLOR TELEVISION SIGNALS—THE TAPE TRANSPORT MECHANISM

A. R. Morgan and M. Artzt
RCA Laboratories
Princeton, N. J.

ABSTRACT

The problem of providing a tape transport mechanism for recording and reproducing video signals might be specified by a statement to the effect that the reproduced picture on a kinescope must not have more "jitter" than one or two picture elements.

The approach to meeting such a specification has been the use of two servomechanisms in tandem. The first is a servomechanism controlling the motion of the capstan so as to minimize the irregularities of recording and reproducing of the video signal. The second servomechanism controls the motion of a movable reproducing head so as to reduce further the irregularities remaining from capstan operation.

Considerable attention must be given to such details as tape tension and guiding, minute adjustment of all aspects of head alignment, reel configuration, starting and stopping of the tape, and perhaps most important of all the precision of mechanical design and shop work.

In the present system it has been established that commercially "jitter" free pictures can be reproduced with a tape speed of 20 feet per second. Reels with a diameter of 20 inches can give a playing time, per reel, of 15 minutes. Starting time with a full reel of tape is the order of 5 to 7 seconds.

The capstan synchronizing system will be most effective when the tape loading is constant. This effect is obtained if the tape tension is maintained at a fixed value. Two separate servo systems are required to accomplish this, one controlling the braking applied to the supply reel and one controlling torque on the take-up reel drive. Two methods of obtaining constant tension in both supply and take-up reels have been developed and are described. Both are apparently satisfactory in operation; choice between them largely depends on practical rather than theoretical considerations.

A MAGNETIC TAPE SYSTEM FOR RECORDING AND REPRODUCING STANDARD FCC COLOR TELEVISION SIGNALS--AUDIO SYSTEMS

J. G. Woodward
RCA Laboratories
Princeton, N. J.

ABSTRACT

Because of certain requirements of the video portions of the television tape-recording system, conventional audio-recording methods are not satisfactory, and the audio program signals are recorded by means of a modulated carrier. Both amplitude- and frequency-modulated carriers have been used. Tape noise and distortion are serious limitations in a simple AM carrier system. A two-carrier AM system provides a degree of noise reduction, but here too, the tape is the limiting element. With a wide-deviation fm system the tape does not contribute significantly to noise and distortion, and tape speed constancy in the television recorder permits an adequate signal-to-noise ratio.

The Technical Boundary Conditions of Subscription Television

Alexander Ellett and Robert Adler

Research Department

Zenith Radio Corporation

Chicago 39, Illinois

Summary

This paper undertakes to state the engineering problem which we set ourselves when we undertook the development of a system of subscription television and to outline in broad terms the direction in which we have sought solutions. Briefly, this problem has been to devise a system of subscription television, using the regular broadcast channels and existing television sets. These requirements impose some rather stringent technical conditions -- the boundary conditions of the problem, if we may borrow a phrase from the mathematicians.

It is necessary that the program should not be available to non-subscribers and that there be a way of collecting fees from those subscribers who choose to pay or to obligate themselves to pay for a particular program. Hence, the transmissions must be scrambled.

We consider several ways of scrambling and ask ourselves whether adequate scrambling will result and whether the picture may be unscrambled without degradation when the signal is received through a commercial receiving set. It is well known that video amplifiers and deflection circuits of commercial sets show appreciable departures from linearity. It is indicated how this fact influences the choice of a preferred means of scrambling and unscrambling the picture.

Problems due to non-linearity are avoided and the picture effectively scrambled by the introduction of a sideways jitter at a faster than field rate. This is accomplished by changing the phase of the video relative to the synchronizing signals. This can be done by the use of a delay line at the transmitter and compensated by a similar delay line at the receiver. A delay of a few microseconds corresponds to a sideways shift of the picture of about an inch on picture tubes used today.

If the receiver is told whether video is to be transmitted in the delayed or non-delayed mode, it can eliminate the scrambling and put the picture back together again.

If this information which the receiver requires is supplied over a controlled channel, means is thereby provided for recording the subscriber's use of the program and for making appropriate charges.

In the simulated commercial test conducted in Chicago in 1951 by Authorization of the FCC, this controlled channel was provided by the use of telephone circuits. This means of controlling the distribution of decoding information is simple, at least in principle, but it appears to be too expensive.

It seems that it might be possible to construct a decoder which would get its decoding information directly from the picture content; for example, by correlation of successive lines of video. We have constructed decoders of this kind and have made them perform fairly well. To do even fairly well, such a decoder must be quite elaborate, and the chance of simplifying it to the point where it could conceivably be used commercially seems to be infinitely remote. Since it turns out to be impractical to obtain decoding information from the picture content, or over wire circuits, you may ask how this information can be furnished to subscribers.

Systems have been developed which use

repetitive cycles of mode information. A fixed sequence of modes repeats itself over and over throughout the program. Information regarding the sequence is sold to subscribers.

In experimenting with systems of this kind, we found them not very secure. Short sequences can be determined rather easily by a simple cut and try procedure. Long sequences require impractically expensive storage devices for each subscriber. They also make it difficult for late arrivals to get into the theatre.

A system providing adequate security is based on an apparent paradox. Mode information is transmitted together with the scrambled television signal during the vertical retrace period preceding each field. At first glance, this seems to make no sense at all. The system is apparently devoid of security. The trick consists in the manner of transmitting the mode information; the message takes the form of a multi-digit pulse code signal which permits millions by permutations. Each of these is assigned to one of the relatively few modes in which the picture may be presented.

This method, which we refer to as Air Code, is analogous to sending the letter R by picking at random a name which starts with R in the telephone directory and transmitting the seven-digit number listed with that name. This is a highly wasteful method of transmitting information, but there is little information to transmit. To translate the number back into the letter R, the subscriber needs, of course, a reverse directory, and we assume that everyone has a nice collection of such directories. The information for which the subscriber pays is an important detail - namely, that the directory to be used for the specific program which he has selected is the one for Iowa City, Iowa. For the next program it will be a different one, and if he wants to see that program, too, he will have to pay again in order to find out which directory it is.

So much for analogy. In practice, the decoding instruments for this air code system are equipped with a switching mechanism which works something like a combination lock. Any one combination of settings corresponds to a specific directory which assigns a specific mode of presentation to each possible pulse code group. Moreover, the combination lock type switching mechanism is made unique to the individual subscriber. This can be done using identical parts but differently assembled, very much as it is done in the case of combination locks.

In solving the problems here depicted in broad outline, it has been necessary to solve a host of special technical problems. We think the solutions of many of these problems are ingenious and interesting. Mr. Roschke will present the first of a series of papers which we purpose to submit to this Institute, dealing with technical problems in the field of subscription television.

AN INTEGRATED SYSTEM OF CODED PICTURE TRANSMISSION

E. M. Roschke, W. S. Druz, Carl Eilers
and Jan Pulles
Zenith Radio Corporation
Chicago, Illinois

SUMMARY

This paper discusses principles and engineering details of the Zenith PHONE-VISION system, its method of picture scrambling, system of code transmission and its security.

The picture is scrambled by delaying alternate 16-line groups with respect to the horizontal synchronizing pulses; the delay is under control of a square wave which has a period equal to 32 horizontal lines.

While many switching circuits are known which might be used to introduce video delay, difficulties such as circuit complexity, switching spikes and varying non-linear tube characteristics have led to the development of a simple circuit using a beam deflection tube. The tube (the 6AR8) employs two anodes; a delay line is connected between these anodes. Video fed to the grid is delayed or not delayed under control of a square wave applied to the deflectors.

By applying inverse delay to the video signal at the receiver which contains a similar 6AR8-delay line circuit, unscrambling is achieved. Specifically, those portions of the video signal which are delayed at the transmitter are not delayed at the receiver and vice versa. This assures proper time relationship between adjacent groups of 16 horizontal lines.

While scrambling as described will make the picture unintelligible, the system would have no security. It would be possible to use a 32 to 1 countdown generator actuated by horizontal pulses and by trial and error obtain phase locking of the decoding square wave. Such a trial and error procedure should, of course, not be required of subscribers; with regard to non-subscribers, security measures must be added.

Phase locking of the square wave can be accomplished by sending information to both transmitter coder and receiver decoder to reset the 32 to 1 countdown unit which in this system consists of an 8 to 1 blocking oscillator followed by 2 binary stages or mode multivibrators. Resetting is accomplished by applying pulses to the blocking oscillator and to a reset grid of each binary stage. Intermittent reset pulses, applied simultaneously to transmitter and receiver, will cause the system to lock in.

Security is added by introducing additional code pulses, sent during the vertical blanking period, which cause the square wave to assume a specific phase condition among the 32 possible conditions. The code pulses are applied to six input points: the two reset inputs and the common or counter input of each binary stage. Application of the same code pulses to corresponding points of the mode determining circuits in coder and decoder results in phase locking of the system.

The code pulses can be sent in numerous combinations each of which may be considered equivalent to a code word. But they can result in only one of 32 phase conditions of the square wave. The high level of redundancy which exists between words and final phase conditions is an important factor governing the security of the system.

Subscribers' decoders contain a switching device which permits variable permutation of the pulses applied to the mode determining circuits. Unique setting of the switches is required to distribute the pulses properly among the six inputs. The large number of ways in which the pulses can be applied to the inputs of the mode circuits permits the use of multiple permutation for individualizing subscriber decoders. This provides inter-subscriber as well as inter-program security.

CHROMATICITY COORDINATE-PLOTTING PHOTOMETER

W. H. Highleyman*
M. J. Cantella**
V. A. Babits

Rensselaer Polytechnic Institute
Troy, New York

Summary

An instrument which will respond to a colored light source and will compute and plot the chromaticity coordinates of the color on the screen of a cathode-ray tube is described.

The instrument consists of three parts. The first part is the known Sziklai tristimulus photometer. The second part is an analog computer which determines the chromaticity coordinates of the plotter. The third part of the instrument plots the computed chromaticity coordinates on an oscilloscope screen. The analysis of the instrument system and the response characteristics will be discussed.

Introduction

In the study and analysis of color television systems, it would be very desirable to have an instrument which would not only measure color parameters accurately, but would also indicate the results rapidly. As for the particular parameters to be measured, several systems are in use today, but the most common system for scientific specification of a color is the trichromatic system as standardized by the International Commission on Illumination (CIE). In this system, three primaries are defined such that any color may be created by an additive combination of the three, the relative amounts of the three primaries required being termed the tristimulus values of the color being measured, (Fig. 1a).

The chromaticity coordinates of a color are defined by the equations:

$$x = \frac{X}{X + Y + Z}$$

$$y = \frac{Y}{X + Y + Z}$$

$$z = \frac{Z}{X + Y + Z}$$

where X, Y, and Z are the tristimulus values, and x, y, and z are the chromaticity coordinates. Since the sum of the chromaticity coordinates is always 1, then only two of the coordinates need be specified, and these may then be plotted in rectangular coordinates.

The CIE has standardized on the x and y coordinates as abcissa and ordinate respectively, and the resulting plot of the chromaticity coordinates of pure and saturated spectral colors and their complements is termed the chromaticity diagram[1] (Fig. 1b). Since there are only two coordinates, only two of the three color parameters are specified: dominant wavelength (hue) and saturation (purity) in this case. The chromaticity coordinates are independent of luminance (brightness).

Instruments which will measure the tristimulus values of a color rapidly have been constructed [2,3,4,5], as has a computer which will calculate the chromaticity coordinates of a color from manually inserted data[6]. Described herein is an instrument which will measure the chromaticity coordinates of an illuminated color directly, and will plot the result on a cathode-ray oscilloscope.

General Description

The chromaticity coordinate photometer consists essentially of a Sziklai tristimulus photometer followed by a logarithmic analog computer. The photometer furnishes three currents, each proportional to one of the tristimulus values of the color being measured. These currents are fed into the computer which determines the x and y chromaticity coordinates according to the previous formulae, delivering the results as voltages.

In steady-state analysis, the tristimulus-photometer outputs may be converted directly to chromaticity coordinates by the use of current-ratio meters, as discussed later. For dynamic studies, the output of the computer may be displayed as a point plotted on a cathode ray oscilloscope, as is the case in the described instrument. For this type of display, the outputs of the computer are time sampled at a high rate, and the sampled data is fed through the amplifiers of the oscilloscope for ease of adjustment of the axis magnitude and position.

The Tristimulus Photometer

By multiplying the response of a given photoelectric transducer by that of certain combinations of chromatic filters, reasonable approximations to the CIE tristimulus value curves may be obtained. Proceeding in this manner, an instrument may be designed which will derive electrical analogs of the tristimulus values of an

---

* Presently at Lincoln Laboratory, M.I.T., Lexington, Massachusetts.

** Presently with U. S. Navy, USS Valley Forge CVS-45.

illuminated color. Sziklai has described just such an instrument[2], and it was his tristimulus photometer that was chosen for the first section of the chromaticity coordinate-plotting photometer

In this system (Fig.2) the incoming chromatic light is split into three directions by a crossed semitransparent mirror arrangement, each resulting component then passing through suitable filters and impinging upon the cathode of its respective photomultiplier. Type IP22 photomultipliers were selected, and the filters used are Corning Glass Works filters, Corning numbers CS 3-113, CS 4-111, and CS 5-79 for the X, Y, and Z characteristics respectively. In order to obtain a closer approximation to the X curve in the 400 to 500 millimicron region (see Fig. 1a), an undirectional current path is afforded from the Z channel to the X channel by means of a diode and a variable resistor, so that an attenuated Z characteristic is added to the X characteristic. Since the input to the computer is an interconnected resistive summing network, it is necessary to place another diode in series with the Z channel output to prevent undesirable cross currents. Variable resistors are provided in each of the photomultiplier circuits so that their luminous sensitivities may be adjusted to obtain the proper relationships. The Z-channel output is adjusted for twice its relative value for reasons discussed later.

The high voltage for the photomultipliers is furnished from a high frequency oscillator. Care must be taken to insure that the D.C. power furnished to the oscillator is free from 60 or 120 cycle ripple, since this may then impress a similar ripple on the high voltage supply which will pass unattenuated through the high frequency filter. With regard to color television work, this will vary the sensitivity of the photomultipliers at the same rate as the vertical sweep, and consequently the photometer will exhibit different characteristics for different areas of the picture.

Chromaticity Coordinate Computer

The chromaticity coordinates are computed from the tristimulus values by logarithmic means[7], thus affording a substantial saving in components in this specialized computer as compared to regular analog techniques. In general (Fig. 3), the photometer output currents are first converted to voltages proportional to X, Y, and Z, and these are then added, giving (X + Y + Z) Through the use of logarithmic amplifiers, log X, log Y, and log (X + Y + Z) are found, and then the differences

$$\log X - \log (X + Y + Z) = \log \frac{X}{X + Y + Z}$$

and

$$\log Y - \log (X + Y + Z) = \log \frac{Y}{X + Y + Z}$$

are taken by means of difference amplifiers. Finally an antilogarithmic amplifier derives the antilogarithms of these, giving the desired x- and y-chromaticity coordinates.

The addition is performed by a standard resistive summing network[8], the input resistors of which perform the necessary current-to-voltage conversion. The Z channel input resistor is smaller than either of the respective X- or Y-channel input resistors. This is to afford necessary attenuation, since the Z channel in the tristimulus photometer is far more sensitive than the others due to the S-8 phosphor of the photomultipliers which peaks in the blue region.

A stage of amplification is needed before the logarithmic amplifiers to obtain the necessary input voltages (100 volts maximum). These amplifiers use negative feedback for both D.C. stabilization and for gain adjustment of the X- and Y- amplifiers. Since the feedback resistors are connected to the outputs of the voltage-zeroing potentiometers, gain adjustment of an amplifier will not affect its zeroing, thus making these two functions independent. The gain of the X- and Y-amplifiers should be adjusted so that the three amplifiers (including the summing network) have equal gain. D.C. zeroing of these amplifiers has to be accomplished iteratively due to the negative feedback and the interconnected inputs. Adjusting the output voltage of one amplifier simultaneously changes the input voltages of the other two, and consequently changes their output voltages. Neon bulbs were placed at the output of each of the three linear amplifiers as overload indicators. Their ionization potential is slightly less than 100 volts, the upper limit of the linear region of operation, and will ionize if the input luminosity is too great.

The logarithmic amplifiers use the principle that there is a logarithmic relationship between grid current and plate current in a vacuum tube for small values of positive grid current[9,10]. It will be noted that, although log 1 = 0, no offset voltage is included in the logarithmic amplifiers so that this restraint may be complied with, since this constant voltage would only be cancelled out in the following difference amplifiers, and would therefore be superfluous. The output of the logarithmic amplifier is linear on a semilogarithmic plot for input voltages ranging from 0.15 volts to more than 100 volts, or over almost three decades.

Following the logarithmic amplifiers are standard difference amplifiers in a long-tailed configuration. The logarithmic outputs must be attenuated so that they will not drive the difference amplifiers into their non-linear region. Similarly, the outputs of the difference amplifiers must also be attenuated so that the antilogarithmic amplifiers will remain in their linear range. Each difference amplifier output-balancing potentiometer should be adjusted for zero voltage output when equal voltages are applied to both inputs of the respective amplifier.

The antilogarithmic amplifiers are of rather novel design. Ideally the output should vary from 0 to 1 for respective input variations from $-\infty$ to 0. Since the input voltage must of course have a finite maximum, the amplifier was designed to be linear on a semilogarithmic plot only for a range of output voltages corresponding to the numerical range .01 to 1, or over a range of two decades. This entails no functional loss

since the minimum chromaticity coordinates of realizeable colors are approximately equal to this. (In color television measurements, the lower coordinate limit is even higher: $x_{min} = .140$, $y_{min} = .080$. This is due to the real primaries used, since no color can be reproduced by an additive process that lies outside of the triangle formed by the location of these primaries on the chromaticity diagram (see Fig. 1b)). The logarithmic amplifier ideally approaches infinite output for infinite input, but if the circuitry is so arranged that the amplifier saturates quickly for increasing inputs, then the voltage asymptotically approaches a constant voltage. If an offset voltage is now furnished so that the resulting asymptotic voltage is equal to zero, then (disregarding sign) an antilogarithmic characteristic may be approximated. A 6SJ7 is used for proper saturation characteristics, and the stage is otherwise similar to the logarithmic amplifiers. The proper offset voltage (equal to the negative of the saturation voltage of the antilogarithmic stage) may be obtained from the output D. C. balancing network. However when used in conjunction with the presently described plotter for oscilloscope display of the chromaticity coordinates, there should be no offset voltage as such, but rather the output level should be shifted so that a zero voltage corresponds to the numerical value of 1.

The Chromaticity-Coordinate Plotter

In order to display the computed chromaticity coordinates on an oscilloscope screen, the representative voltages must first be amplified from the 27-volt maximum swing obtainable at the computer output to a value determined by the deflection sensitivity of the cathode-ray tube used. Since steady-state as well as transient measurements are desirable, this amplification must be accomplished either with additional D. C. amplifiers or by using a carrier-modulated system.

The latter method[11] was chosen for various reasons. Primarily, it would minimize D. C. drift, a problem which is small in the computer itself, but one which might grow with increasing D. C. amplification. In addition, by modulating the computer outputs with a square wave, the results may be amplified by the oscilloscope amplifiers, consequently allowing the scale magnitude to be adjusted by the oscilloscope gain controls, and the origin location to be controlled by the horizontal and vertical positioning controls. Furthermore, in the steady-state condition, the selected point is energized for only a portion of the time, and consequently there is no fear of burning a spot in the screen .

The modulation source is a conventional 50 kilocycle multivibrator (Fig. 4). Its output is shaped by a clipper and fed to the control grid of each modulator, a sharp-cutoff pentode. Here the positive portion of the square wave is clamped to the computer output voltage. When this voltage is zero, it corresponds to a chromaticity -coordinate value of one, and when it is equal to the control-grid-cutoff voltage, it corresponds to a zero value. The peak-to-peak amplitude of the square wave is greater than the cutoff voltage of the modulator under the operating conditions present. Therefore, the modulator output is a square wave whose amplitude is proportional to the output of the chromaticity-coordinate computer. The computer output swing must be adjusted so that it will vary from ground to modulator cutoff, a range of about 3 volts.

This of course, is ideal. Actually, in the region near cutoff, the modulator transfer characteristic becomes rather non-linear. To overcome this difficulty, the lowest value of clamping voltage (computer output voltage) for which the transfer characteristic is still linear is defined as corresponding to a chromaticity-coordinate value of zero, and the small value of signal occuring in this state is subtracted from the output by a biased diode clipper, as follows. The modulator output, after amplification, is first clamped negatively with respect to ground, and then only that portion of the square wave more negative than a certain critical value passes through the series diode to the output. This critical voltage is determined by the amount of negative bias applied to the anode of the diode through the adjusting potentiometer, which is adjusted for zero output with a D. C. input voltage corresponding to a zero value. The biasing network is isolated from the clipper AC-wise by a low-pass filter. The output of the x and y channels are now fed through the horizontal and vertical amplifiers respectively of an oscilloscope for display on its screen.

A positive pulse is also derived from the multivibrator and is timed to occur during the middle of the positive portion of the square wave. To form this pulse, the multivibrator output is first delayed about 5 microseconds (one-fourth of a period), and then differentiated. The resulting negative pulse is amplified and the positive pulse clipped off, so that the output is a positive pulse occuring at the correct time. This pulse is then fed to the intensity grid of the cathode-ray tube so that only a portion of the positive part of the square wave is displayed. This eliminates a mirror effect that would otherwise be obtained due to the negative portion of the signal. It also reduces the phosphor-energization time to a fraction of a period, so that the screen is in no danger of burning in steady-state conditions.

PERFORMANCE CHARACTERISTICS

The overall accuracy of the chromaticity coordinate-plotting photometer is in the order of 10%. A closer look will reveal that the accuracy of the tristimulus photometer is not much better than this due to the approximation methods used. It is entirely feasible that more accurate and probably more complex methods may be used to obtain closer approximations to the C.I.E. tristimulus values [5], and consequently this will increase the overall accuracy of the instrument almost proportionally. It is also interesting to note

that the results, although accurate to only 10% on a linear coordinate scale, are much more consistent than this. In fact, no variance of results within the resolution of a five-inch oscilloscope were noticed over an extended period of time. Hence, this suggests that, by distorting the coordinate axes, a very accurately calibrated instrument may be obtained.

One of the factors contributing to the consistency of results is the high D.C. stability of the computer, assuming good regulated power is furnished to it (including a D. C. filament supply). This is due to the fact that most of the stages have very low gain, and the high-gain stages (X, Y, and summing amplifiers) employ negative feedback for effective D.C. stabilization. This also means that, once the instrument has been warmed up and the D.C. balancing potentiometers have been adjusted, these adjustments need be checked only once in a while during operation. In the laboratory model constructed, each of the balancing-network outputs were brought out to a sampling switch and V.T.V.M. for ease of adjustment. The remaining adjustments in the system need only be made once, and until component aging has taken its toll or a tube has been replaced, they need not be touched.

The frequency response of the system was measured by holding one or more inputs of the computer at a constant voltage, while impressing a sinusoidal voltage of appropriate amplitude and D.C. level on the remaining inputs. This caused a certain variation in the output, the amplitude of which was measured with increasing frequency. The point at which the output amplitude was 0.7 of its low frequency value was called the upper frequency limit of the system or its frequency response. (Note that this is not the true half-power point since the output is not necessarily sinusoidal.)

The overall frequency response of this system, as measures by the preceeding methods, is about 10 kilocycles. The main detriments to the response are the large plate resistors in the computer necessary for the proper characteristics, and the excessive capacitance created by the large number of adjusting potentiometers used in the laboratory model for flexibility.

As mentioned earlier, the tristimulus photometer results may also be converted directly to chromaticity coordinates by using a current-ratio meter (Weston Electrical Instrument Corp.). By summing the three output currents and using this total current (after suitable amplification) for driving one of the coils, and the amplified X or Y current for driving the other, a very accurate conversion may be obtained for steady-state measurements.

Acknowledgement

The authors are indebted to G. C. Sziklai for his helpful discussions on the subject of tristimulus-value measurement.

References

1. Benson, J.E., A SURVEY OF THE METHODS AND COLORIMETRIC PRINCIPLES OF COLOR TELEVISION, Amalgamated Wireless (Australasia) Limited, Sidney, September, 1951.

2. Sziklai, G. C., A TRISTIMULUS PHOTOMETER, Journal of the Optical Society of America, Vol. 41, No. 5, May, 1951.

3. Olson, O.H., COLOR BASICS FOR THE CONTROL ENGINEER, PART 2-MEASURING INSTRUMENTS, Control Engineering, Vol. 2, No. 11, November, 1955, pg. 90.

4. INTEGRATOR COMPUTES TRISTIMULUS VALUES, Control Engineering, Vol. 3, No. 1, January, 1956, pg. 91.

5. Chatten, J. B., WIDE RANGE CHROMATICITY MEASUREMENTS WITH PHOTOELECTRIC COLORIMETER, Proc. I. R. E., Vol. 42, No. 1, January, 1954, pg. 156.

6. Burr, White, SIMPLE COLOR COMPUTER GIVES TRISTIMULUS VALUES, Electronics, Vol. 28 No. 10 October, 1955, pg. 166.

7. Cantella, M. J., A TRISTIMULUS COMPUTER, RPI, May, 1954.

8. Seely, S., ELECTRON TUBE CIRCUITS, first edition, 1950, pp 146-162.

9. LINEAR TO LOGARITHMIC VOLTAGE CONVERTER, Electronics, July, 1953, pg. 156.

10. Valley, Wallman; VACUUM TUBE AMPLIFIERS, MIT Radiation Laboratory Series, Vol. 18, pp. 418-420, 441-456.

11. Highleyman, W. H., A TRICHROMATIC PHOTOMETER, RPI, May, 1955.

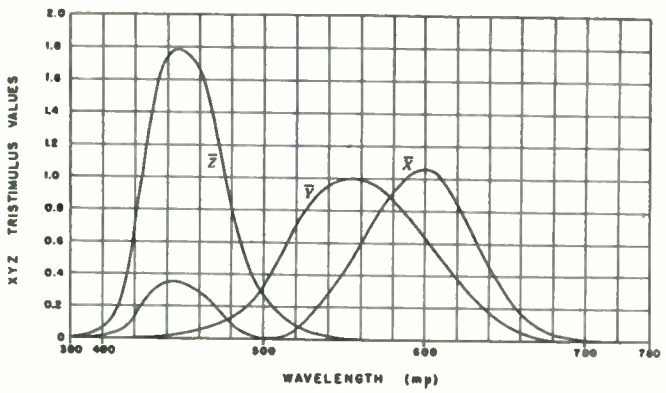

Fig. 1a
Tristimulus Value Curves

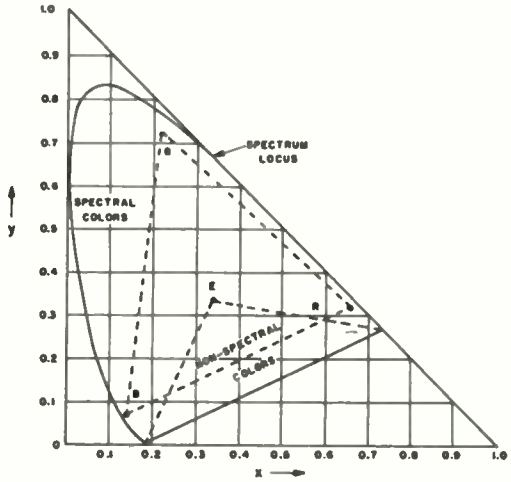

Fig. 1b
CIE Chromaticity Diagram

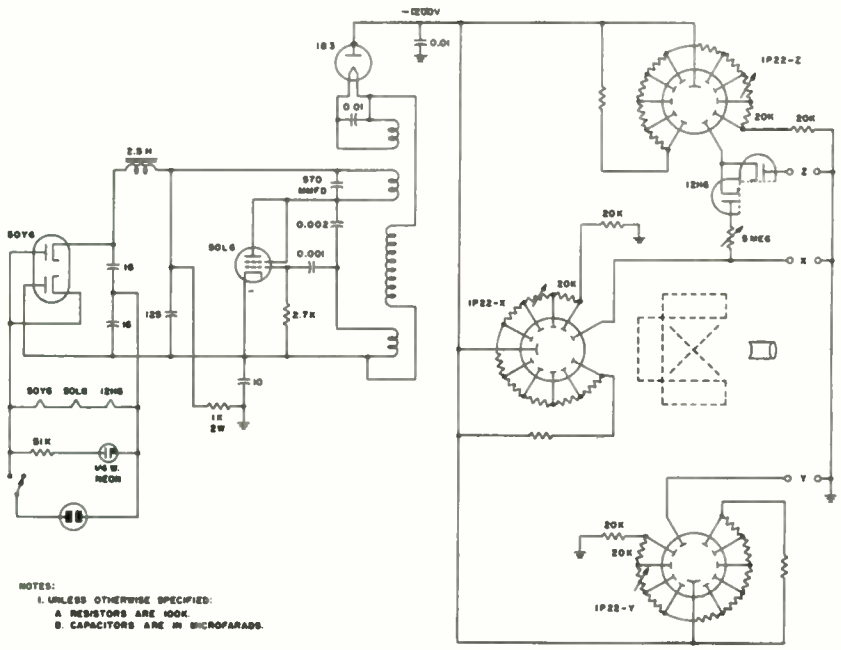

Fig. 2
Tristimulus Photometer

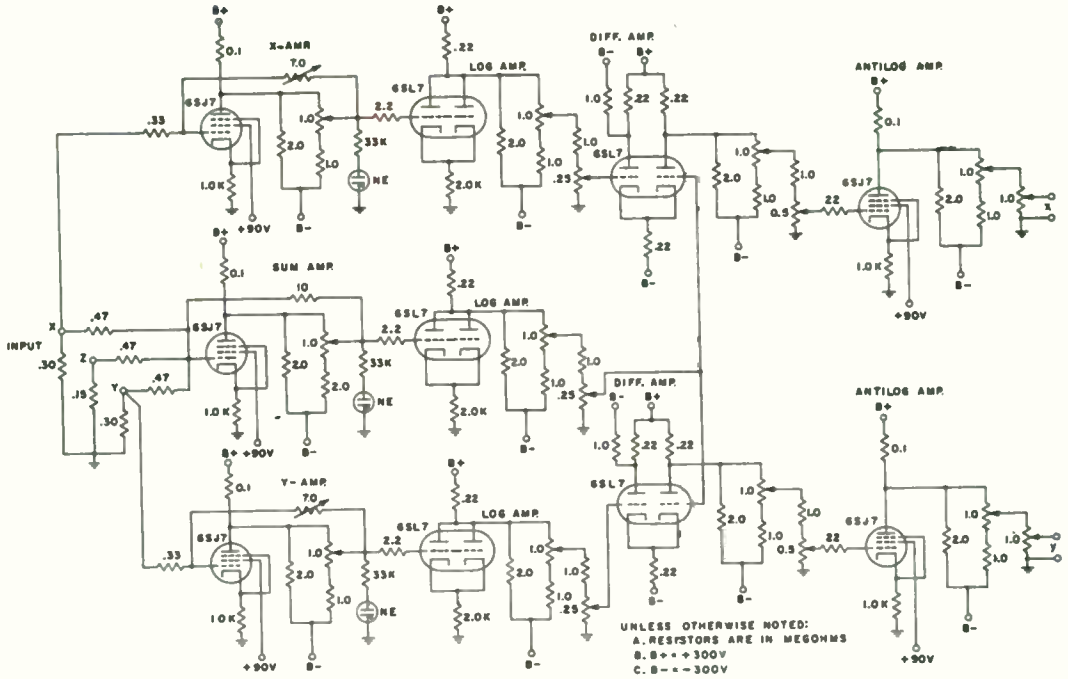

Fig. 3
Chromaticity-Coordinate Computer

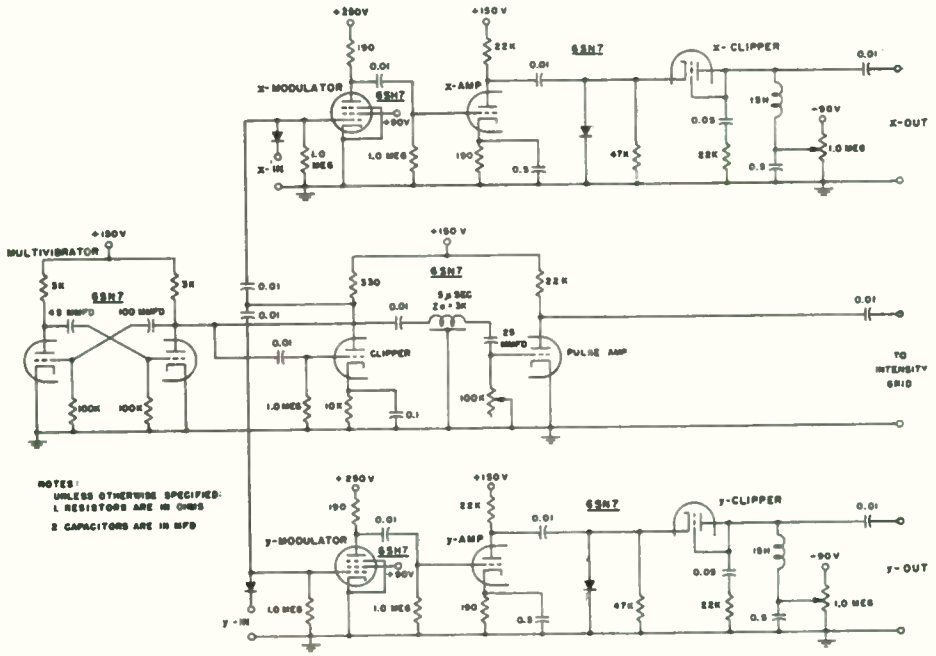

Fig. 4
Chromaticity-Coordinate Plotter

RECENT IMPROVEMENTS IN BLACK-AND-WHITE FILM RECORDING FOR COLOR TELEVISION USE

by

William L. Hughes
Engineering Experiment Station
Iowa State College

SUMMARY

At the 1954 national convention of the Institute of Radio Engineers, a system was proposed for recording and reproducing color television images using black-and-white film as a storage medium. At the national convention in the following year, a complete experimental system was described. There were certain problems connected with this system which were yet to be resolved. It is the purpose of this paper to describe how those problems have been resolved.

The first part of the paper will be concerned with a brief review of the basic theory of operation. At the time that the system was first put into operation, it became apparent that the most serious problem was the need for greater resolution in both horizontal and vertical directions. The lack of resolution was due primarily to the inability of the 5ZP16 scanner tube to meet conflicting requirements in the system. It was desired to have a single line scan when film was running since the vertical sweep was produced by the continuous film movement. In order to prevent rapid deterioration of the scanning tube phosphor, it was necessary to lower beam current and accelerating voltage appreciably. In order to get reasonable life from the scanner tube, these tube parameters fell at about 10 microamperes and 15,000 volts respectively. This very low value of accelerating voltage made it quite difficult to get adequate definition in the pictures. This problem was compounded with respect to vertical definition because the anamorphic nature of the images makes a slightly defocused spot a more serious detriment to vertical definition than to horizontal definition.

It should probably be said at this point that no definition problems have been encountered with the film itself. Both horizontal and vertical definition capabilities of the film exceed the highest values necessary for good television transmission.

The definition problem just described was solved in two steps. The second and major part of the paper will be concerned with this solution. The first step was to insert a special cylindrical optical system between the flying spot scanner tube and the spherical lenses of the regular optical system.

The complete optical system will be considered in some detail in the paper. This cylindrical optical system was designed to provide a virtual image of the scanner tube face which was scanned with a full raster. This image was greatly compressed in the vertical direction and thus approximated a scanning line. Quite incidentally, it can be shown that an oblong raster, with a very little height (such as is provided by this cylindrical optical system) is actually better for the purpose than a single scanning line because it permits use of film area which would otherwise be scanned during the vertical blanking period. This will be discussed in detail in the paper. The second step was to use a scanner tube with a more efficient phosphor (re: P 24) which operates at 27,000 volts and 200 microamperes beam current with a full raster. The combined results of these two steps were as follows: The scanning spot was anamorphosed in the same direction as the image so that full definition is obtainable in both directions if the scanner tube is focused normally. The higher accelerating voltage makes it quite easy to get excellent focusing characteristics. The higher voltage, beam current, and more efficient phosphor together provide a tremendous light increase so that the inherent inefficiency of the cylindrical optics is overcome, the regular lenses can be stopped down, and the resulting definition is extremely good in both directions. Furthermore, the pictures are essentially noise free. Several color photographs of images produced on a dichroic display from the system will be shown.

An additional problem in the initial system was concerned with stability of the film transport mechanism. A standard Simplex 35 mm film trap assembly has been modified to be used with a synchronous motor-reducer combination which was specially machined. This simple film transport mechanism will be described in some detail. When the mechanism is properly adjusted, film stability is quite satisfactory.

REVIEW OF SYSTEM PRINCIPLES

In the last two years, three papers have been presented which describe a method of recording color television images on black-and-white film. *

*(See next page.)

The system is, in theory, capable of all of the recording functions currently required by the color television broadcast industry. First, films can be taken by a mechanical camera and played directly after development on the flying spot scanner reproducer. Secondly, the system is adaptable to a relatively easy method of making kinescope recordings. In addition, there are certain obvious advantages with regard to ease and cost of operation as well as picture quality theoretically obtainable when compared with present day 16 mm color film. These advantages are discussed in detail in the previous papers and will not be elaborated on here.

The basic reproducer system is illustrated in figure 1. Vertically compressed television fields are shown on a continuously moving piece of film. The left hand column of images represents successive fields of the luminance signal. The right hand column of images represents alternate fields of chrominance information which in this illustration are red and blue. As the film moves continuously, an image from the scanner tube is focused by means of a beam splitter on each of three film images; they are a luminance image, the chrominance image beside that luminance image, and the chrominance image directly above and to the right of the luminance image. The cathode ray scanner tube produces either a single line scan or a very narrow raster. This narrow raster might be produced either optically or electronically. Photomultipliers gather the light from each of the three scanned images. Photomultiplier 1 continuously reads luminance information at the same time that photomultipliers 2 and 3 are continuously reading chrominance information. If the recorded chrominance information is red and blue, then photomultiplier 2 will read red one field, blue the next field, red the third field, and so on. Photomultiplier 3 reads different color information on successive fields as does photomultiplier 2; but in any given field, one of them reads blue and the other reads red. An electronic switch keyed at a field rate is used to sort this information out so that one luminance signal and two consistent chrominance signals are always available. There is one sprocket hole on the film per television field so that if 35 mm film is used, the film is consumed at a rate of 56 feet per minute. Field recognizer marks are shown on the film in figure 1. These marks might be used to provide a check on switching phase. Since the film is driven by a synchronous motor, however, they have been dispensed with in the initial experimental model. Once the film is started correctly, it stays in proper switching sequence unless some external cause disrupts it.

The possibility that color fringing might occur during fast motion has been mentioned at various times. It is not likely that this will be objectionable. If it does become a problem, however, a relatively simple modification of the basic switching and scanning scheme will eliminate it. This modification is discussed in detail in one of the previous papers and will not be further elaborated on here.

A possible type of kinescope recorder is illustrated in figure 2. Here the unexposed film is moved continuously at a synchronous rate. The left hand column of images is recorded directly from a cathode ray tube with a single line or compressed raster. The tube is modulated by the luminance signal. The right hand column of images is recorded directly from a second cathode ray tube with similar sweep characteristics. This second tube is modulated on odd fields by one piece of chrominance information and on even fields by the other piece of chrominance information. This alternate throwing away of chrominance information results in a loss of vertical chrominance detail. The total loss of vertical chrominance detail is, however, considerably less than the horizontal chrominance detail lost in the standard encoding process. It is reasonably certain, therefore, that the resulting color information remaining should be more than adequate to produce a good color picture which really hinges on the quality of the luminance image. It appears desirable, in both direct and kinescope recording, to keep as much of the luminance information as possible coming from the luminance image and as little luminance information as possible coming from the chrominance images.

INITIAL OPERATION OF THE EXPERIMENTAL SCANNER

An experimental model of the previously described scanning system was first put in operation late in 1954. It used a 5ZP16 scanner tube with a single line scan (no vertical raster). A test pattern film was made to use with the scanner and to evaluate its capabilities. The individual images on the test film were approximately 4.75 mm high and 10 mm wide. This width is standard for a regular 16 mm frame. The definition in both horizontal and vertical directions on the film was

---

*I. Feasibility and Technique of Storing Color Video Information on Black-and-White Film. Presented at 1954 National I.R.E. Convention; II. Experimental Equipment for Recording and Reproducing Color Television Images on Black-and-White Film. Presented at 1955 National Convention of I.R.E. and at Chicago Convention of S.M.P.T.E.; III. A New Recording Method for Color TV Using Black-and-White Film. Presented at Pacific Coast Convention of A.I.E.E.

more than adequate to provide a very good television picture. Getting that information off the film, however, presented certain complications. The initial color pictures obtained from the scanner suffered from some obvious defects. The definition was rather poor in both horizontal and vertical directions and the pictures were quite noisy. These defects were directly traceable to one fundamental problem. To prevent rapid phosphor deterioration on the scanner tube due to the single line scan, the beam current was cut to 10 microamperes and the ultor voltage to approximately 15,000 volts. Even at these values it was necessary to move the scanning line often. Reasonable scanner tube life could have been achieved by this method, but at best it was quite inconvenient. Further, the light output was quite low at the ultor voltage and beam current mentioned, which accounted for the objectionable noise characteristics. A further and perhaps more serious difficulty was that at the low ultor voltage the scanner tube would not focus well enough to give a really high definition image. Still another and even more fundamental problem occurred which caused considerable degradation in the vertical definition of the reproduced image. The image on the film was compressed to a little over 0.6 of the height of a normal 16 mm image. Even though this allows good vertical definition as far as the film is concerned, the spot of the scanner tube is essentially round and therefore discriminates against vertical detail as compared to horizontal detail in a vertically compressed image. This can be corrected by either using a much smaller scanner spot (which is not a particularly practical solution with present scanner tubes) or by optically compressing the scanning spot in the vertical direction.

To get an idea of resolution obtainable by compression of the scanning spot, let us choose a few numbers regarding resolution that might be expected from film and from a television scanning tube. A rather conservative figure for film resolution that might be expected under field conditions is 100 television lines per mm. This is equivalent to 50 photographic lines per mm. An image with a height of 7.5 mm then would be capable of about 750 lines. If this is scanned with a scanner tube with 600 line definition (ignoring for the moment that we only have 500 or so usable lines in the television display), the resulting definition would be about 470 lines. Now let us suppose that we have a film image 4.75 mm high which is scanned with a spot that is compressed vertically by a factor of 6:1 or so. The resultant definition capability of the film alone is 475 lines, but the scanning system is capable of reading out essentially all of that definition; provided, of course, that there are more than 475 scanning lines in the first place. In other words, we can increase definition either by increasing film area or by decreasing equivalent scanning aperture size. It is true that the limiting definition of the 7.5 mm image would be improved by using the compressed spot. However, we begin to enter the area in which the absolute upper working limit is controlled to a greater and greater extent by the television scanning standards.

There is one other factor regarding vertical resolution in a video signal that is worth considering. Essentially all of the vertical resolution present in the video signal usually does reach the grid of the picture tube in the home receiver. Further, in a properly focused receiver, the vertical resolution displayed exceeds horizontal resolution displayed because of the transmitter and receiver band pass characteristics. It is probably much less desirable to degrade horizontal resolution even by a small factor than it is to degrade vertical resolution by the same factor as long as vertical limiting resolution still exceeds horizontal.

DESIGN AND USE OF COMPRESSION OPTICAL SYSTEMS

From the preceding discussion, and from the experience gained in the initial operation of the scanner, several things were successively apparent. To get good focusing characteristics and a high light output from the scanner tube, much higher values of beam current and ultor voltage were required. Therefore, the use of a single scanning line was not feasible because of the rapid phosphor deterioration. If a raster was required on the scanner tube, then some sort of compression optical system was needed to get the proper image aspect ratio as well as to improve vertical resolution characteristics.

As has been implied, it is not necessary to compress the raster vertically until it is approximately the height of a normal single line. As a matter of fact, if the vertical raster is compressed to about 1/26 of the normal raster height, the net result is to eliminate the area on the film that would normally be black during the vertical blanking period. Thus, the film is used with absolute minimum waste area. In practice, a compression of 10:1 or more gives a perfectly satisfactory aspect ratio and the result is essentially undistinguishable from the ideal compression figure.

It is necessary to arrive at some compromise between electronic raster compression and optical raster compression. If compression is completely electronic, there is a loss in vertical definition for reasons explained earlier; and it is quite likely that the life of the scanner tube phosphor will be shortened. On the other hand, it has proved impractical to get all of the required compression

optically and still use cylindrical lenses of reasonable cost.

Still another factor must be considered. If such a device is to become commercially practical, it is probably necessary that the system be capable of showing still frame pictures. If good vertical definition is to be available in these still frame pictures, the spot must be compressed vertically by a factor of about two to one. Also the resultant image of the scanner tube on the film must have a proper television aspect ratio. Since the picture image on the film is compressed by a factor of about 0.6, then the image of the cathode ray tube on the film is approximately 0.6 times as high as it would be if it were scanning a standard 16 mm film image. The raster on the scanner tube, then, must be 1.2 times as high as it would be if it were scanning a standard 16 mm film. This allows for the desirable 2:1 compression in the vertical direction which is obtained optically. The width of the raster on the scanner tube has been nominally about 4 inches. This width gives good horizontal definition, and it is desirable to avoid sacrificing this feature. The height of the raster for still frame pictures is then 3.6 inches. A little corner trimming occurs on a five inch scanner tube with this raster height, but this probably can be ignored for still frame purposes.

For running film, it appears that optical systems with a vertical compression of 6:1 can be designed with nominal complexity. Beyond this figure the optical systems either get quite complex or have too great a light loss. The remaining theoretical compression of 4.33 (26 divided by 6) can be obtained by electronic compression of the raster; although it has been found that 2:1 or greater electronic compression is quite satisfactory. If any objectionable overlap of successive fields occurs at the top or bottom of the picture, it is easily removed by reversal of vertical sweep direction on the scanner tube, and the resulting aspect ratio distortion is insignificant.

From the preceding discussion, the requirements of a practical optical compression system can be stated.
It should have a vertical compression of 2:1 for still frames.
It should have a vertical compression of about 6:1 for running film.
In addition, when switching from running film to still frame, it is necessary to disable the electronic switch and increase the size of the vertical sweep.

The first compression optical system that was used is shown in figures 3 and 4. Figure 3 shows the arrangement of the optical elements when the film is running. Its operation is described briefly as follows: The negative plano-cylinders, C_1, produce a virtual image (vertical only) of the scanner tube face approximately 31 mm to the right of their geometric center. The single positive plano-cylinder, C_2, has a relatively long focal length. The distance from C_2 to the virtual image produced by C_1 is considerably less than the focal length of C_2. The net result is that C_2 forms a second virtual image (in the vertical only) at the face of the scanner tube. The height of this second virtual image is 1/6 of the height of the actual raster. Thus, the spherical Tessar lens "sees" a raster of normal horizontal dimension but with the vertical dimension compressed 6:1. Figure 4 illustrates the optical configuration when the film is not running. The only thing that is changed is that the negative cylinders are removed and two positive plano-cylinders, C_3, are inserted in another position which is closer to the scanner tube. The function of C_3 is to form a real image of the scanner tube face (vertical only) at the same position as the virtual image of the negative cylinders which were removed. The remainder of the optical system can then be left alone. This configuration gives the net compression of 2:1, which is required for still film.

The overall system was satisfactory in every respect for still film. The compression characteristics and optical image quality were quite satisfactory for running film. There was, however, an overall light loss in the system of about 6:1 for running film. The basic reason for this light loss can be explained from a fundamental rule of optics. It is not possible to increase the radiant flux per unit area per steradian of solid angle. This means that to place a compressed raster on the film with the same radiant energy as a normally uncompressed raster it is necessary to increase the lens aperture or make provisions for an auxiliary lens closer to the film. There was, of course, a considerable increase in the light output of the scanner tube due to the higher ultor voltage and beam current. This increase very roughly made up for the light loss in the compression optical system. The overall results, therefore, were that image quality and definition were much improved but the noise characteristics remained about the same.

The noise problem was largely overcome by using a scanner tube with considerably more total light output than the 5ZP16. That tube is the 5AUP24. The 5AUP24 has its main application for color film flying spot scanners and has a relatively wide band spectral output. This characteristic is, of course, relatively unimportant when used with a system of the type discussed in this paper. The phosphor correction requirements for the 5AUP24

are somewhat more severe than those of the 5ZP16, but the light output is sufficient to overcome this disadvantage and still have a light advantage over the 5ZP16 of perhaps 4:1 or more. The overall noise characteristics are satisfactory with this arrangement, but there is not enough leeway to allow for losses that invariably occur when such devices are used in commercial applications instead of in a development laboratory.

A safety factor can be built into the equipment rather easily by redesigning the optical system. Figures 5 and 6 illustrate a new compression optical system which performs the same geometrical functions as the original system, but is between two and three times as efficient. Figure 5 illustrates the system for running film.

The operation of the second optical system is as follows: The two negative cylinders, C_1, produce a virtual image (vertical only) approximately 75 mm to the right of C_1. The 75 mm spherical Tessar lens produces a real image (of the virtual image of C_1) approximately 25 mm to the left of the film plane. The function of the two positive plano-cylinders, C_2, is to move the vertical image of S_1 back to the film plane. The overall compression of this system is 6:1 over the image reduction effect of the 75 mm spherical lens alone. Figure 6 illustrates the system for the film stopped. The only change is that the negative cylinders have been removed and two positive plano-cylinders, C_3, have been inserted at the position shown. The function of C_3 is to produce a real image (vertical only) in the same place as the virtual image produced by C_1 when the film is running. The overall vertical compression beyond the image reduction effects of S_1 alone is 2:1.

At the time of writing of this paper, this optical system is being constructed. It is hopefully expected that there will be no further need to increase the system light efficiency.

For purposes of clarity, it should probably be mentioned that the optical systems illustrated in figures 3 through 6 are shown for only one channel. In the actual system, the cylindrical lenses in front of the spherical Tessar lenses are made physically quite large. It is thus possible to split the light for each Tessar lens by using rhomboid prisms and to use the same cylindrical lenses for all three channels. In the second optical system described, the positive cylinders, C_2, must for physical reasons be very small, and thus, one complete set of them must be used for each channel. Figure 7 illustrates how the light is split for the two chrominance channels. The luminance channel is left out for clarity. Figure 8 is a photograph showing the mounting of the lenses and three of the rhomboid prisms.

At the oral presentation of this paper, a number of color slides of color television pictures produced by this system are shown. Some of them show "before" and "after" characteristics of the system for some of the difficulties which have been overcome.

FILM TRANSPORT MECHANISM

One of the more serious problems often encountered in continuous motion systems is the difficulty in obtaining sufficient stability in the film transport mechanism. A number of elaborate systems have been built involving moving optical systems and feedback loops to position the scanning raster in agreement with the film position. It was considered desirable to avoid these complications if possible. A number of simple transport mechanisms have been tried.

In this experimentation, it has been found that the stability of a small synchronous motor-reducer combination can be made with adequate stability. A difficulty arises, however, in getting the same stability in the film gate. The current transport mechanism (and the best one obtained thus far) consists of a standard Simplex film trap assembly that has been machined to make provisions for mounting the three photomultipliers and their associated optical lucite light pipes and prisms. A Bodine synchronous motor-reducer with a drive sprocket mounted on it is placed directly beneath the Simplex film trap. The stability of this mechanism compares reasonably well with the stability of the average 16 mm motion picture projector and probably would be adequate for television broadcasting with films of moving objects. A system for kinescope recording would have to be somewhat better. It is quite possible, however, that the film could be recorded directly on a drive sprocket assembly and would not have to go through a gate, since there is no need to gather the light into a photomultiplier behind the film. If this were done, the stability of the motor assembly alone might be quite adequate. Figure 9, a photograph of the entire transport mechanism, shows the photomultiplier housing mounted on the film trap assembly and the film drive mechanism.

THE ELECTRONIC SWITCH

In previous papers, the circuit of an electronic switch that would perform satisfactorily was presented. There were eight adjustments in this switch. Each time the switch was balanced, it was necessary to use an oscilloscope and check each of the eight adjustments. In recent months, the General Electric Company has manufactured a new tube for electronic switching purposes. Its designation number is 6AR8. Basically, it is a multi-grid tube with beam deflecting electrodes

and two anodes. Either anode can be selected, depending on the potential applied to the beam deflecting electrodes. The valuable feature of the tube in this application is that its transconductance is essentially independent of the anode being used. This means that when one channel is dynamically balanced, the other must be also.

If two of these tubes are used as shown in the electronic switch circuit of figure 10, only four adjustments (two d-c and two dynamic) are necessary. Further, if the two tubes are once balanced d-c wise and sufficient low frequency degeneration is introduced, the little d-c drift which occurs is easily removed by the keyed clamping circuits. When one of the dynamic adjustments is set to some medium value, the entire electronic switch can then be balanced by the other dynamic adjustment. This means that it can be rebalanced visually without using an oscilloscope while the film is running should some severe change in gain occur in a chrominance channel. Thus, no shutdown of the equipment is necessary.

KINESCOPE RECORDER

As yet, a kinescope recorder for this system has not been built. A kinescope recorder for black-and-white television which has similar problems (i.e., a continuously moving film and a compressed vertical raster) has been built and operated successfully in England.* The optics for a kinescope recorder in this system are quite simple since the light does not have to be gathered behind the film after passing through it. It is hoped that this work might be undertaken in the near future.

CONCLUSIONS

It is believed that the principles upon which this device operates are sound and that good quality color pictures can be obtained from it. Further the versatility of this system in doing all television jobs would seem to be a great advantage. Also, the amount of black-and-white film used per minute is a little over half that used by other systems of this general type.

The writer is indebted to many people for assistance in this project. In particular, Mr. Paul Kristensen of Iowa State College has lent considerable help. Assistance with the optical system has come from Mr. Arthur Cox, Optical Director of Bell and Howell, and from Messrs. Larry Iverson and Albert Anderson of Benson Optical Company in Ames, Iowa, and Minneapolis, Minnesota, respectively.

*16 mm Television-Recording for Sequential Television Systems. V.B. Hulme. Electronic Engineering, December, 1955, pages 516-522.

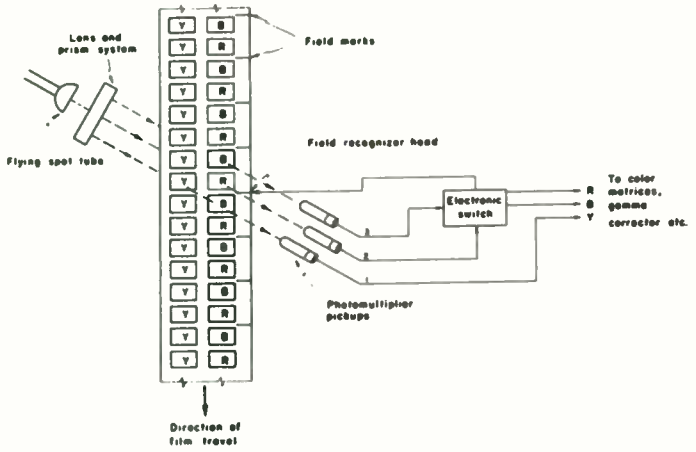

Fig. 1
Continuous film scanner for color television (first type).

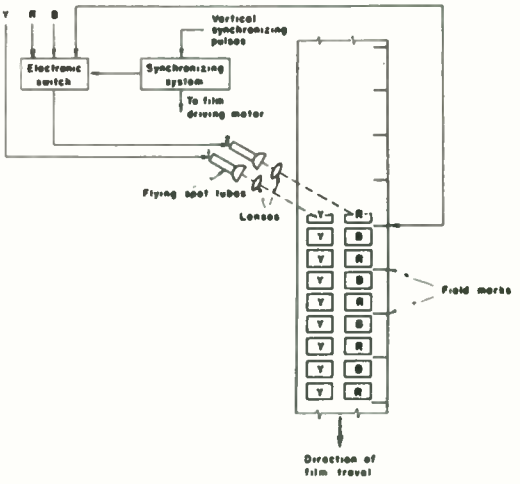

Fig. 2
Continuous motion kinescope recorder for color television.

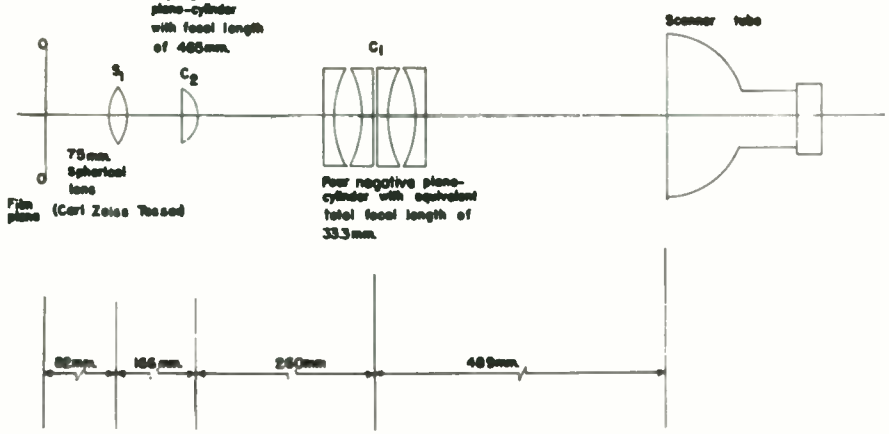

Fig. 3
First type of compression optical system
(film running).

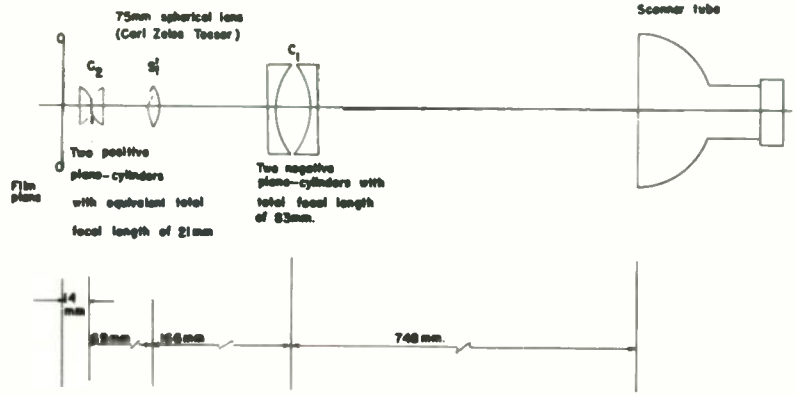

Fig. 5
Second type compression optical system
(film running).

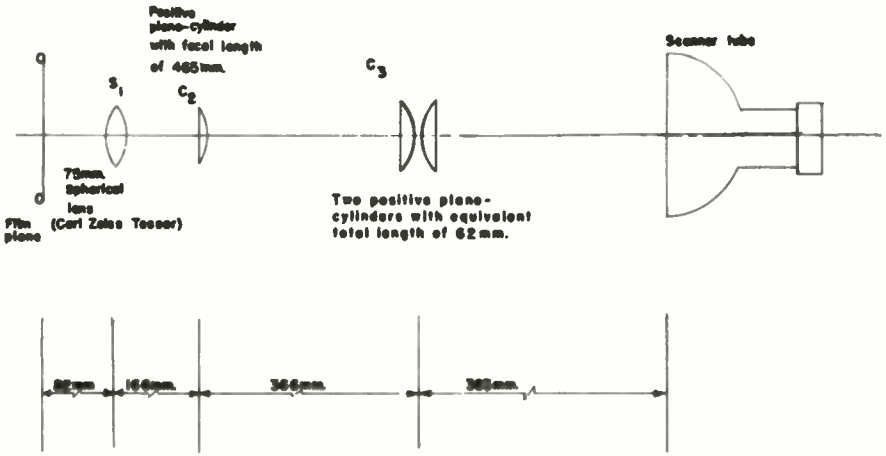

Fig. 4
First type of compression optical system
(film stopped).

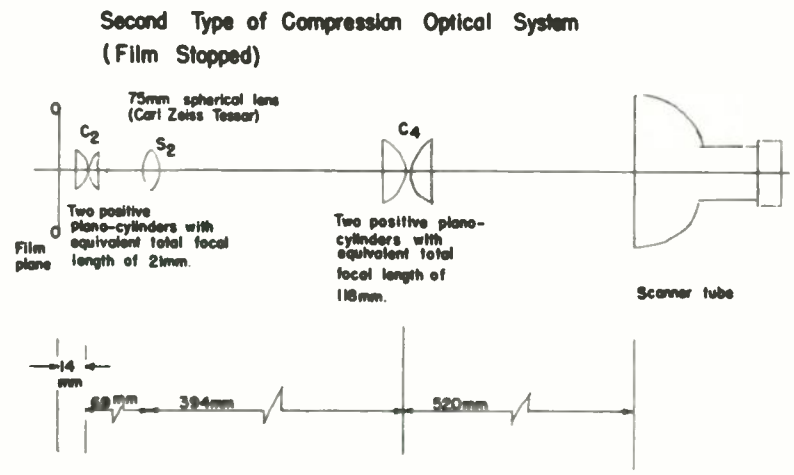

Fig. 6
Second type of compression optical system
(film stopped).

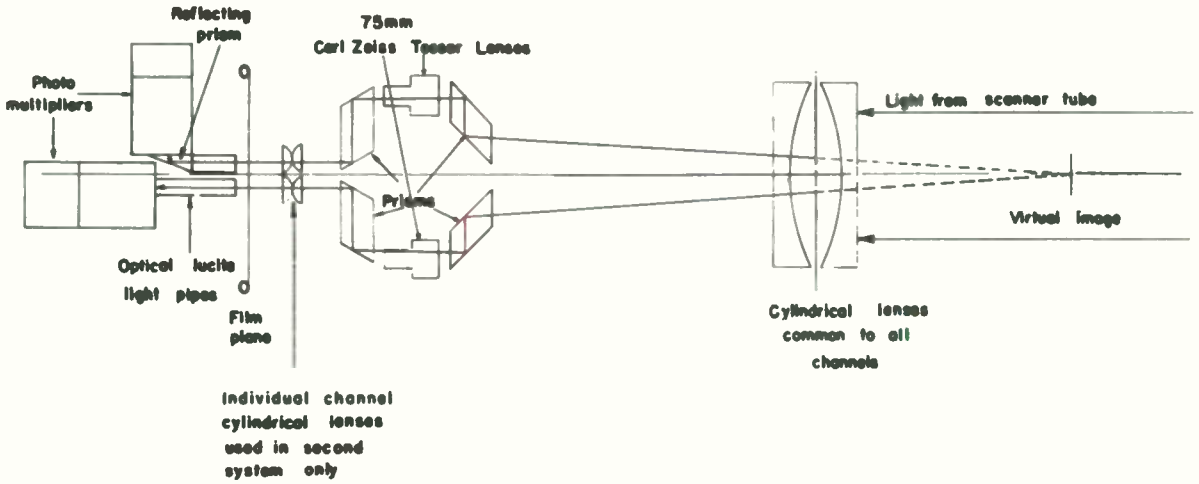

Fig. 7
Diagram, light paths for chrominance channels.

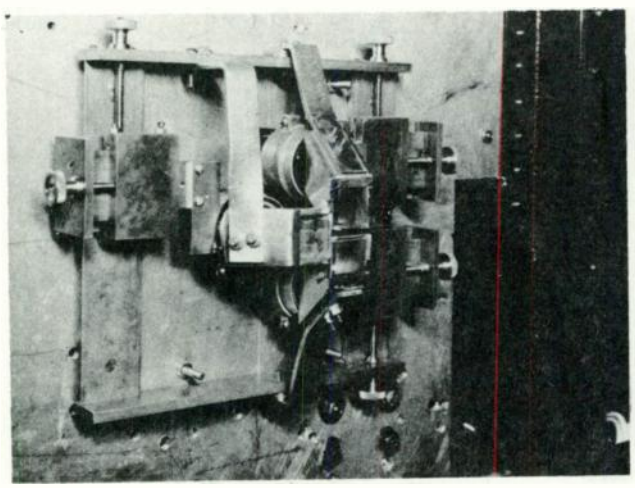

Fig. 8
Lens mounting.

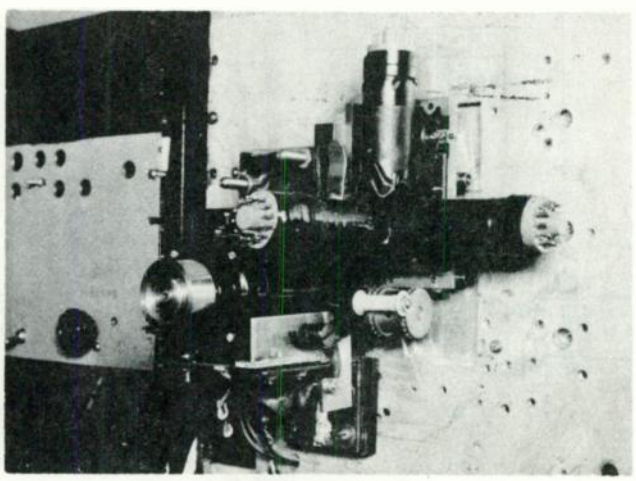

Fig. 9
Film transport mechanism.

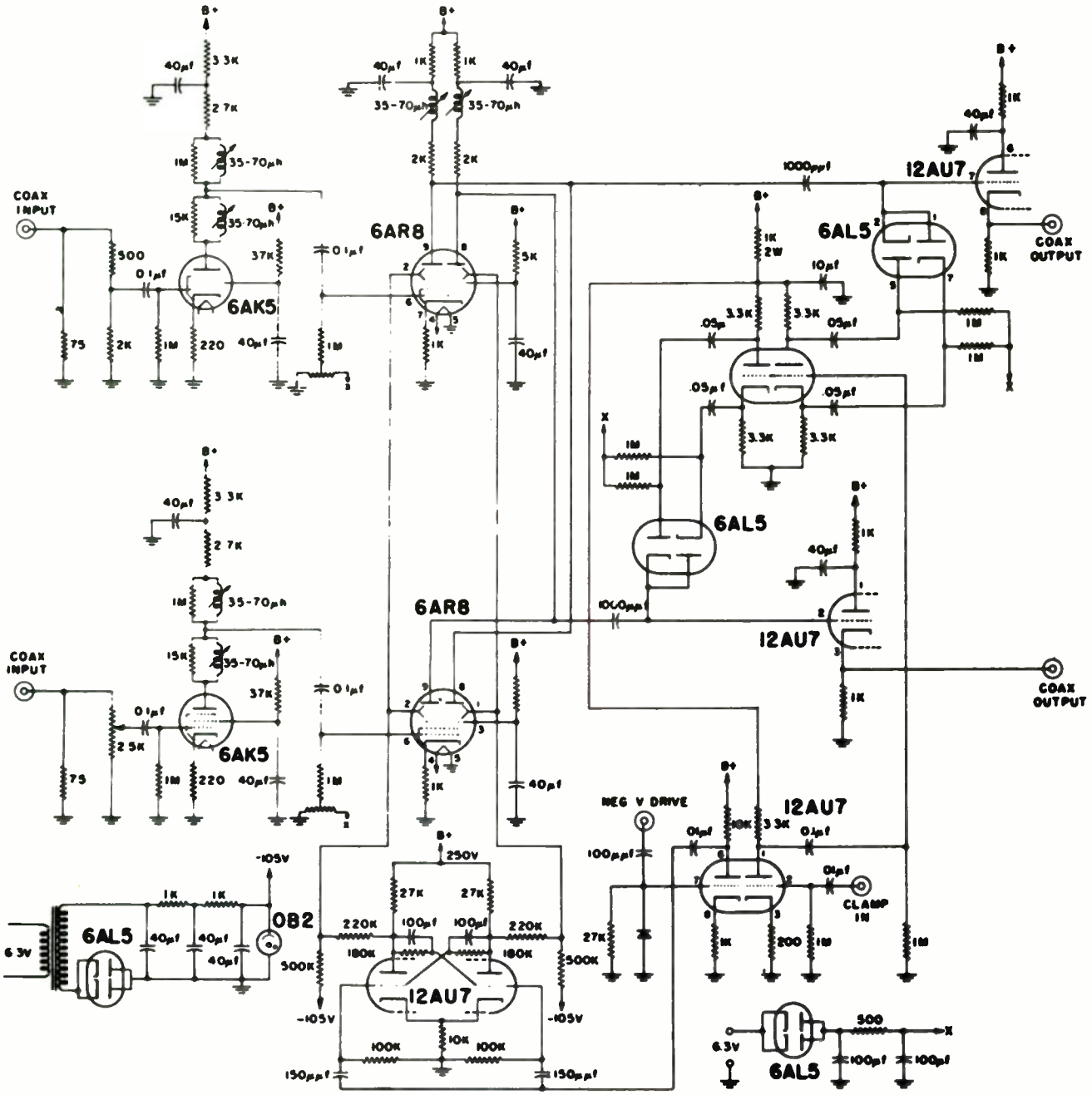

Fig. 10
Electronic switch.

DESIGN CONSIDERATIONS FOR A HIGH QUALITY TRANSISTORIZED PROGRAM AMPLIFIER FOR REMOTE BROADCAST USE

John K. Birch
Gates Radio Company
Quincy, Illinois

Summary

Small size and extremely low battery drain make transistors attractive for use in portable broadcast equipment. However, they present many unique problems, including temperature sensitivity and non-linearity, which conflict with the high standards set up for broadcast equipment. Solutions have been found in special circuit techniques, which are embodied in a program amplifier available commercially in several forms.

Introduction

Manufacturers of remote broadcast amplifiers work in a field where miniaturization is very desirable, but extremely difficult to attain. Such factors as A and B battery packs and high quality attenuators and transformers place a definite limit on unit size, limiting further improvement to the areas of styling and deluxe features. The appearance of the improved low cost junction transistor made possible the development of a remote amplifier of small size, light weight and long battery life.

Early in the development of transistorized audio amplifiers a number of problems arose which are peculiar to transistor circuits and which require special techniques to solve. Four of the most important of these problems are:

1. Temperature sensitivity.

2. Distortion due to non-linearity in the output stage.

3. Transformer design.

4. Narrow range of input levels for the preamplifier stage.

It is the purpose of this paper to illustrate these problems, and to present solutions which are feasible for standard production techniques.

Objectives

In the beginning, it was necessary to list the design goals, which it was felt must be included in the new equipment at any cost:

1. The remote amplifier must be as small as possible, limited mainly by transformer and battery size.

2. Only battery operation would be considered, since the small size of the equipment would make it ideal for use in locations far removed from power sources, or where a line cord would be a needless encumbrance. The use of mercury batteries could possibly provide operation for a whole season without change.

3. Frequency response and distortion must be held close to ratings of previous equipment. Response must be held within 2 db from 70 to 10,000 cps., and distortion under 2% at full output.

4. An adequate overload factor must be included; at least 6 db over the normal output level of +8 dbm, or +14 dbm out of the isolation pad.

5. A line isolation pad of sufficient attenuation must be included to reduce the effect of variations in line impedance to a negligible amount. The loading of the output stage is rather critical and requires an isolation pad of 4 db attenuation for dependable results. Allowing 1 db for a production safety factor and as a margin for battery aging, the maximum amplifier output level must be +19 dbm, or 80 milliwatts.

6. Although the nominal output level of a microphone is -60 dbm, it can easily increase by 20 db with some types of program material. Thus the desired specifications must be obtained at an input level of -40 dbm.

7. Noise must be as low as with vacuum tube equipment, calling for an equivalent input noise figure of -115 to -120 dbm.

Temperature Sensitivity

The first design problem, temperature sensitivity, results from the increase in collector cut-off current with temperature. This increase appears in the collector circuit multiplied by the factor 1-a, and is especially serious in stages operating at low collector voltages and with a high value of collector load resistance. A change in 15 degrees C. in one circuit tested increased the

collector current from .73 ma to 1.0 ma and dropped the collector voltage from 6 volts to 0.5 volts, resulting in extreme clipping.

Methods of temperature stabilization are well known and will not be described in detail here. The most common procedure consists of biasing the base from a bleeder across the battery, and supplying emitter current from a constant current source, which is done effectively by connecting a resistance in series with the emitter.[1] Stabilization to 60°C. is obtained in this manner in the amplifier being described.

The Output Stage

Design of the output stage centers around two choices: between Class A and Class B operation, and between the common base and common emitter configurations.

Class B operation cannot be considered for high quality performance, in spite of its offer of high power output and low quiescent current. Biasing is extremely critical and is subject to shifting with temperature changes. Distortion is difficult to control due to the notch effect, and is especially serious at high frequencies where variations in current gain and phase shift between transistors cause unbalance.

Push-pull Class A operation eliminates the notch effect, and the bias point is more easily stabilized. It is the logical choice, at the price of higher battery drain.

Distortion in the power stage is due to two factors: non-linearity of the collector family curves, and non-linearity of the emitter-base diode.

Figure 1 shows the collector family for the common emitter configuration,[2] with a load line of 4000 ohms superimposed. The crowding at the high current end indicates a source of distortion for operation at maximum output, which in this case is about 43 mw.

Figure 2 shows the 4000 ohm load line plotted on the common base curves.[3] The constant spacing makes operation at the maximum output of 45 mw. possible with low distortion.

Measurements made on a push-pull amplifier at 2% distortion using 2N44's show maximum output for common emitter to be ∔15 dbm; for common base, ∔19 dbm, or more than twice as much power.

The disadvantage of the common base circuit is its low gain. A difference of 20 db was measured in the comparison just described, and part of this is due to an intentional input impedance mismatch to be described later. The extra undistorted power available was considered to be more important than the power gain in this application.

Figure 3 shows the second source of distortion - non-linearity of the transistor input circuit. This is a graph of collector current vs. emitter volts for zero generator resistance in the common base circuit. A sine wave output can be obtained only by supplying signal to the emitter from a constant current source, which is accomplished by employing a source impedance higher than the input impedance. The input impedance of the common base power stage under consideration is about 40 ohms.

With a source impedance of 50 ohms, the distortion for maximum output is 3%; for 150 ohms, 1.5%; and for 600 ohms, 1.2%. Loss in gain is 3 db at 150 ohms, & db at 600 ohms. 150 ohms is chosen as the best compromise between gain and distortion.

Transformer Design

The transformer is the most critical factor in high quality transistor amplifier design, and the most serious obstacle to miniaturization.

Although many extremely small transformers are available, they are unusable below about 200 cps. for the equipment under consideration. Extending the range another octave and a half requires a larger core and involves a juggling process between core materials, D.C. in windings, and efficiency to determine the optimum combination for the size allowable. Nickle alloy cores are used, and shielding is provided by the mu-metal case.

The Input Stage

Distortion in the microphone preamplifier is produced mainly by two factors.

First, the low collector voltage required for low noise operation limits the a.c. collector voltage swing to a few volts, beyond which clipping occurs. In a typical common emitter amplifier, with a collector to emitter voltage of 3 volts, source impedance 600 ohms, voltage gain of 460, clipping occurs at an input voltage of 5 mv., or -43 dbm.

Second, the non-linearity of the emitter-base diode causes even-harmonic distortion, as in the case of the output stage described earlier. In this case, however, the impedance of the source - a microphone - is fixed. Linearity can be improved by adding an unbypassed resistance in series with the emitter, with results as shown in Figure 4. This is a plot of collector current vs. base voltage, for emitter resistances of 0 and 200 ohms.

This procedure also results in degenerative current feedback, which further reduces the even harmonic distortion in the same manner as cathode degeneration in vacuum tube amplifiers. Degeneration has a valuable side effect, in almost completely equalizing the gain figure for transistors of any one type, and providing good predictability for the overall gain of the amplifier. In a sampling of fifteen transistors, gain variation was only 0.5 db.

Figure 5 shows the effect of emitter degeneration on the signal handling capabilities of the preamplifier. The decreasing slope of the curves as resistance increases is due to the improving linearity. In each case, however, the curve turns up sharply when the clipping point is reached.

Degeneration also increases the transistor input impedance. A 200 ohm emitter resistor raises the input impedance to 2500 ohms, which is low enough to eliminate the need for an input transformer, and high enough to satisfy the requirement that the microphone must work into an unloaded input circuit for optimum performance.

The noise figure for the overall amplifier is about 10 db better than the average vacuum tube remote amplifier with low-level mixing. This is accomplished through the use of high-level mixing, low noise transistors and low collector voltages for the first two stages. With an input level of -60 dbm and +8 dbm output, the noise is down -55 to -60 db.

Commercial Applications

These design factors have been utilized in the development of three new pieces of equipment for the broadcast station - a single channel remote amplifier, a two channel remote amplifier, and a microphone booster amplifier.

Figure 6 shows a simplified schematic diagram of the single channel remote amplifier. All biasing and stabilizing resistors have been omitted for clarity. Low noise 2N106 transistors are used in the preamplifier and booster stages; the driver and push-pull output transistors are type 2N44 medium power units.

All the design specifications mentioned at the beginning are included in this amplifier. In addition, the weight is 3 pounds, size is 9" x 3" x 2", and battery life is about 80 hours.

Figure 7 is an external view of the amplifier.

Figure 8 shows the internal construction, with the printed wiring chassis for the amplifier and line isolation pad.

Figure 9 shows the two-channel remote amplifier. The principle differences are the extra input circuit, the VU meter, and provision for a spare battery.

The booster amplifier shown in Figure 10 is a single stage preamplifier with a gain of 15 db, output impedances of 150 or 50 ohms. It is designed to be used with boom or overhead microphones, and will run continuously for a year on its self-contained battery, permitting placement in difficult locations.

These units illustrate the most appropriate use at present for transistors in broadcast equipment. They provide the closest approach yet to perfect portability, benefitting station and listener alike.

References

1. Shea, R. F. (ed.), "Principles of Transistor Circuits", John Wiley & Sons, 1953, pp. 97-108.

2, 3. Tentative Data Sheet ECG-21B for 2N44 Transistor, General Electric Co.

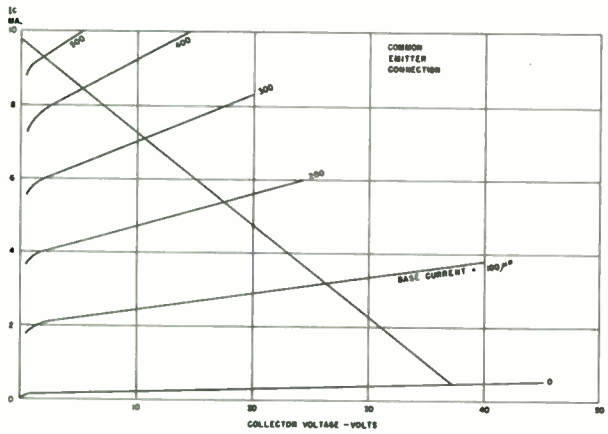

Fig. 1
Collector characteristics for 2N44 in the common emitter connection, illustrating crowding at high collector current.

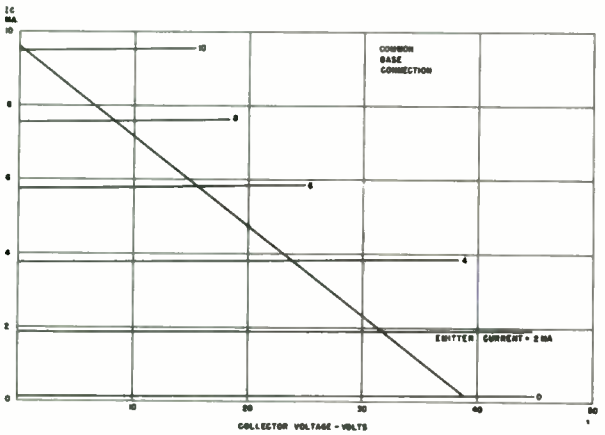

Fig. 2
Collector characteristics for 2N44 in the common base connection, illustrating even spacing.

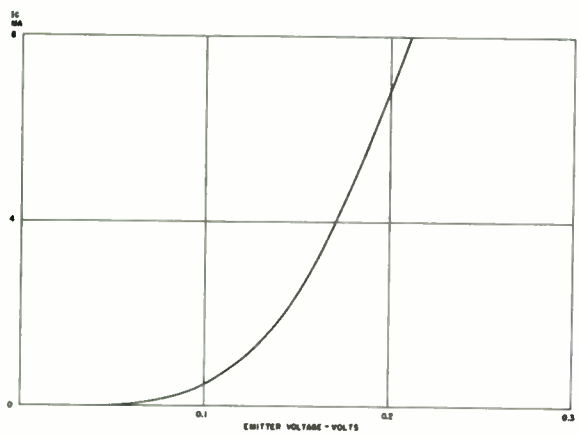

Fig. 3
Non-linear relationship between collector current and emitter voltage in the common base connection.

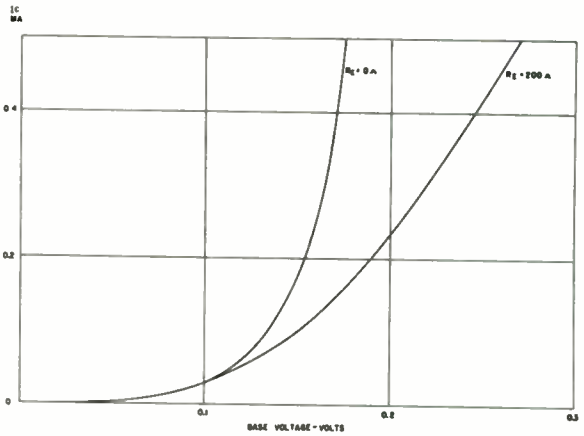

Fig. 4
Effect of external emitter resistance on linearity of emitter-base diode.

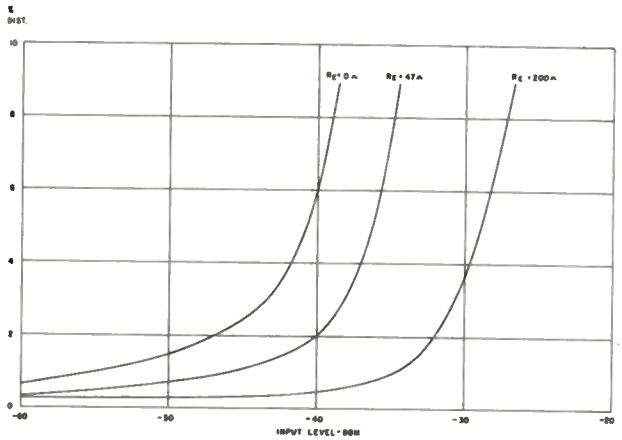

Fig. 5
Effect of external emitter resistance on maximum input signal.

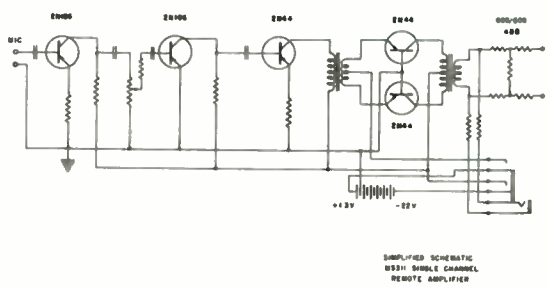

Fig. 6
Simplified schematic diagram of single channel remote amplifier. Bias and stabilizing circuits omitted for clarity.

Fig. 7
External view of single channel remote amplifier.

Fig. 9
Two-channel remote amplifier with carrying case.

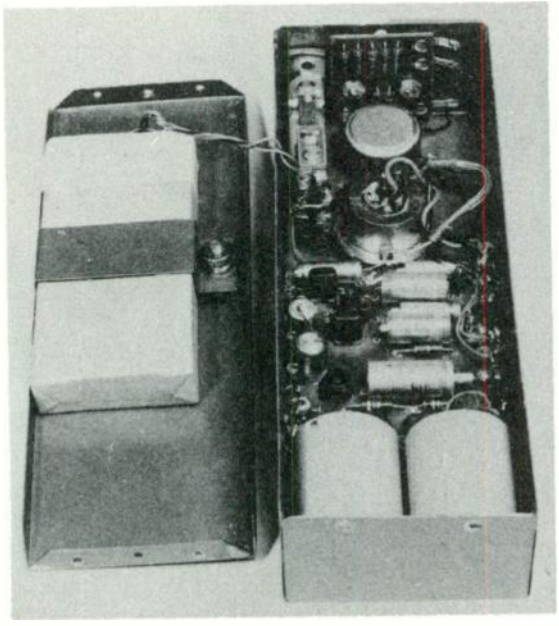

Fig. 8
Internal view of single channel remote amplifier, showing printed chassis for amplifier and line pad.

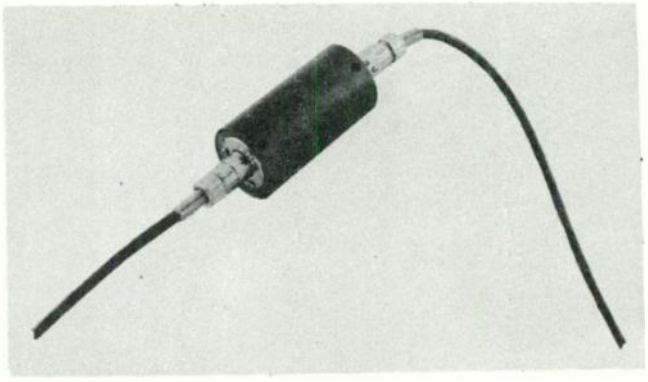

Fig. 10
Microphone booster amplifier.